
**Pacific Northwest
National Laboratory**

Operated by Battelle for the
U.S. Department of Energy

**Deep Downhole Seismic Testing at the
Waste Treatment Plant Site,
Hanford, WA**

Volume V

**S-Wave Measurements in Borehole C4996
Seismic Records, Wave-Arrival Identifications and
Interpreted S-Wave Velocity Profile**

K. H. Stokoe
S. Li
B. Cox
F. Menq

June 2007



Prepared by The University of Texas at Austin
for the Pacific Northwest National Laboratory
under Contract DE-AC05-76RL01830
with the U.S. Department of Energy

DISCLAIMER

This report was prepared as an account of work sponsored by an agency of the United States Government. Neither the United States Government nor any agency thereof, nor Battelle Memorial Institute, nor any of their employees, makes **any warranty, express or implied, or assumes any legal liability or responsibility for the accuracy, completeness, or usefulness of any information, apparatus, product, or process disclosed, or represents that its use would not infringe privately owned rights.** Reference herein to any specific commercial product, process, or service by trade name, trademark, manufacturer, or otherwise does not necessarily constitute or imply its endorsement, recommendation, or favoring by the United States Government or any agency thereof, or Battelle Memorial Institute. The views and opinions of authors expressed herein do not necessarily state or reflect those of the United States Government or any agency thereof.

PACIFIC NORTHWEST NATIONAL LABORATORY
operated by
BATTELLE
for the
UNITED STATES DEPARTMENT OF ENERGY
under Contract DE-AC05-76RL01830

Printed in the United States of America

Available to DOE and DOE contractors from the
Office of Scientific and Technical Information,
P.O. Box 62, Oak Ridge, TN 37831-0062;
ph: (865) 576-8401
fax: (865) 576-5728
email: reports@adonis.osti.gov

Available to the public from the National Technical Information Service,
U.S. Department of Commerce, 5285 Port Royal Rd., Springfield, VA 22161
ph: (800) 553-6847
fax: (703) 605-6900
email: orders@ntis.fedworld.gov
online ordering: <http://www.ntis.gov/ordering.htm>



This document was printed on recycled paper.

Deep Downhole Seismic Testing at the Waste Treatment Plant Site, Hanford, WA

Volume V of VI

**S-Wave Measurements in Borehole C4996
Seismic Records, Wave-Arrival Identifications and Interpreted S-
Wave Velocity Profile**

for

Pacific Northwest National Laboratory
Richland, WA

by

Kenneth H. Stokoe, II
Songcheng Li
Brady Cox
Farn-Yuh Menq

June 28, 2007

Geotechnical Engineering Report GR07-10
Geotechnical Engineering Center
Civil Engineering Department
The University of Texas at Austin

**Volume V: S-Wave Measurements in Borehole C4996
Seismic Records, Wave-Arrival Identifications and Interpreted
S-Wave Velocity Profile**

Table of Contents

Section 1	Introduction	1
Section 2	Explanation of Terminology.....	4
Section 3	Vs Profile at Borehole C4996.....	16
Section 4	Unfiltered S-Wave Records of Lower Horizontal Receiver and Derived Rotated In-Line Signals	30
4.1	Forward S-wave records of the lower in-line receiver.....	33
4.2	Reversed S-wave records of the lower in-line receiver	43
4.3	Forward S-wave records of the lower cross-line receiver	53
4.4	Reversed S-wave records of the lower cross-line receiver	63
4.5	Forward S-wave signals of the lower rotated in-line receiver	73
4.6	Reversed S-wave signals of the lower rotated in-line receiver	83
Section 5	Unfiltered S-Wave Records of Reaction Mass.....	93
Section 6	Unfiltered S-Wave Records of Reference Receiver.....	104
Section 7	Filtered S-Wave Signals of Lower Rotated In-Line Receiver	115
Section 8	Filtered S-Wave Signals of Reaction Mass Acceleration ...	126
Section 9	Filtered S-Wave Signals of Reference Receiver	137

Section 10	Expanded and Filtered S-Wave Signals of Lower Rotated In-Line Receiver.....	148
Section 11	Waterfall Plots of Unfiltered S-Wave Signals of Lower Rotated In-Line Receiver.....	159
Section 12	Waterfall Plots of Filtered S-Wave Signals of Lower Rotated In-Line Receiver.....	165
Section 13	References.....	171

Volume V: S-Wave Measurements in Borehole C4996 Seismic Records, Wave-Arrival Identifications and Interpreted S-Wave Velocity Profile

Section 1: Introduction

The U.S. Department of Energy (DOE) and the Pacific Northwest National Laboratory (PNNL) installed three boreholes to a depth of approximately 1400 feet below ground surface (bgs) in 2006 at the Waste Treatment and Immobilization Plant (WTP) construction site on the Hanford Site in southeastern Washington State. The purpose of the new boreholes was to obtain direct shear (S) and compressional (P) wave velocity measurements in the subsurface for use in reducing the uncertainty in the seismic response spectra and design basis for the WTP. The University of Texas at Austin (UTA) was contracted by PNNL to collect S- and P-wave measurements in each of the three new boreholes identified as C4993, C4996 and C4997 (Barnett et al. 2007; Gardner and Price 2007).

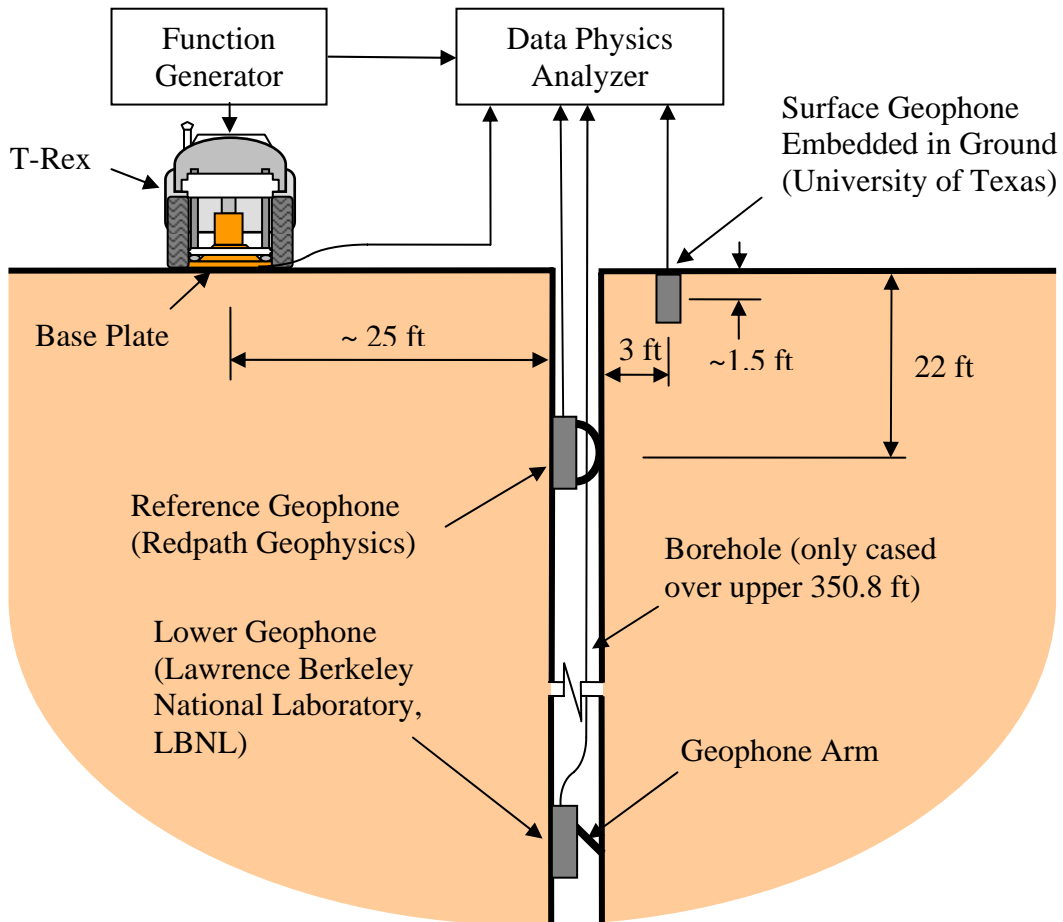
Velocity measurements in shallow sediments from the ground surface to approximately 370 to 400 feet bgs were collected by Redpath Geophysics using impulsive S- and P-wave seismic sources (Redpath 2007). Measurements below this depth within basalt and sedimentary interbeds were made by UTA between October and December 2006 using the T-Rex vibratory seismic source (Stokoe et al. 2004) in each of the three boreholes. Results of these measurements including seismic records, wave-arrival identifications and interpreted velocity profiles are presented in the following six volumes:

- I. P-Wave Measurements in Borehole C4993,
- II. P-Wave Measurements in Borehole C4996,
- III. P-Wave Measurements in Borehole C4997,
- IV. S-Wave Measurements in Borehole C4993,
- V. S-Wave Measurements in Borehole C4996, and
- VI. S-Wave Measurements in Borehole C4997.

In this volume (V), all S-wave measurements are presented that were performed in Borehole C4996 at the WTP with T-Rex as the seismic source and the Lawrence

Berkeley National Laboratory (LBNL) 3-D wireline geophone as the at-depth borehole receiver. S-wave measurements were performed over the depth range of 360 to 1300 ft, typically in 10-ft intervals. However, in some interbeds, 5-ft depth intervals were used, while below about 1180 ft, depth intervals of 20 ft were used. The field setup is illustrated in Figure 1.1.

Figure 1.1 Field Setup for P- and S-Wave Measurement in Borehole C4996



Shear (S) waves were generated by moving the base plate of T-Rex for a given number of cycles at a fixed frequency as discussed in Section 2. This process was repeated so that signal averaging in the time domain was performed using 3 to about 15 averages, with 5 averages typically used. In addition, a second average shear wave record

was recorded by reversing the polarity of the motion of the T-Rex base plate. In this sense, all the signals recorded in the field were averaged signals.

In all cases, the base plate was moving perpendicular to a radial line between the base plate and the borehole which is in and out of the plane of the figure shown in Figure 1.1. The definition of “in-line”, “cross-line”, “forward”, and “reversed” directions are presented in of Section 2. The definitions are based on the direction of the movement of the base plate.

In addition to the LBNL 3-D geophone, called the lower receiver herein, a 3-D geophone from Redpath Geophysics was fixed at a depth of 22 ft in Borehole C4996, and a 3-D geophone from the University of Texas (UT) was embedded near the borehole at about 1.5 ft below the ground surface. The Redpath geophone and the UT geophone were properly aligned so that one of the horizontal components in each geophone was aligned with the direction of horizontal shaking of the T-Rex base plate.

This volume is organized into 13 sections as follows.

Section 1: Introduction,

Section 2: Explanation of Terminology,

Section 3: Vs Profile at Borehole C4996,

Sections 4 to 6: Unfiltered S-wave records of lower horizontal receiver, reaction mass, and reference receiver, respectively,

Sections 7 to 9: Filtered S-wave signals of lower horizontal receiver, reaction mass and reference receiver, respectively,

Section 10: Expanded and filtered S-wave signals of lower horizontal receiver,

Sections 11 and 12: Waterfall plots of unfiltered and filtered lower horizontal receiver signals, respectively, and

Section 13: References.

Section 2 Explanation of Terminology

1. Record or Signal

The recorded and sampled time series of analog voltage from a geophone or an accelerometer is called a record. A signal can generally be a raw record, a processed record or any designed or generated (as by function generator) time series.

The magnitude of any signals related to this test is by default in voltage. All signal amplitudes (y-axis for time series, both axes for hodograph) in figures of this report, if not otherwise explicitly labeled, have a unit of volt.

All figures for time series have the y axis scaled independently for legibility for each trace (gain-normalized). This makes them legible when the amplitude varies from trace to trace (large close to the surface, small at depth).

2. Input Signal or Drive Signal

At each measurement depth, an independent fixed sine wave with a frequency of 50 Hz or 30 Hz was sent from a function generator to T-Rex. This signal is called the Input Signal to T-Rex, or the T-Rex Drive Signal. The input signal was a perfect sine wave, with 5 cycles of 50 Hz, 4 cycles of 20 Hz, or 4 cycles of 30 Hz. Input signals of all measurements were aligned so that they all began at the same instant, which is called time zero, and was marked as time zero (at $t = 0$) on all recorded signals. The input signal, with 5 cycles of 50 Hz, 4 cycles of 20 Hz or 4 cycles of 30 Hz, was sent to T-Rex anywhere from 3 to about 15 times to allow signal averaging of the shear wave to be performed in the time domain. In addition, the polarity of the drive signal was then reversed and the whole process repeated to allow an averaged shear wave signal with reversed polarity to be recorded at the same depth.

3. In-Line and Cross-Line (X-Line)

As discussed in Section 1, in all cases, the base plate was moving perpendicular to a radial line between the base plate and the borehole which is in and out of the plane of the figure shown in Figure 1.1. The radial line is called cross-line (x-line) direction, while the tangential line, which represents the direction of the base plate, is called in-line direction.

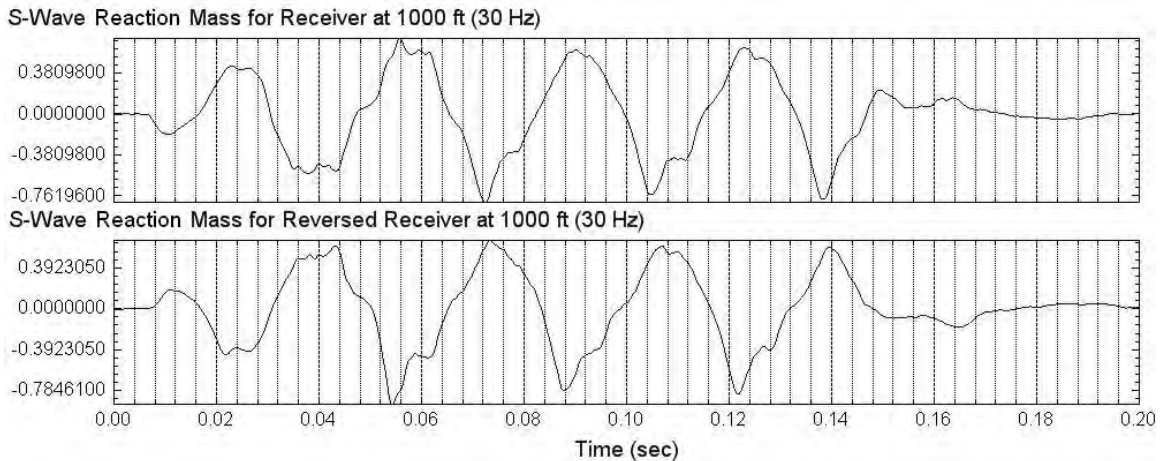
4. Forward Signal and Reversed Signal

The initial horizontal direction in which T-Rex was excited is called the forward direction. The opposite initial direction of excitation that was created by reversing the polarity of the drive signal to T-Rex is called the reversed direction. The forward and reversed motions should be out of phase or have a 180-degree in-phase difference. Examples of these two records are shown in Figures 2.1 and 2.2.

5. Reaction Mass Acceleration or T-Rex Output Signal

The horizontal output force of T-Rex was transmitted to the ground surface by a square base plate located on the bottom of T-Rex. The base plate directly contacted the ground surface. The acceleration of the reaction mass that loads the base plate, also called T-Rex Output Signal, was recorded by a horizontal accelerometer on the reaction mass. An example of the reaction mass output signal is presented in Figure 2.1. The upper one represents the forward initial motion, while the lower one represents the reversed input motion.

Figure 2.1 Unfiltered Horizontal (S-Wave) Acceleration Signals of the Reaction Mass
Input Signal: 4 Cycles of 30-Hz Sine Wave



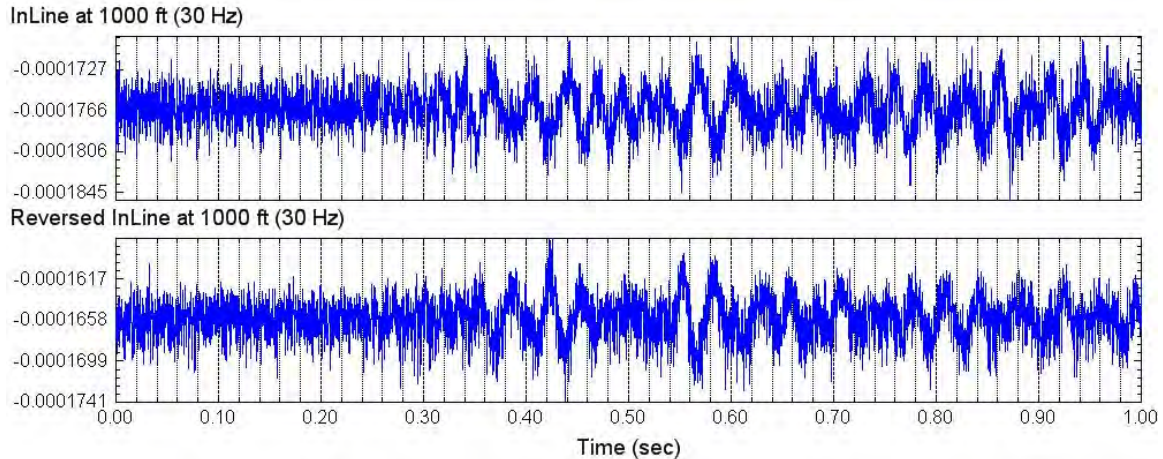
6. Unfiltered Signals

Unfiltered signals are the averaged original time series directly recorded with the Data Physics Analyzer¹. They are the averaged horizontal outputs of the reaction mass accelerometer or the receiver geophones due to the 50-Hz, 20-Hz or 30-Hz input signal. The average amplitude of the unfiltered signal over the record length may not be zero due

¹ System No. 70270 Mobilyzer II – 16C2S – HS, Data Physics Corporation, San Jose, California

to the non-zero initial voltage. Figure 2.2 shows that the average amplitude of an unfiltered signal is less than zero.

Figure 2.2 Unfiltered Lower InLine Receiver (S-Wave) Signals
Input Signal: 4 Cycles of 30-Hz Sine Wave

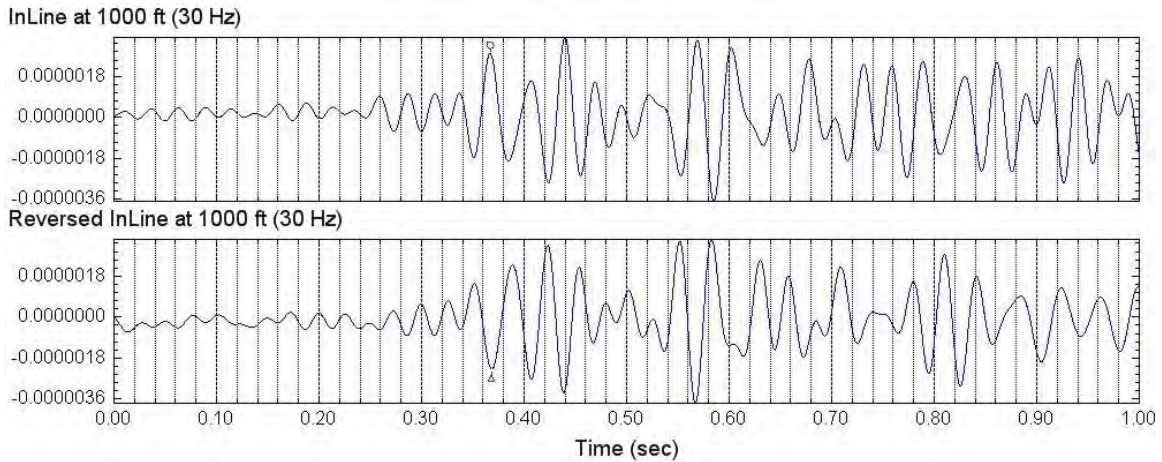


7. Filters and Filtered Signals

Filters were used in processing the averaged unfiltered signals. A filter is a transfer function that can modify magnitudes and phases of the signal. A low-pass filter is a filter that attenuates or removes undesired high frequencies. The filtered signal is then smoother, and the input signal transmitted through the geologic column is easier to identify. Unfiltered signals in the time domain were transformed into the frequency domain using the discrete Fast Fourier Transform (FFT), where a low-pass filter was applied by multiplying filter coefficients with both the real and imaginary parts of the frequency magnitudes to get a modified frequency response. Then the inverse FFT was performed on the modified frequency response to obtain a filtered signal in the time domain. Figure 2.3 is the filtered version of the recorded signal in Figure 2.2.

The exact same filtering was performed on all signals with a given fixed frequency. Therefore, any minor shifting in the time domain due to the filtering was the same for each fixed-frequency signal. As a result, the relative travel times determined herein are unaffected by this filtering. Also, the wave-arrival identification on the filtered waveform is denoted by a symbol added to the waveform (the small circle or triangle at $t \sim 0.37$ sec in Figure 2.3) as discussed below in item "Relative Travel Times".

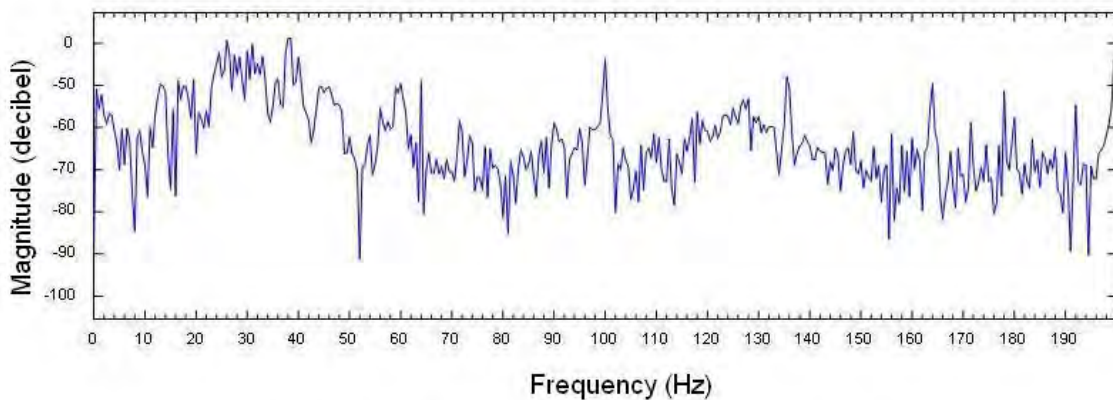
Figure 2.3 Filtered Lower InLine Receiver (S-Wave) Signals
 Input Signal: 4 Cycles of 30-Hz Sine Wave



8. Pass Band or Low Pass

By signal processing convention, the “pass band” of a filter is the band of frequencies that lie within 3 decibels of the peak magnitude. The “stop band” or “reject band” is all other frequencies. The word “band” refers to a frequency range. The frequency corresponding to 3 decibels of the peak value is called the “cut-off” frequency. If a pass band of a filter is the frequency range between zero and the cut-off frequency, it is called a “low pass” filter.

Figure 2.4 Power Spectrum of 30-Hz S-Wave Signal
 Expanded from 0 to 200 Hz



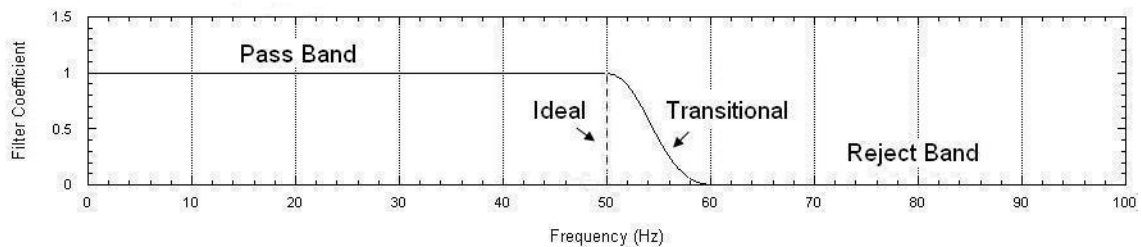
Unfiltered signals are all digital discrete time series, whose frequency domain is also discrete, as shown in Figure 2.4, where the input signal is a 30-Hz sine wave. As demonstrated in the figure, except for the 60-Hz noise, the largest magnitude in the

spectrum is the frequency near 30-Hz. Because the 60-Hz noise and other noise have a significant contribution in the unfiltered signal, they must be filtered or removed to retrieve and view the desired measurement of the 30-Hz input signal.

A discrete filter in the frequency domain, as shown in Figure 2.5, is applicable to these discrete time series. The pass band is 0 to 50 Hz, the reject band is 60 Hz to the Nyquist frequency (not shown), and there is a transitional band between 50 Hz and 60 Hz, which is a cubic spline curve in this work.

A transitional band is preferred if the magnitude of the reject band is not negligible compared with the magnitude of the desired dominant frequency. For example, in Figure 2.4, if the pass band is 0 to 40 Hz, a transitional band of 40 to 60 Hz would make the filtered signal better. If the contribution of the reject band to the spectrum (or energy) is negligible, an ideal filter makes little difference compared to a transitional filter. For example, if the pass band is 0 to 50 Hz, there is no significant difference between a transitional filter and an ideal filter. If there was a general trough (near 52 Hz) following the peak of the signal energy (near 30 Hz), a cut-off frequency (50 Hz) was chosen near the trough, and an ideal filter was used. Otherwise, a transitional filter was used.

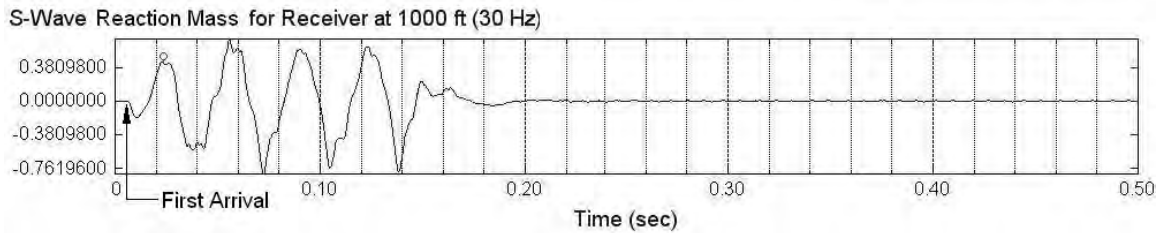
Figure 2.5 Filter Pass Band and Stop Band Coefficient



9. Time Shift

The input signal to the ground, represented by the acceleration of the reaction mass, is not a perfect sine wave, as shown in Figure 2.6. It can be distorted when the initial state of the T-Rex mass is not consistently the same, or the soil below the reaction mass is loaded nonlinearly. Therefore, even if the drive signal is always aligned to zero time, the reaction mass initial response may be shifted from zero time, which is called a time shift.

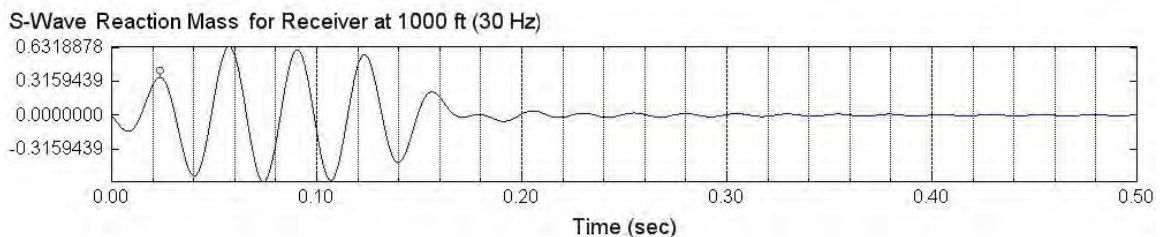
Figure 2.6 Initial Response of the Reaction Mass



In Figure 2.6, the denoted first arrival is the best point for wave-arrival identification. However, it is not reliable because of the nonlinear initial response of the reaction mass, which may produce different first arrival times for reaction mass and receivers even if the drive signals are exactly aligned. This effect is demonstrated by the first cycle right after the first arrival that shows a transient amplitude and frequency.

Figure 2.7 is used to further explain the unreliability of the first arrival or first movement of the reaction mass, and the transient effect on both frequency and magnitude. The filter is a 40-Hz low pass that removed all frequencies higher than 40 Hz. The first arrival point or “first break” in Figure 2.6 no longer exists in Figure 2.7 because it contains transient frequencies that are higher than 30 Hz. On the other hand, the amplitude of the first peak denoted by a small circle is smaller than other peaks, because reaction mass is beginning to move at 30 Hz. This first peak is the correct point to use in evaluating the relative travel time of a 30-Hz S wave.

Figure 2.7 Filtered Initial Response of the Reaction Mass



Further analysis confirmed that different non-causal low pass filters for the 30-Hz signal in Figure 2.6 will shift the first arrival and first trough, but only slightly shift the first peak if the transient state extends to it, while other peaks and troughs that are in steady state stay unchanged and perfectly aligned. The shift of the first arrival is systematically backward (time is less) and stable because the desired 30-Hz signal remains dominant. Steady-state peaks of output signals have no time shift if the input

signals have no time shift. An FFT low-pass filter can do an excellent job in tracking the desired fixed frequencies.

Nevertheless, steady state peaks and troughs are not a perfect reference for wave-arrival identification because of reflected waves and mode conversions that can enter the direct signal and distort the steady-state peaks and troughs.

As a compromise and for convenience, the first-arrival wave identification method is replaced with the first peak or first trough of the waveform for the reaction mass acceleration and other receiver signals. There is little shifting from the steady state of the desired signal frequency (for example 30 Hz), and less interference from reflections and mode conversions.

As an alternative for the non-causal filter, a Butterworth filter may secure the first arrival to be stationary, but it falls short if the frequency of the dominant noise (38-Hz noise in Figure 2.4 has greater magnitude than the desired signal at 30 Hz) is very close to that of the signal. The filtering of the 60-Hz noise from the 50-Hz signal was used in all three boreholes. If the noise can not be significantly attenuated or removed, it will shift not only the first arrival, but also the steady-state peaks and troughs, and the shift is irregular because it is controlled by the noise. The FFT low pass filter, which is non-causal, can remove undesired 60-Hz noise completely and track the desired frequency effectively. Therefore, the FFT low-pass filter was used herein.

10. Relative Travel Times

Relative travel times are the time intervals between the same points on the averaged waveforms of the reaction mass and receivers (lower receiver or reference receiver). The time on each filtered waveform that is used to determine the relative travel time is denoted by a small symbol that has been added to all waveforms. Examples are shown in Figures 2.3 and 2.7 by the small circles or triangles. These points (representing times) are not the wave arrivals but are the same point on the waveform from one measurement depth to the next. These points are called “wave-arrival identifications” herein.

11. Long Lever Arm and Short Lever Arm

The lower borehole geophone from Lawrence Berkeley National Laboratory (LBNL) was fixed to the borehole wall at a depth by rotating the pivoting lever arm that

was attached to the geophone case. As the lever arm rotated outward, the geophone case was pushed into contact with the borehole wall. Two lengths of lever arms were used, the longer one called a long lever arm and the shorter one called a short lever arm. Because of irregularities in the borehole diameter (Gardner and Price 2007), the long lever arm was used to avoid inadequate contact with the borehole wall in regions where washouts may have substantially increased the borehole diameter. Both long and short arms were used at depths 1240 and 1260 ft in Borehole C4993, only the long arm was used for all depths in Borehole C4996.

12. Reference Receiver

The reference receiver is the horizontal receiver that was always fixed at depth of 22 ft in Borehole C4996 while the lower 3-D receiver of LBNL was moved downward along the borehole.

13. Lower Horizontal Receivers: In-Line Receiver and Cross-Line (X-Line) Receiver

The lower horizontal receivers are the two horizontal components of the LBNL 3-D geophone. They are at the deeper depth or lower location than the reference receiver. They are the components in the only 3-D geophone that was moved in the borehole.

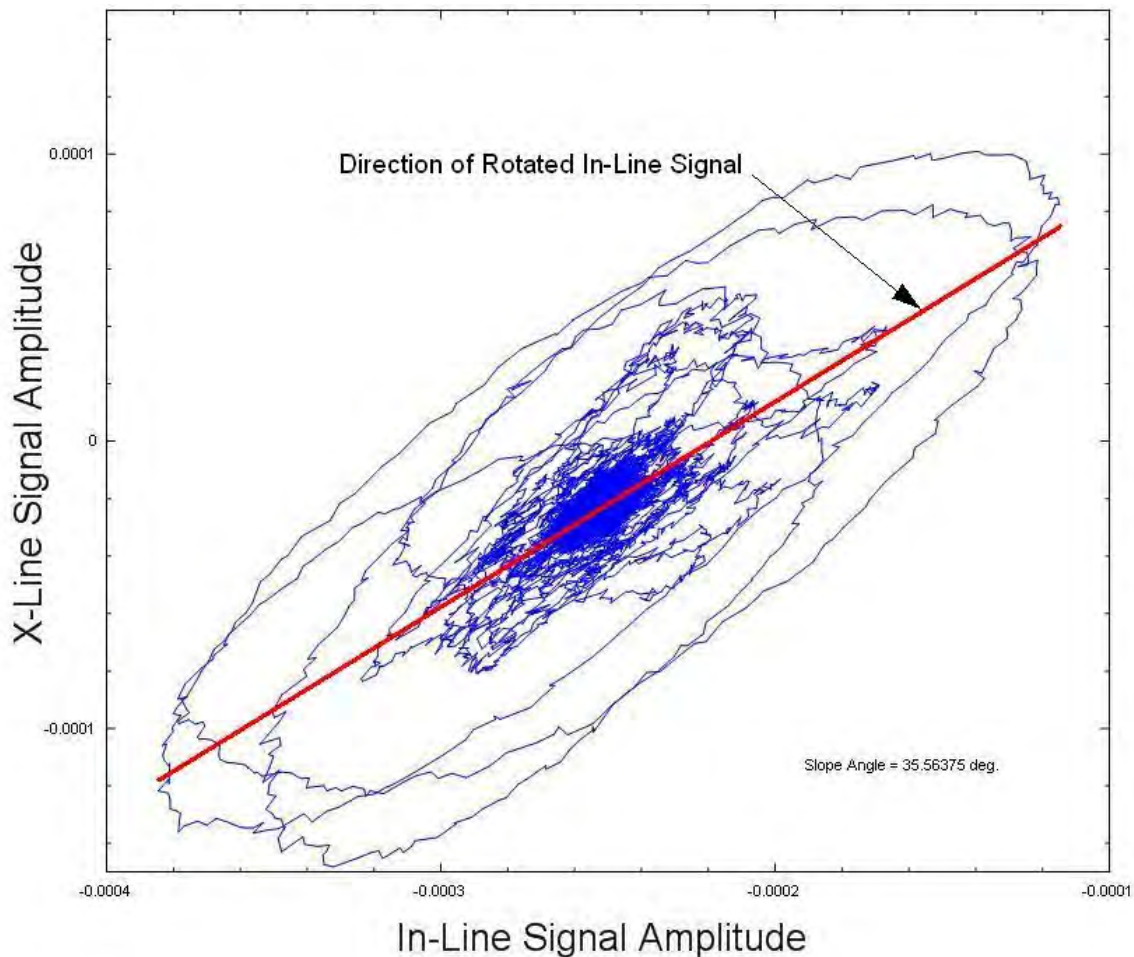
The two horizontal components are perpendicular to each other. One is called in-line receiver, and the other cross-line (x-line) receiver. These receivers were on a wireline and, hence, their orientation could not be controlled while the 3-D geophone was moved along the borehole. Nevertheless, for convenience, the names of “in-line” and “cross-line” were used, though they were actually not related to the direction of motion of the base plate. The signals of the two components were used to obtain the actual in-line signal, which is called rotated in-line signal or rotated in-line receiver herein.

14. Rotated In-Line Receiver

As discussed in the item above, the in-line and cross-line (x-line) receivers in the field are generally not aligned with the T-Rex shaking direction. From the signal records of the in-line and cross-line (x-line) receivers, the shaking orientation can be found by the hodograph as shown in Figure 2.8. The red line represents the statistically strongest motion direction, called the rotated in-line direction. The rotated in-line signal can be composed by combining the directional components of the in-line and cross-line

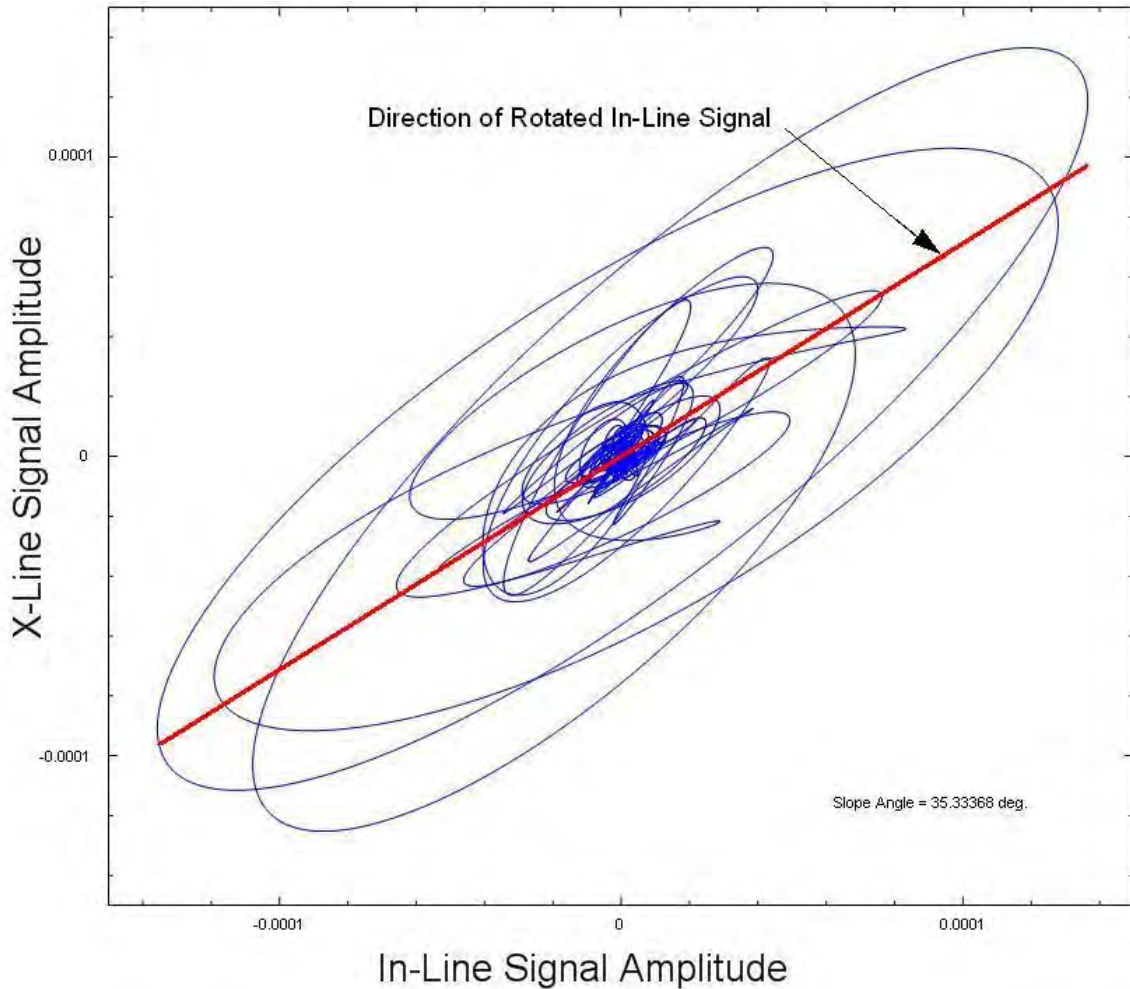
receivers in time. This composition was performed for each waveform record. The resultant waveform is termed the rotated in-line signal. Because the rotated cross-line signal is not our interest, only the rotated in-line signals were used for the relative travel times, and are presented in the subsequent sections.

Figure 2.8 Composition of the Rotated In-line Signal Using the Unfiltered Signals of Both Horizontal Geophones



When the measurements were deep, the strongest motion may be difficult to determine in the unfiltered signals. Reflected, refracted and converted waves can exist in the S-wave records which make the S-wave signal with a fixed frequency and given number of cycles difficult to recover. In this situation, filtered in-line and cross-line (x-line) signals were used to obtain the rotated in-line signal, as shown in Figure 2.9.

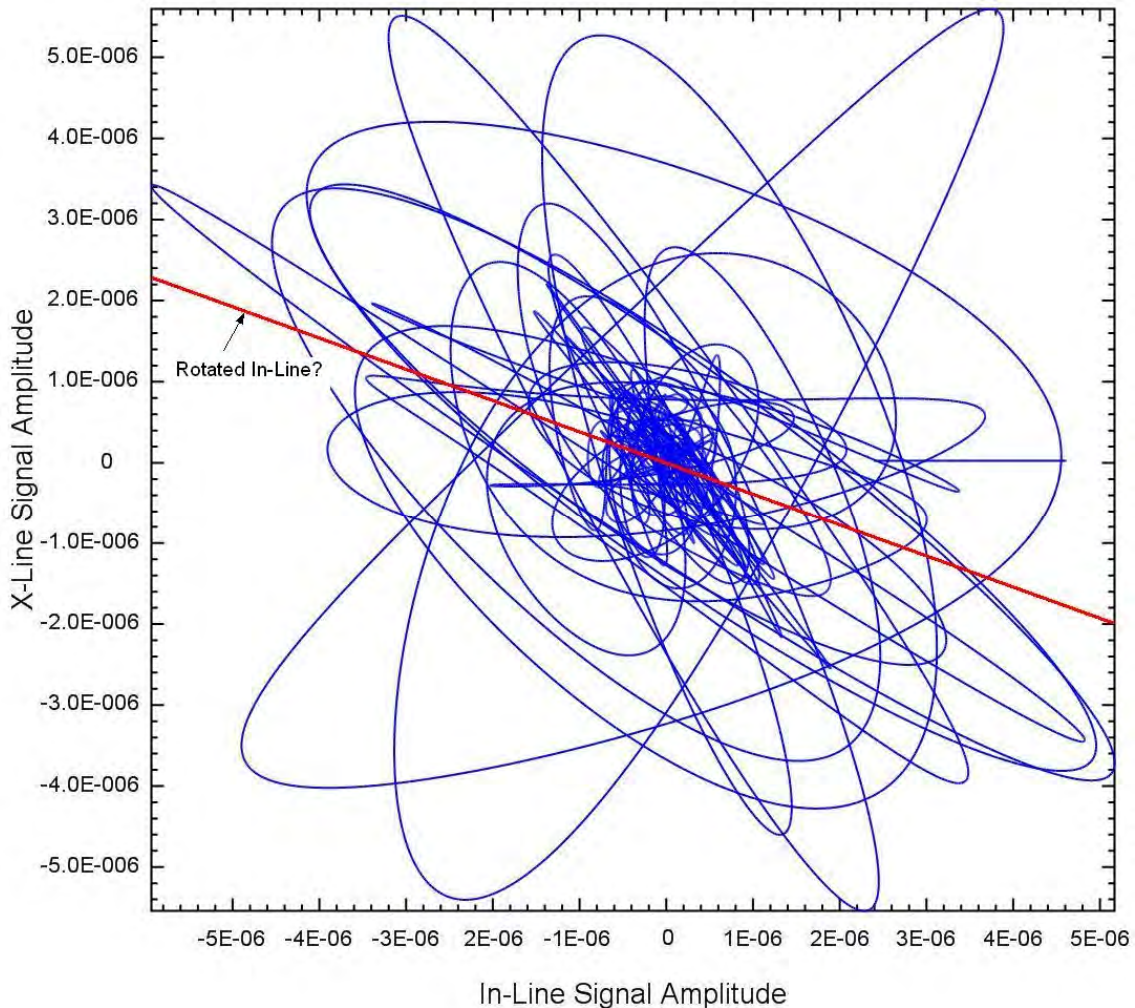
Figure 2.9 Composition of the Rotated In-line Signal Using the Filtered Signals of Both Horizontal Geophones



However, the strongest motion direction is not always available when the desired signal can hardly be detected at significant depths. Figure 2.10 is the hodograph of the filtered in-line and cross-line (x-line) signals at a depth of 1100 ft. Two possible factors can contribute to the loss of the strongest motion. One factor is that the energy of the noise remaining in the filtered signal is rather large compared with the input signal so that the signal-to-remaining-noise ratio becomes smaller and smaller. The other factor is that the P-wave component generated during the S-wave shaking is no longer negligible at depth. When the energy of the derivative vertical P-wave component is of the same magnitude as the horizontal S-wave components, the particle motion is no longer strongest in the horizontal 2-D surface that is parallel to the base plate; rather, it is a 3-D

motion, the projection of which onto the horizontal surface can demonstrate an instantaneous strongest motion in any direction. It is possible that beyond a certain depth, combined with complex layering, only the derivative P-wave survives and determines the strongest motion, which can be vertically oriented.

Figure 2.10 Unreliable Composition of the Rotated In-line Signal Using the Filtered Signals of Both Horizontal Geophones



Even though, based on the statistics, there may exist a relatively stronger horizontal motion for the records as indicated by the red line in Figure 2.10, the horizontal motion can be misleading because the stronger motion may be determined by remaining noise or the derivative P-wave component rather than the desired signal. An

invalid strongest motion direction results in a wrongly interpreted rotated in-line signal, whose phase can be shifted up to 180 degrees. When this case was suspected by an unreasonable trend in the data, waveforms were presented but not picked for travel times.

When the signal condition was between the conditions shown in Figures 2.9 and 2.10, the error in the orientation of the red line (rotated in-line direction) probably increased with depth. Scatter was found in the wave-arrival identification of these signals. However, their waveforms were picked and presented. When the trend in the relative travel times was evident, the shear wave velocity was reported. When only a few waveforms could be interpreted (in a thin layer) the scatter in the relative travel times resulted in a lower confidence level in the shear wave velocity.

Section 3: Vs Profile at Borehole C4996

Section 3 contains the geologic profile, interpreted Vs profile and relative S-wave travel times.

1. Figure 3.1 presents the geologic profile.
2. Figure 3.2 presents all relative S-wave travel times and the interpreted Vs profile at Borehole C4996.
3. Figures 3.3 to 3.5 are the expanded relative S-wave travel times and the interpreted Vs profile at Borehole C4996.
4. Tables 3.1 to 3.9 list the relative S-wave travel times at Borehole C4996, including the times of the wave-arrival identifications for the peaks or troughs of the reaction-mass acceleration, reference receiver and lower rotated receiver signals.

Figure 3.1 General Stratigraphy of Borehole C4996

(Depths source: Barnett et al. 2007; Rohay and Brouns 2007)

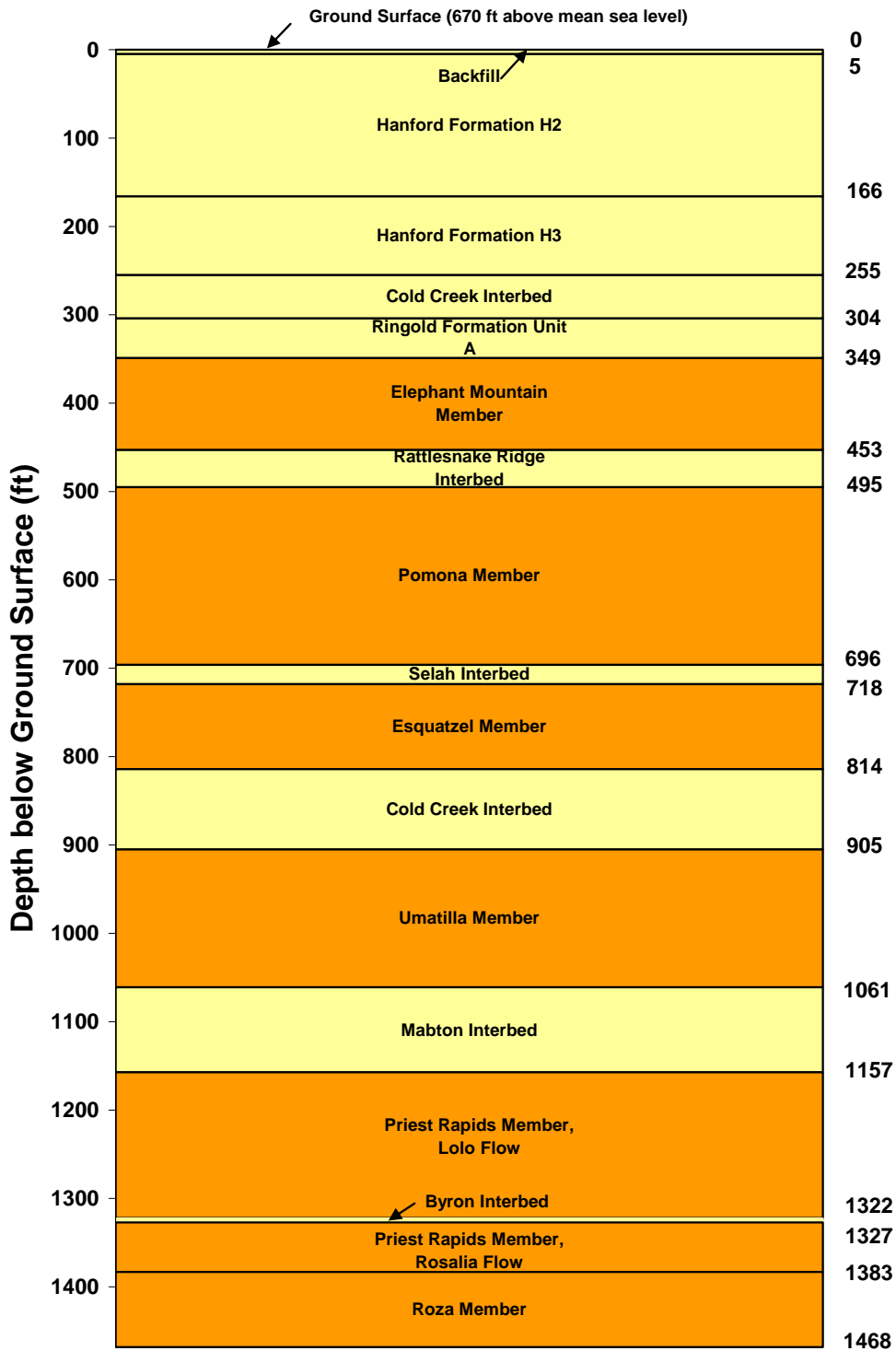


Figure 3.2 Relative S-Wave Travel Times and Interpreted Vs Profile at Borehole C4996

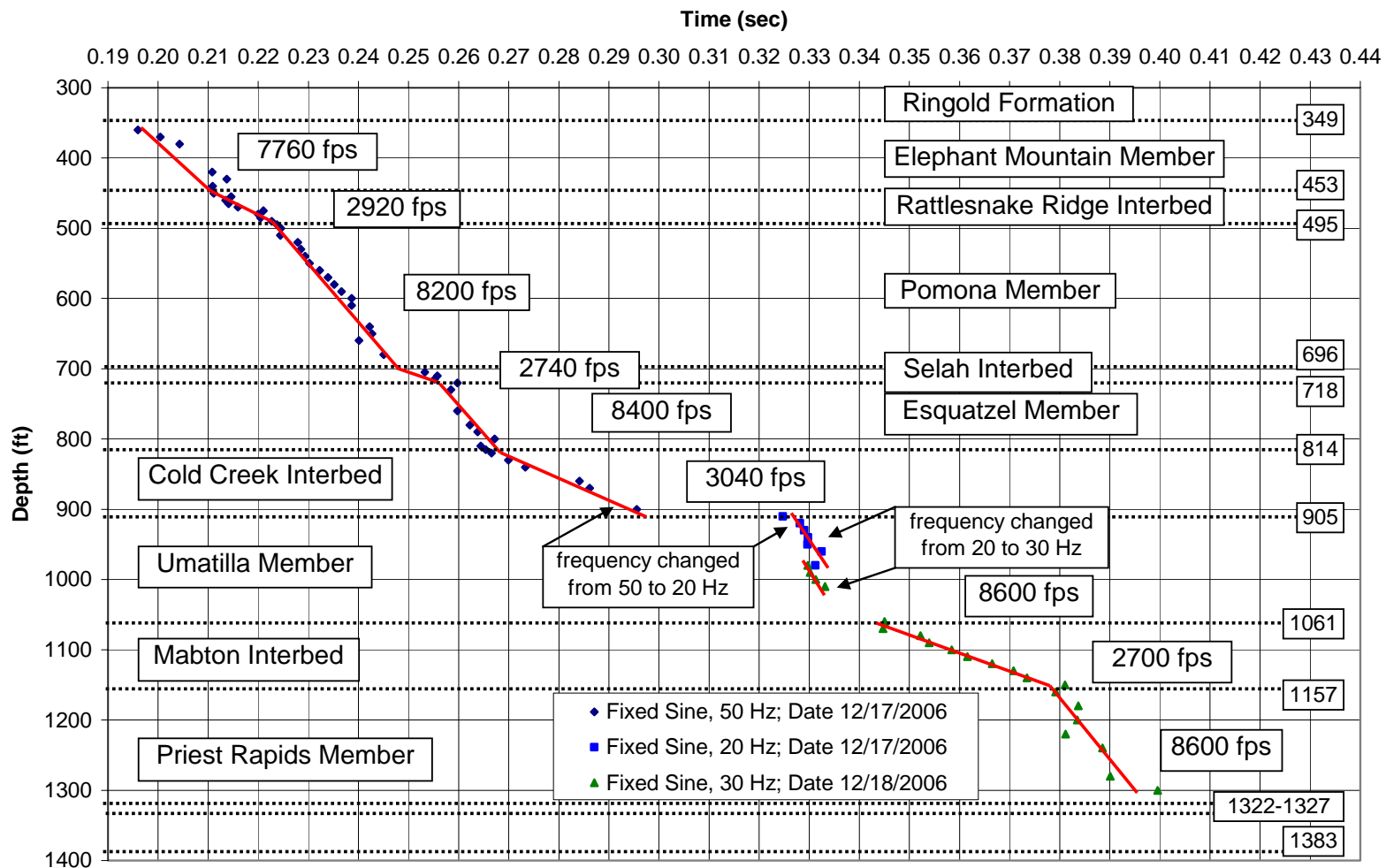


Figure 3.3 Expanded Relative S-Wave Travel Times and Interpreted Vs Profile at Borehole C4996, Depths 300 to 800 ft

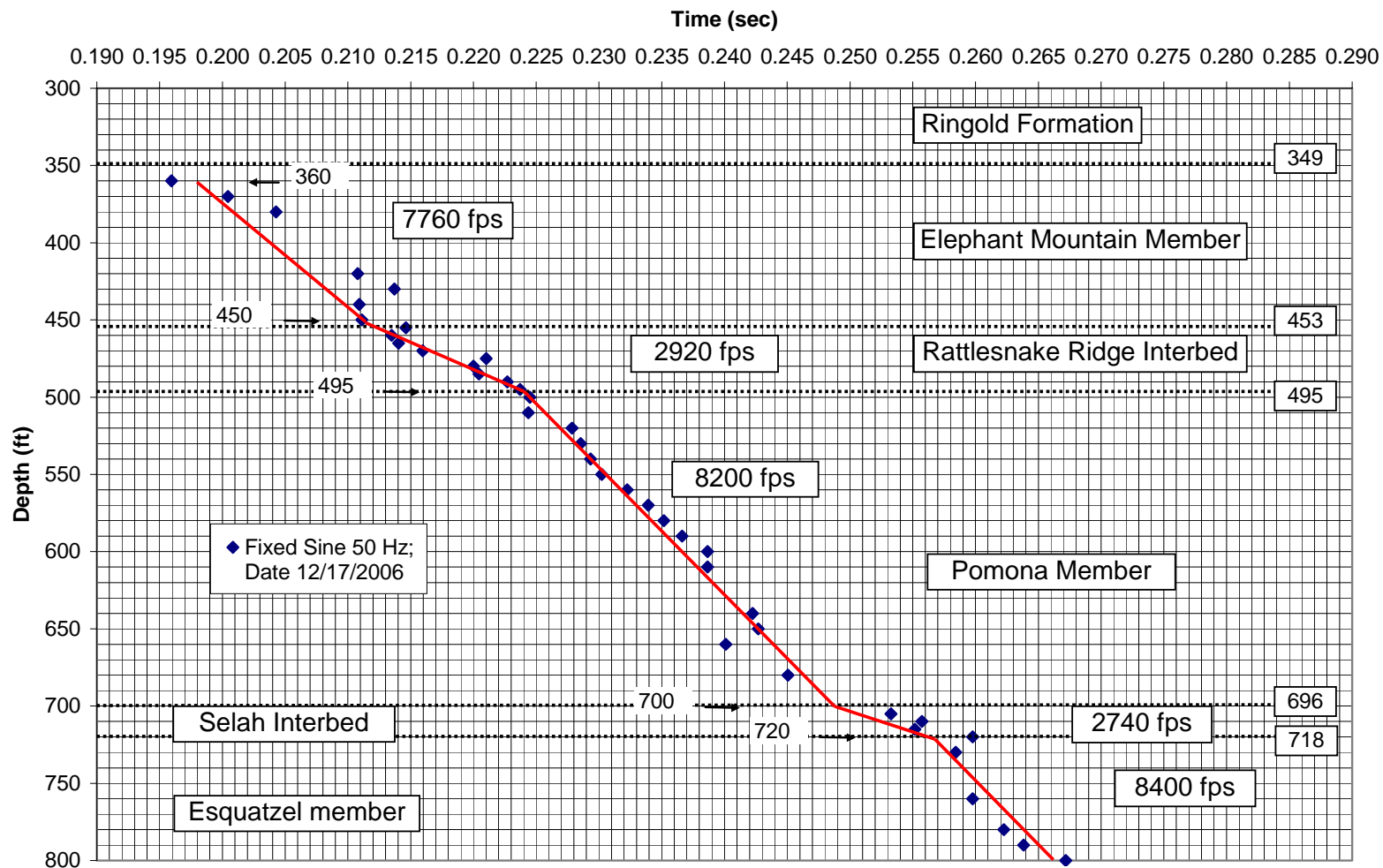


Figure 3.4 Expanded Related S-Wave Travel Times and Interpreted Vs Profile at Borehole C4996, Depths 600 to 1100 ft

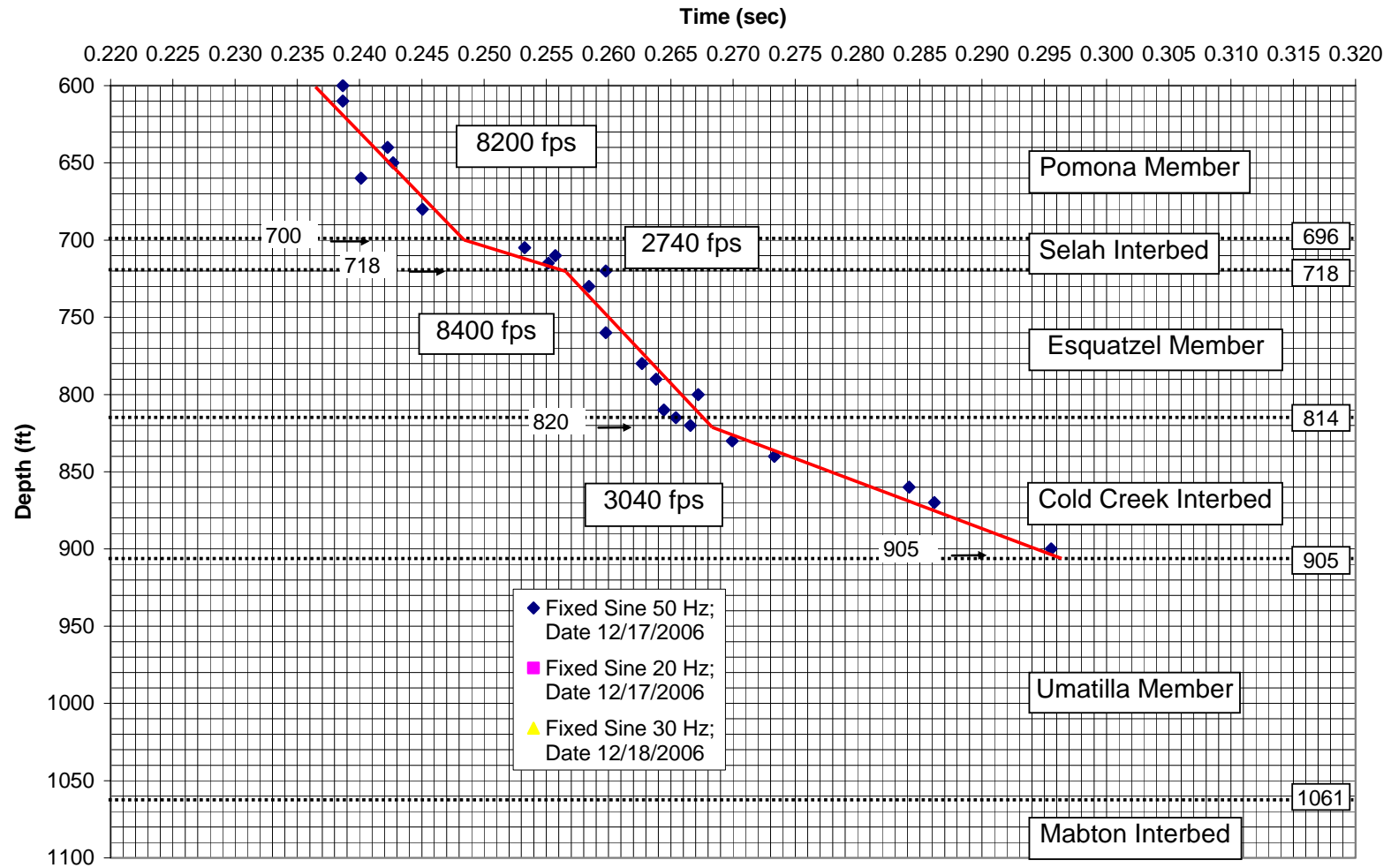


Figure 3.5 Expanded Relative S-Wave Travel Times and Interpreted Vs Profile at Borehole C4996, Depths 900 to 1400 ft

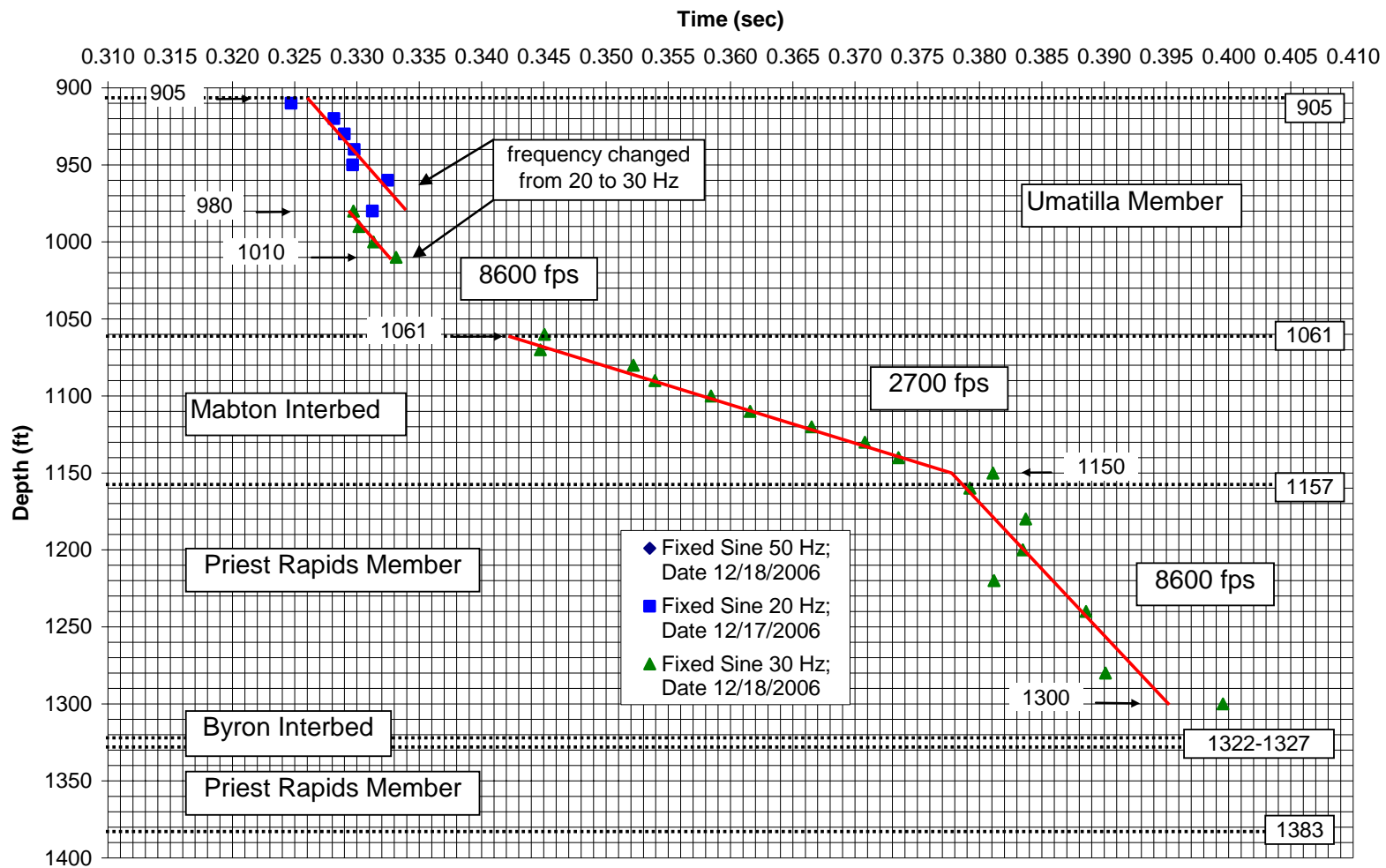


Table 3.1 Relative S-Wave Travel Times at Borehole C4996

Lower Receiver Depth (ft)	Reference Receiver Depth (ft)	T-Rex Drive Freq./ No. of Cycles (Hz/No.)	T-Rex Excitation Direction	Time: Peak or Trough at Reaction Mass (sec)	Time: Peak or Trough at Ref. Receiver (sec)	Time: Peak or Trough at Lower Receiver (sec)	Travel Time Relative to Ref. Receiver (sec)	Travel Time Relative to Reaction Mass (sec)	Average Travel Time * Relative to Reaction Mass (sec)
360	22	50/5	Forward	0.01933	0.06584	0.21461	0.14876	0.19528	0.19596
360	22	50/5	Reversed	0.01933	0.06584	0.21596	0.15011	0.19663	-
370	22	50/5	Forward	0.01933	0.06584	0.22045	0.15461	0.20112	0.20045
370	22	50/5	Reversed	0.01933	0.06584	0.21910	0.15326	0.19978	-
380	22	50/5	Forward	0.01933	0.06584	0.22360	0.15775	0.20427	0.20427
380	22	50/5	Reversed	0.01933	0.06584	0.22360	0.15775	0.20427	-
390	22	50/5	Forward	0.01933	0.06584	**	-	-	-
390	22	50/5	Reversed	0.01933	0.06584	**	-	-	-
400	22	50/5	Forward	0.01933	0.06584	**	-	-	-
400	22	50/5	Reversed	0.01933	0.06584	**	-	-	-
410	22	50/5	Forward	0.01933	0.06584	**	-	-	-
410	22	50/5	Reversed	0.01933	0.06584	**	-	-	-
420	22	50/5	Forward	0.01933	0.06584	0.23034	0.16449	0.21101	0.21079
420	22	50/5	Reversed	0.01933	0.06584	0.22989	0.16404	0.21056	-
430	22	50/5	Forward	0.01933	0.06584	0.23303	0.16719	0.21371	0.21371
430	22	50/5	Reversed	0.01933	0.06584	0.23303	0.16719	0.21371	-
440	22	50/5	Forward	0.01933	0.06584	0.23034	0.16449	0.21101	0.21090
440	22	50/5	Reversed	0.01933	0.06584	0.23011	0.16427	0.21079	-
450	22	50/5	Forward	0.01933	0.06652	0.23034	0.16382	0.21101	0.21112
450	22	50/5	Reversed	0.01933	0.06652	0.23056	0.16404	0.21124	-
455	22	50/5	Forward	0.01933	0.06652	0.23393	0.16742	0.21461	0.21461
455	22	50/5	Reversed	0.01933	0.06652	0.23393	0.16742	0.21461	-
460	22	50/5	Forward	0.01933	0.06652	0.23281	0.16629	0.21348	0.21348
460	22	50/5	Reversed	0.01933	0.06652	0.23281	0.16629	0.21348	-
465	22	50/5	Forward	0.01933	0.06652	0.23326	0.16674	0.21393	0.21404
465	22	50/5	Reversed	0.01933	0.06652	0.23348	0.16697	0.21416	-
470	22	50/5	Forward	0.01933	0.06652	0.23528	0.16876	0.21596	0.21596

* Use of the reaction mass as a reference for calculating relative travel times exhibited less scatter than using the reference receiver.

** Waveform was distorted making arrival time unidentifiable.

Table 3.2 Relative S-Wave Travel Times at Borehole C4996

Lower Receiver Depth (ft)	Reference Receiver Depth (ft)	T-Rex Drive Freq./ No. of Cycles (Hz/No.)	T-Rex Excitation Direction	Time: Peak or Trough at Reaction Mass (sec)	Time: Peak or Trough at Ref. Receiver (sec)	Time: Peak or Trough at Lower Receiver (sec)	Travel Time Relative to Ref. Receiver (sec)	Travel Time Relative to Reaction Mass (sec)	Average Travel Time * Relative to Reaction Mass (sec)
470	22	50/5	Reversed	0.01933	0.06652	0.23528	0.16876	0.21596	-
475	22	50/5	Forward	0.01933	0.06652	0.24067	0.17416	0.22135	0.22101
475	22	50/5	Reversed	0.01933	0.06652	0.24000	0.17348	0.22067	-
480	22	50/5	Forward	0.01933	0.06652	0.23888	0.17236	0.21955	0.22000
480	22	50/5	Reversed	0.01933	0.06652	0.23978	0.17326	0.22045	-
485	22	50/5	Forward	0.01933	0.06652	0.23978	0.17326	0.22045	0.22045
485	22	50/5	Reversed	0.01933	0.06652	0.23978	0.17326	0.22045	-
490	22	50/5	Forward	0.01933	0.06674	0.24292	0.17618	0.22360	0.22270
490	22	50/5	Reversed	0.01933	0.06719	0.24112	0.17393	0.22180	-
495	22	50/5	Forward	0.01933	0.06674	0.24315	0.17640	0.22382	0.22371
495	22	50/5	Reversed	0.01933	0.06719	0.24292	0.17573	0.22360	-
500	22	50/5	Forward	0.01933	0.06674	0.24427	0.17753	0.22494	0.22449
500	22	50/5	Reversed	0.01933	0.06719	0.24337	0.17618	0.22404	-
510	22	50/5	Forward	0.01933	0.06719	0.24360	0.17640	0.22427	0.22438
510	22	50/5	Reversed	0.01933	0.06719	0.24382	0.17663	0.22449	-
520	22	50/5	Forward	0.01933	0.06742	0.24697	0.17955	0.22764	0.22787
520	22	50/5	Reversed	0.01933	0.06764	0.24742	0.17978	0.22809	-
530	22	50/5	Forward	0.01933	0.06742	0.24787	0.18045	0.22854	0.22854
530	22	50/5	Reversed	0.01933	0.06719	0.24787	0.18067	0.22854	-
540	22	50/5	Forward	0.01933	0.06742	0.24876	0.18135	0.22944	0.22933
540	22	50/5	Reversed	0.01933	0.06742	0.24854	0.18112	0.22921	-
550	22	50/5	Forward	0.01933	0.06764	0.24966	0.18202	0.23034	0.23022
550	22	50/5	Reversed	0.01933	0.06809	0.24944	0.18135	0.23011	-
560	22	50/5	Forward	0.01933	0.06764	0.25146	0.18382	0.23213	0.23225
560	22	50/5	Reversed	0.01933	0.06787	0.25169	0.18382	0.23236	-
570	22	50/5	Forward	0.01933	0.06809	0.25371	0.18562	0.23438	0.23393
570	22	50/5	Reversed	0.01933	0.06831	0.25281	0.18449	0.23348	-

* Use of the reaction mass as a reference for calculating relative travel times exhibited less scatter than using the reference receiver.

Table 3.3 Relative S-Wave Travel Times at Borehole C4996

Lower Receiver Depth (ft)	Reference Receiver Depth (ft)	T-Rex Drive Freq./ No. of Cycles (Hz/No.)	T-Rex Excitation Direction	Time: Peak or Trough at Reaction Mass (sec)	Time: Peak or Trough at Ref. Receiver (sec)	Time: Peak or Trough at Lower Receiver (sec)	Travel Time Relative to Ref. Receiver (sec)	Travel Time Relative to Reaction Mass (sec)	Average Travel Time * Relative to Reaction Mass (sec)
580	22	50/5	Forward	0.01933	0.06787	0.25438	0.18652	0.23506	0.23517
580	22	50/5	Reversed	0.01933	0.06831	0.25461	0.18629	0.23528	-
590	22	50/5	Forward	0.01933	0.06809	0.25596	0.18787	0.23663	0.23663
590	22	50/5	Reversed	0.01933	0.06831	0.25596	0.18764	0.23663	-
600	22	50/5	Forward	0.01933	0.06831	0.25775	0.18944	0.23843	0.23865
600	22	50/5	Reversed	0.01933	0.06831	0.25820	0.18989	0.23888	-
610	22	50/5	Forward	0.01933	0.06809	0.25775	0.18966	0.23843	0.23865
610	22	50/5	Reversed	0.01933	0.06831	0.25820	0.18989	0.23888	-
620	22	50/5	Forward	0.01933	0.06809	**	-	-	-
620	22	50/5	Reversed	0.01933	0.06831	**	-	-	-
630	22	50/5	Forward	0.01933	0.06809	**	-	-	-
630	22	50/5	Reversed	0.01933	0.06831	**	-	-	-
640	22	50/5	Forward	0.01933	0.06809	0.26157	0.19348	0.24225	0.24225
640	22	50/5	Reversed	0.01933	0.06831	0.26157	0.19326	0.24225	-
650	22	50/5	Forward	0.01933	0.06809	0.26270	0.19461	0.24337	0.24270
650	22	50/5	Reversed	0.01933	0.06831	0.26135	0.19303	0.24202	-
660	22	50/5	Forward	0.01933	0.06809	0.26022	0.19213	0.24090	0.24011
660	22	50/5	Reversed	0.01933	0.06831	0.25865	0.19034	0.23933	-
670	22	50/5	Forward	0.01933	0.06809	**	-	-	-
670	22	50/5	Reversed	0.01933	0.06831	**	-	-	-
680	22	50/5	Forward	0.01933	0.06809	0.26472	0.19663	0.24539	0.24506
680	22	50/5	Reversed	0.01933	0.06831	0.26405	0.19573	0.24472	-
690	22	50/5	Forward	0.01933	0.06809	**	-	-	-
690	22	50/5	Reversed	0.01933	0.06831	**	-	-	-
700	22	50/5	Forward	0.01933	0.06809	**	-	-	-
700	22	50/5	Reversed	0.01933	0.06831	**	-	-	-

* Use of the reaction mass as a reference for calculating relative travel times exhibited less scatter than using the reference receiver.

** Waveform was distorted making arrival time unidentifiable.

Table 3.4 Relative S-Wave Travel Times at Borehole C4996

Lower Receiver Depth (ft)	Reference Receiver Depth (ft)	T-Rex Drive Freq./ No. of Cycles (Hz/No.)	T-Rex Excitation Direction	Time: Peak or Trough at Reaction Mass (sec)	Time: Peak or Trough at Ref. Receiver (sec)	Time: Peak or Trough at Lower Receiver (sec)	Travel Time Relative to Ref. Receiver (sec)	Travel Time Relative to Reaction Mass (sec)	Average Travel Time * Relative to Reaction Mass (sec)
705	22	50/5	Forward	0.01933	0.06809	0.27258	0.20449	0.25326	0.25326
705	22	50/5	Reversed	0.01933	0.06831	0.27258	0.20427	0.25326	-
710	22	50/5	Forward	0.01933	0.06809	0.27528	0.20719	0.25596	0.25573
710	22	50/5	Reversed	0.01933	0.06831	0.27483	0.20652	0.25551	-
715	22	50/5	Forward	0.01933	0.06809	0.27438	0.20629	0.25506	0.25517
715	22	50/5	Reversed	0.01933	0.06831	0.27461	0.20629	0.25528	-
720	22	50/5	Forward	0.01933	0.06809	0.27933	0.21124	0.26000	0.25978
720	22	50/5	Reversed	0.01933	0.06831	0.27888	0.21056	0.25955	-
730	22	50/5	Forward	0.01933	0.06809	0.27798	0.20989	0.25865	0.25843
730	22	50/5	Reversed	0.01933	0.06831	0.27753	0.20921	0.25820	-
740	22	50/5	Forward	0.01933	0.06809	**	-	-	-
740	22	50/5	Reversed	0.01933	0.06831	**	-	-	-
750	22	50/5	Forward	0.01933	0.06809	**	-	-	-
750	22	50/5	Reversed	0.01933	0.06831	**	-	-	-
760	22	50/5	Forward	0.01933	0.06809	0.27955	0.21146	0.26022	0.25978
760	22	50/5	Reversed	0.01933	0.06831	0.27865	0.21034	0.25933	-
770	22	50/5	Forward	0.01933	0.06809	**	-	-	-
770	22	50/5	Reversed	0.01933	0.06831	**	-	-	-
780	22	50/5	Forward	0.01933	0.06809	0.26180	0.26180	0.26180	0.26225
780	22	50/5	Reversed	0.01933	0.06831	0.28202	0.21371	0.26270	-
790	22	50/5	Forward	0.01933	0.06809	0.28337	0.21528	0.26404	0.26382
790	22	50/5	Reversed	0.01933	0.06876	0.28292	0.21416	0.26360	-
800	22	50/5	Forward	0.01933	0.06921	0.28629	0.21708	0.26697	0.26719
800	22	50/5	Reversed	0.01933	0.06876	0.28674	0.21798	0.26742	-
810	22	50/5	Forward	0.01933	0.06854	0.28382	0.21528	0.26449	0.26444
810	22	50/5	Reversed	0.01933	0.06854	0.28371	0.21517	0.26438	-

* Use of the reaction mass as a reference for calculating relative travel times exhibited less scatter than using the reference receiver.

** Waveform was distorted making arrival time unidentifiable.

Table 3.5 Relative S-Wave Travel Times at Borehole C4996

Lower Receiver Depth (ft)	Reference Receiver Depth (ft)	T-Rex Drive Freq./ No. of Cycles (Hz/No.)	T-Rex Excitation Direction	Time: Peak or Trough at Reaction Mass (sec)	Time: Peak or Trough at Ref. Receiver (sec)	Time: Peak or Trough at Lower Receiver (sec)	Travel Time Relative to Ref. Receiver (sec)	Travel Time Relative to Reaction Mass (sec)	Average Travel Time * Relative to Reaction Mass (sec)
815	22	50/5	Forward	0.01933	0.06876	0.28472	0.21596	0.26539	0.26539
815	22	50/5	Reversed	0.01933	0.06854	0.28472	0.21618	0.26539	-
820	22	50/5	Forward	0.01933	0.06876	0.28607	0.21730	0.26674	0.26657
820	22	50/5	Reversed	0.01933	0.06876	0.28573	0.21697	0.26640	-
830	22	50/5	Forward	0.01933	0.06854	0.28876	0.22022	0.26944	0.26994
830	22	50/5	Reversed	0.01933	0.06876	0.28978	0.22101	0.27045	-
840	22	50/5	Forward	0.01933	0.06854	0.29348	0.22494	0.27416	0.27331
840	22	50/5	Reversed	0.01933	0.06809	0.29180	0.22371	0.27247	-
850	22	50/5	Forward	0.01933	0.06933	**	-	-	-
850	22	50/5	Reversed	0.01933	0.06921	**	-	-	-
860	22	50/5	Forward	0.01933	0.06876	0.30401	0.23525	0.28468	0.28414
860	22	50/5	Reversed	0.01933	0.06876	0.30292	0.23416	0.28360	-
870	22	50/5	Forward	0.01933	0.06876	0.30461	0.23584	0.28528	0.28617
870	22	50/5	Reversed	0.01933	0.06899	0.30639	0.23740	0.28706	-
880	22	50/5	Forward	0.01933	0.06854	**	-	-	-
880	22	50/5	Reversed	0.01933	0.06854	**	-	-	-
890	22	50/5	Forward	0.01933	0.06876	**	-	-	-
890	22	50/5	Reversed	0.01933	0.06876	**	-	-	-
900	22	50/5	Forward	0.01933	0.06831	0.31506	0.24674	0.29573	0.29556
900	22	50/5	Reversed	0.01933	0.06854	0.31472	0.24618	0.29539	-
910	22	50/5	Forward	0.01933	0.06876	**	-	-	-
910	22	50/5	Reversed	0.01933	0.06876	**	-	-	-
920	22	50/5	Forward	0.01933	0.06899	**	-	-	-
920	22	50/5	Reversed	0.01933	0.06921	**	-	-	-
960	22	50/5	Forward	0.01933	0.06899	0.32382	0.25483	0.30449	0.30517
960	22	50/5	Reversed	0.01933	0.06966	0.32517	0.25551	0.30584	-

* Use of the reaction mass as a reference for calculating relative travel times exhibited less scatter than using the reference receiver.

** Waveform was distorted making arrival time unidentifiable.

Table 3.6 Relative S-Wave Travel Times at Borehole C4996

Lower Receiver Depth (ft)	Reference Receiver Depth (ft)	T-Rex Drive Freq./ No. of Cycles (Hz/No.)	T-Rex Excitation Direction	Time: Peak or Trough at Reaction Mass (sec)	Time: Peak or Trough at Ref. Receiver (sec)	Time: Peak or Trough at Lower Receiver (sec)	Travel Time Relative to Ref. Receiver (sec)	Travel Time Relative to Reaction Mass (sec)	Average Travel Time * Relative to Reaction Mass (sec)
910	22	20/4	Forward	0.02876	0.07903	0.35348	0.27445	0.32472	0.32472
910	22	20/4	Reversed	0.02876	0.07910	0.35348	0.27438	0.32472	-
920	22	20/4	Forward	0.02876	0.07976	0.35719	0.27743	0.32843	0.32815
920	22	20/4	Reversed	0.02876	0.07978	0.35663	0.27685	0.32787	-
930	22	20/4	Forward	0.02876	0.07976	0.35753	0.27777	0.32876	0.32899
930	22	20/4	Reversed	0.02876	0.08022	0.35798	0.27775	0.32921	-
940	22	20/4	Forward	0.02876	0.07955	0.35820	0.27865	0.32944	0.32978
940	22	20/4	Reversed	0.02876	0.08000	0.35888	0.27888	0.33011	-
950	22	20/4	Forward	0.02876	0.08000	0.35843	0.27843	0.32966	0.32966
950	22	20/4	Reversed	0.02876	0.08000	0.35843	0.27843	0.32966	-
960	22	20/4	Forward	0.02876	0.07978	**	-	-	0.33247
960	22	20/4	Reversed	0.02876	0.07978	0.36124	0.28146	0.33247	-
970	22	20/4	Forward	0.02876	0.08000	**	-	-	-
970	22	20/4	Reversed	0.02876	0.08022	**	-	-	-
980	22	20/4	Forward	0.02876	0.08000	**	-	-	-
980	22	20/4	Reversed	0.02876	0.07978	**	-	-	-
980	22	20/4	Forward	0.02876	0.07843	0.36022	0.28180	0.33146	0.33124
980	22	20/4	Reversed	0.02876	0.07843	0.35978	0.28135	0.33101	-
980	22	30/4	Forward	0.02427	0.07393	0.35281	0.27888	0.32854	0.32972
980	22	30/4	Reversed	0.02427	0.07393	0.35517	0.28124	0.33090	-
990	22	30/4	Forward	0.02427	0.07393	0.35236	0.27843	0.32809	0.33017
990	22	30/4	Reversed	0.02427	0.07393	0.35652	0.28258	0.33225	-
1000	22	30/4	Forward	0.02427	0.07393	**	-	-	0.33132
1000	22	30/4	Reversed	0.02427	0.07393	0.35559	0.28166	0.33132	-
1010	22	30/4	Forward	0.02427	0.07393	0.35921	0.28528	0.33494	0.33313
1010	22	30/4	Reversed	0.02427	0.07393	0.35559	0.28166	0.33132	-

* Use of the reaction mass as a reference for calculating relative travel times exhibited less scatter than using the reference receiver.

** Waveform was distorted making arrival time unidentifiable.

Table 3.7 Relative S-Wave Travel Times at Borehole C4996

Lower Receiver Depth (ft)	Reference Receiver Depth (ft)	T-Rex Drive Freq./ No. of Cycles (Hz/No.)	T-Rex Excitation Direction	Time: Peak or Trough at Reaction Mass (sec)	Time: Peak or Trough at Ref. Receiver (sec)	Time: Peak or Trough at Lower Receiver (sec)	Travel Time Relative to Ref. Receiver (sec)	Travel Time Relative to Reaction Mass (sec)	Average Travel Time * Relative to Reaction Mass (sec)
1020	22	30/4	Forward	0.02427	0.07393	**	-	-	-
1020	22	30/4	Reversed	0.02427	0.07393	**	-	-	-
1030	22	30/4	Forward	0.02427	0.07393	**	-	-	-
1030	22	30/4	Reversed	0.02427	0.07393	**	-	-	-
1040	22	30/4	Forward	0.02427	0.07393	**	-	-	-
1040	22	30/4	Reversed	0.02427	0.07393	**	-	-	-
1050	22	30/4	Forward	0.02427	0.07393	**	-	-	-
1050	22	30/4	Reversed	0.02427	0.07393	**	-	-	-
1060	22	30/4	Forward	0.02427	0.07393	0.36966	0.29573	0.34539	0.34506
1060	22	30/4	Reversed	0.02427	0.07393	0.36899	0.29506	0.34472	-
1070	22	30/4	Forward	0.02427	0.07393	0.36809	0.29416	0.34382	0.34472
1070	22	30/4	Reversed	0.02427	0.07393	0.36989	0.29596	0.34562	-
1080	22	30/4	Forward	0.02427	0.07393	0.37483	0.30090	0.35056	0.35219
1080	22	30/4	Reversed	0.02427	0.07393	0.37809	0.30416	0.35382	-
1090	22	30/4	Forward	0.02427	0.07393	0.37730	0.30337	0.35303	0.35393
1090	22	30/4	Reversed	0.02427	0.07393	0.37910	0.30517	0.35483	-
1100	22	30/4	Forward	0.02427	0.07393	0.38225	0.30831	0.35798	0.35843
1100	22	30/4	Reversed	0.02427	0.07393	0.38315	0.30921	0.35888	-
1110	22	30/4	Forward	0.02427	0.07393	0.38539	0.31146	0.36112	0.36157
1110	22	30/4	Reversed	0.02427	0.07393	0.38629	0.31236	0.36202	-
1120	22	30/4	Forward	0.02427	0.07393	0.39079	0.31685	0.36652	0.36652
1120	22	30/4	Reversed	0.02427	0.07393	0.39079	0.31685	0.36652	-
1130	22	30/4	Forward	0.02427	0.07393	0.39483	0.32090	0.37056	0.37079
1130	22	30/4	Reversed	0.02427	0.07393	0.39528	0.32135	0.37101	-

* Use of the reaction mass as a reference for calculating relative travel times exhibited less scatter than using the reference receiver.

** Waveform was distorted making arrival time unidentifiable.

Table 3.8 Relative S-Wave Travel Times at Borehole C4996

Lower Receiver Depth (ft)	Reference Receiver Depth (ft)	T-Rex Drive Freq./ No. of Cycles (Hz/No.)	T-Rex Excitation Direction	Time: Peak or Trough at Reaction Mass (sec)	Time: Peak or Trough at Ref. Receiver (sec)	Time: Peak or Trough at Lower Receiver (sec)	Travel Time Relative to Ref. Receiver (sec)	Travel Time Relative to Reaction Mass (sec)	Average Travel Time * Relative to Reaction Mass (sec)
1140	22	30/4	Forward	0.02427	0.07393	0.39753	0.32360	0.37326	0.37348
1140	22	30/4	Reversed	0.02427	0.07393	0.39798	0.32404	0.37371	-
1150	22	30/4	Forward	0.02427	0.07393	0.40461	0.33068	0.38034	0.38107
1150	22	30/4	Reversed	0.02427	0.07393	0.40607	0.33213	0.38180	-
1160	22	30/4	Forward	0.02427	0.07393	0.40405	0.33011	0.37978	0.37921
1160	22	30/4	Reversed	0.02427	0.07393	0.40292	0.32899	0.37865	-
1170	22	30/4	Forward	0.02427	0.07393	**	-	-	-
1170	22	30/4	Reversed	0.02427	0.07393	**	-	-	-
1180	22	30/4	Forward	0.02427	0.07393	0.40652	0.33258	0.38225	0.38371
1180	22	30/4	Reversed	0.02427	0.07393	0.40944	0.33551	0.38517	-
1200	22	30/4	Forward	0.02427	0.07393	0.40899	0.33506	0.38472	0.38348
1200	22	30/4	Reversed	0.02427	0.07393	0.40652	0.33258	0.38225	-
1220	22	30/4	Forward	0.02427	0.07393	0.40410	0.33017	0.37983	0.38115
1220	22	30/4	Reversed	0.02427	0.07393	0.40674	0.33281	0.38247	-
1240	22	30/4	Forward	0.02427	0.07393	0.41281	0.33888	0.38854	0.38506
1240	22	30/4	Reversed	0.02427	0.07393	0.40584	0.33191	0.38157	-
1260	22	30/4	Forward	0.02427	0.07393	**	-	-	-
1260	22	30/4	Reversed	0.02427	0.07393	**	-	-	-
1280	22	30/4	Forward	0.02427	0.07393	0.41438	0.34045	0.39011	0.39011
1280	22	30/4	Reversed	0.02427	0.07393	**	-	-	-
1300	22	30/4	Forward	0.02427	0.07393	**	-	-	0.39955
1300	22	30/4	Reversed	0.02427	0.07393	0.42382	0.34989	0.39955	-

* Use of the reaction mass as a reference for calculating relative travel times exhibited less scatter than using the reference receiver.

** Waveform was distorted making arrival time unidentifiable.

Section 4: Unfiltered S-Wave Records of Lower Horizontal Receiver and Derived Rotated In-Line Signals

Section 4 includes all unfiltered S-wave records at the lower horizontal receiver and signals of rotated in-line receiver. There are 6 groups: forward in-line, reversed in-line; forward cross-line (x-line), reversed cross-line (x-line); forward rotated in-line and reversed rotated in-line.

4.1 Forward S-wave records of the lower in-line receiver.

1. Figures 4.1.1 to 4.1.6 present unfiltered lower in-line receiver (forward S-wave) records in Borehole C4996, depths 360 to 960 ft; input signal: 5 cycles of 50-Hz sine wave.
2. Figure 4.1.7 presents unfiltered lower in-line receiver (forward S-wave) signals in Borehole C4996, depths 910 to 980 ft; input signal: 4 cycles of 20-Hz sine wave.
3. Figures 4.1.8 to 4.1.10 present unfiltered lower in-line receiver (forward S-wave) signals in Borehole C4996, depths 980 to 1300 ft; input signal: 4 cycles of 30-Hz sine wave.

4.2 Reversed S-wave records of the lower in-line receiver.

1. Figures 4.2.1 to 4.2.6 present unfiltered lower in-line receiver (reversed S-wave) records in Borehole C4996, depths 360 to 960 ft; input signal: 5 cycles of 50-Hz sine wave.
2. Figure 4.2.7 presents unfiltered lower in-line receiver (reversed S-wave) signals in Borehole C4996, depths 910 to 980 ft; input signal: 4 cycles of 20-Hz sine wave.
3. Figures 4.2.8 to 4.2.10 present unfiltered lower in-line receiver (reversed S-wave) signals in Borehole C4996, depths 980 to 1300 ft; input signal: 4 cycles of 30-Hz sine wave.

- 4.3 Forward S-wave records of the lower cross-line receiver.
1. Figures 4.3.1 to 4.3.6 present unfiltered lower cross-line receiver (forward S-wave) records in Borehole C4996, depths 360 to 960 ft; input signal: 5 cycles of 50-Hz sine wave.
 2. Figure 4.3.7 presents unfiltered lower cross-line receiver (forward S-wave) signals in Borehole C4996, depths 910 to 980 ft; input signal: 4 cycles of 20-Hz sine wave.
 3. Figures 4.3.8 to 4.3.10 present unfiltered lower cross-line receiver (forward S-wave) signals in Borehole C4996, depths 980 to 1300 ft; input signal: 4 cycles of 30-Hz sine wave.
- 4.4 Reversed S-wave records of the lower cross-line receiver.
1. Figures 4.4.1 to 4.4.6 present unfiltered lower cross-line receiver (reversed S-wave) records in Borehole C4996, depths 360 to 960 ft; input signal: 5 cycles of 50-Hz sine wave.
 2. Figure 4.4.7 presents unfiltered lower cross-line receiver (reversed S-wave) signals in Borehole C4996, depths 910 to 980 ft; input signal: 4 cycles of 20-Hz sine wave.
 3. Figures 4.4.8 to 4.4.10 present unfiltered lower cross-line receiver (reversed S-wave) signals in Borehole C4996, depths 980 to 1300 ft; input signal: 4 cycles of 30-Hz sine wave.
- 4.5 Forward S-wave signals of the lower rotated in-line receiver.
1. Figures 4.5.1 to 4.5.6 present unfiltered lower rotated in-line receiver (forward S-wave) records in Borehole C4996, depths 360 to 960 ft; input signal: 5 cycles of 50-Hz sine wave.
 2. Figure 4.5.7 presents unfiltered lower rotated in-line receiver (forward S-wave) signals in Borehole C4996, depths 910 to 980 ft; input signal: 4 cycles of 20-Hz sine wave.
 3. Figures 4.5.8 to 4.5.10 present unfiltered lower rotated in-line receiver (forward S-wave) signals in Borehole C4996, depths 980 to 1300 ft; input signal: 4 cycles of 30-Hz sine wave.

- 4.6 Reversed S-wave signals of the lower rotated in-line receiver.
1. Figures 4.6.1 to 4.6.6 present unfiltered lower rotated in-line receiver (reversed S-wave) records in Borehole C4996, depths 360 to 960 ft; input signal: 5 cycles of 50-Hz sine wave.
 2. Figure 4.6.7 presents unfiltered lower rotated in-line receiver (reversed S-wave) signals in Borehole C4996, depths 910 to 980 ft; input signal: 4 cycles of 20-Hz sine wave.
 3. Figures 4.6.8 to 4.6.10 present unfiltered lower rotated in-line receiver (reversed S-wave) signals in Borehole C4996, depths 980 to 1300 ft; input signal: 4 cycles of 30-Hz sine wave.

Figure 4.1.1 Unfiltered Forward S-Wave Signals of Lower In-Line Receiver (C4996)
Depths 360 to 455 ft; Input Signal: 5 Cycles of 50-Hz Sine Wave

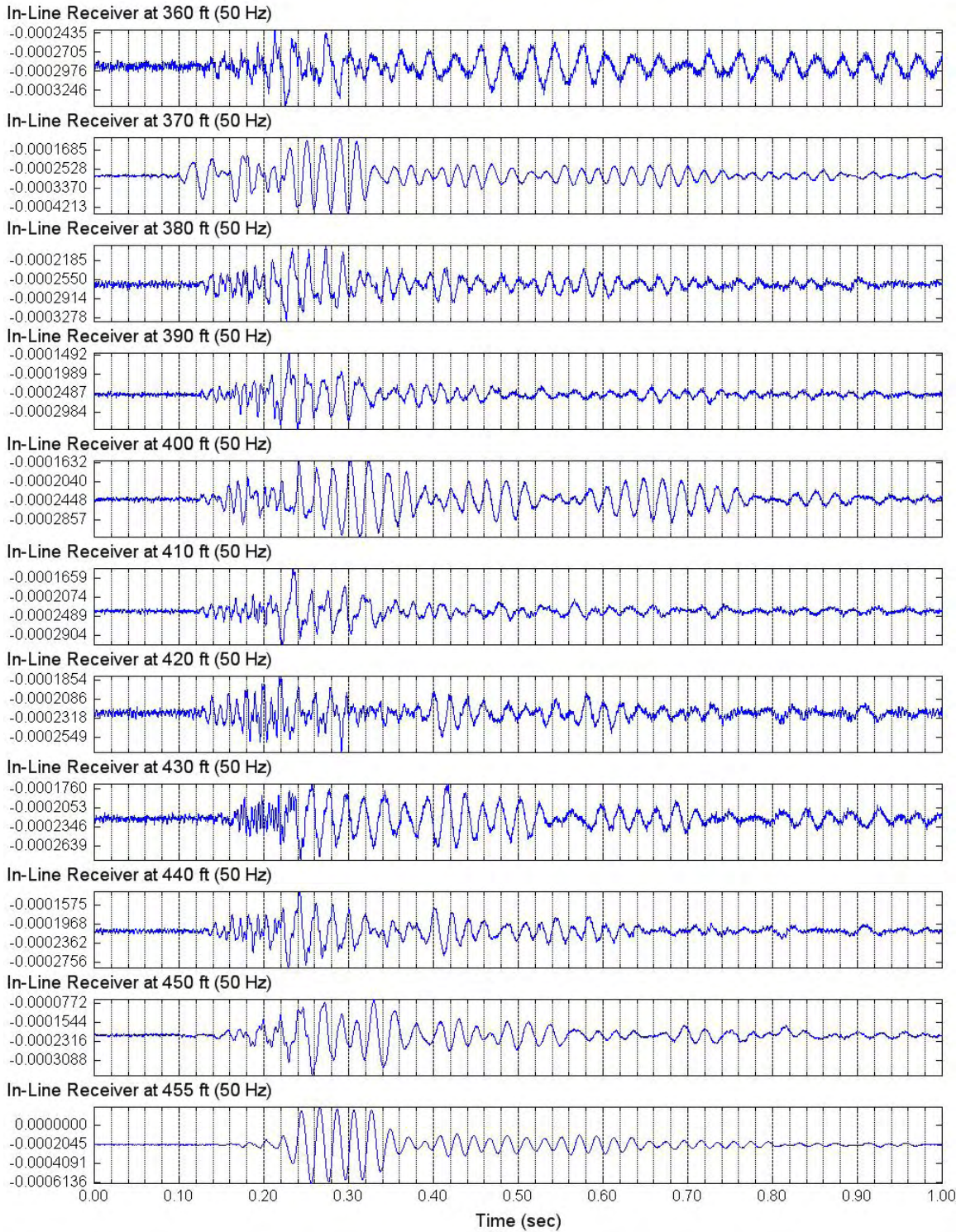


Figure 4.1.2 Unfiltered Forward S-Wave Signals of Lower In-Line Receiver (C4996)
Depths 460 to 520 ft; Input Signal: 5 Cycles of 50-Hz Sine Wave

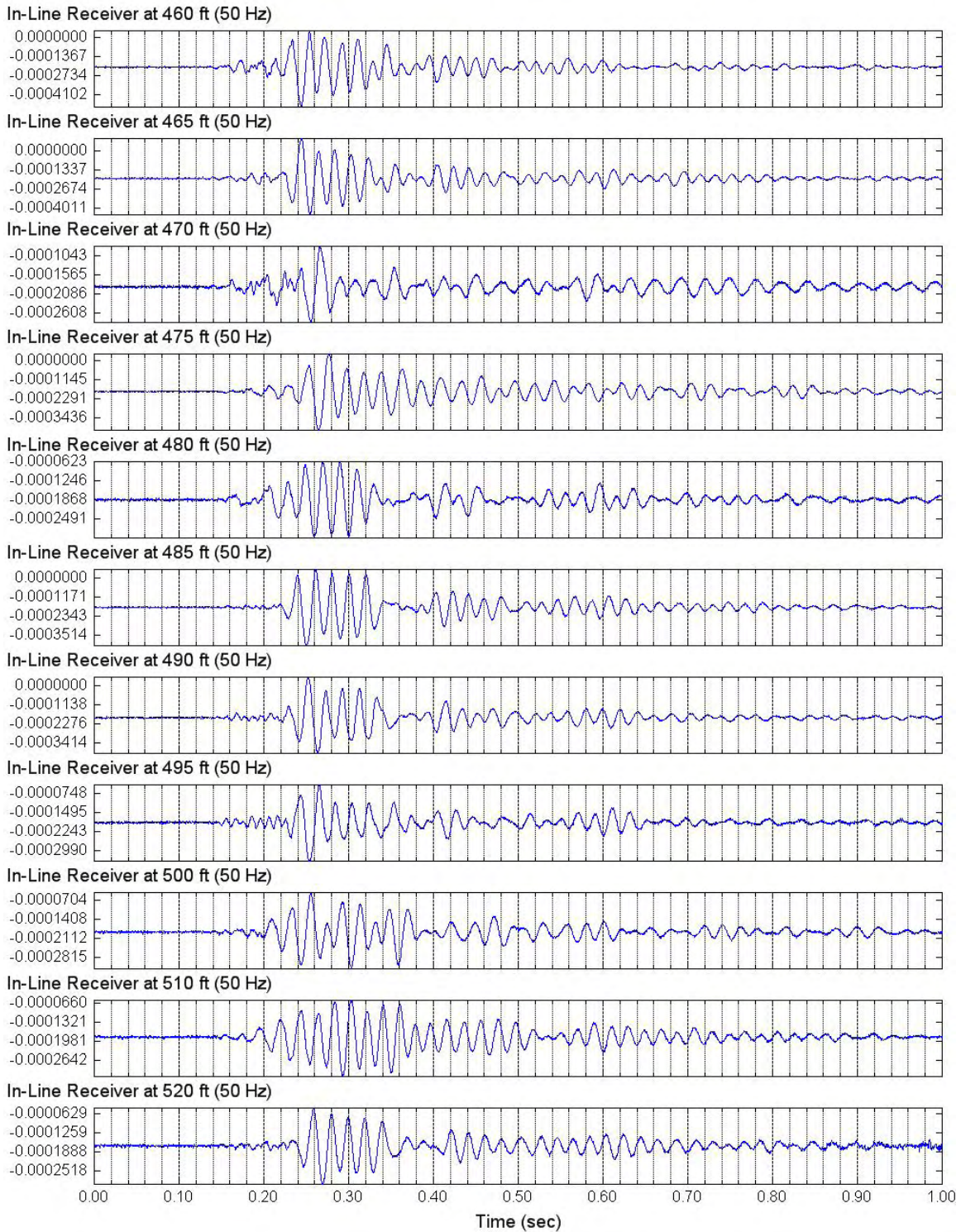


Figure 4.1.3 Unfiltered Forward S-Wave Signals of Lower In-Line Receiver (C4996)
Depths 530 to 630 ft; Input Signal: 5 Cycles of 50-Hz Sine Wave

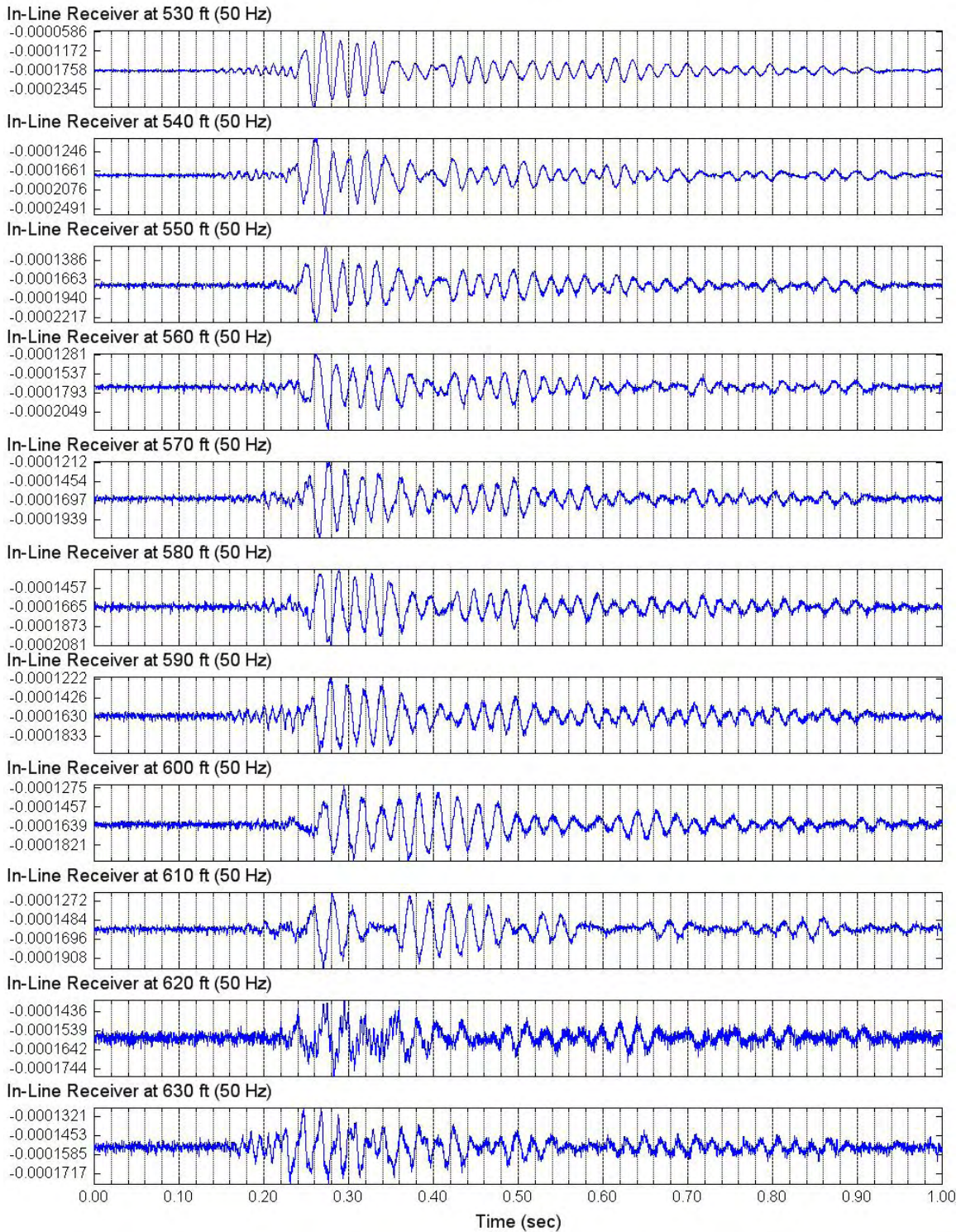


Figure 4.1.4 Unfiltered Forward S-Wave Signals of Lower In-Line Receiver (C4996)
 Depths 640 to 720 ft; Input Signal: 5 Cycles of 50-Hz Sine Wave

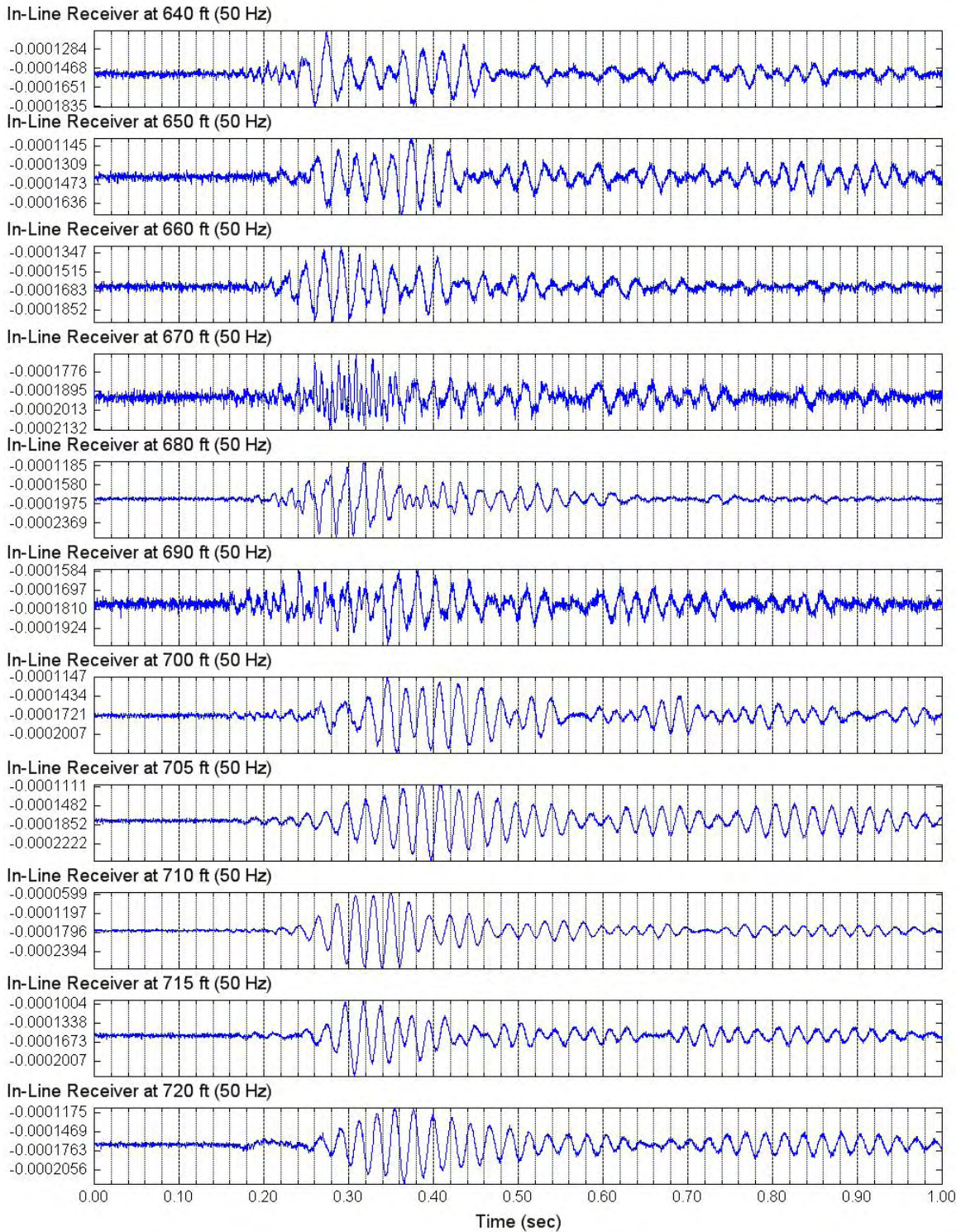


Figure 4.1.5 Unfiltered Forward S-Wave Signals of Lower In-Line Receiver (C4996)
Depths 730 to 820 ft; Input Signal: 5 Cycles of 50-Hz Sine Wave

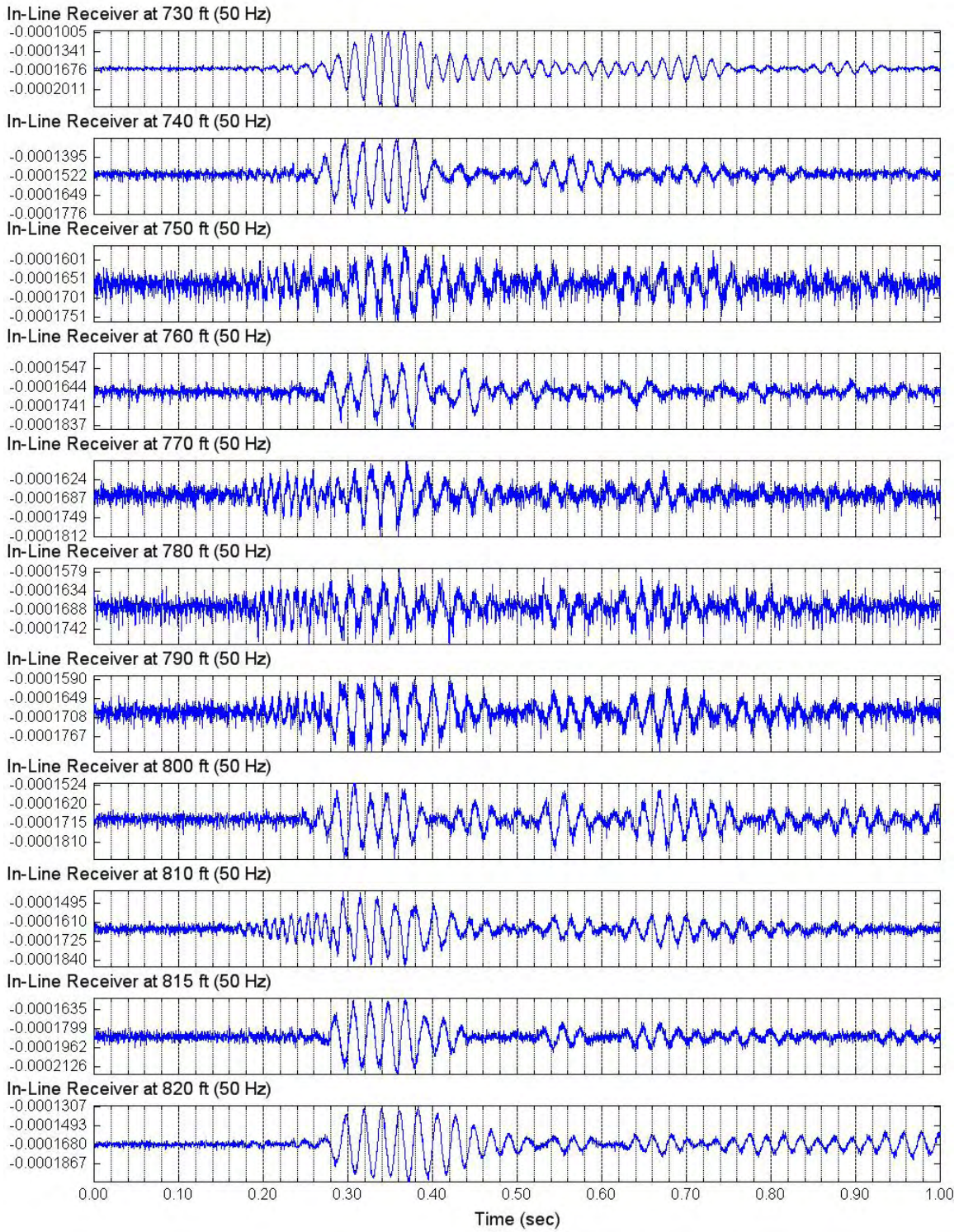


Figure 4.1.6 Unfiltered Forward S-Wave Signals of Lower In-Line Receiver (C4996)
Depths 830 to 960 ft; Input Signal: 5 Cycles of 50-Hz Sine Wave

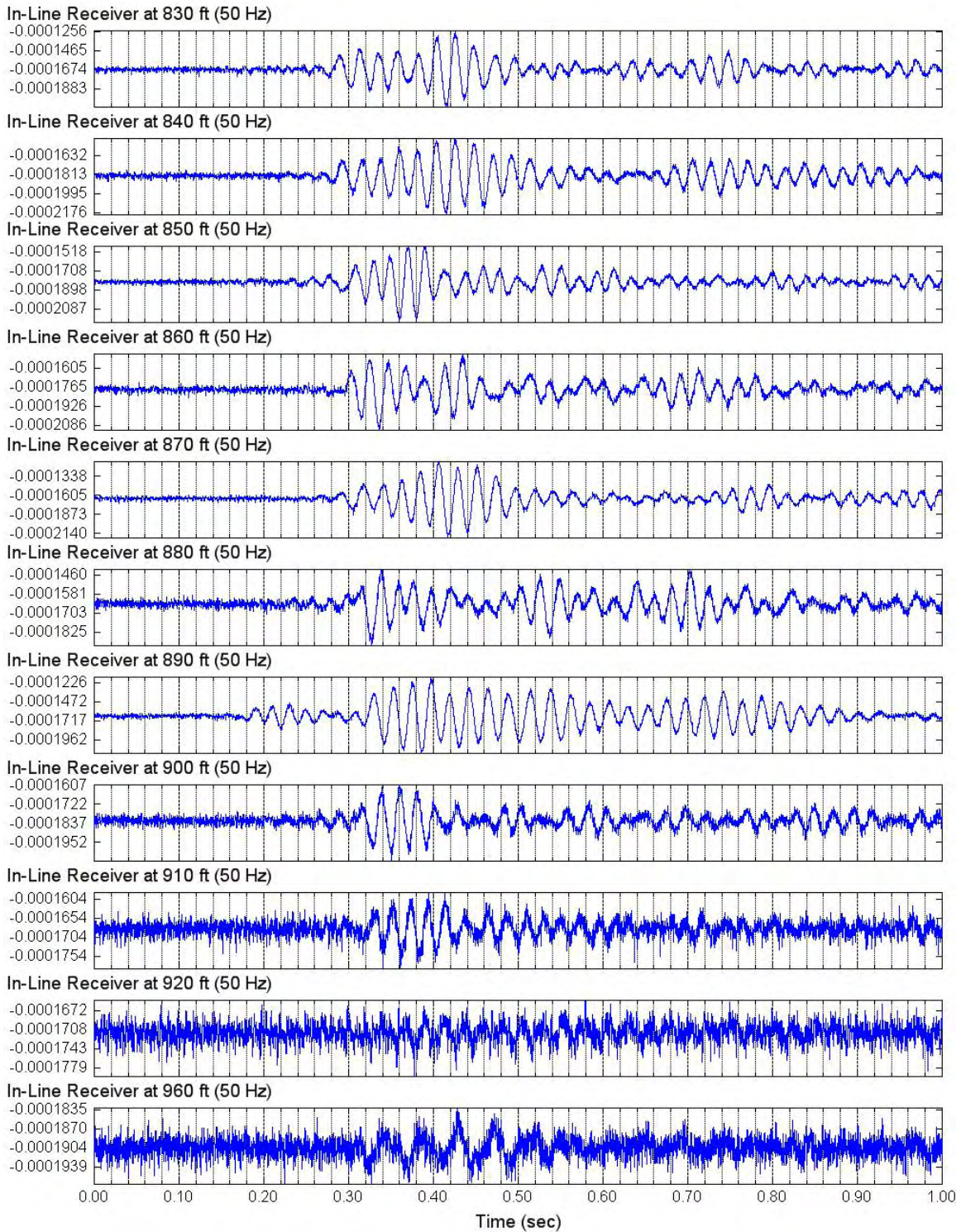


Figure 4.1.7 Unfiltered Forward S-Wave Signals of Lower In-Line Receiver (C4996)
Depths 910 to 980 ft; Input Signal: 4 Cycles of 20-Hz Sine Wave

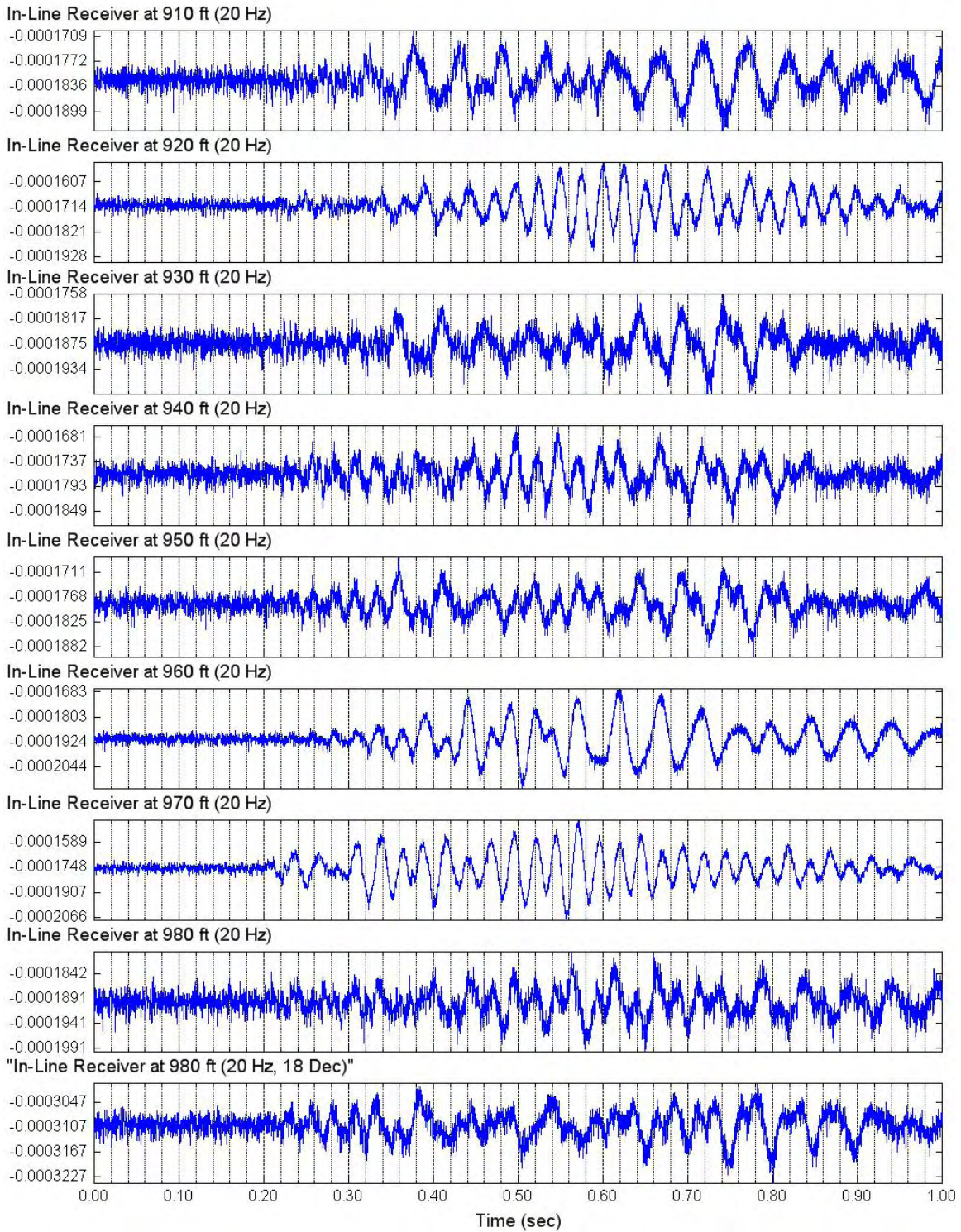


Figure 4.1.8 Unfiltered Forward S-Wave Signals of Lower In-Line Receiver (C4996)
Depths 980 to 1060 ft; Input Signal: 4 Cycles of 30-Hz Sine Wave

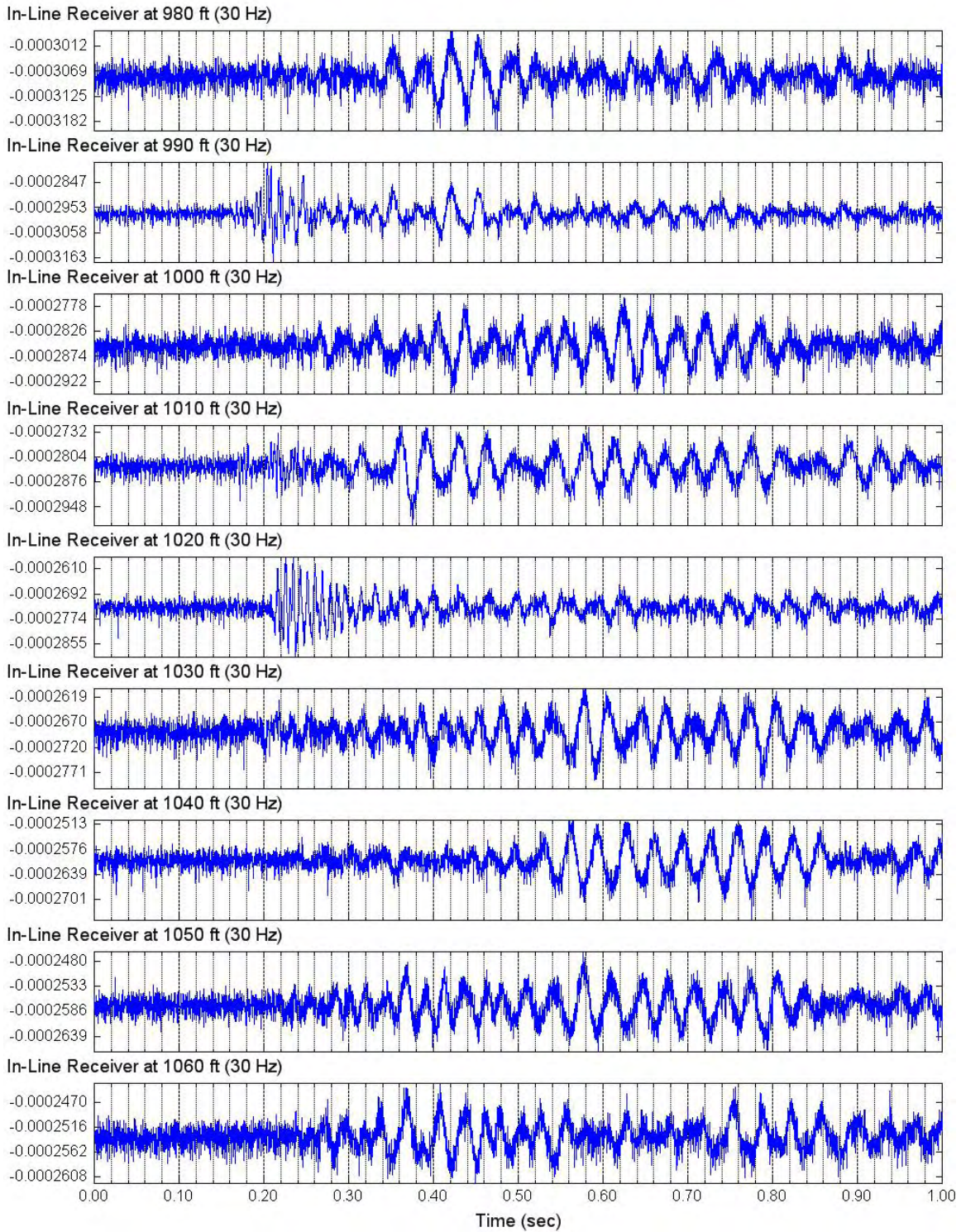


Figure 4.1.9 Unfiltered Forward S-Wave Signals of Lower In-Line Receiver (C4996)
Depths 1070 to 1150 ft; Input Signal: 4 Cycles of 30-Hz Sine Wave

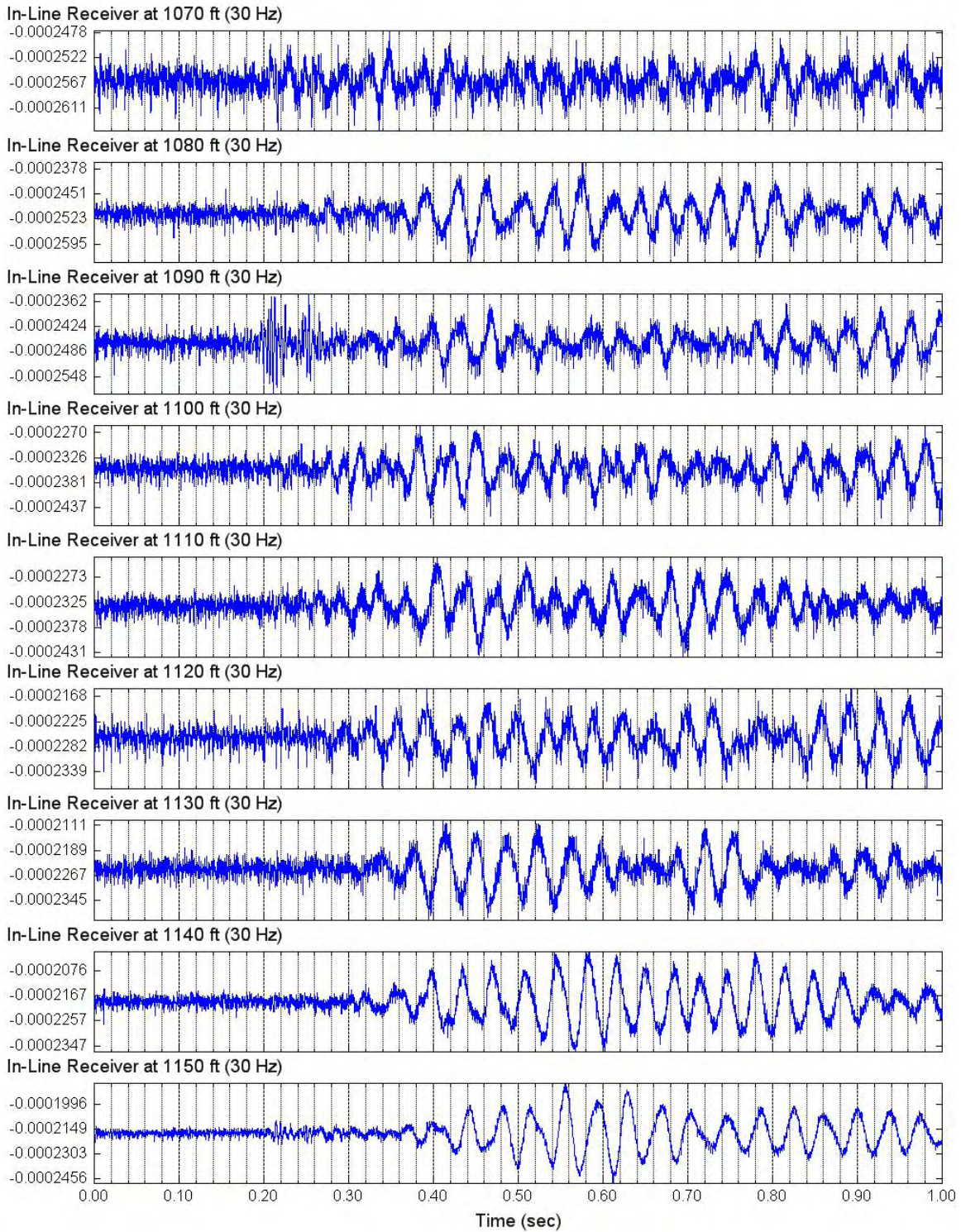


Figure 4.1.10 Unfiltered Forward S-Wave Signals of Lower In-Line Receiver (C4996)
Depths 1160 to 1300 ft; Input Signal: 4 Cycles of 30-Hz Sine Wave

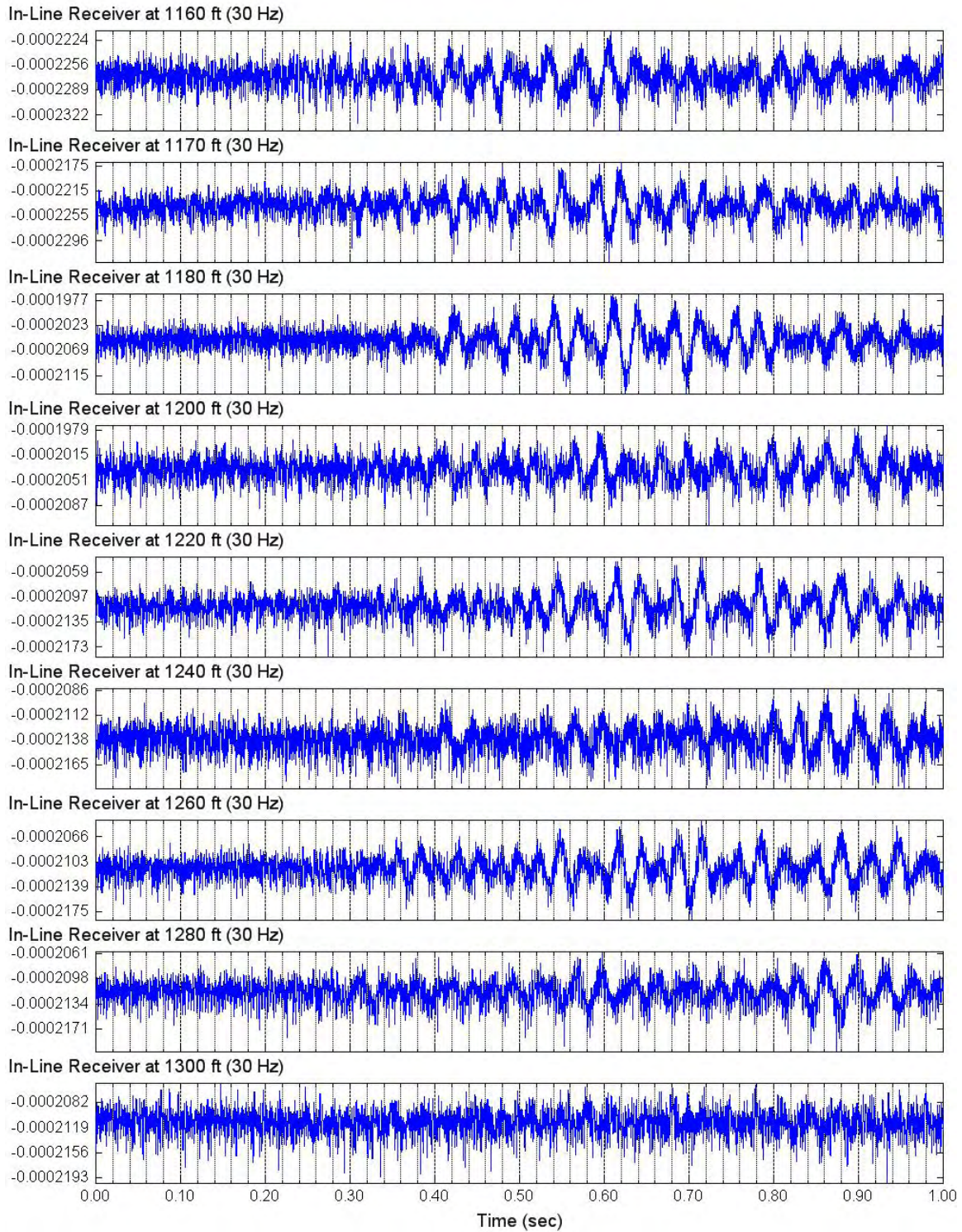


Figure 4.2.1 Unfiltered Reverse S-Wave Signals of Lower In-Line Receiver (C4996)
Depths 360 to 455 ft; Input Signal: 5 Cycles of 50-Hz Sine Wave

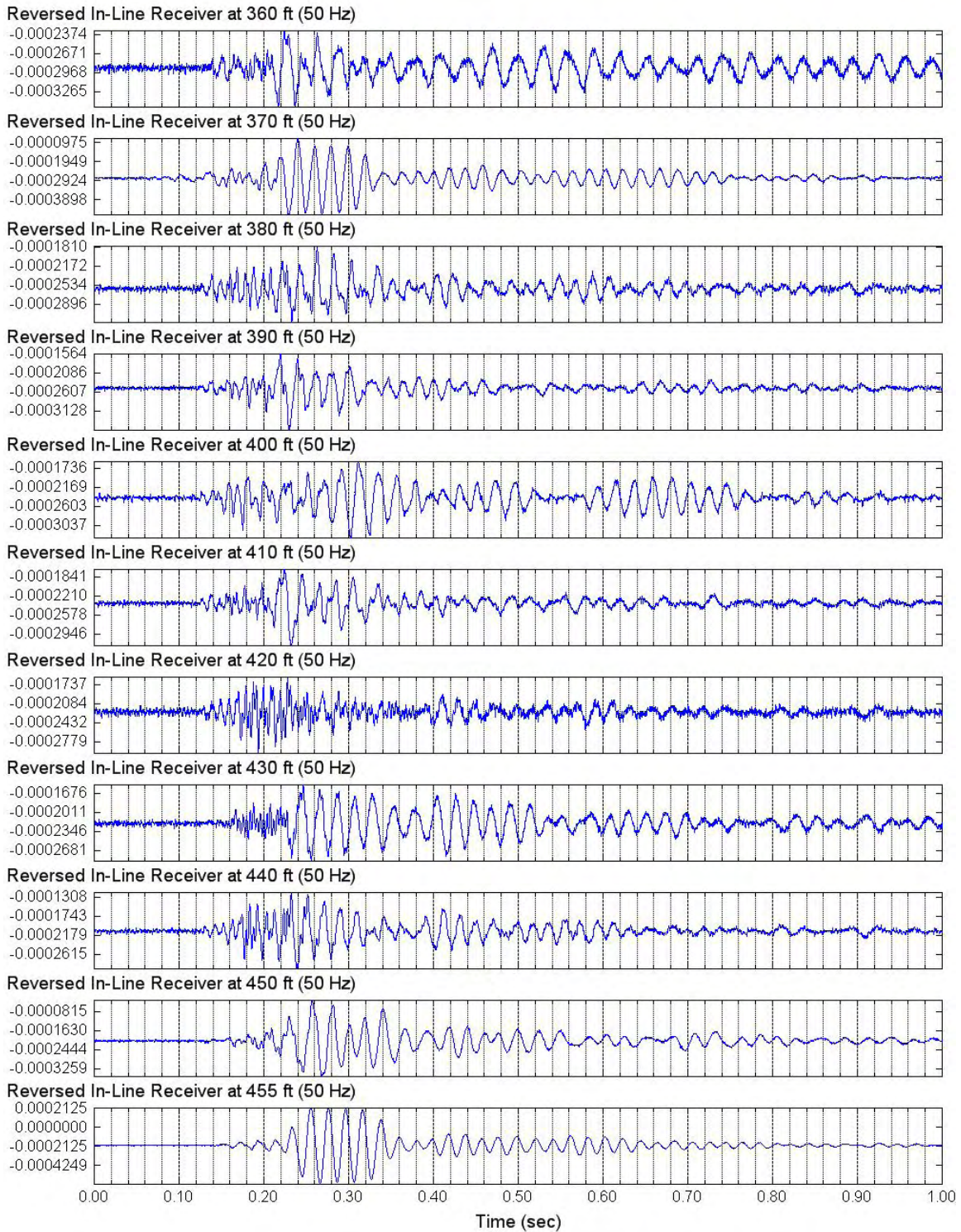


Figure 4.2.2 Unfiltered Reverse S-Wave Signals of Lower In-Line Receiver (C4996)
Depths 460 to 520 ft; Input Signal: 5 Cycles of 50-Hz Sine Wave

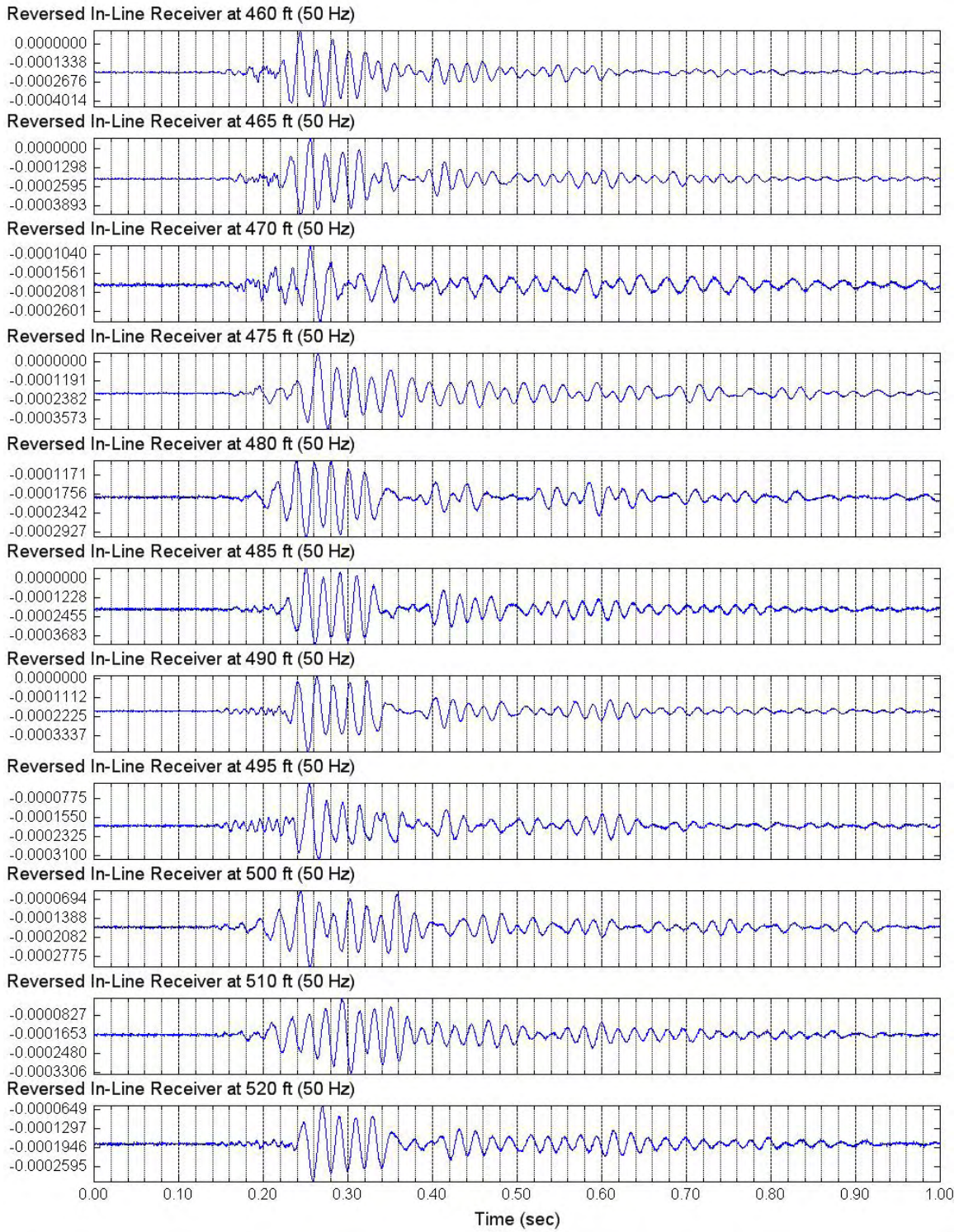


Figure 4.2.3 Unfiltered Reverse S-Wave Signals of Lower In-Line Receiver (C4996)
Depths 530 to 630 ft; Input Signal: 5 Cycles of 50-Hz Sine Wave

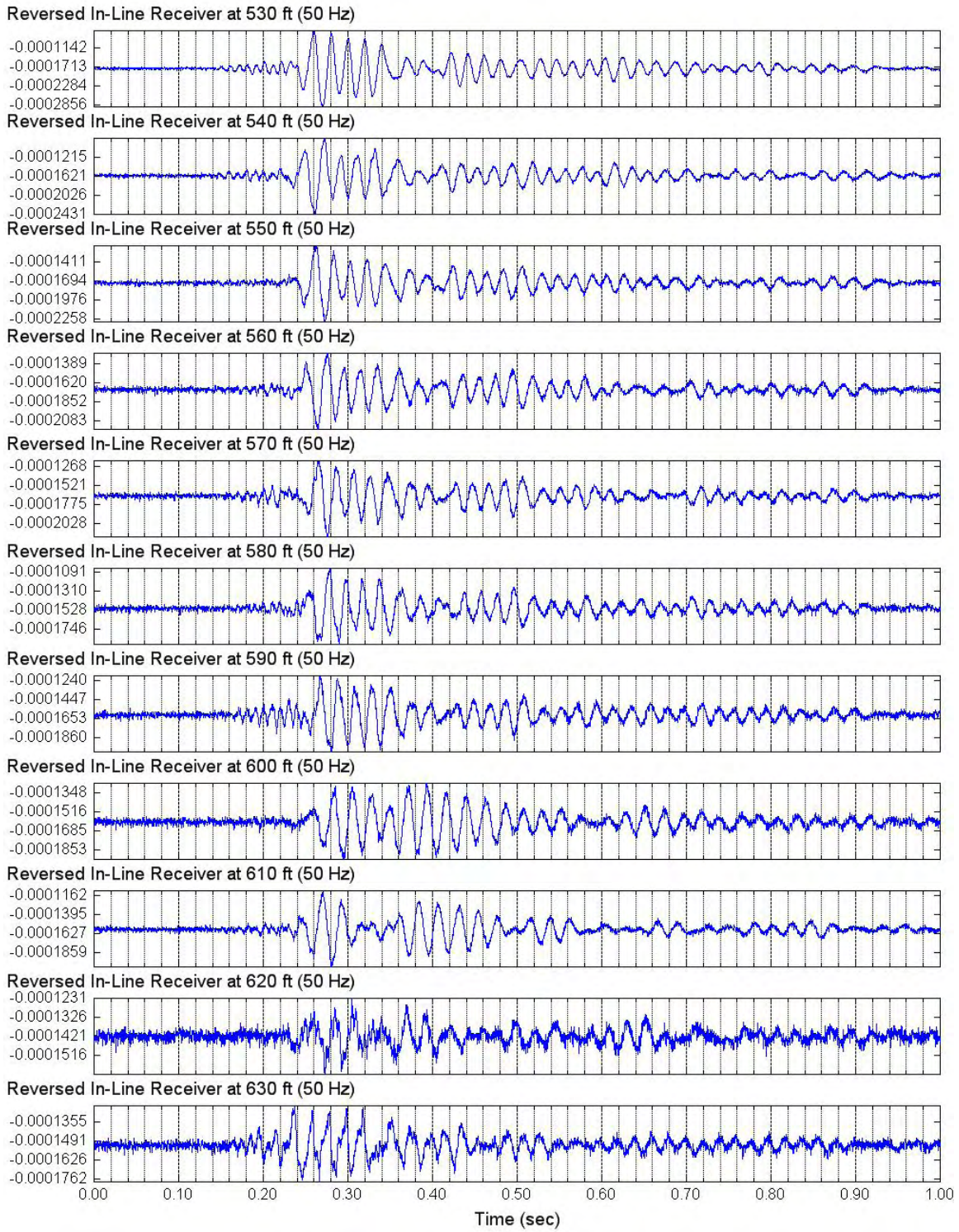


Figure 4.2.4 Unfiltered Reverse S-Wave Signals of Lower In-Line Receiver (C4996)
Depths 640 to 720 ft; Input Signal: 5 Cycles of 50-Hz Sine Wave

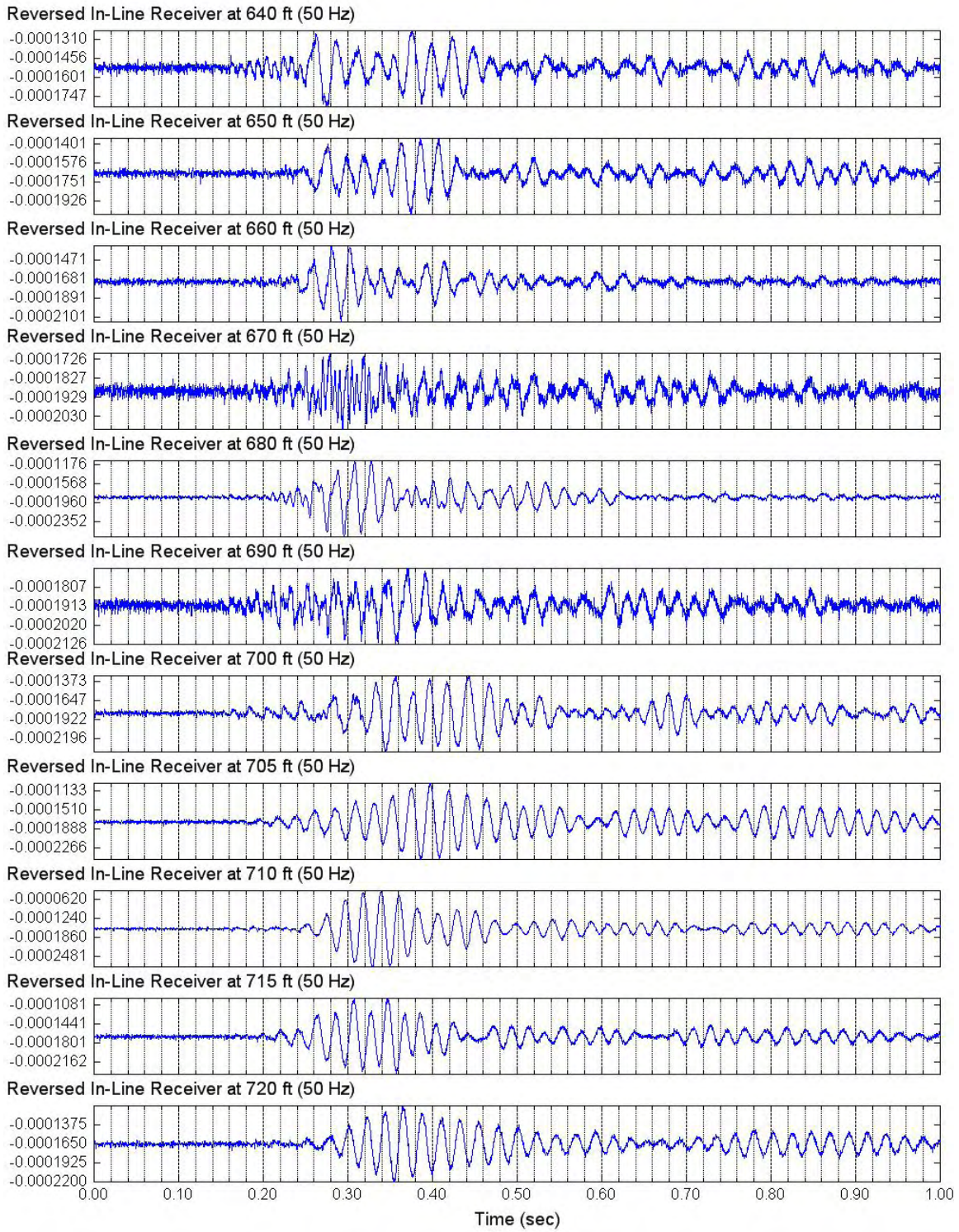


Figure 4.2.5 Unfiltered Reverse S-Wave Signals of Lower In-Line Receiver (C4996)
Depths 730 to 820 ft; Input Signal: 5 Cycles of 50-Hz Sine Wave

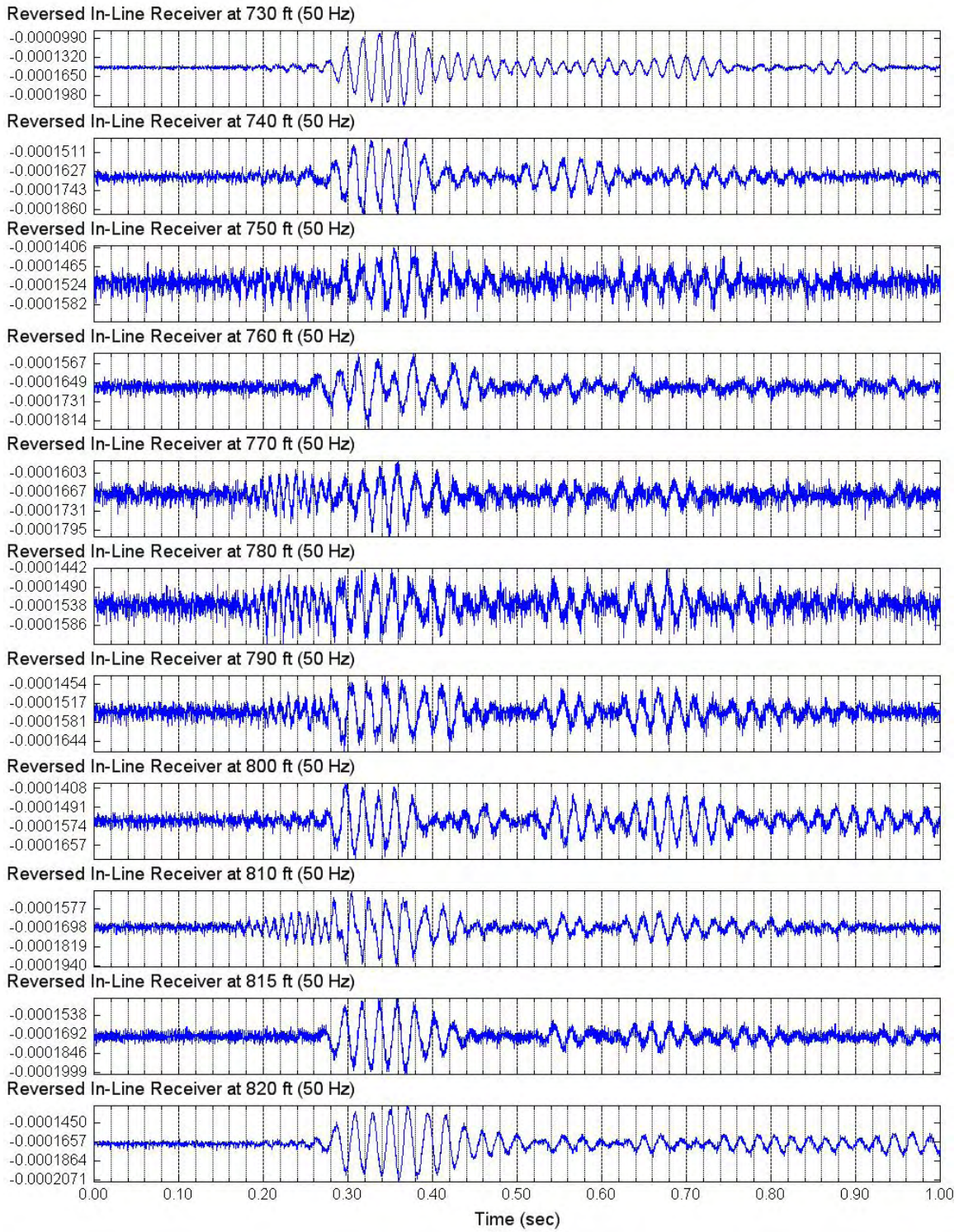


Figure 4.2.6 Unfiltered Reverse S-Wave Signals of Lower In-Line Receiver (C4996)
Depths 830 to 960 ft; Input Signal: 5 Cycles of 50-Hz Sine Wave

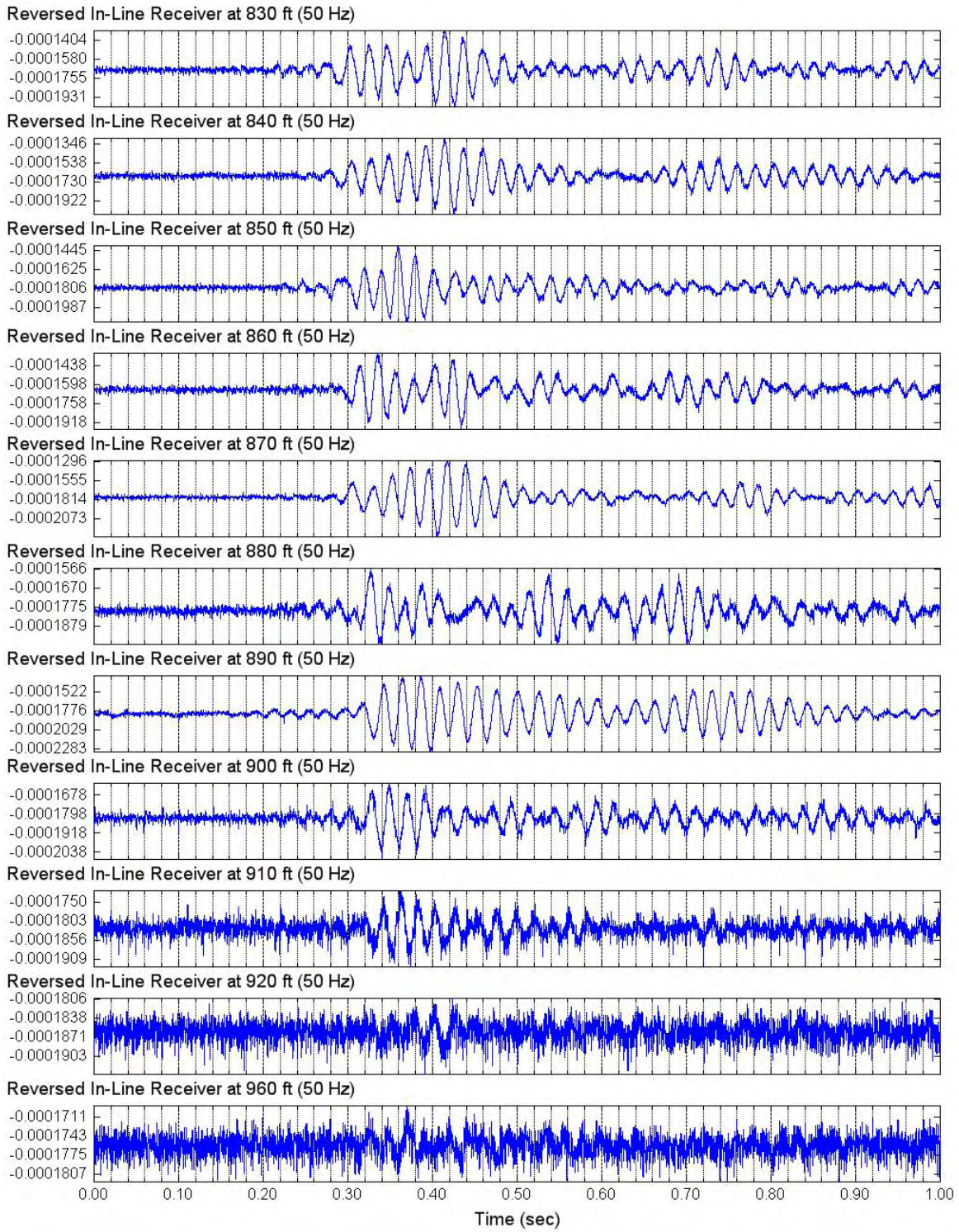


Figure 4.2.7 Unfiltered Reverse S-Wave Signals of Lower In-Line Receiver (C4996)
Depths 910 to 980 ft; Input Signal: 4 Cycles of 20-Hz Sine Wave

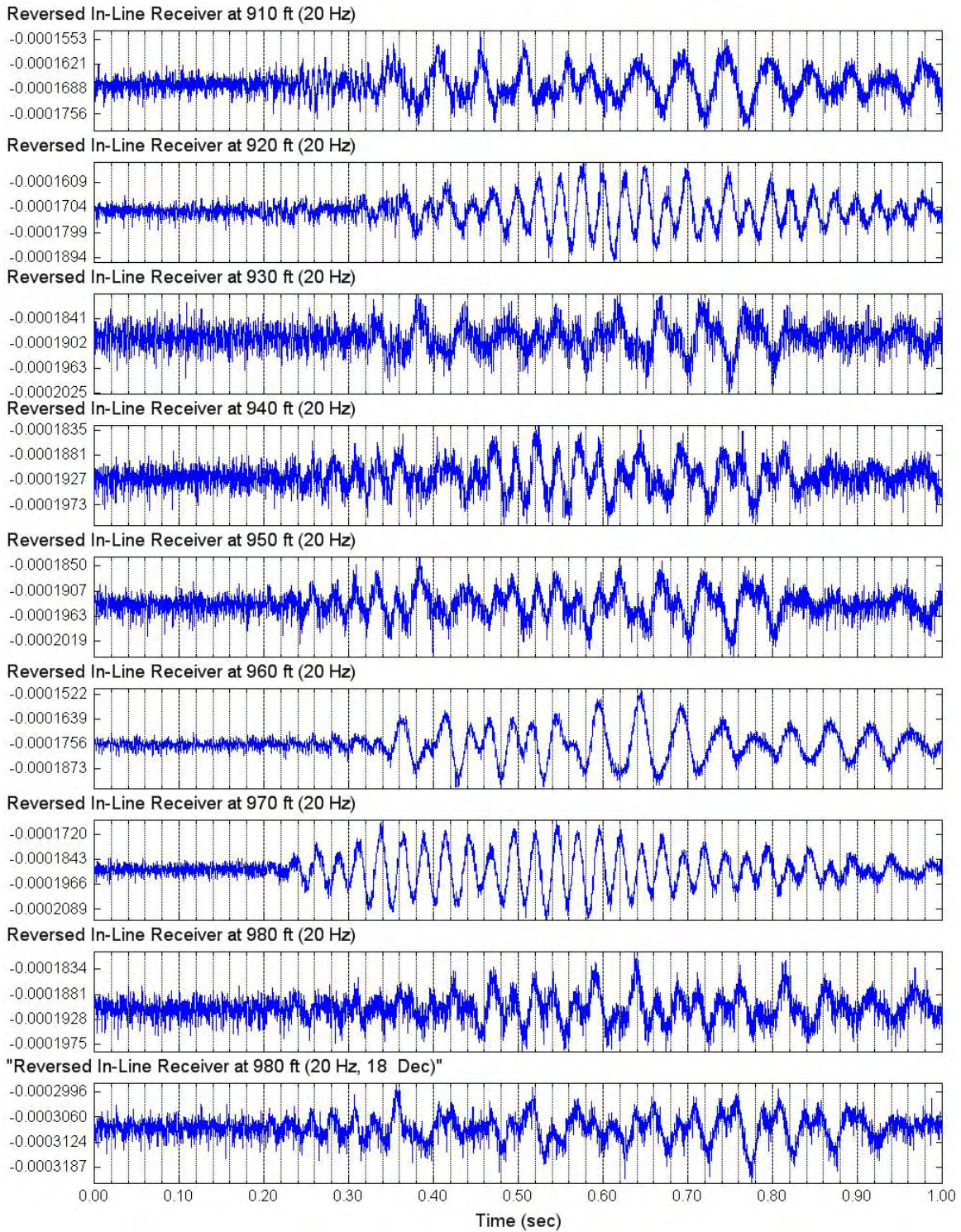


Figure 4.2.8 Unfiltered Reverse S-Wave Signals of Lower In-Line Receiver (C4996)
Depths 980 to 1060 ft; Input Signal: 4 Cycles of 30-Hz Sine Wave

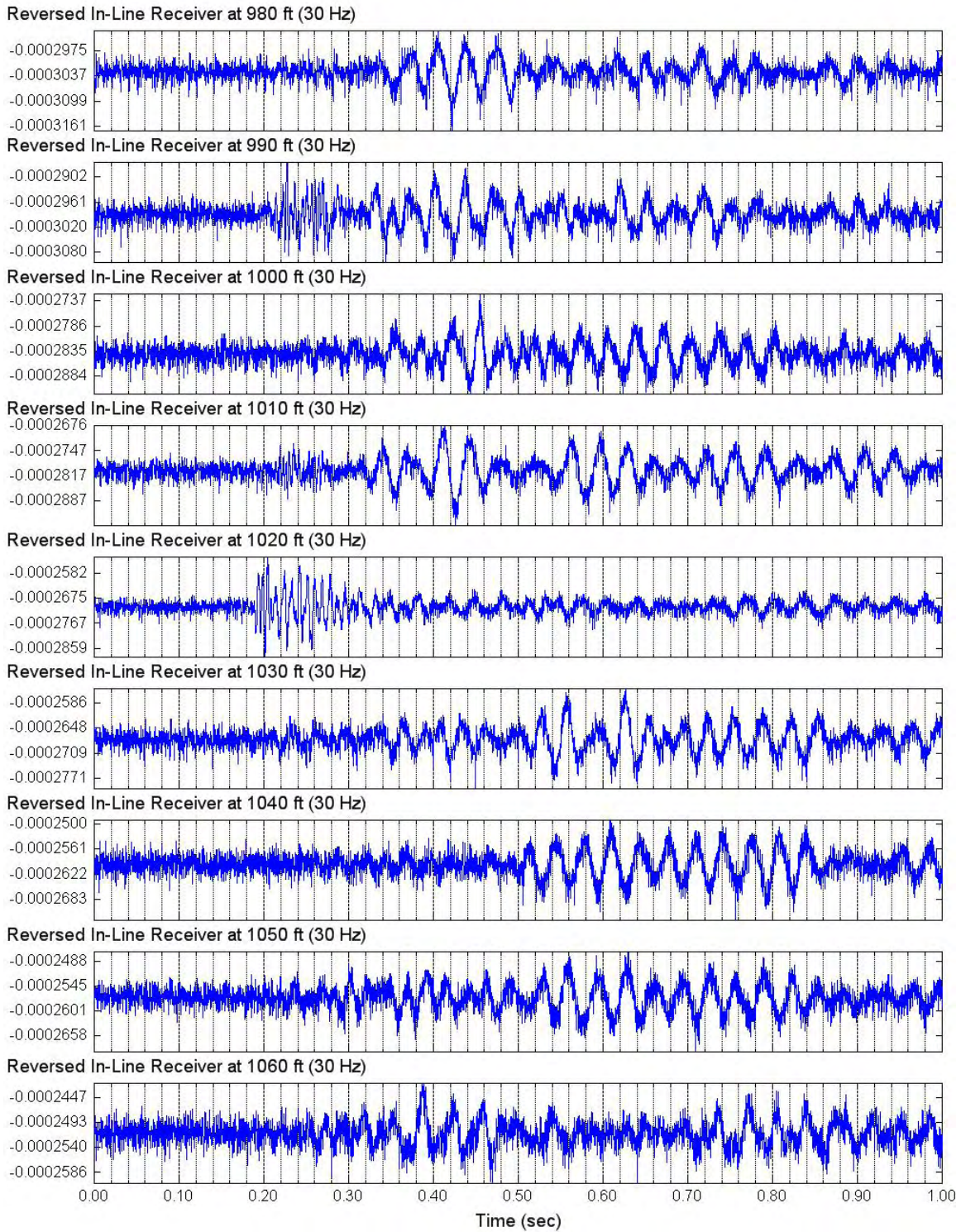


Figure 4.2.9 Unfiltered Reverse S-Wave Signals of Lower In-Line Receiver (C4996)
Depths 1070 to 1150 ft; Input Signal: 4 Cycles of 30-Hz Sine Wave

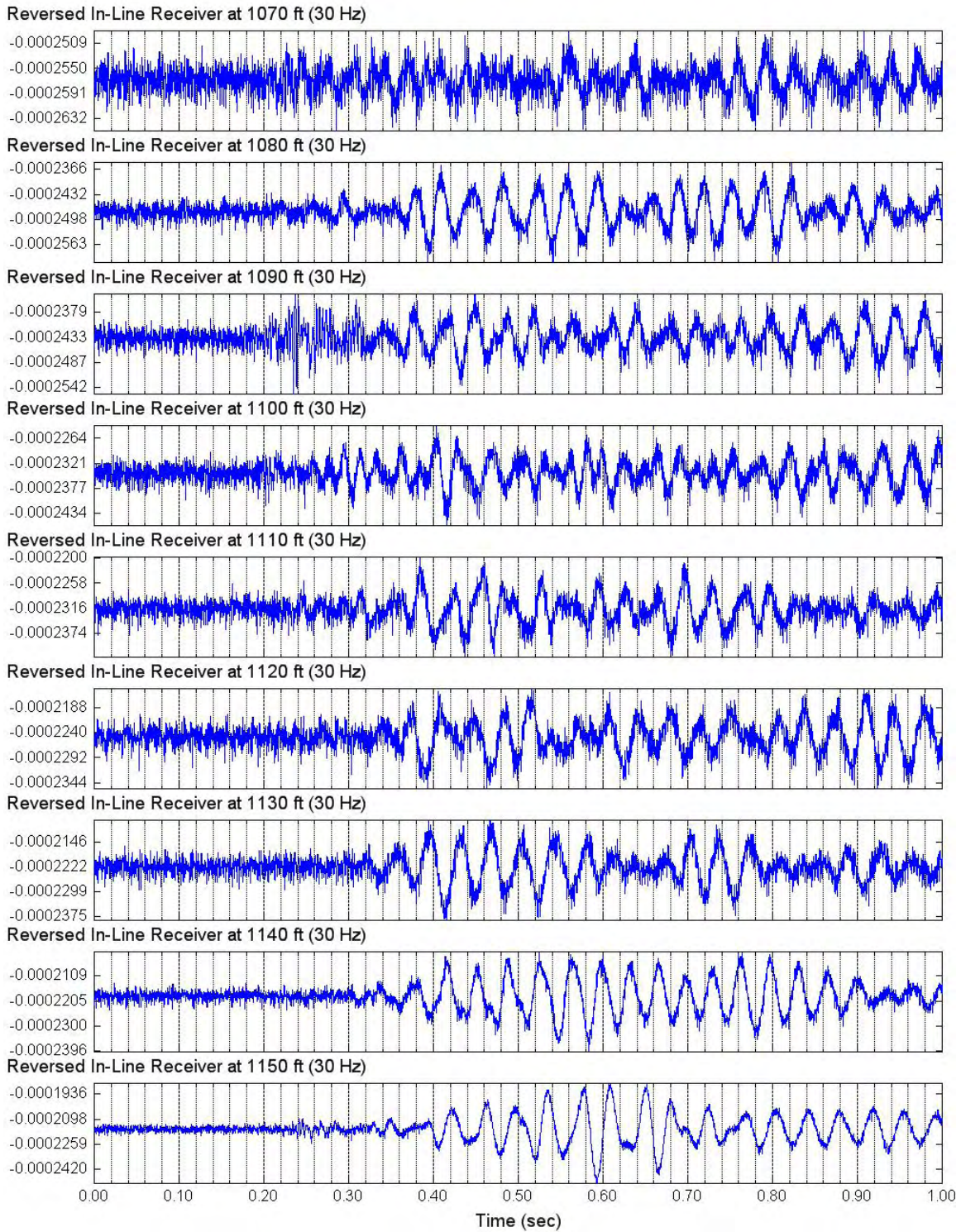


Figure 4.2.10 Unfiltered Reverse S-Wave Signals of Lower In-Line Receiver (C4996)
Depths 1160 to 1300 ft; Input Signal: 4 Cycles of 30-Hz Sine Wave

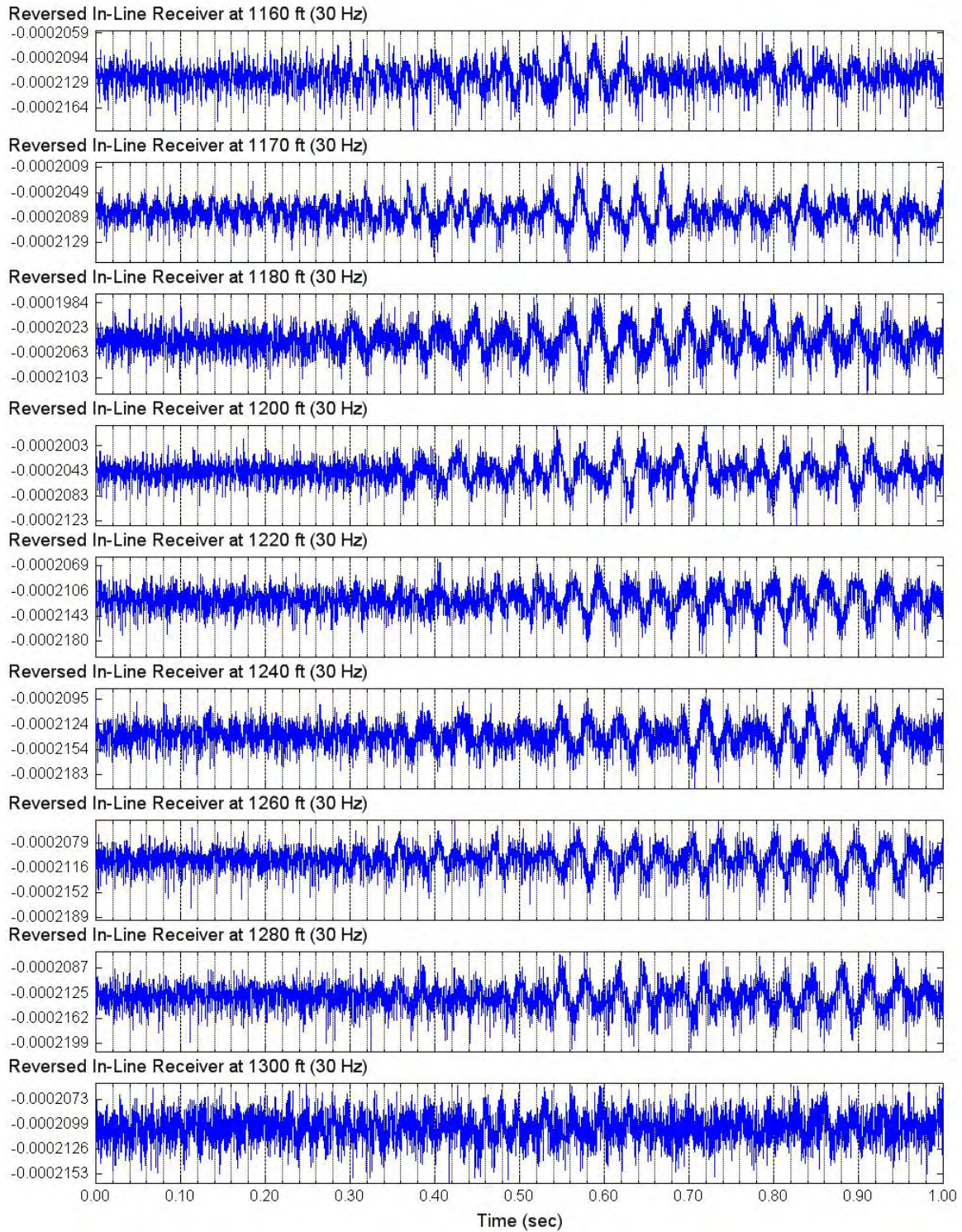


Figure 4.3.1 Unfiltered Forward S-Wave Signals of Lower Cross-Line Receiver (C4996)
Depths 360 to 455 ft; Input Signal: 5 Cycles of 50-Hz Sine Wave

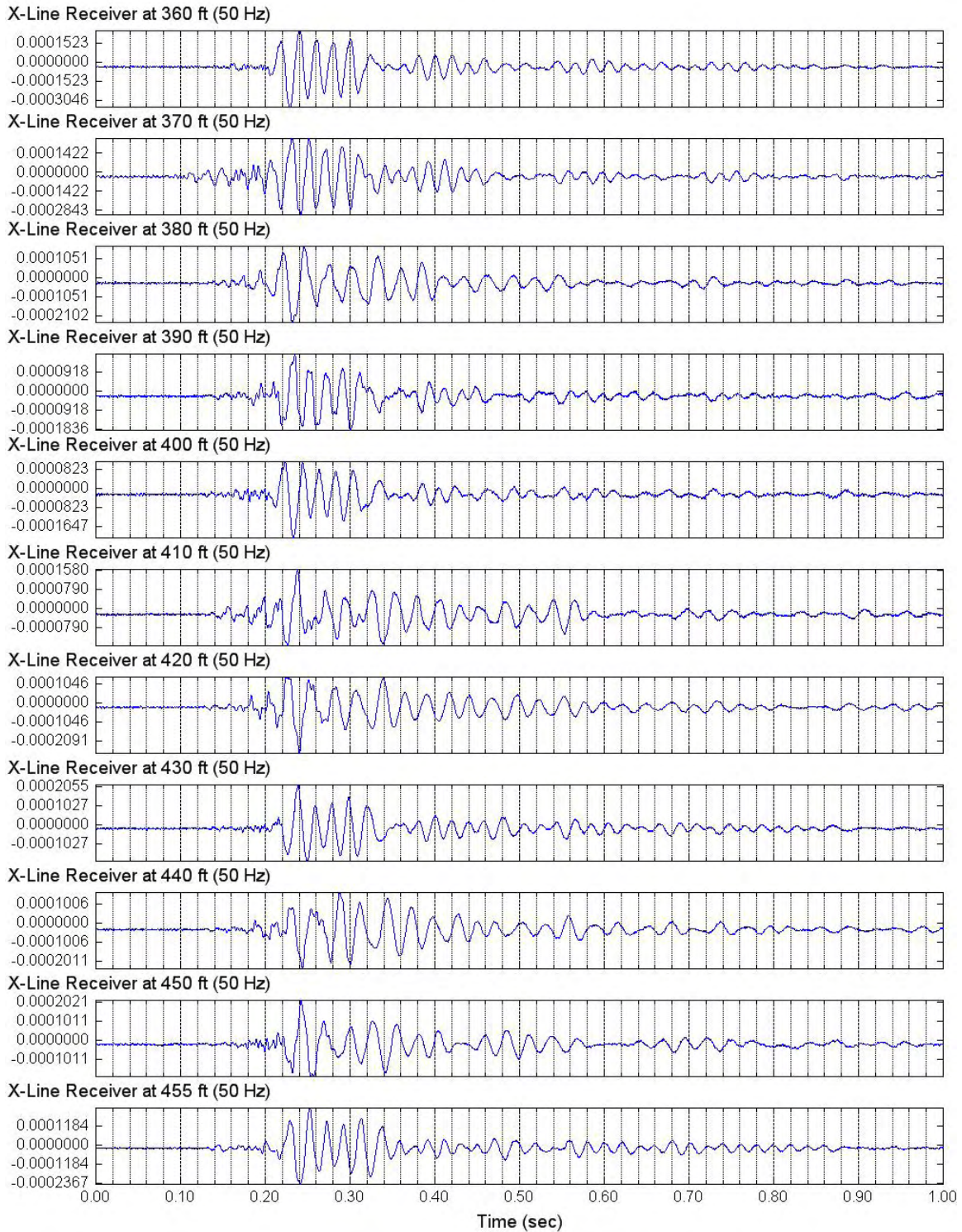


Figure 4.3.2 Unfiltered Forward S-Wave Signals of Lower Cross-Line Receiver (C4996)
Depths 460 to 520 ft; Input Signal: 5 Cycles of 50-Hz Sine Wave

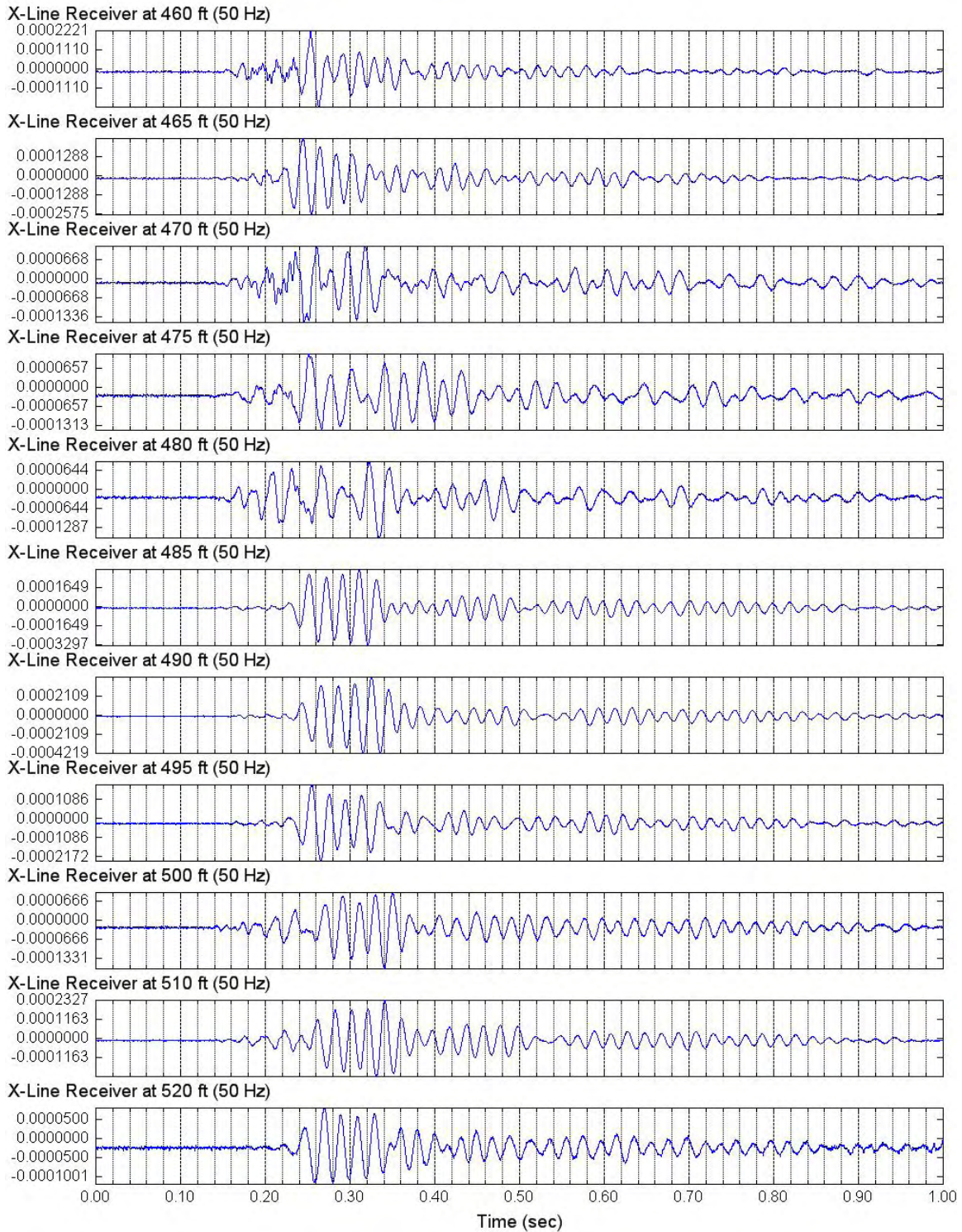


Figure 4.3.3 Unfiltered Forward S-Wave Signals of Lower Cross-Line Receiver (C4996)
Depths 530 to 630 ft; Input Signal: 5 Cycles of 50-Hz Sine Wave

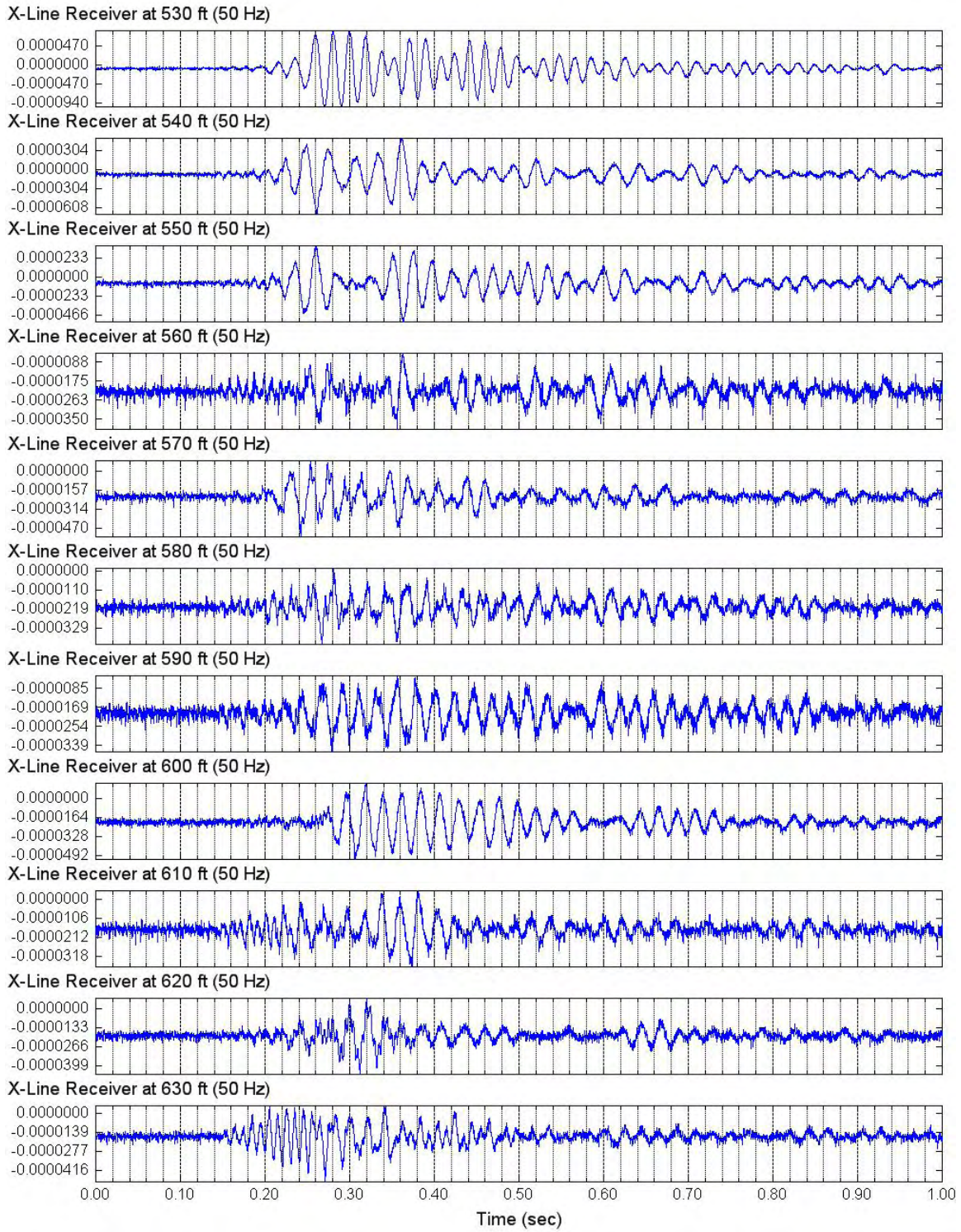


Figure 4.3.4 Unfiltered Forward S-Wave Signals of Lower Cross-Line Receiver (C4996)
Depths 640 to 720 ft; Input Signal: 5 Cycles of 50-Hz Sine Wave

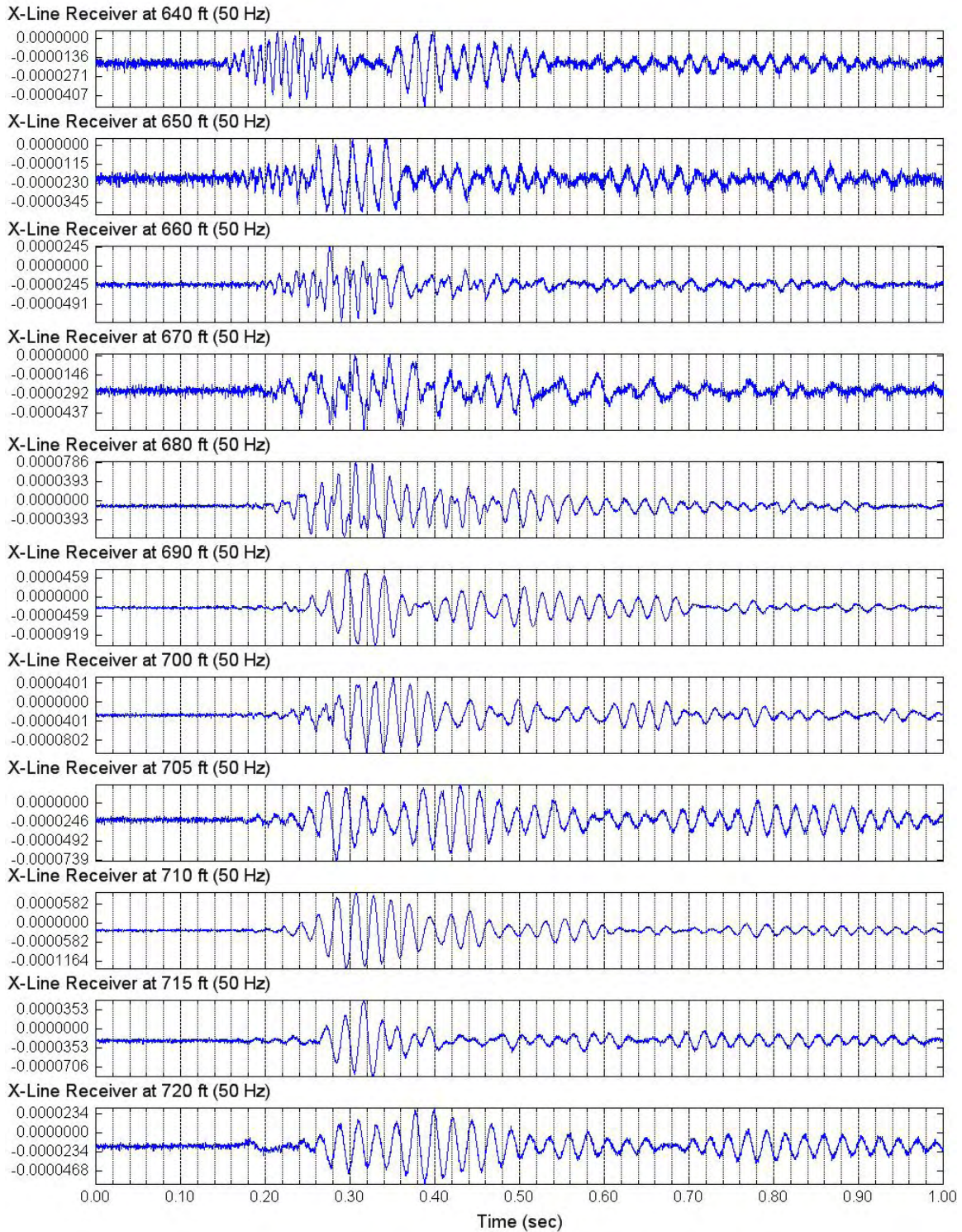


Figure 4.3.5 Unfiltered Forward S-Wave Signals of Lower Cross-Line Receiver (C4996)
Depths 730 to 820 ft; Input Signal: 5 Cycles of 50-Hz Sine Wave

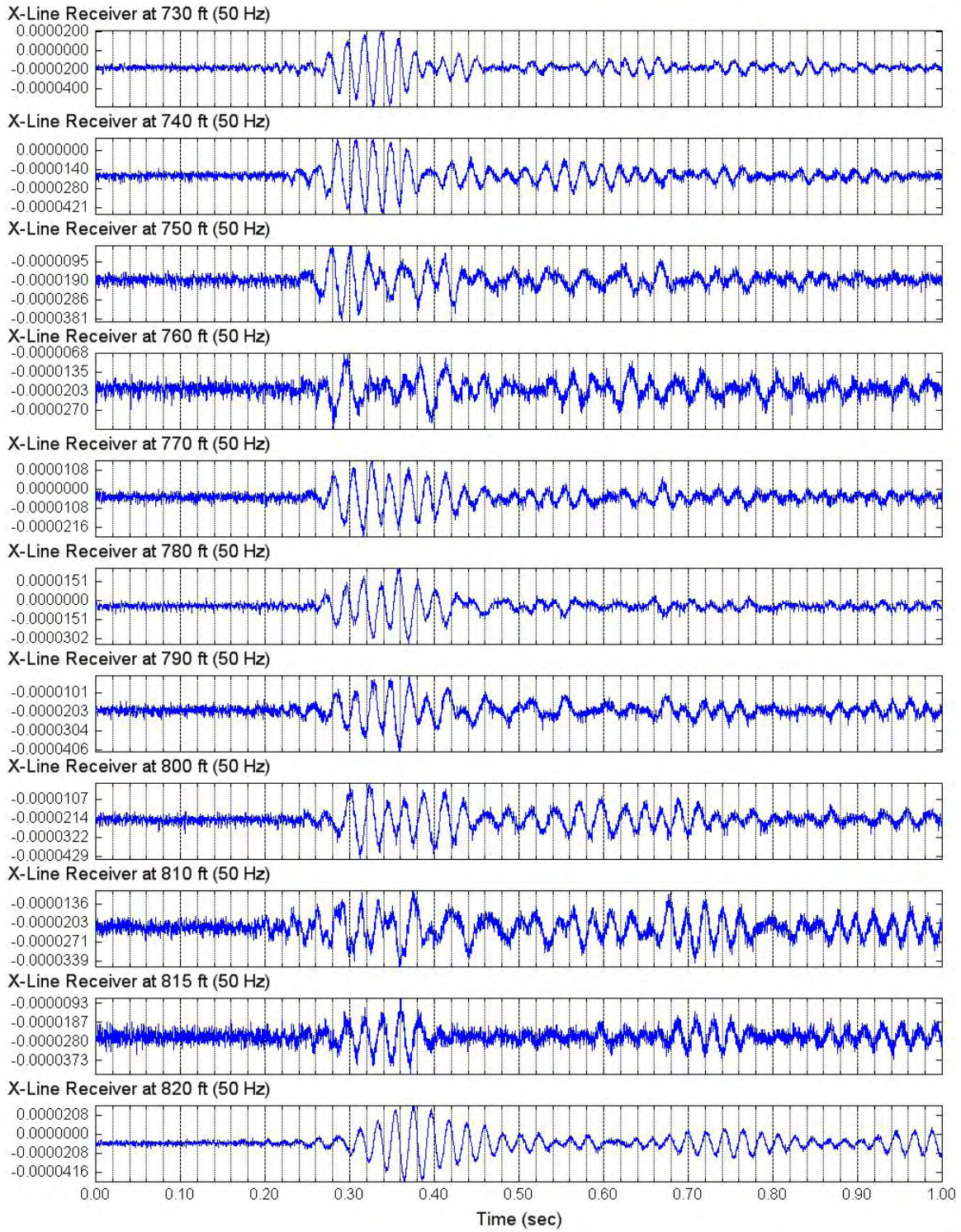


Figure 4.3.6 Unfiltered Forward S-Wave Signals of Lower Cross-Line Receiver (C4996)
Depths 830 to 960 ft; Input Signal: 5 Cycles of 50-Hz Sine Wave

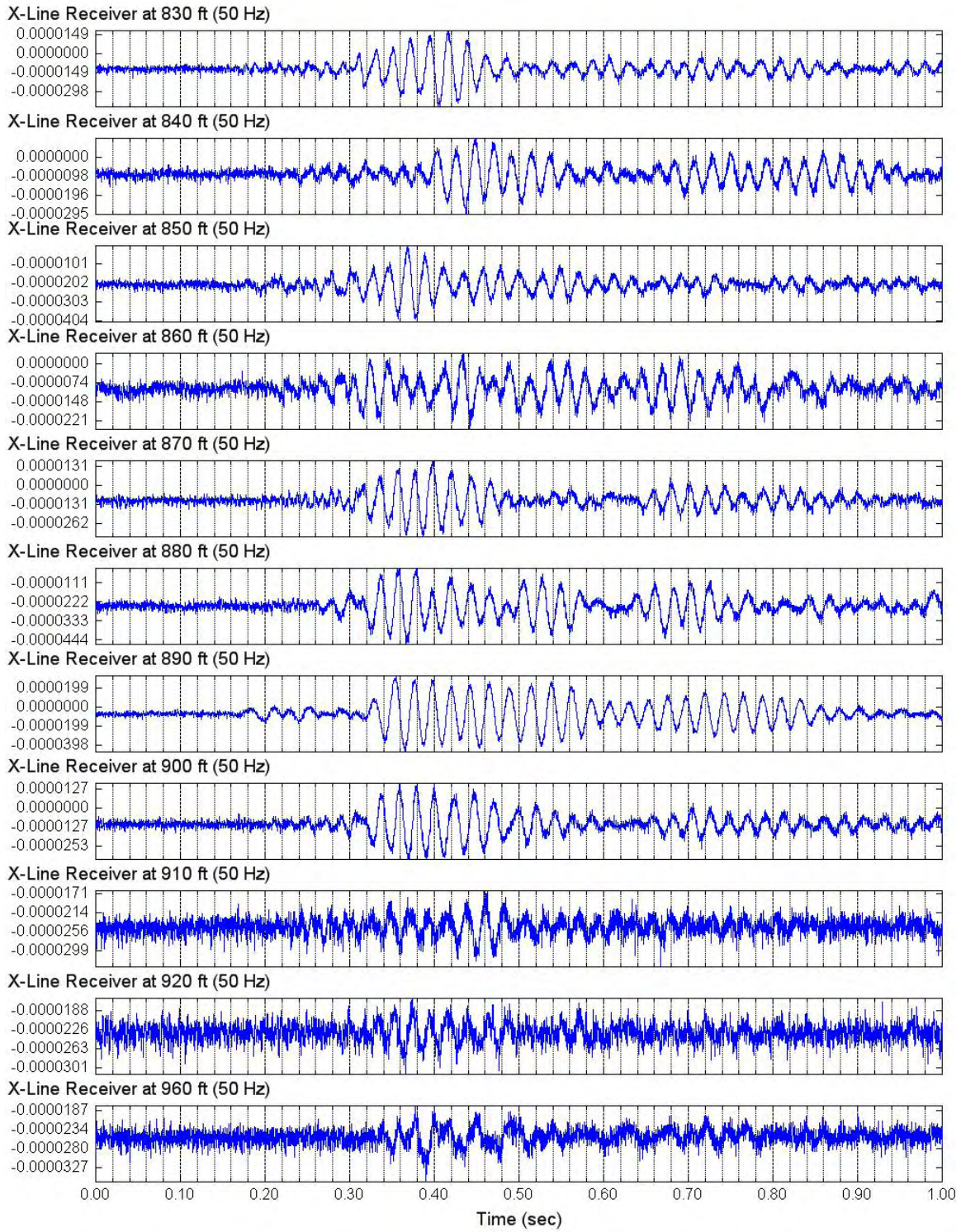


Figure 4.3.7 Unfiltered Forward S-Wave Signals of Lower Cross-Line Receiver (C4996)
Depths 910 to 980 ft; Input Signal: 4 Cycles of 20-Hz Sine Wave

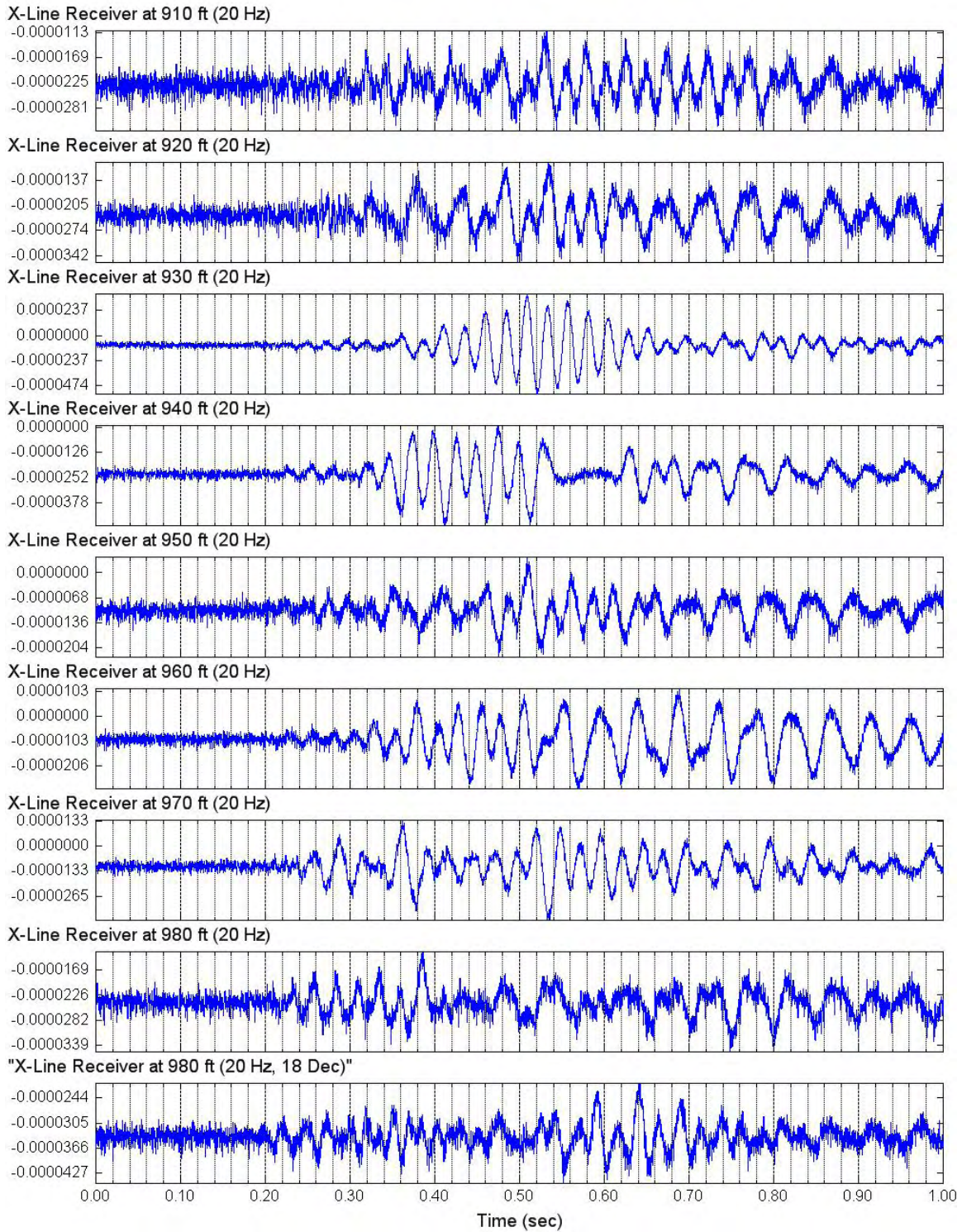


Figure 4.3.8 Unfiltered Forward S-Wave Signals of Lower Cross-Line Receiver (C4996)
Depths 980 to 1060 ft; Input Signal: 4 Cycles of 30-Hz Sine Wave

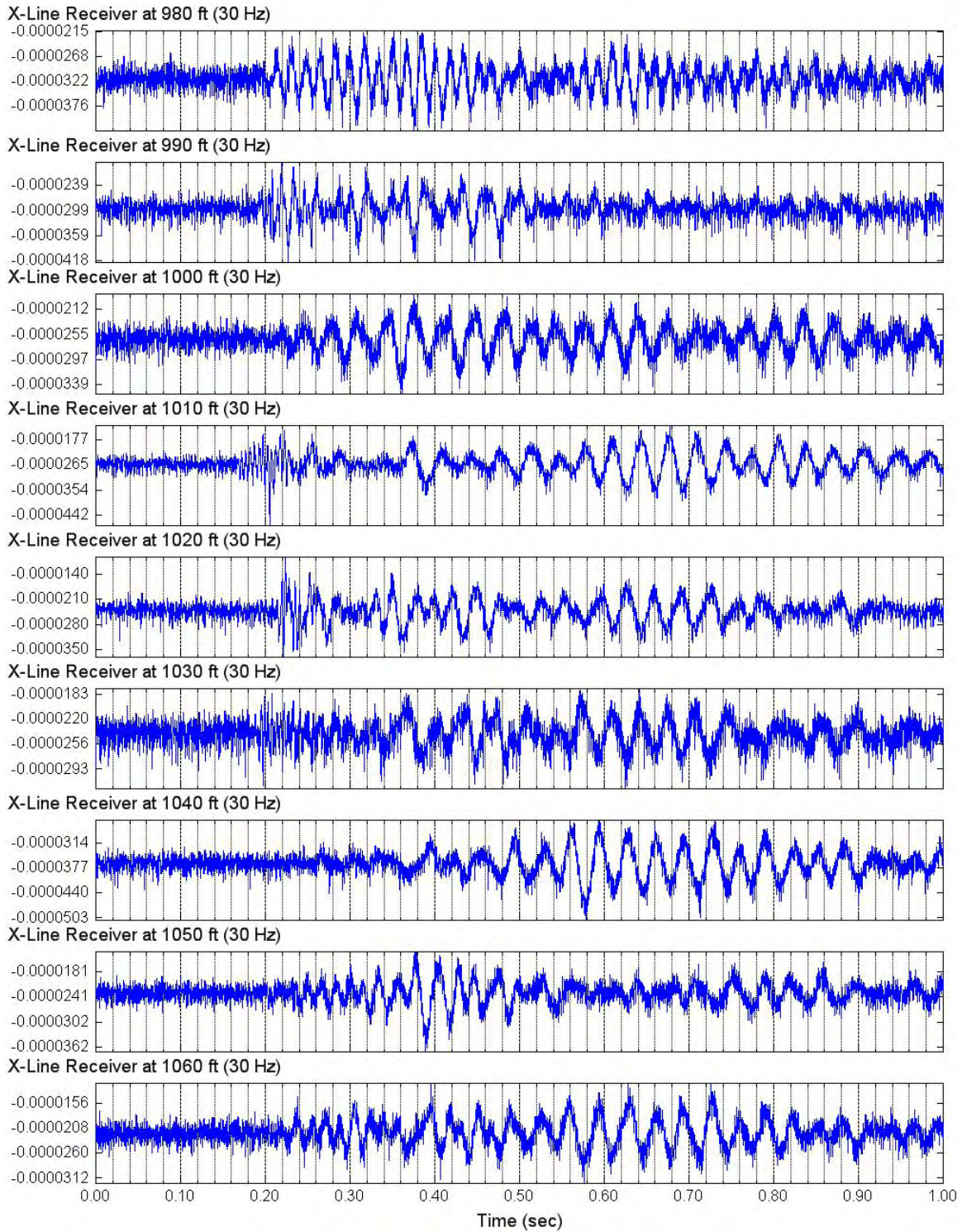


Figure 4.3.9 Unfiltered Forward S-Wave Signals of Lower Cross-Line Receiver (C4996)
Depths 1070 to 1150 ft; Input Signal: 4 Cycles of 30-Hz Sine Wave

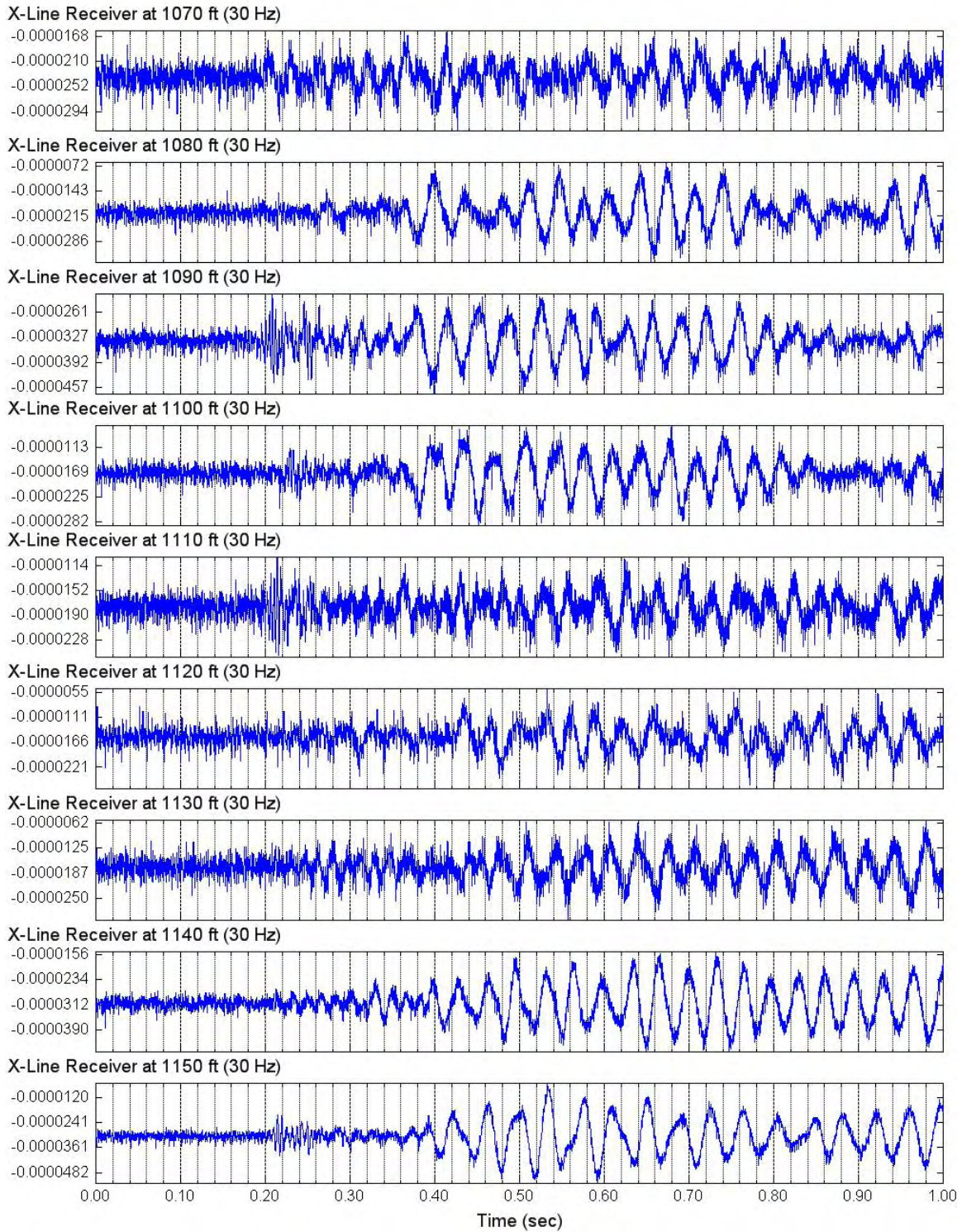


Figure 4.3.10 Unfiltered Forward S-Wave Signals of Lower Cross-Line Receiver (C4996)
Depths 1160 to 1300 ft; Input Signal: 4 Cycles of 30-Hz Sine Wave

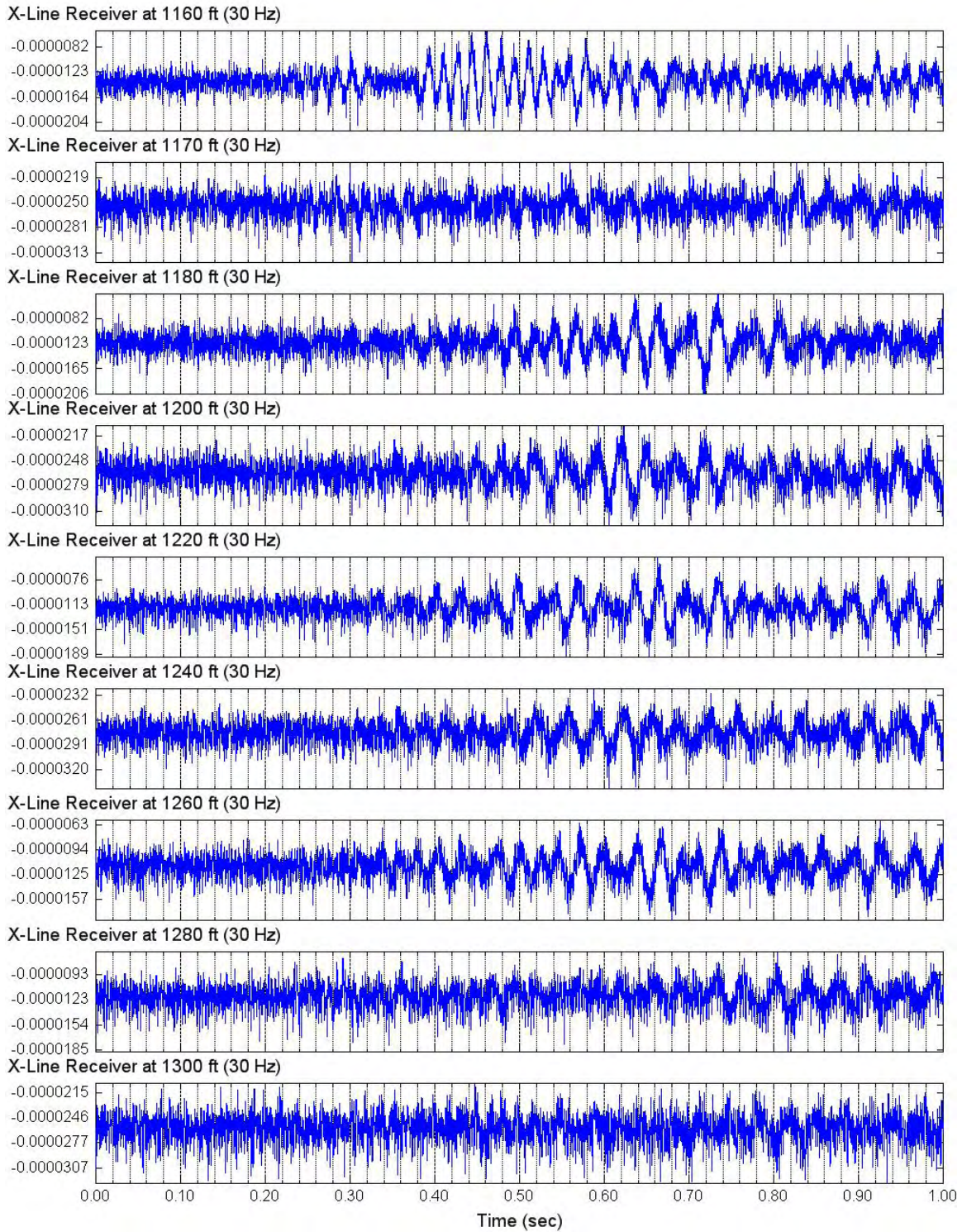


Figure 4.4.1 Unfiltered Reverse S-Wave Signals of Lower Cross-Line Receiver (C4996)
Depths 360 to 455 ft; Input Signal: 5 Cycles of 50-Hz Sine Wave

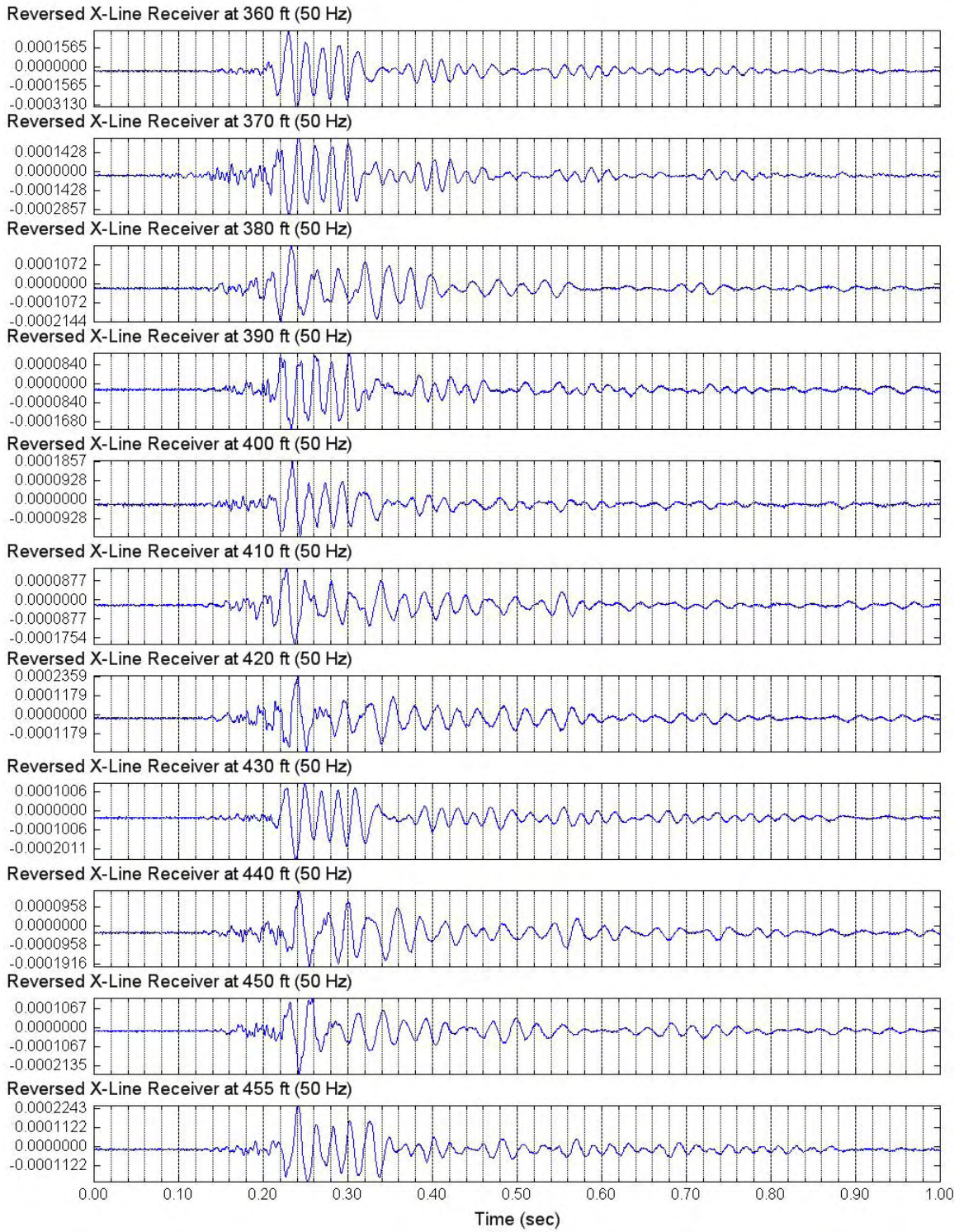


Figure 4.4.2 Unfiltered Reverse S-Wave Signals of Lower Cross-Line Receiver (C4996)
Depths 460 to 520 ft; Input Signal: 5 Cycles of 50-Hz Sine Wave

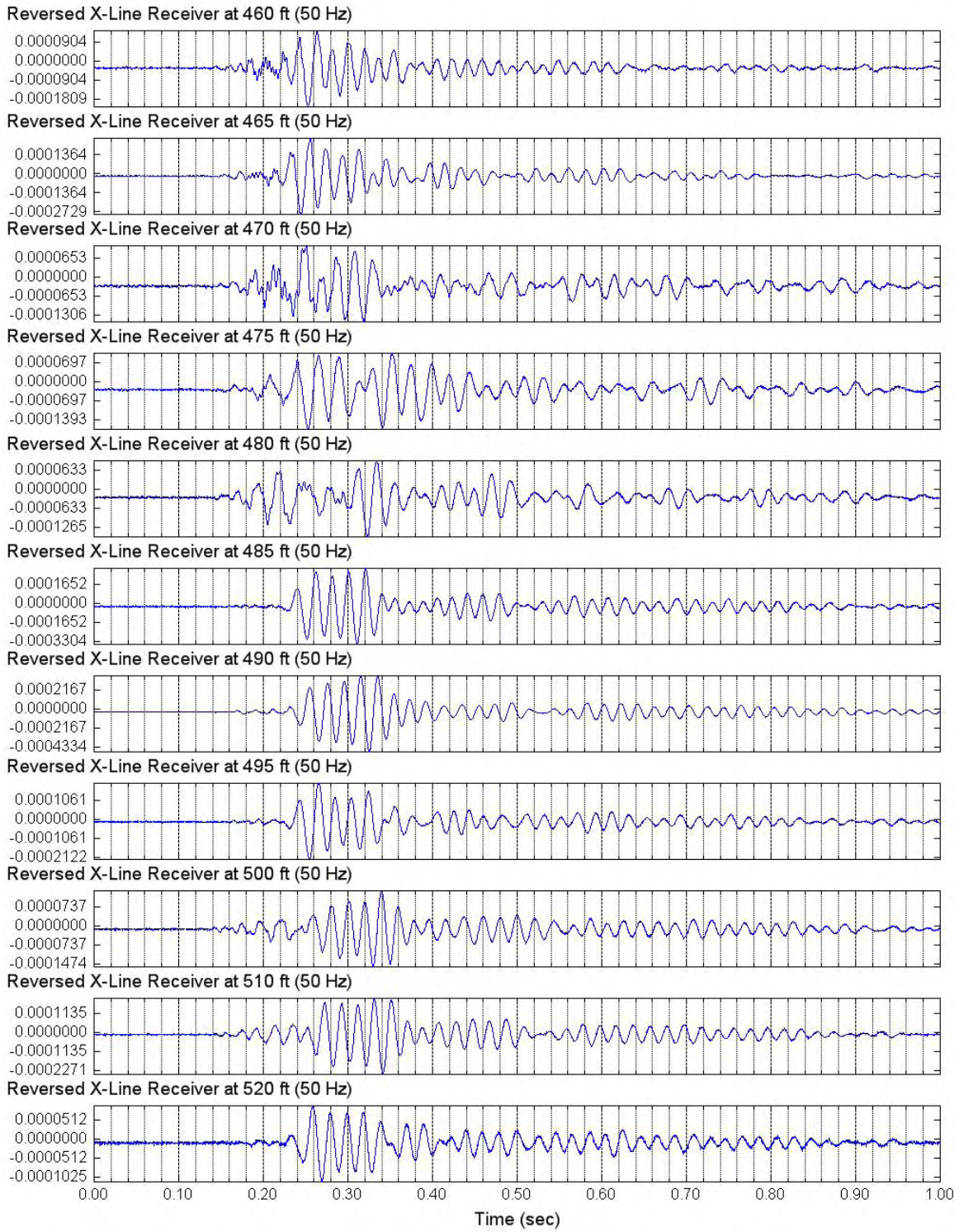


Figure 4.4.3 Unfiltered Reverse S-Wave Signals of Lower Cross-Line Receiver (C4996)
Depths 530 to 630 ft; Input Signal: 5 Cycles of 50-Hz Sine Wave

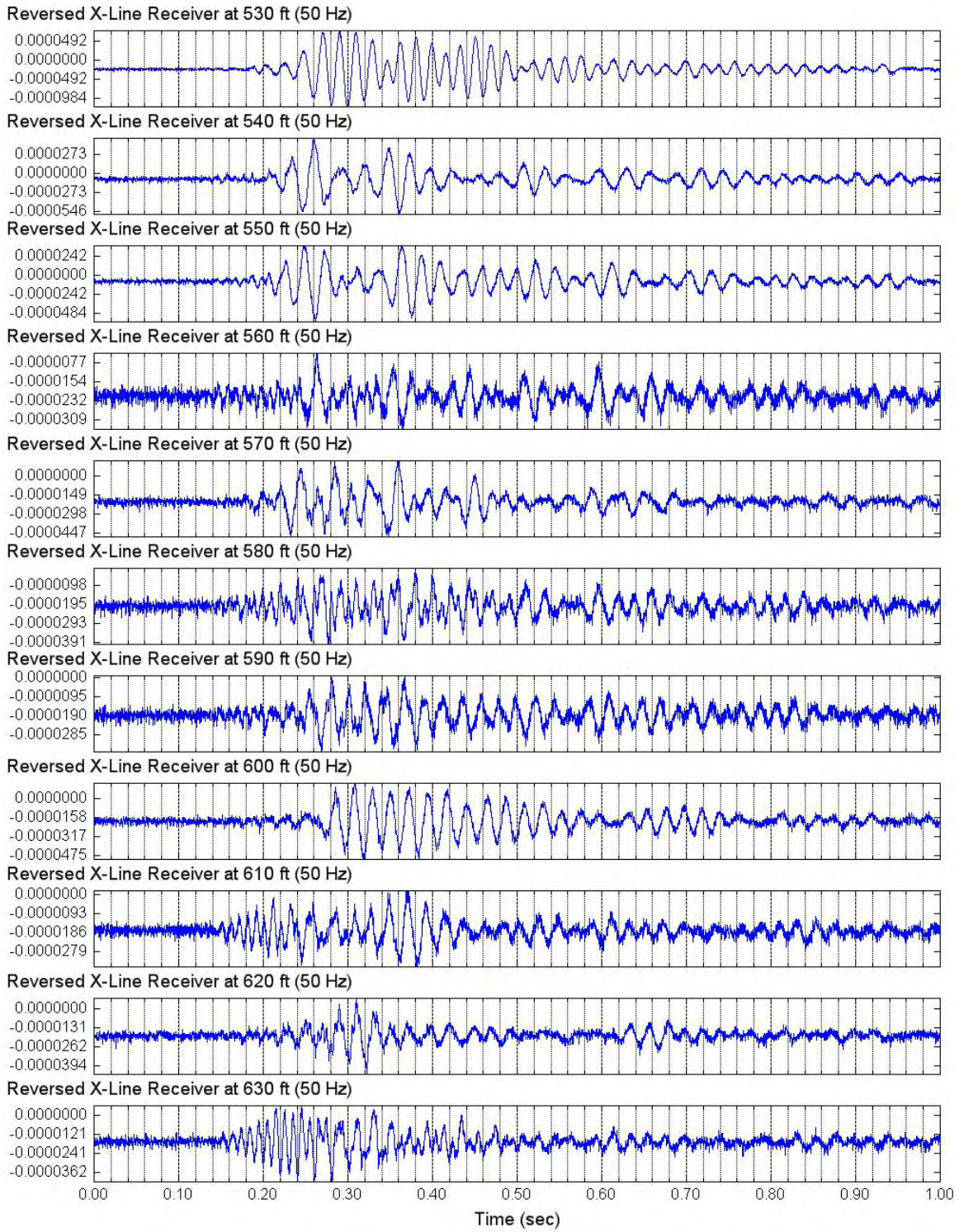


Figure 4.4.4 Unfiltered Reverse S-Wave Signals of Lower Cross-Line Receiver (C4996)
Depths 640 to 720 ft; Input Signal: 5 Cycles of 50-Hz Sine Wave

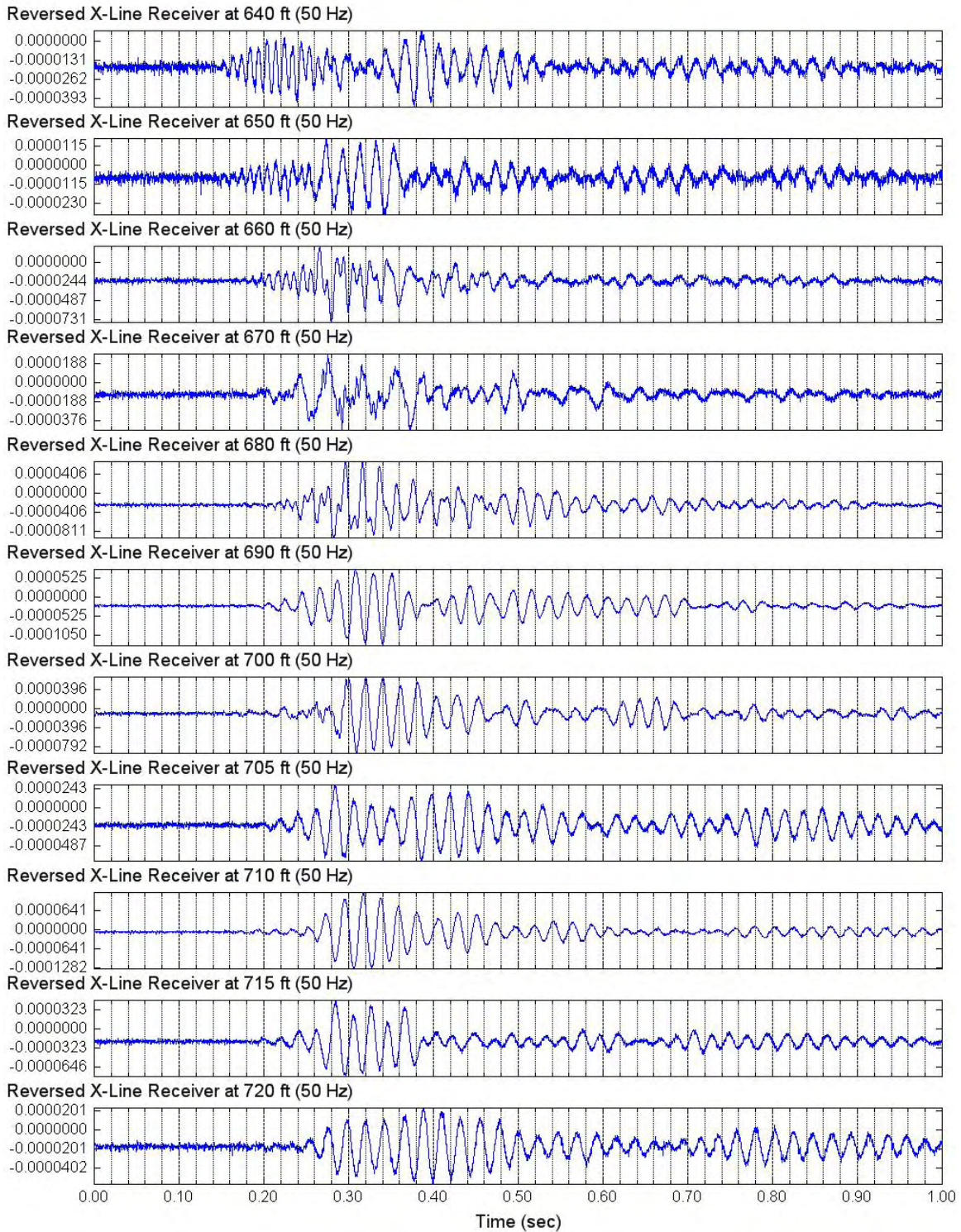


Figure 4.4.5 Unfiltered Reverse S-Wave Signals of Lower Cross-Line Receiver (C4996)
Depths 640 to 720 ft; Input Signal: 5 Cycles of 50-Hz Sine Wave

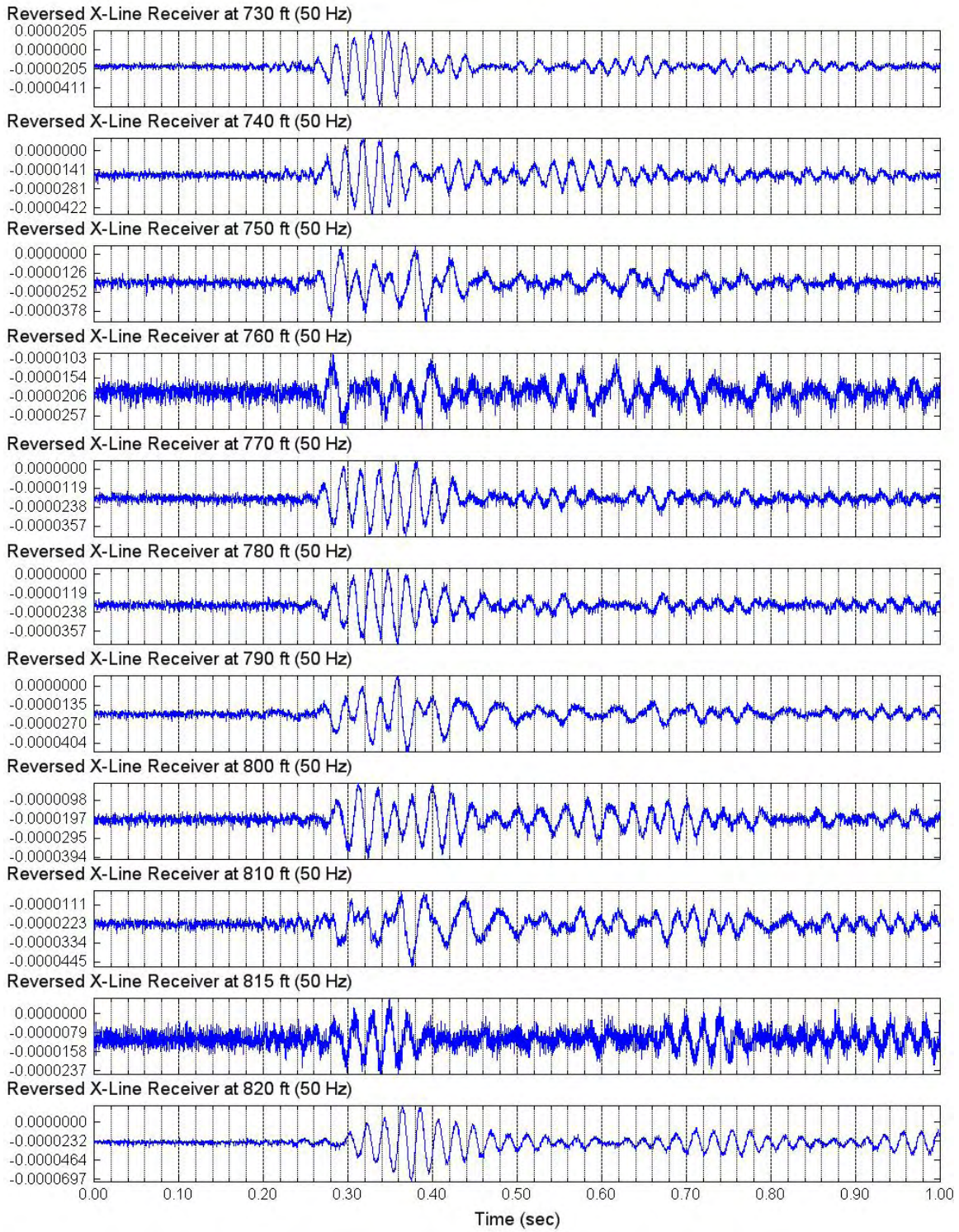


Figure 4.4.6 Unfiltered Reverse S-Wave Signals of Lower Cross-Line Receiver (C4996)
Depths 830 to 960 ft; Input Signal: 5 Cycles of 50-Hz Sine Wave

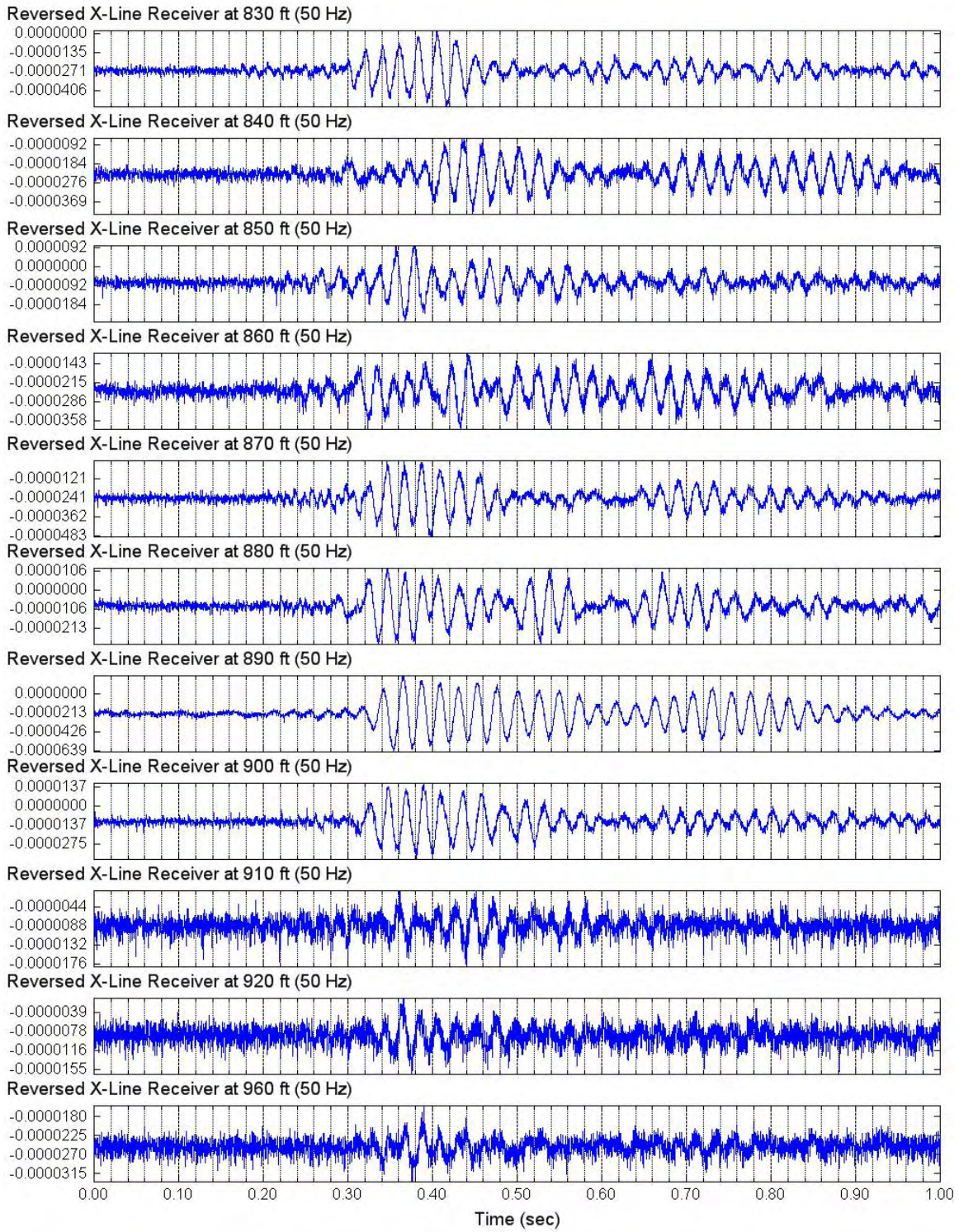


Figure 4.4.7 Unfiltered Reverse S-Wave Signals of Lower Cross-Line Receiver (C4996)
Depths 910 to 980 ft; Input Signal: 4 Cycles of 20-Hz Sine Wave

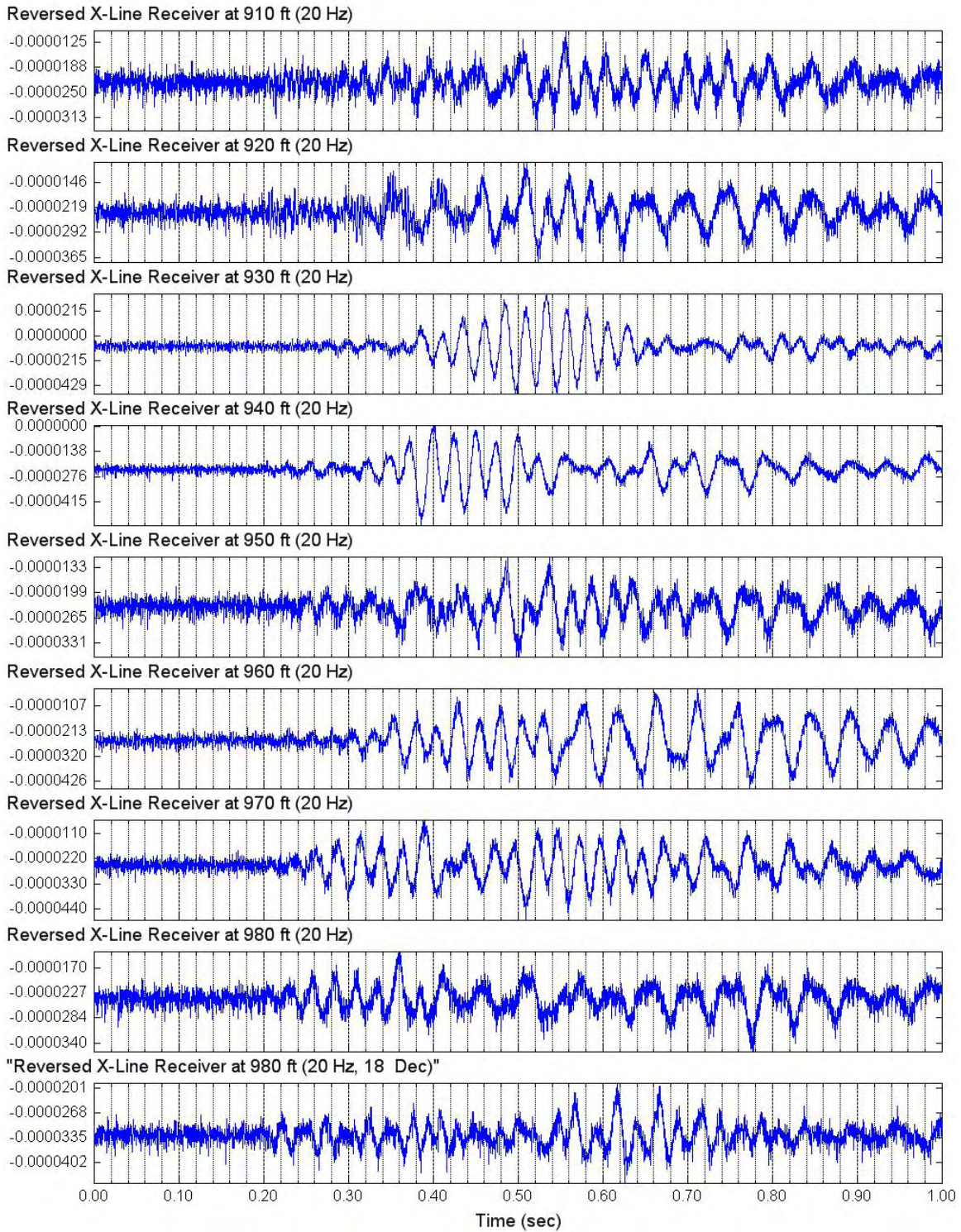


Figure 4.4.8 Unfiltered Reverse S-Wave Signals of Lower Cross-Line Receiver (C4996)
Depths 980 to 1060 ft; Input Signal: 4 Cycles of 30-Hz Sine Wave

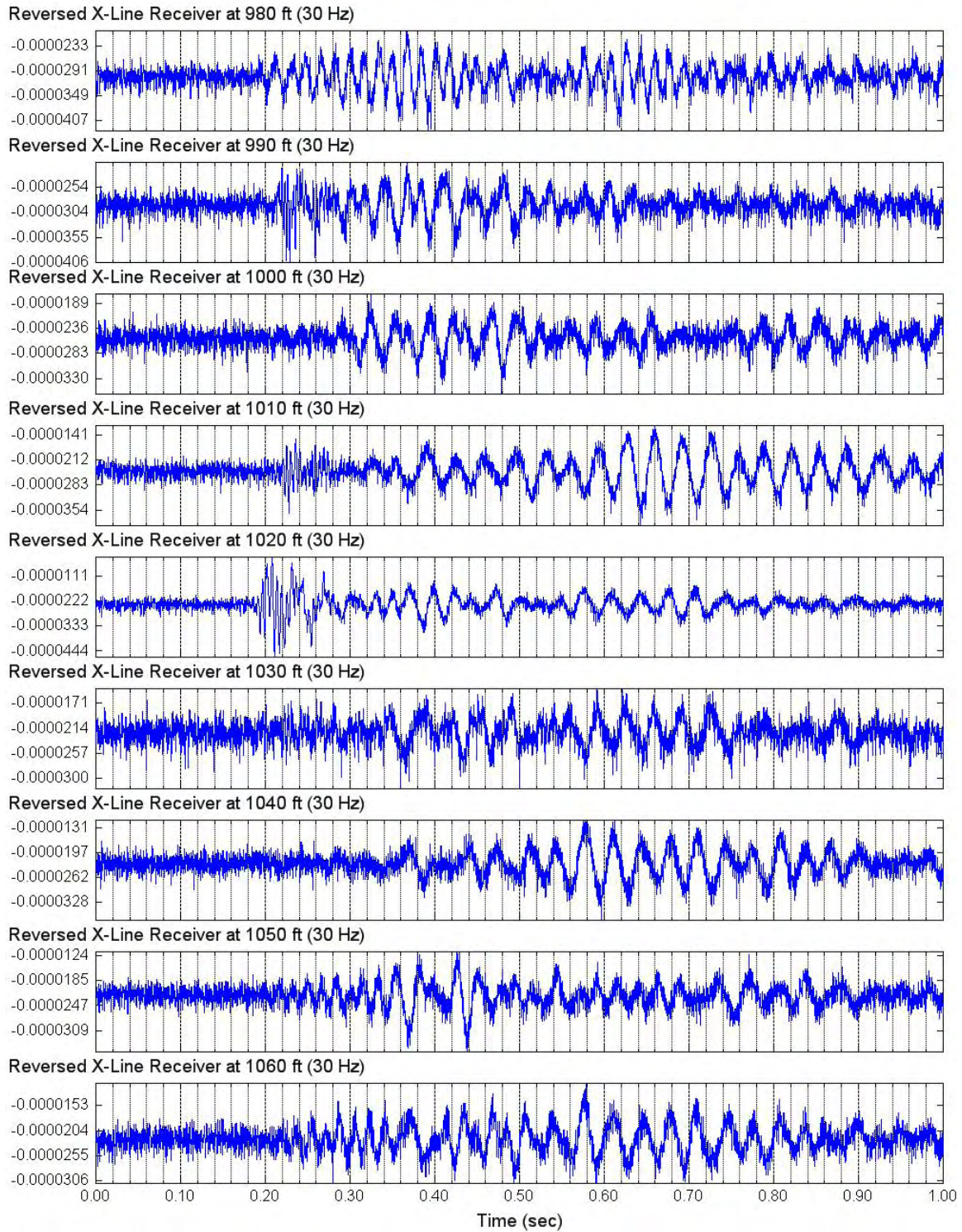


Figure 4.4.9 Unfiltered Reverse S-Wave Signals of Lower Cross-Line Receiver (C4996)
Depths 1070 to 1150 ft; Input Signal: 4 Cycles of 30-Hz Sine Wave

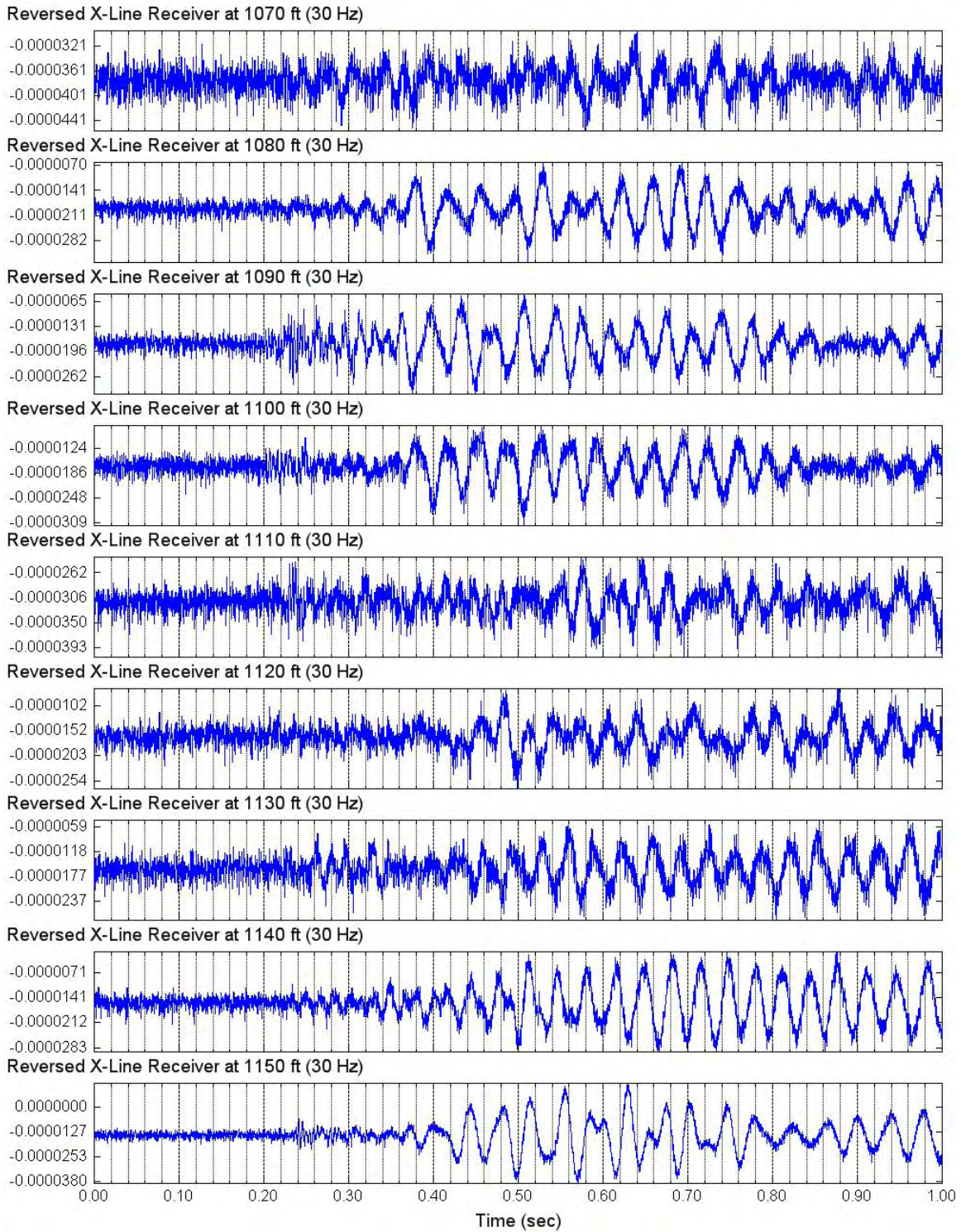


Figure 4.4.10 Unfiltered Reverse S-Wave Signals of Lower Cross-Line Receiver (C4996)
Depths 1160 to 1300 ft; Input Signal: 4 Cycles of 30-Hz Sine Wave

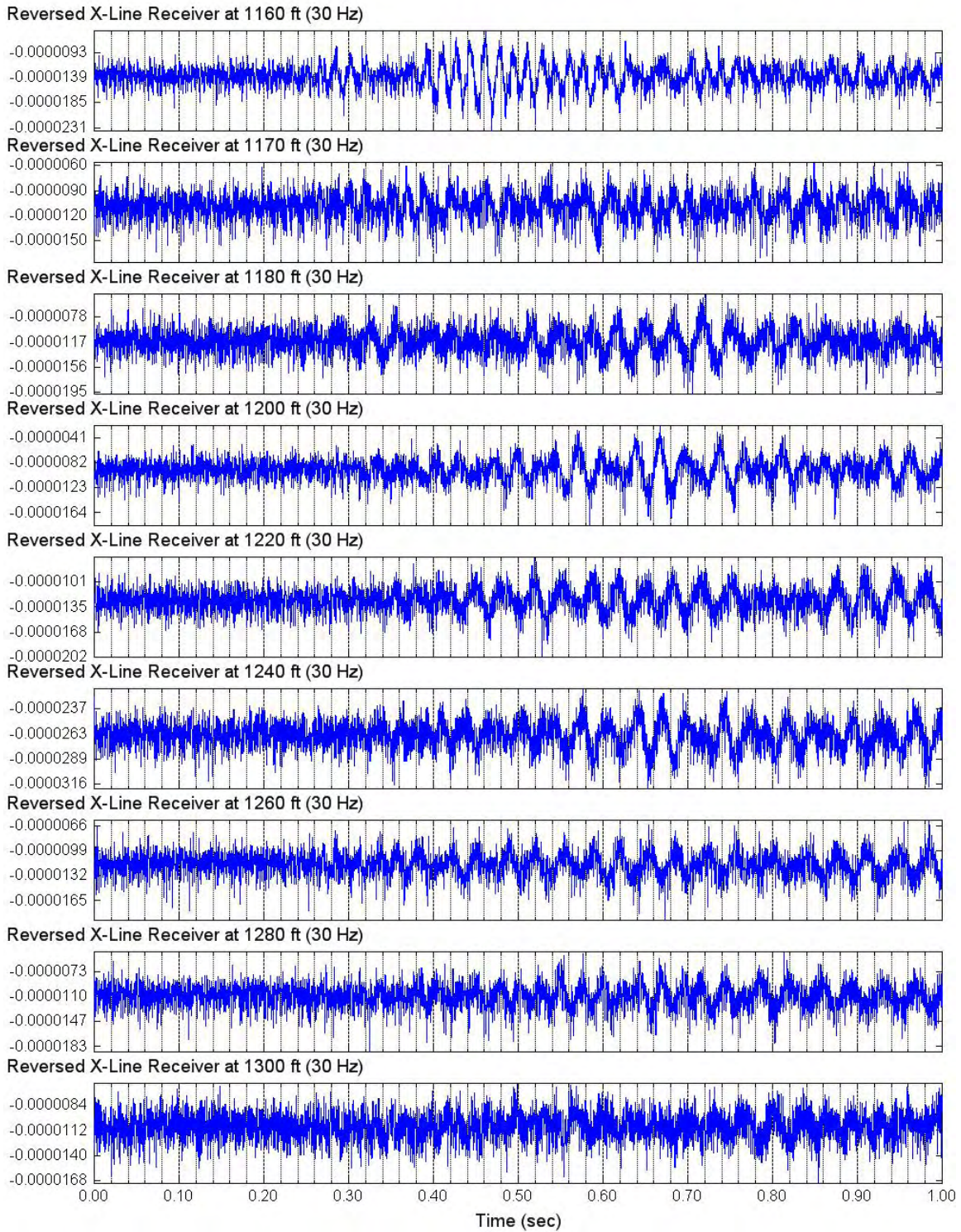


Figure 4.5.1 Unfiltered Forward S-Wave Signals of Lower Rotated In-Line Receiver (C4996)
Depths 360 to 455 ft; Input Signal: 5 Cycles of 50-Hz Sine Wave

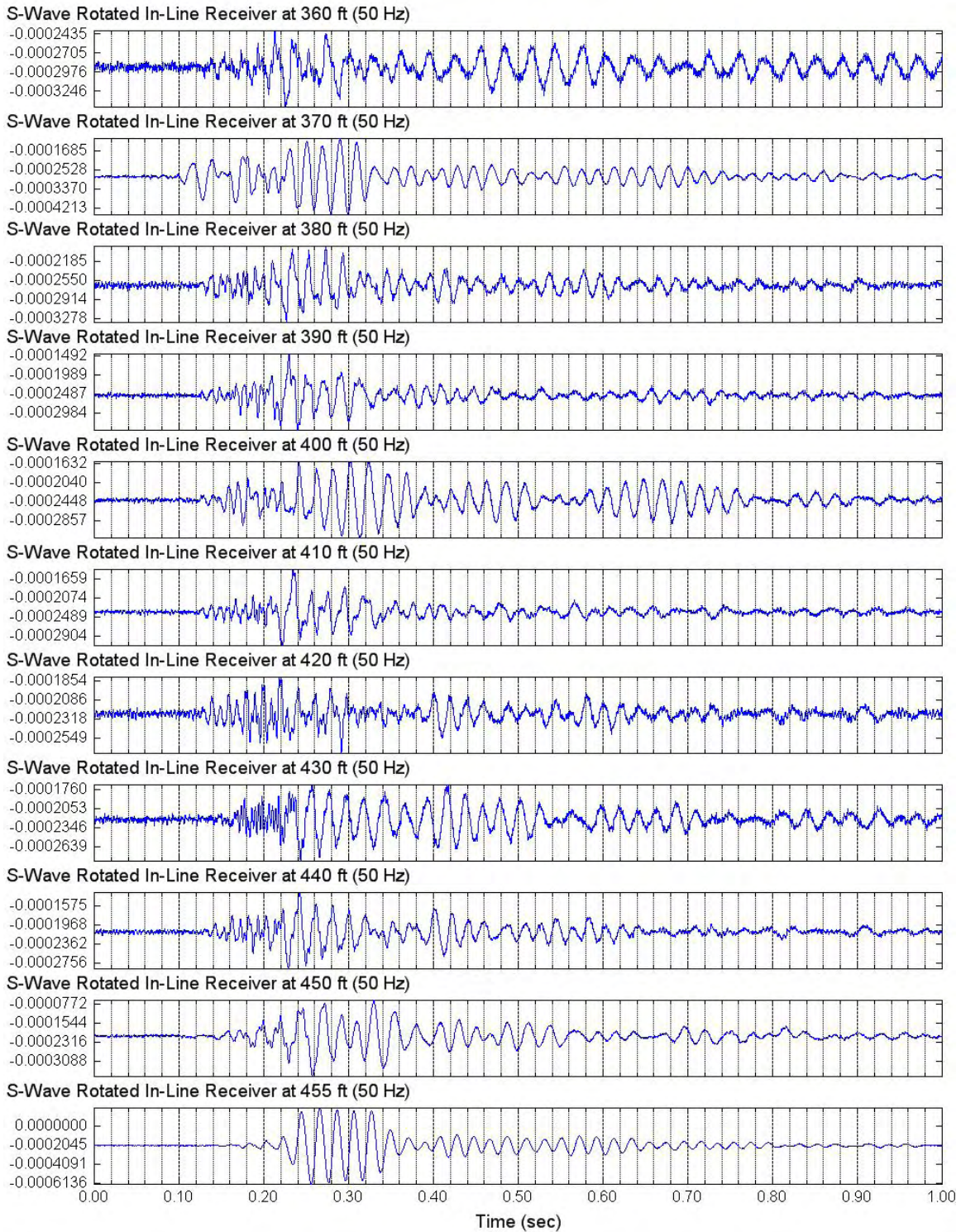


Figure 4.5.2 Unfiltered Forward S-Wave Signals of Lower Rotated In-Line Receiver (C4996)
Depths 460 to 520 ft; Input Signal: 5 Cycles of 50-Hz Sine Wave

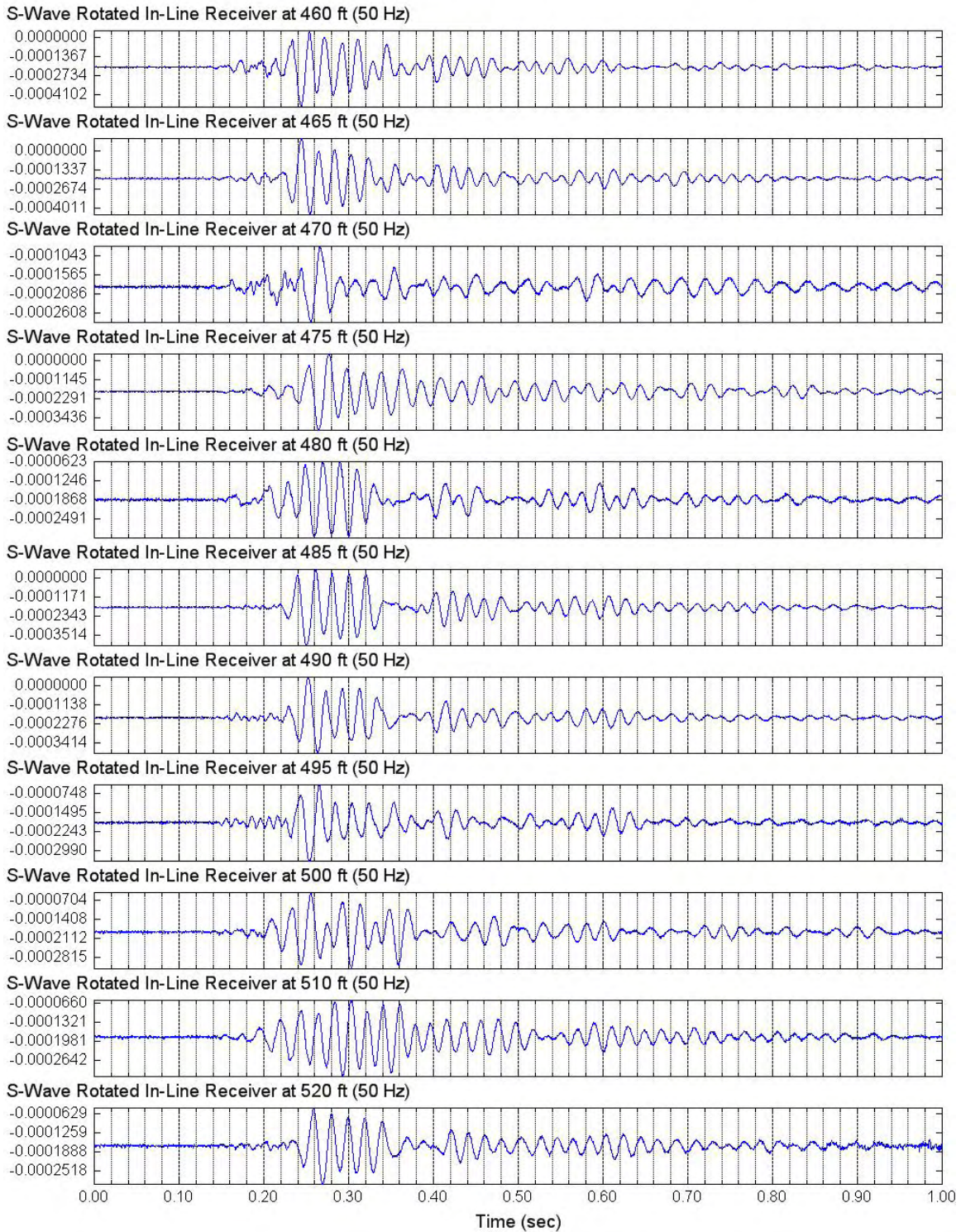


Figure 4.5.3 Unfiltered Forward S-Wave Signals of Lower Rotated In-Line Receiver (C4996)
Depths 530 to 630 ft; Input Signal: 5 Cycles of 50-Hz Sine Wave

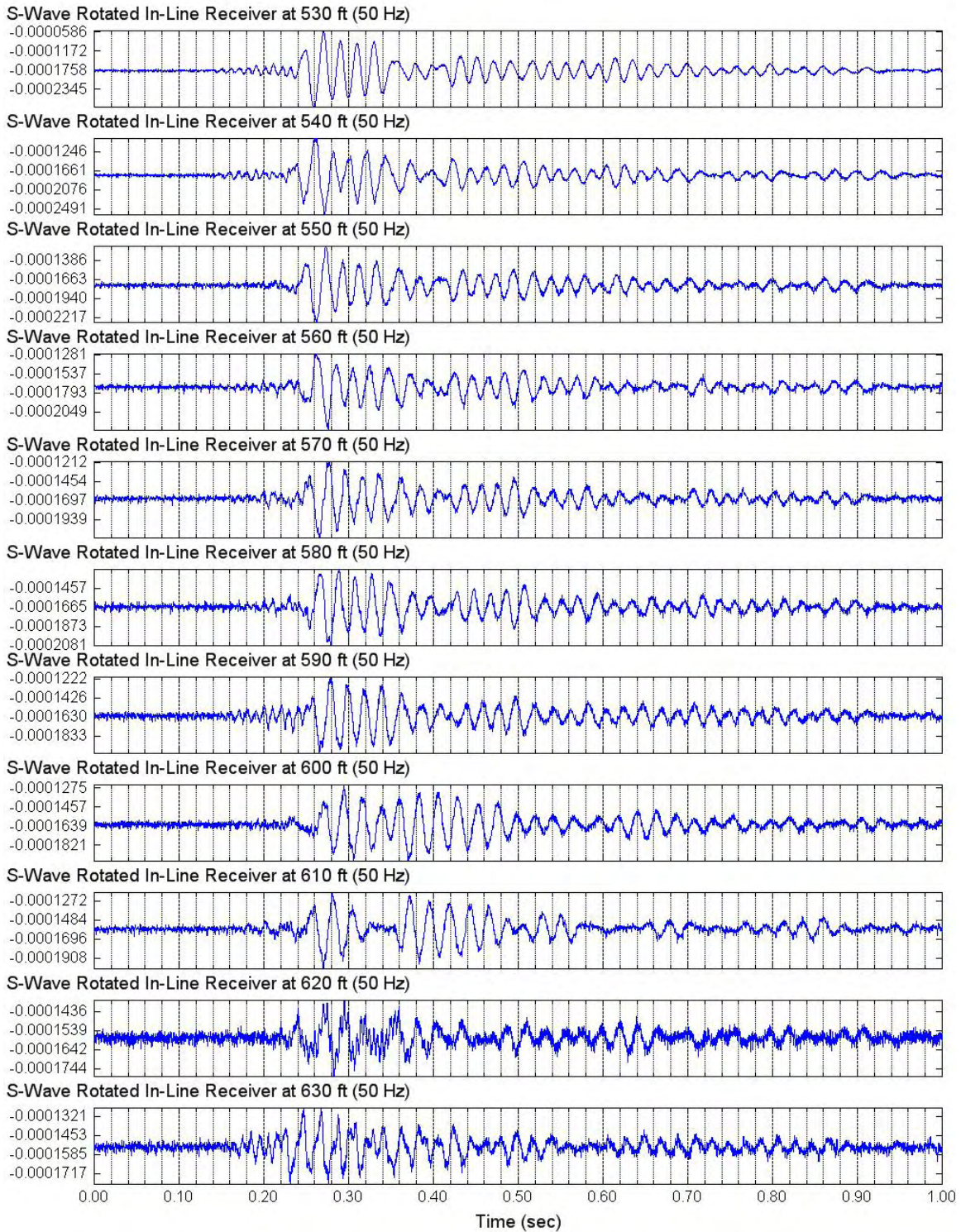


Figure 4.5.4 Unfiltered Forward S-Wave Signals of Lower Rotated In-Line Receiver (C4996)
Depths 640 to 720 ft; Input Signal: 5 Cycles of 50-Hz Sine Wave

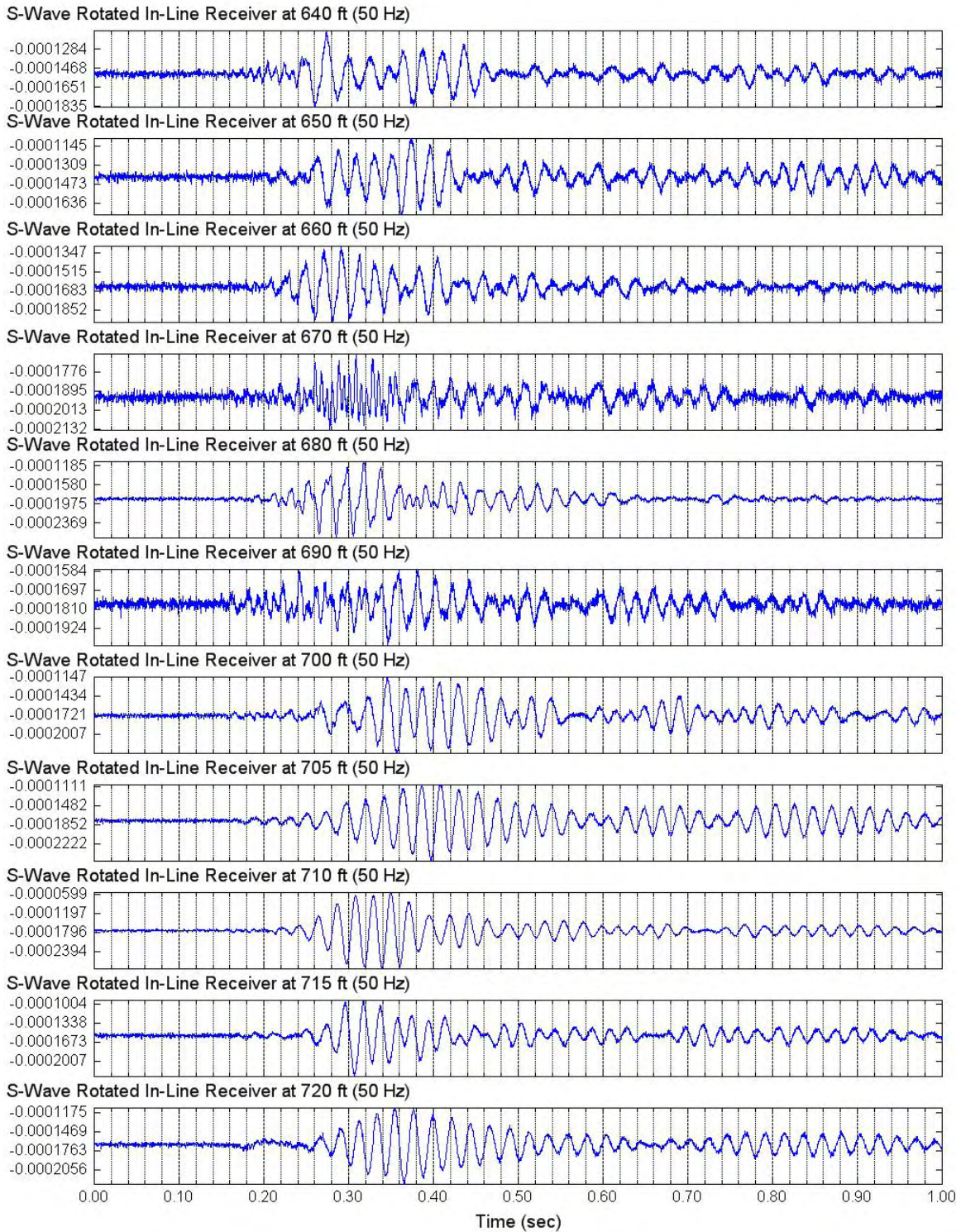


Figure 4.5.5 Unfiltered Forward S-Wave Signals of Lower Rotated In-Line Receiver (C4996)
Depths 640 to 720 ft; Input Signal: 5 Cycles of 50-Hz Sine Wave

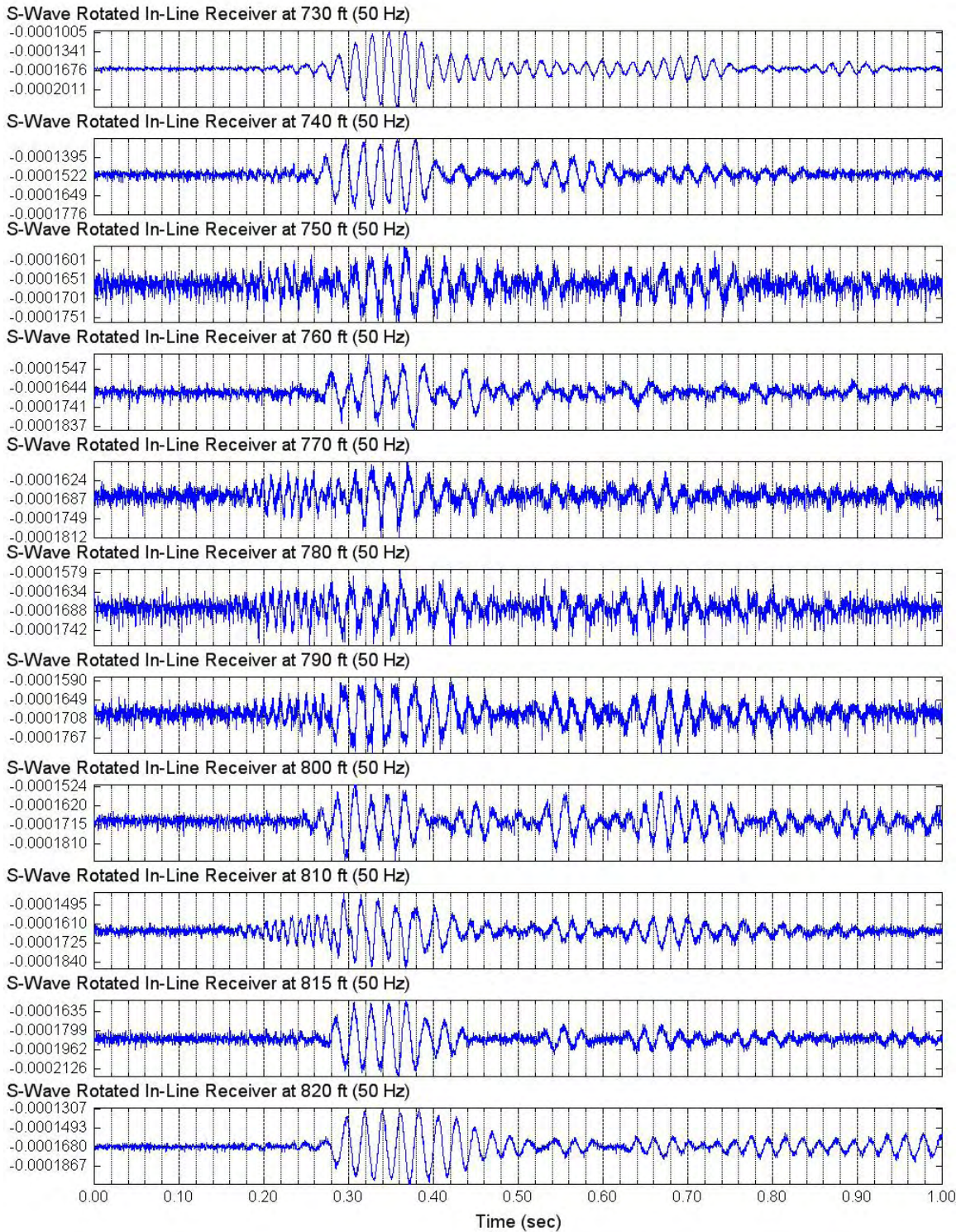


Figure 4.5.6 Unfiltered Forward S-Wave Signals of Lower Rotated In-Line Receiver (C4996)
Depths 830 to 960 ft; Input Signal: 5 Cycles of 50-Hz Sine Wave

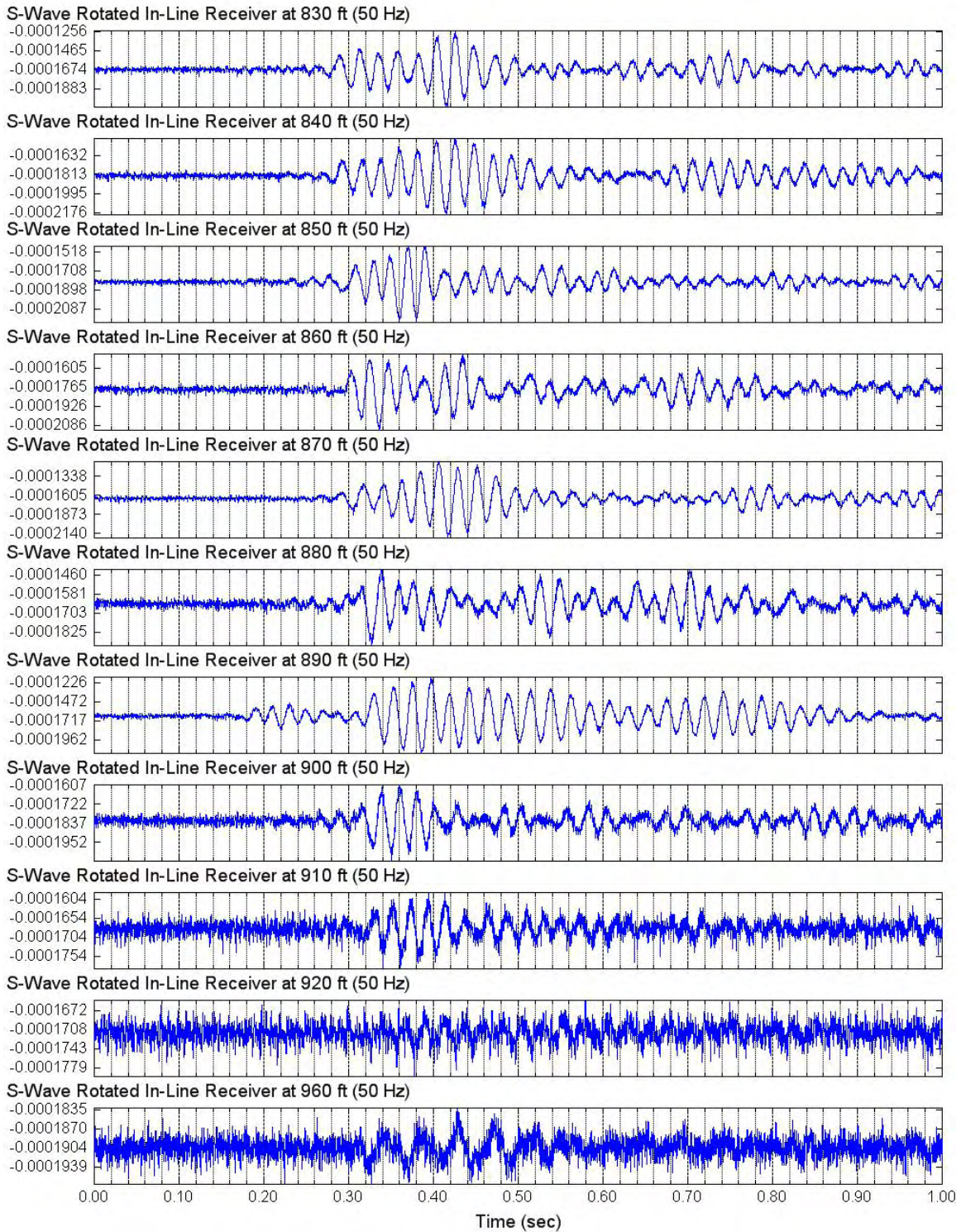


Figure 4.5.7 Unfiltered Forward S-Wave Signals of Lower Rotated In-Line Receiver (C4996)
Depths 910 to 980 ft; Input Signal: 4 Cycles of 20-Hz Sine Wave

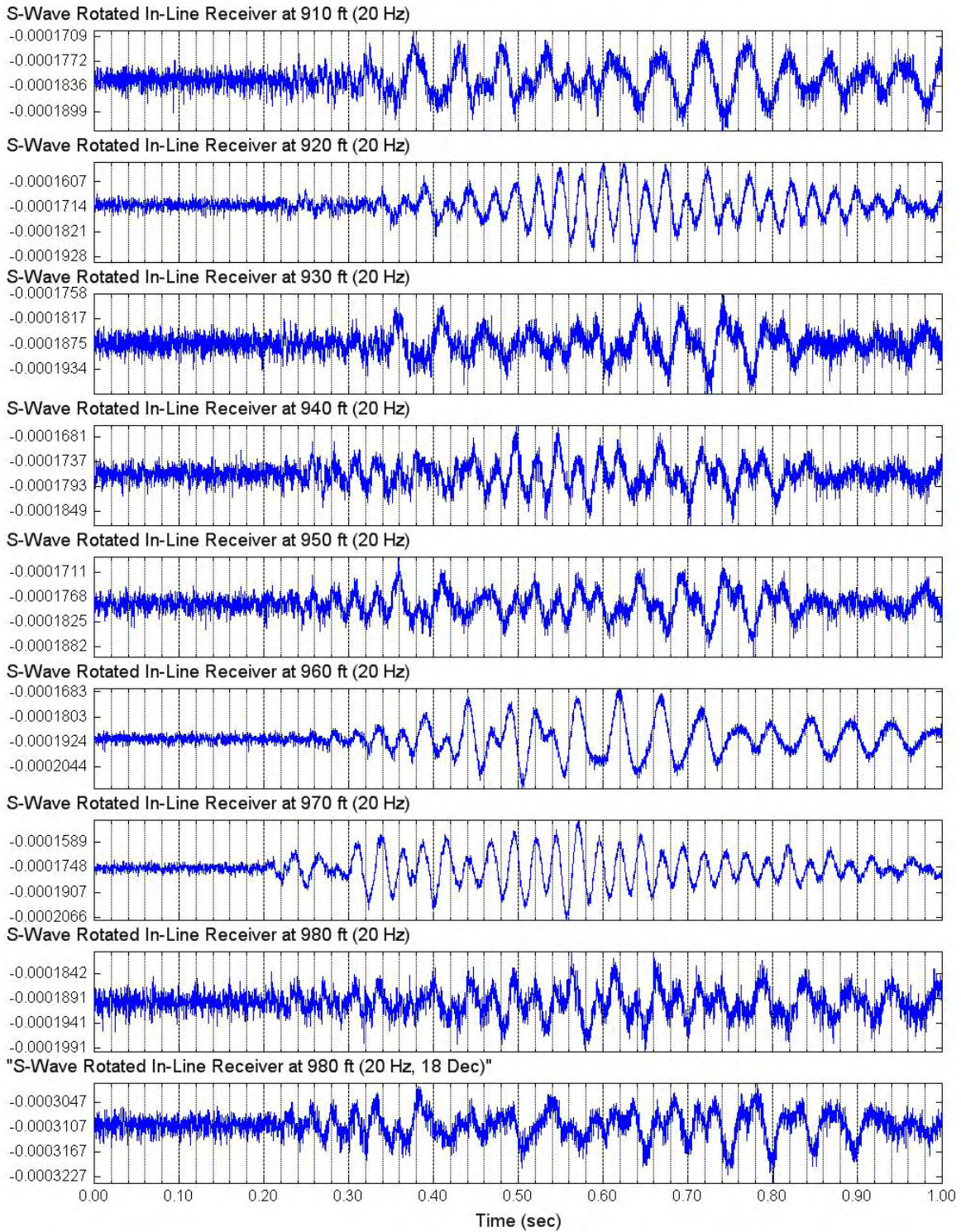


Figure 4.5.8 Unfiltered Forward S-Wave Signals of Lower Rotated In-Line Receiver (C4996)
Depths 980 to 1060 ft; Input Signal: 4 Cycles of 30-Hz Sine Wave

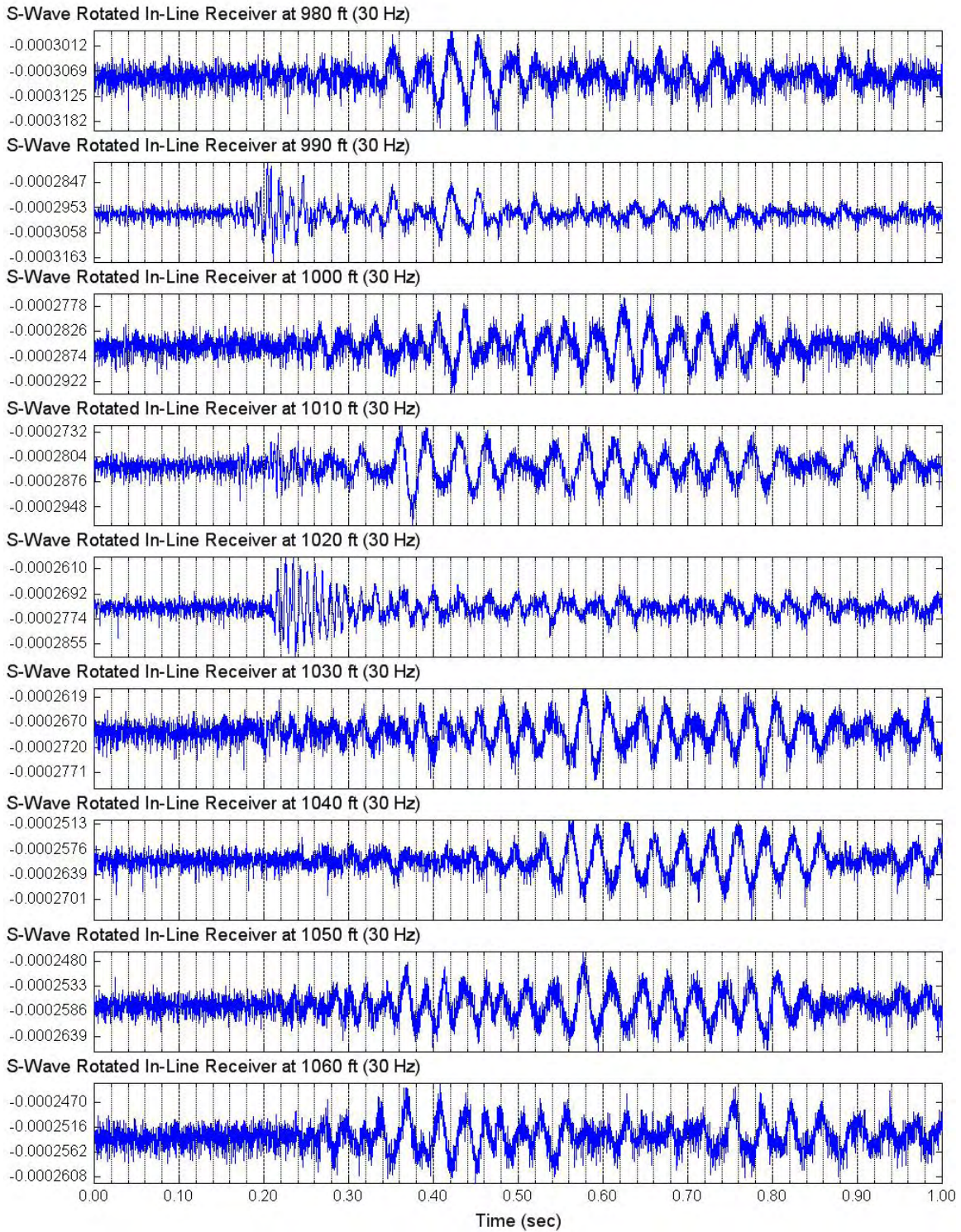


Figure 4.5.9 Unfiltered Forward S-Wave Signals of Lower Rotated In-Line Receiver (C4996)
Depths 1070 to 1150 ft; Input Signal: 4 Cycles of 30-Hz Sine Wave

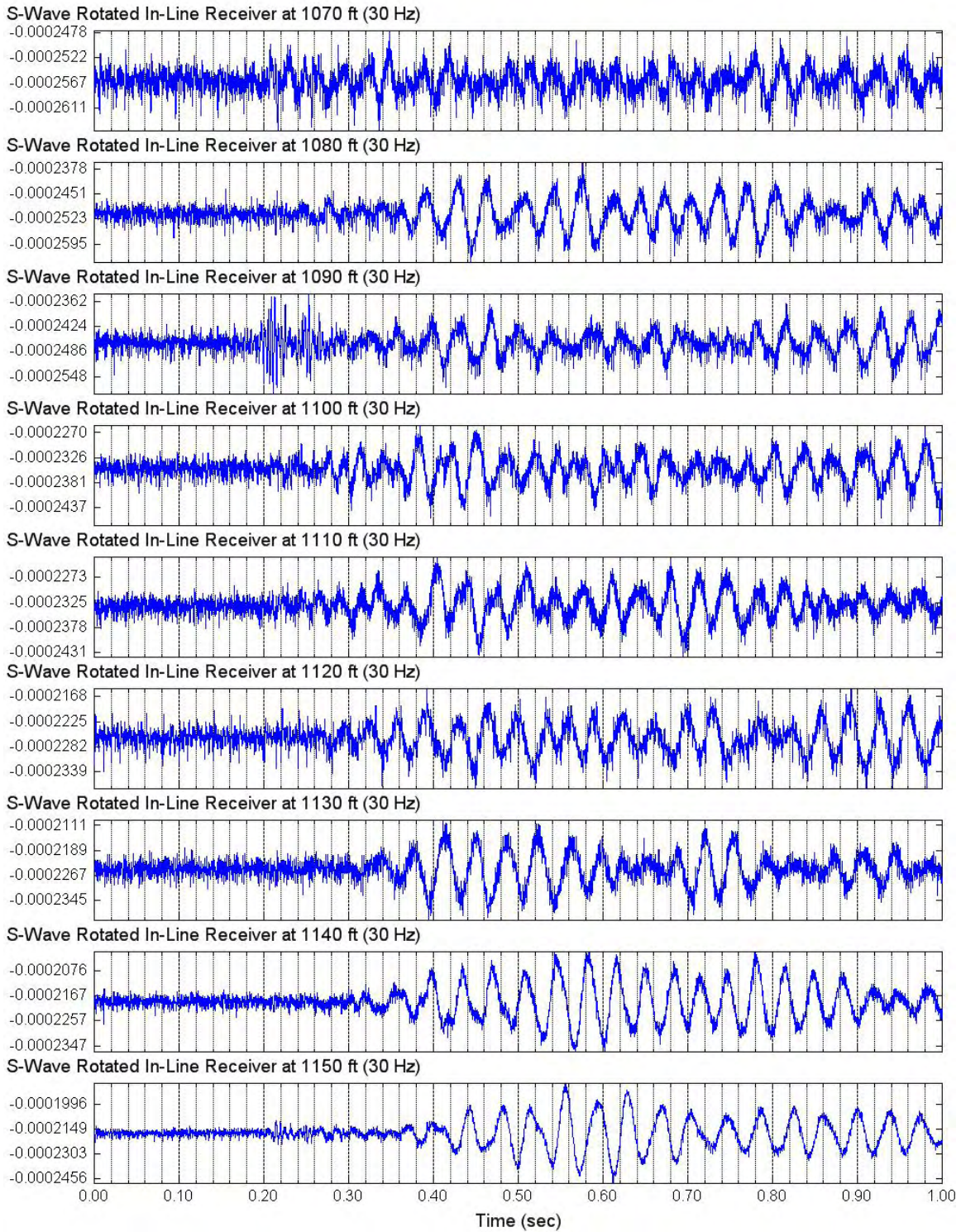


Figure 4.5.10 Unfiltered Forward S-Wave Signals of Lower Rotated In-Line Receiver (C4996)
Depths 1160 to 1300 ft; Input Signal: 4 Cycles of 30-Hz Sine Wave

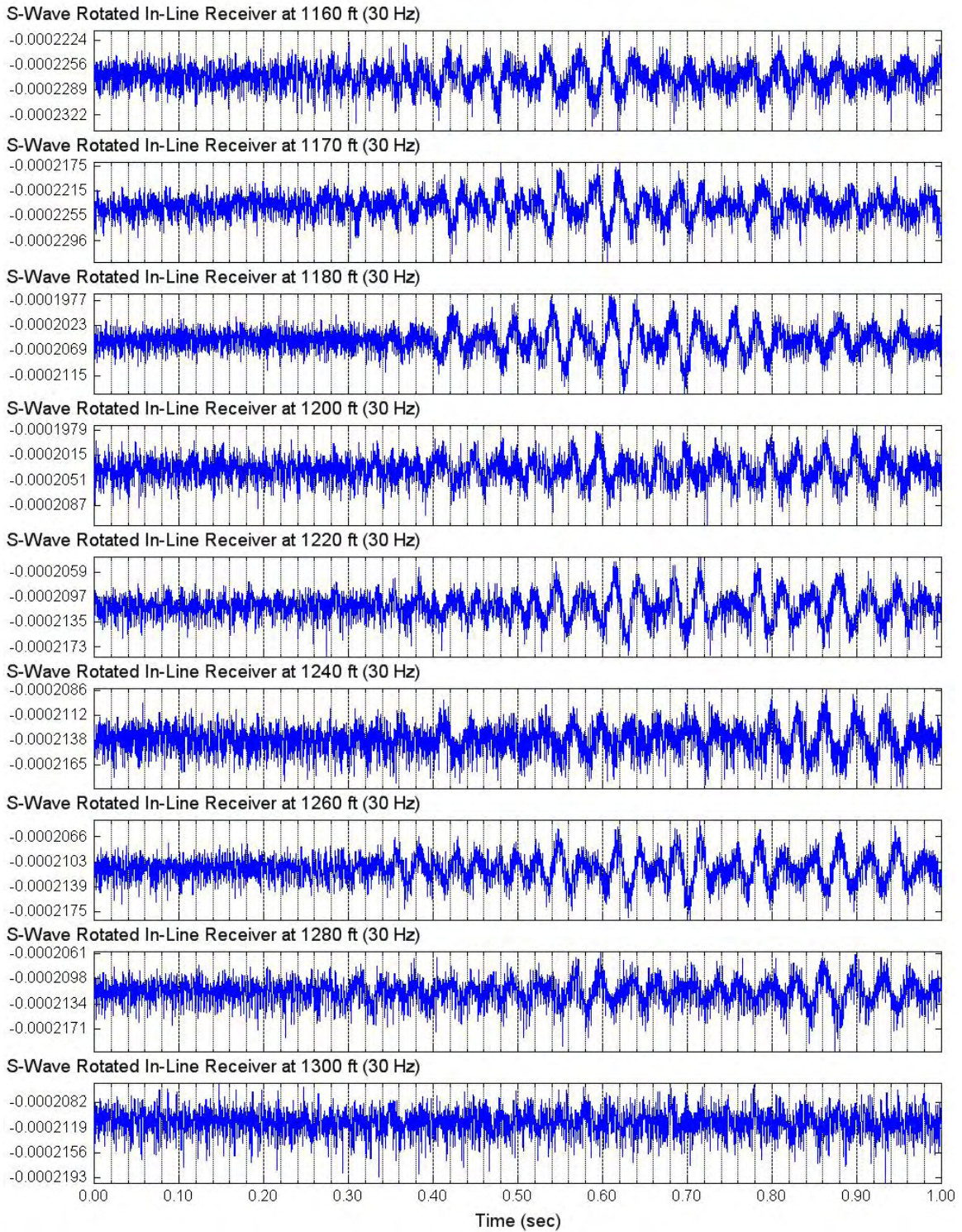


Figure 4.6.1 Unfiltered Reverse S-Wave Signals of Lower Rotated In-Line Receiver (C4996)
 Depths 360 to 455 ft; Input Signal: 5 Cycles of 50-Hz Sine Wave

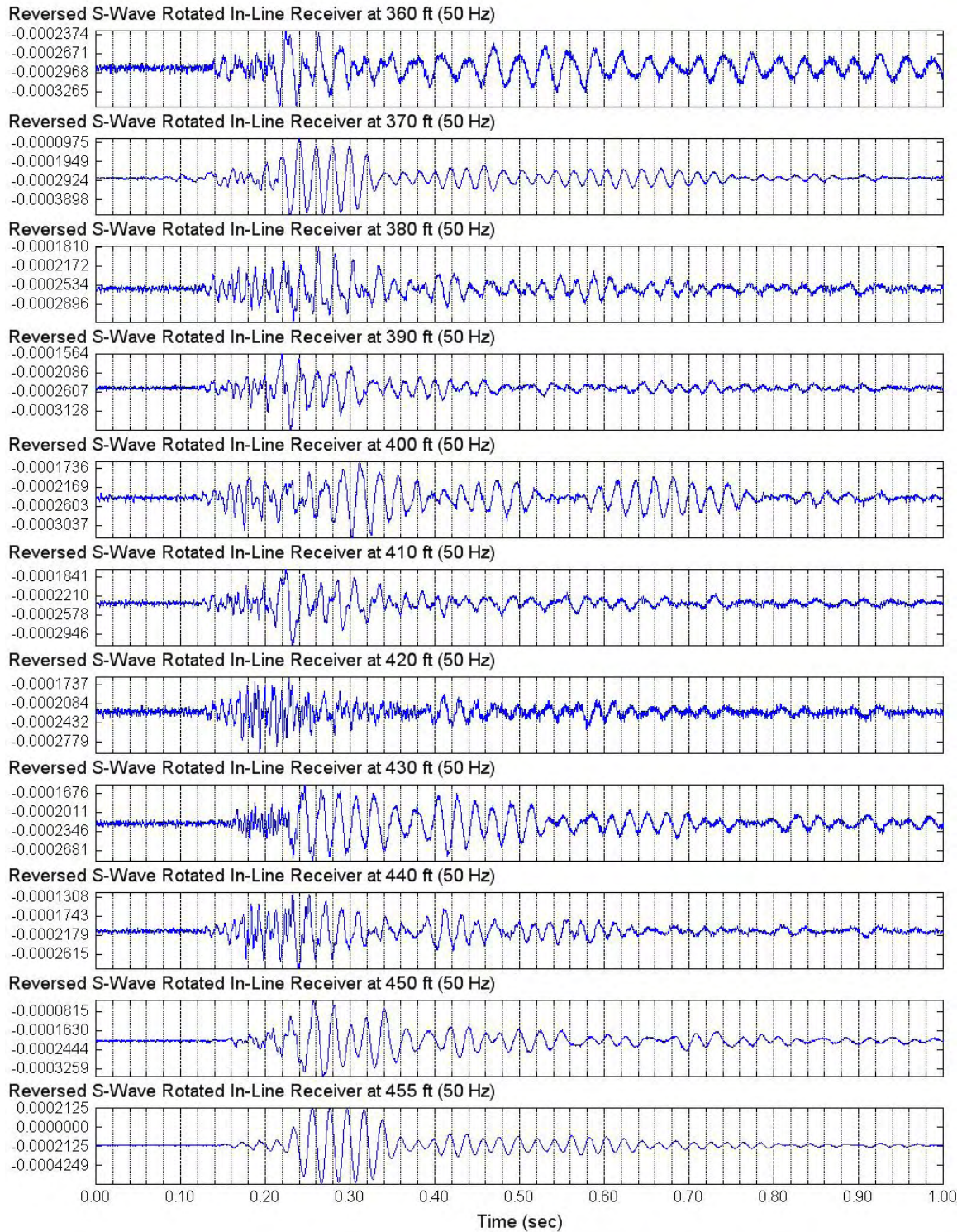


Figure 4.6.2 Unfiltered Reverse S-Wave Signals of Lower Rotated In-Line Receiver (C4996)
 Depths 460 to 520 ft; Input Signal: 5 Cycles of 50-Hz Sine Wave

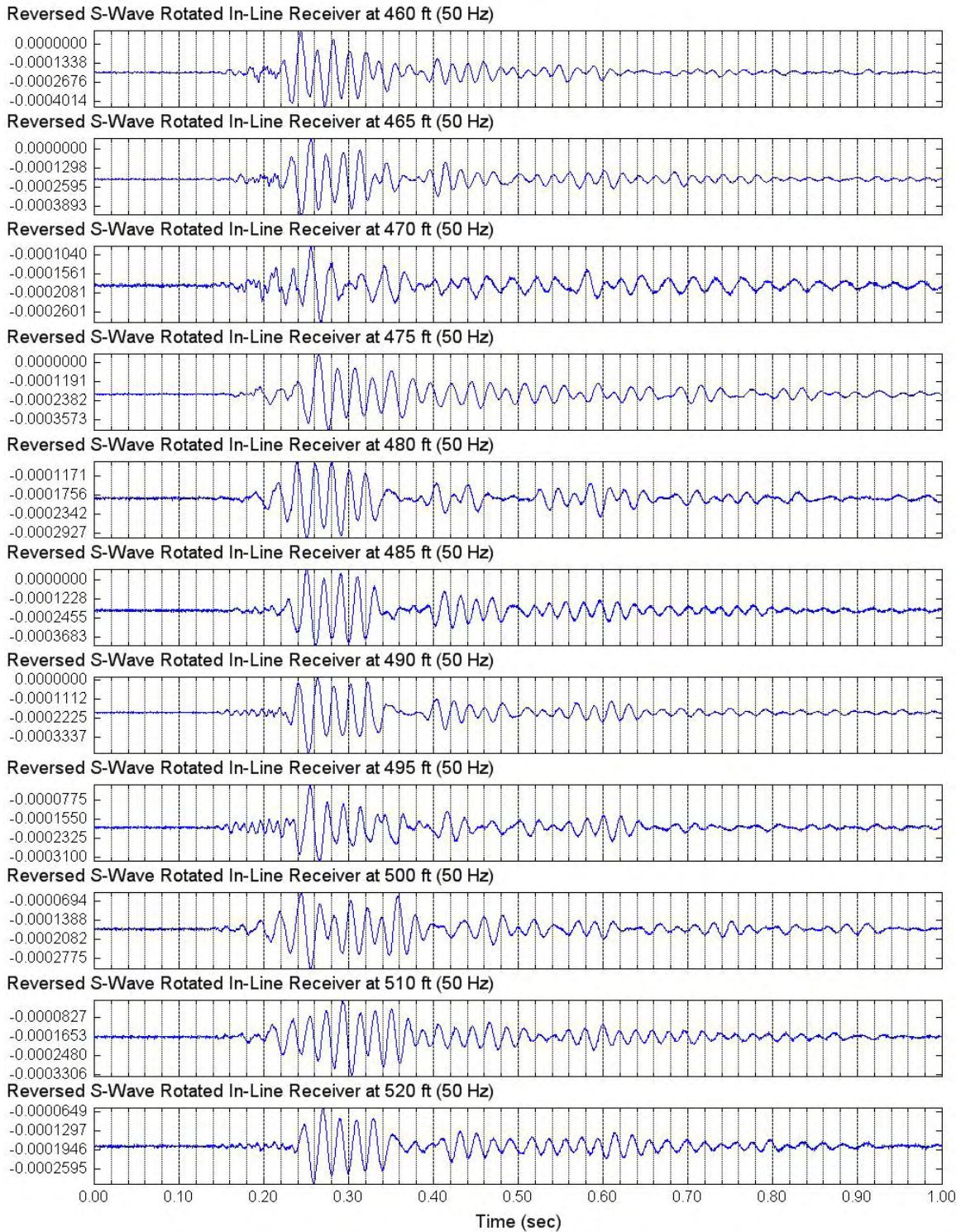


Figure 4.6.3 Unfiltered Reverse S-Wave Signals of Lower Rotated In-Line Receiver (C4996)
Depths 530 to 630 ft; Input Signal: 5 Cycles of 50-Hz Sine Wave

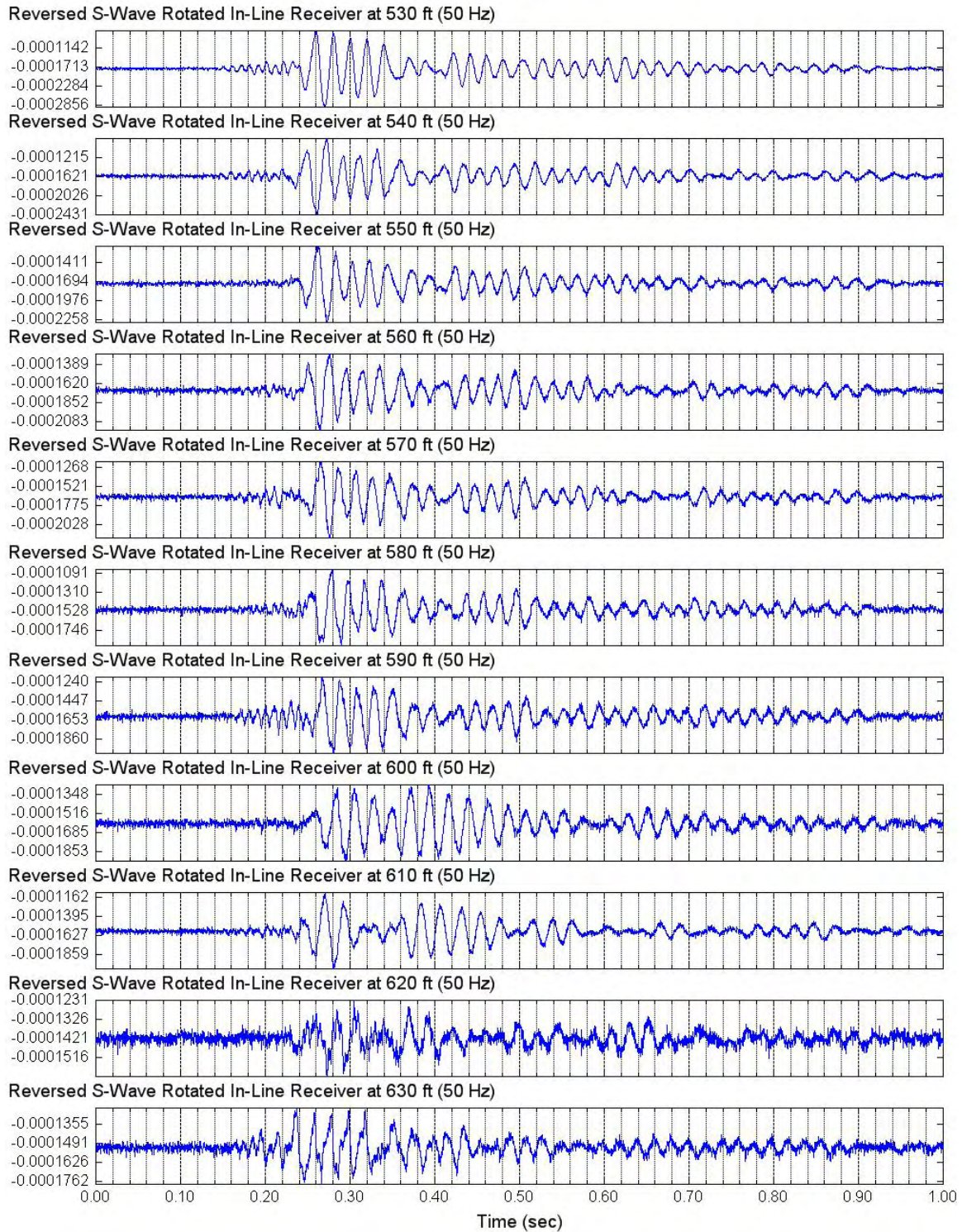


Figure 4.6.4 Unfiltered Reverse S-Wave Signals of Lower Rotated In-Line Receiver (C4996)
Depths 640 to 720 ft; Input Signal: 5 Cycles of 50-Hz Sine Wave

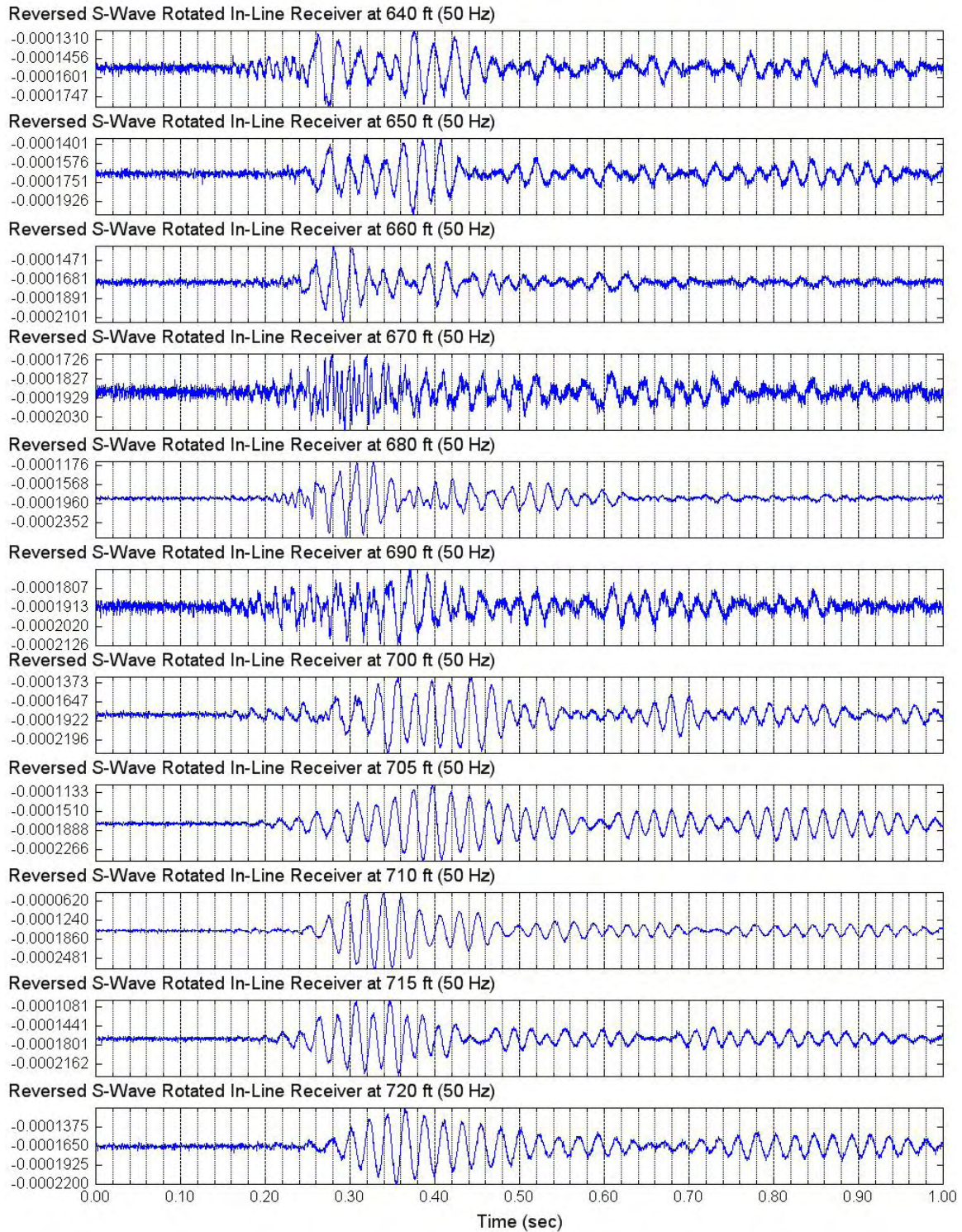


Figure 4.6.5 Unfiltered Reverse S-Wave Signals of Lower Rotated In-Line Receiver (C4996)
Depths 640 to 720 ft; Input Signal: 5 Cycles of 50-Hz Sine Wave

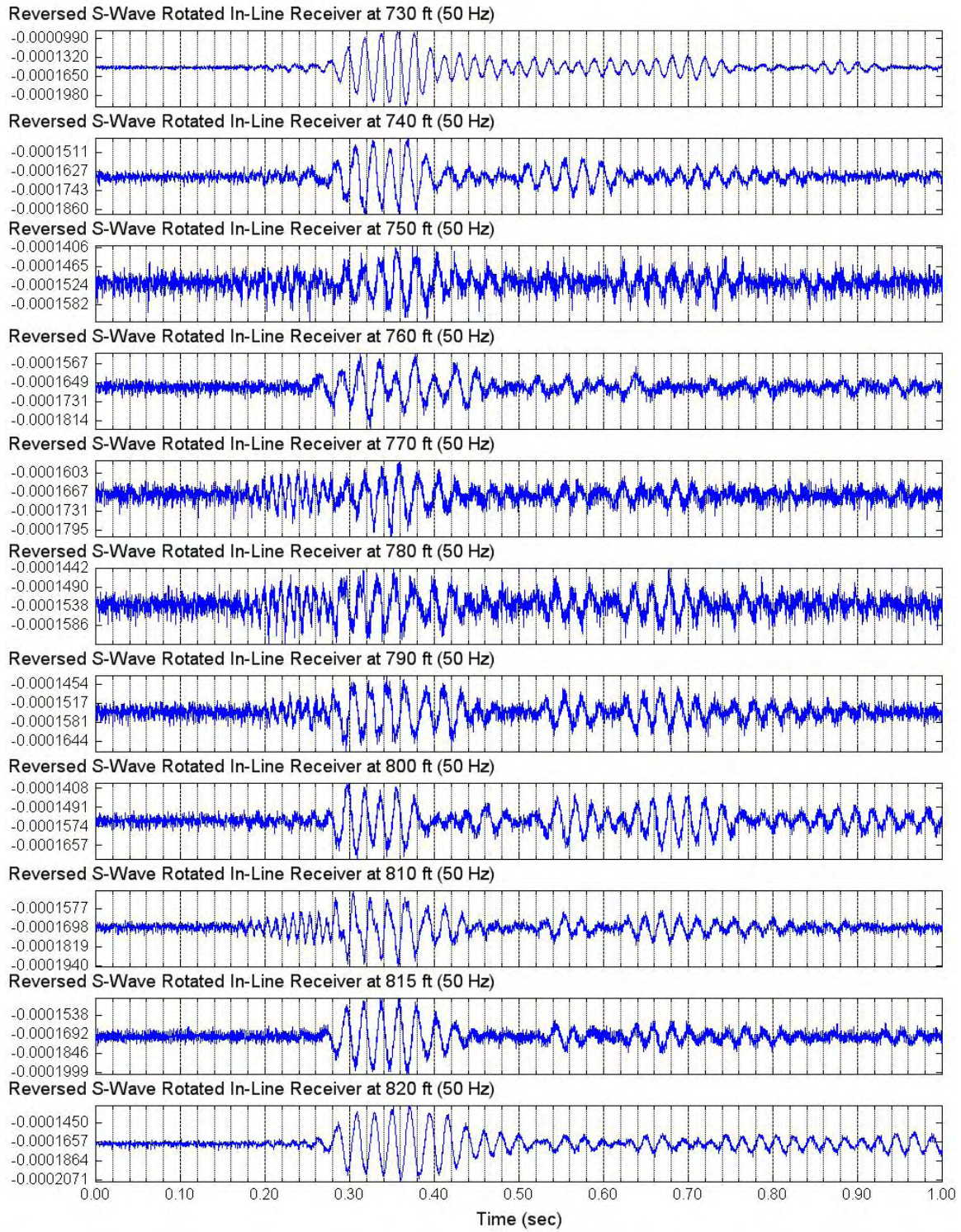


Figure 4.6.6 Unfiltered Reverse S-Wave Signals of Lower Rotated In-Line Receiver (C4996)
Depths 830 to 960 ft; Input Signal: 5 Cycles of 50-Hz Sine Wave

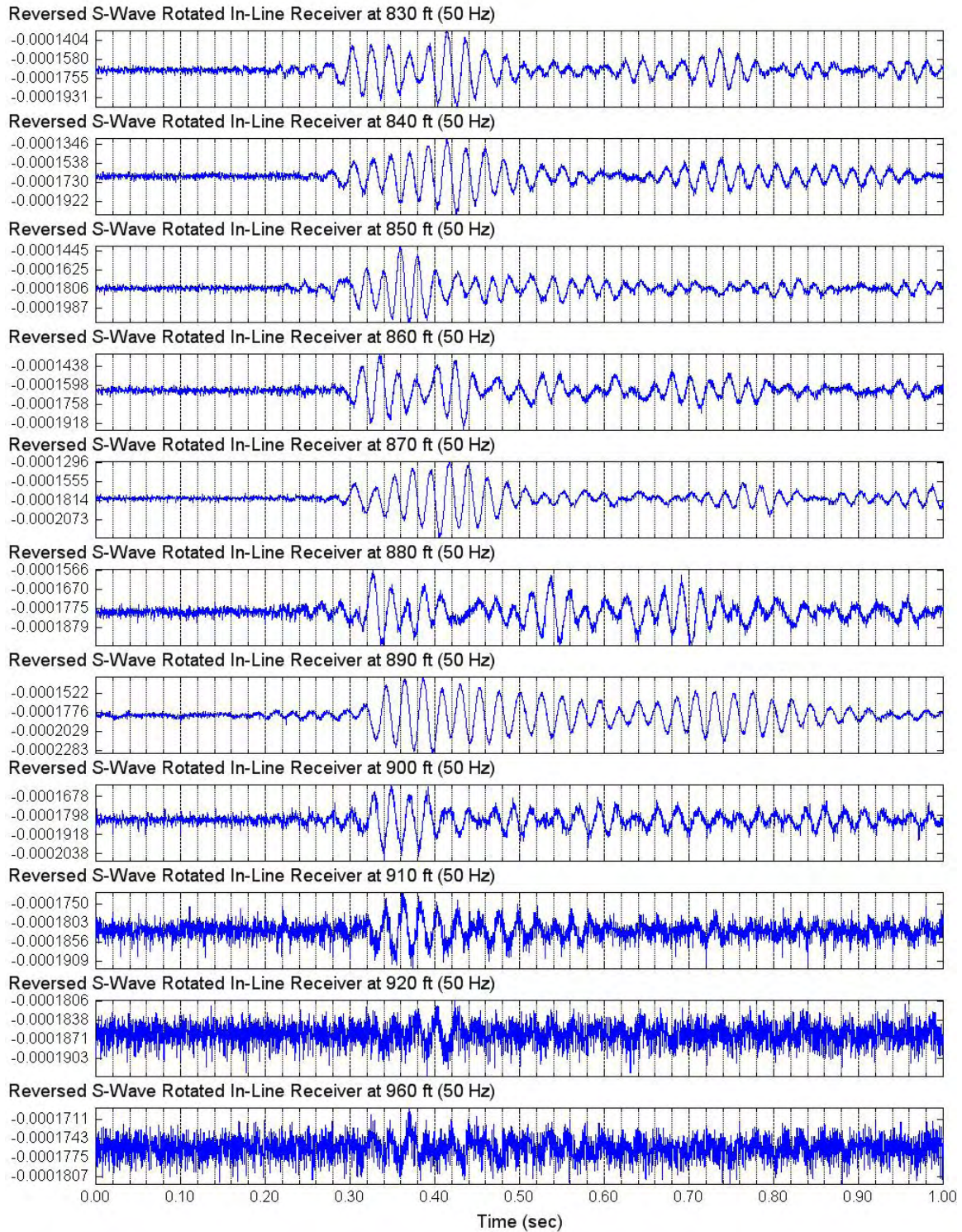


Figure 4.6.7 Unfiltered Reverse S-Wave Signals of Lower Rotated In-Line Receiver (C4996)
Depths 910 to 980 ft; Input Signal: 4 Cycles of 20-Hz Sine Wave

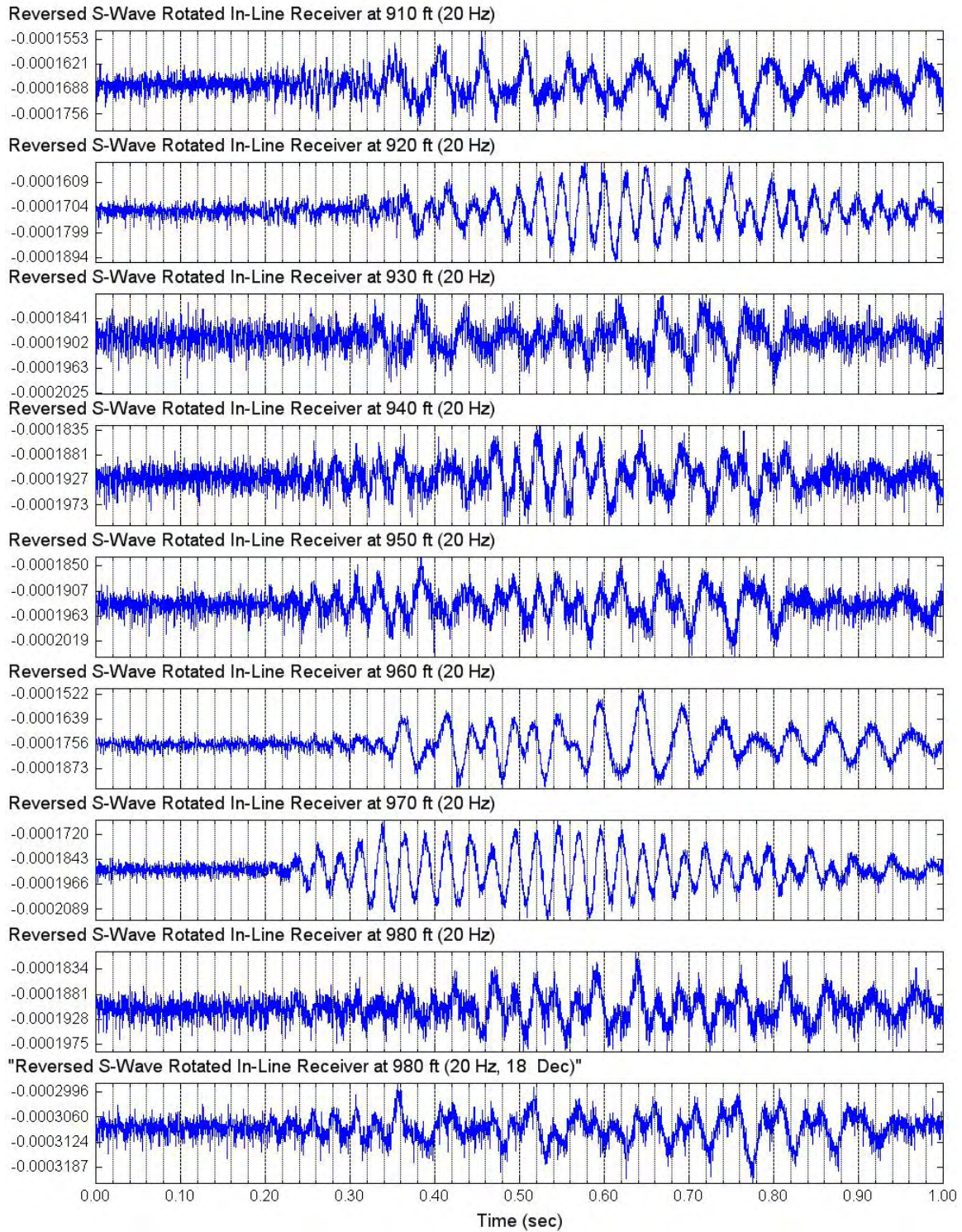


Figure 4.6.8 Unfiltered Reverse S-Wave Signals of Lower Rotated In-Line Receiver (C4996)
Depths 980 to 1060 ft; Input Signal: 4 Cycles of 30-Hz Sine Wave

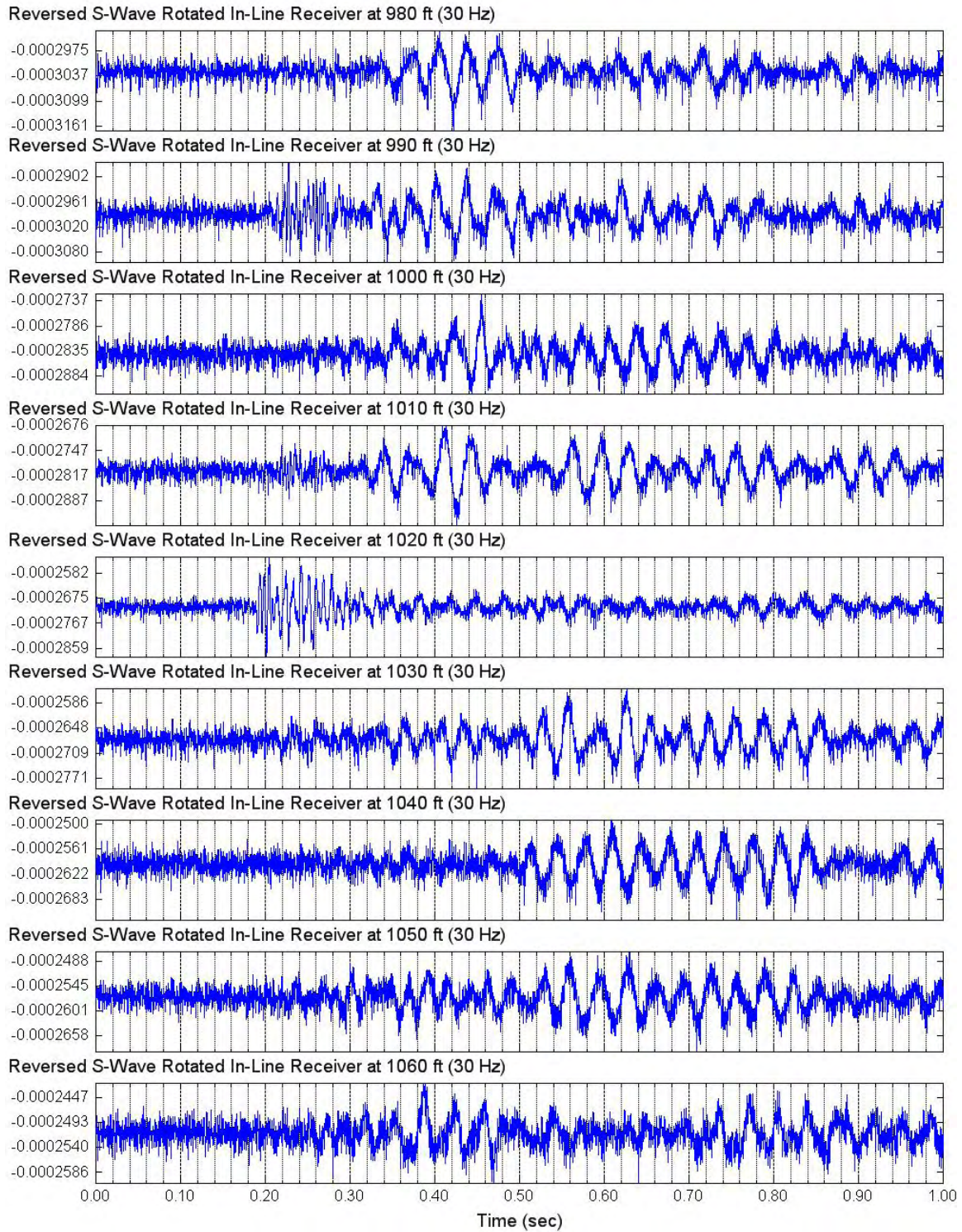


Figure 4.6.9 Unfiltered Reverse S-Wave Signals of Lower Rotated In-Line Receiver (C4996)
Depths 1070 to 1150 ft; Input Signal: 4 Cycles of 30-Hz Sine Wave

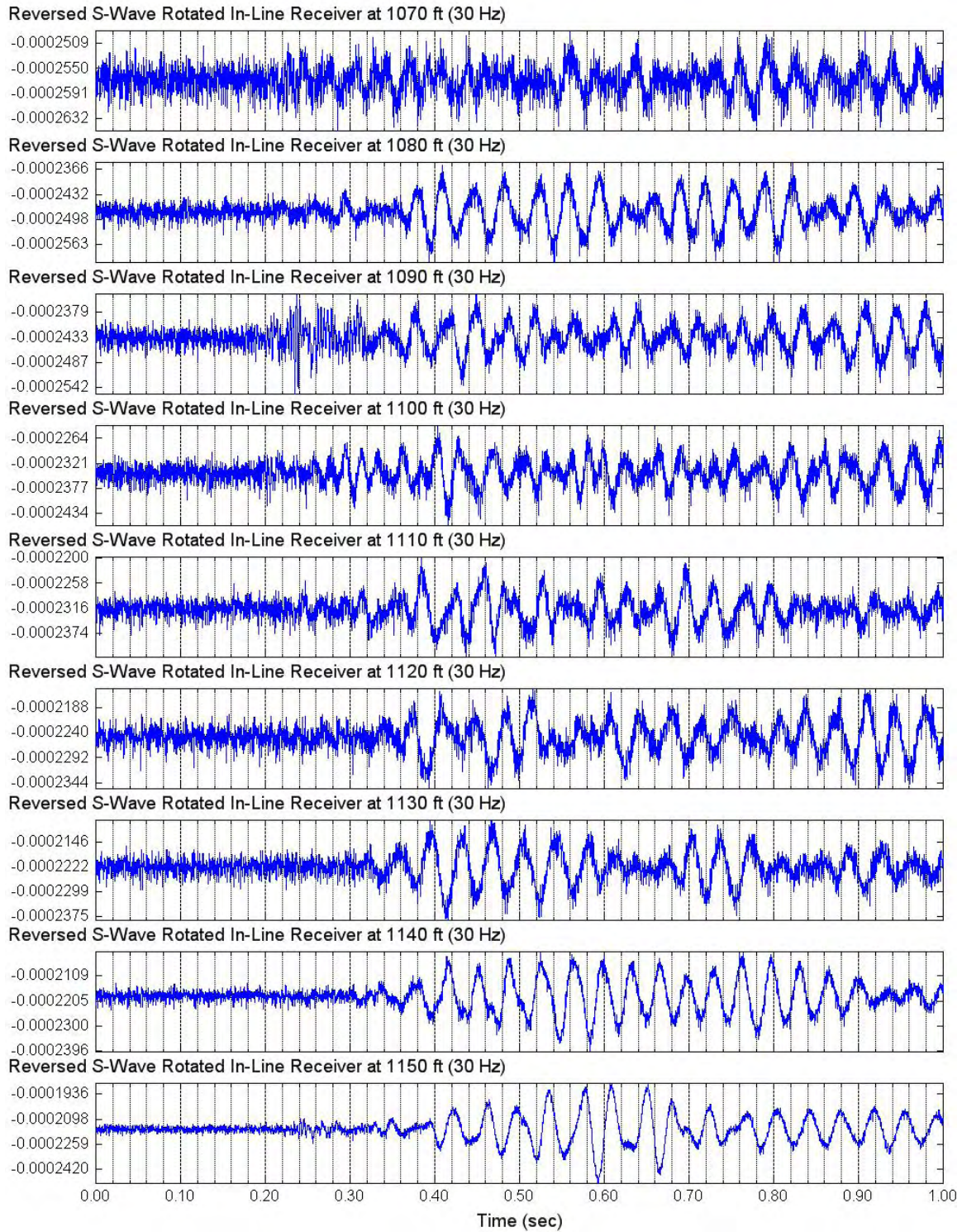
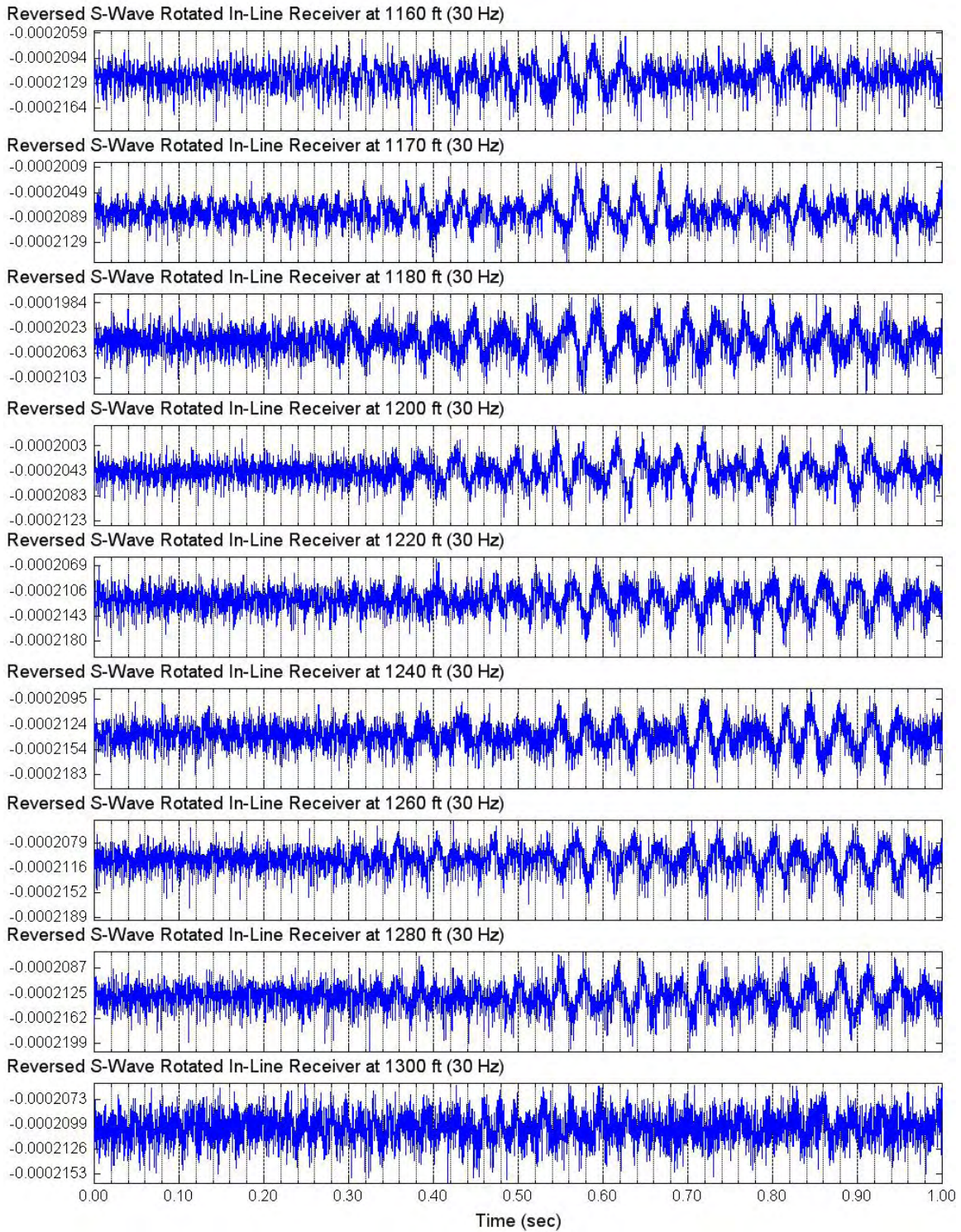


Figure 4.6.10 Unfiltered Reverse S-Wave Signals of Lower Rotated In-Line Receiver (C4996)
Depths 1160 to 1300 ft; Input Signal: 4 Cycles of 30-Hz Sine Wave



Section 5: Unfiltered S-Wave Records of Reaction Mass

Section 5 includes all unfiltered S-wave signals of the reaction mass accelerometer.

1. Figures 5.1 to 5.6 present unfiltered reaction mass horizontal (S-wave) acceleration at Borehole C4996, depths 360 to 960 ft; input signal: 5 cycles of 50-Hz sine wave.
2. Figure 5.7 presents unfiltered reaction mass horizontal (S-wave) acceleration at Borehole C4996, depths 910 to 980 ft; input signal: 4 cycles of 20-Hz sine wave.
3. Figures 5.8 to 5.10 present unfiltered reaction mass horizontal (S-wave) acceleration at Borehole C4996, depths 980 to 1300 ft; input signal: 4 cycles of 30-Hz sine wave.

Figure 5.1 Unfiltered S-Wave Signals of Reaction Mass Accelerometer (C4996)
Depths 360 to 455 ft; Input Signal: 5 Cycles of 50-Hz Sine Wave

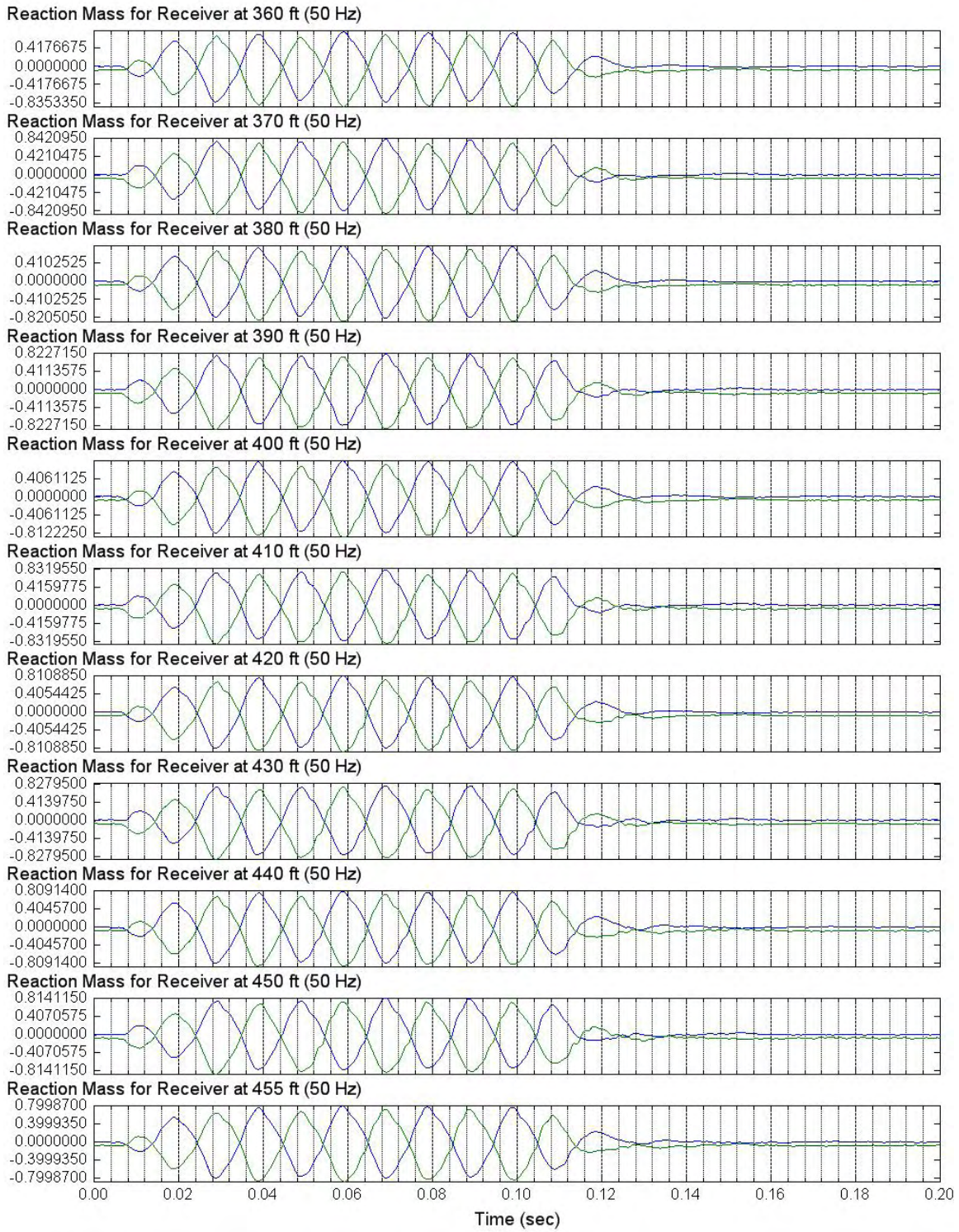


Figure 5.2 Unfiltered S-Wave Signals of Reaction Mass Accelerometer (C4996)
Depths 460 to 520 ft; Input Signal: 5 Cycles of 50-Hz Sine Wave

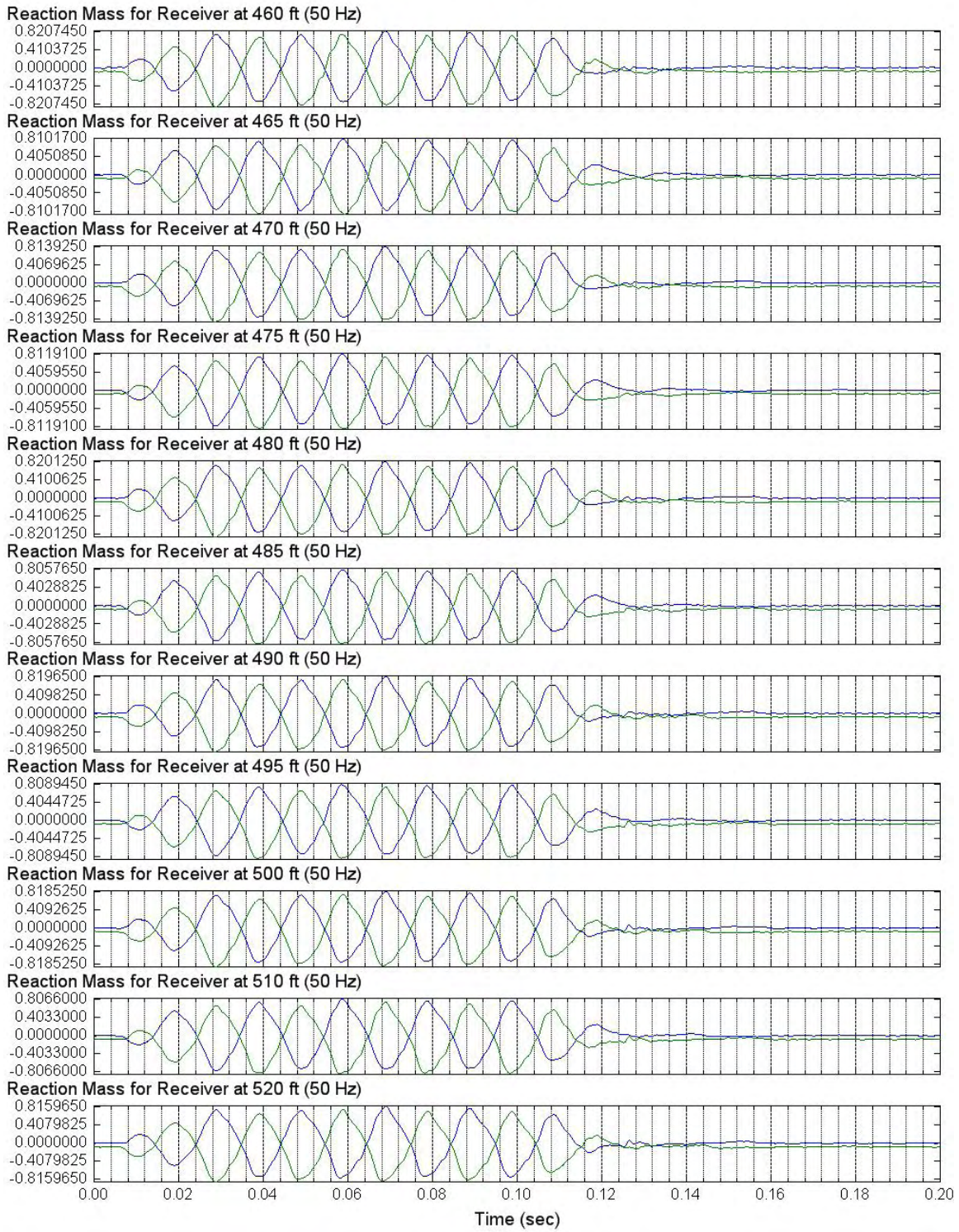


Figure 5.3 Unfiltered S-Wave Signals of Reaction Mass Accelerometer (C4996)
Depths 530 to 630 ft; Input Signal: 5 Cycles of 50-Hz Sine Wave

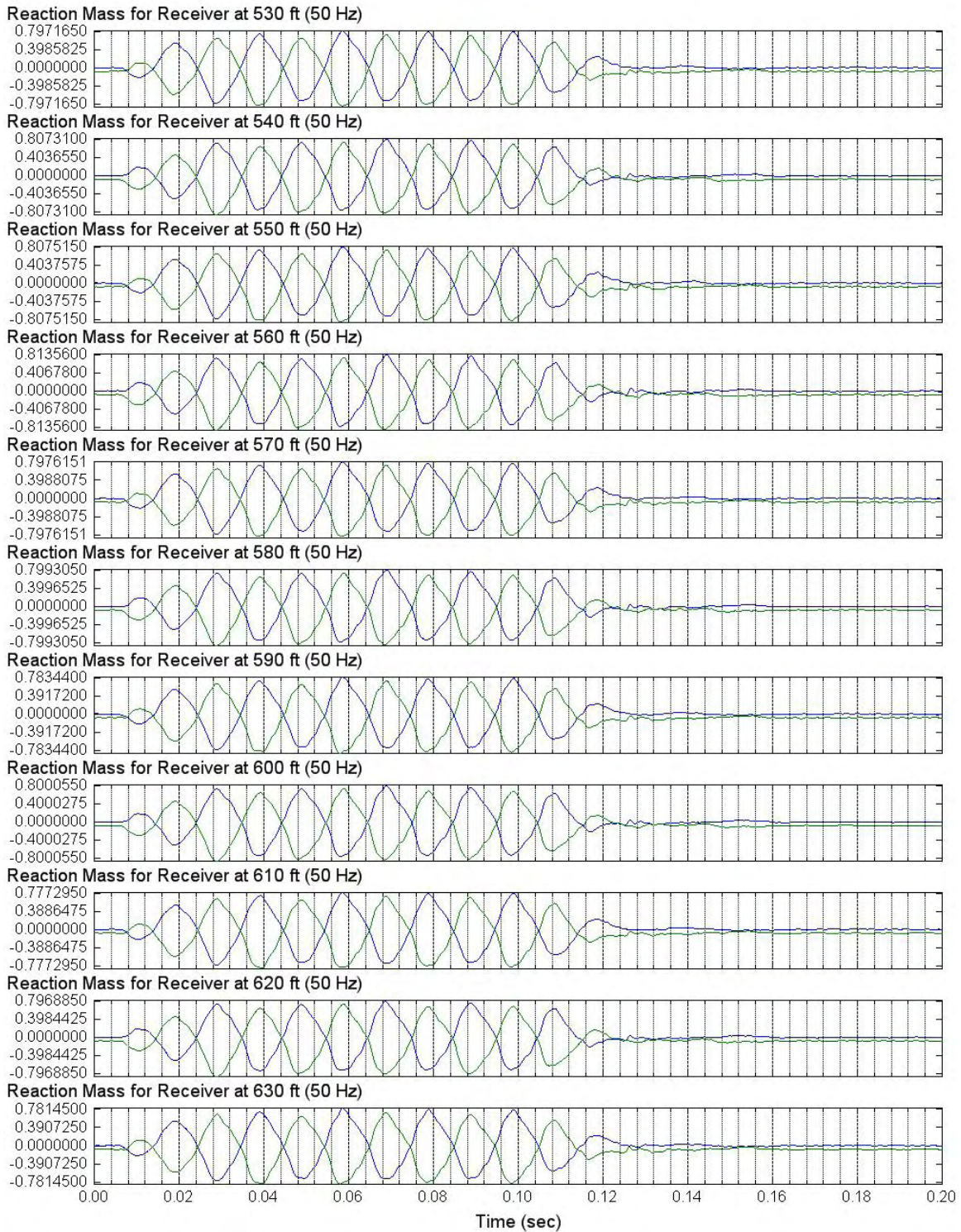


Figure 5.4 Unfiltered S-Wave Signals of Reaction Mass Accelerometer (C4996)
Depths 640 to 720 ft; Input Signal: 5 Cycles of 50-Hz Sine Wave

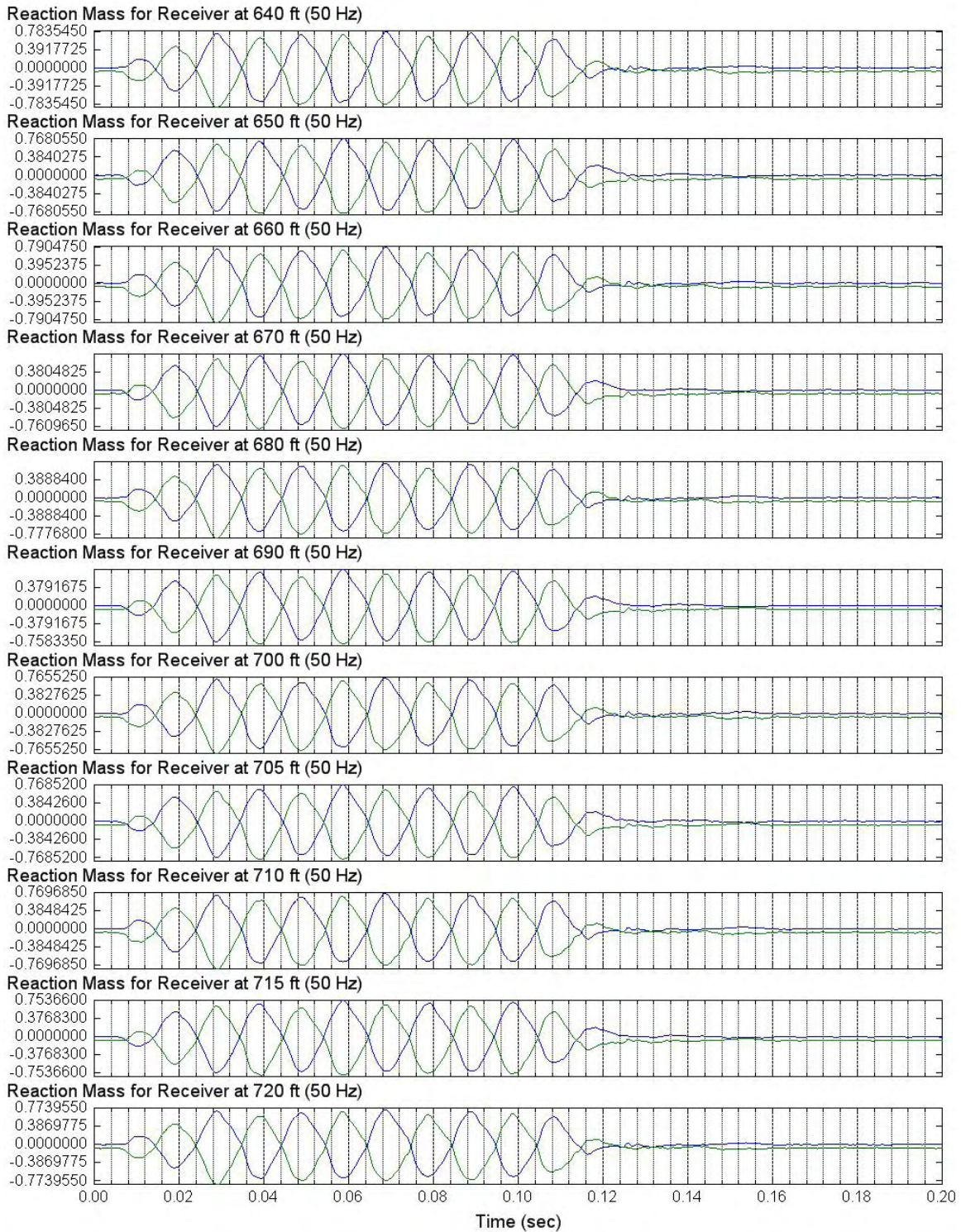


Figure 5.5 Unfiltered S-Wave Signals of Reaction Mass Accelerometer (C4996)
Depths 730 to 820 ft; Input Signal: 5 Cycles of 50-Hz Sine Wave

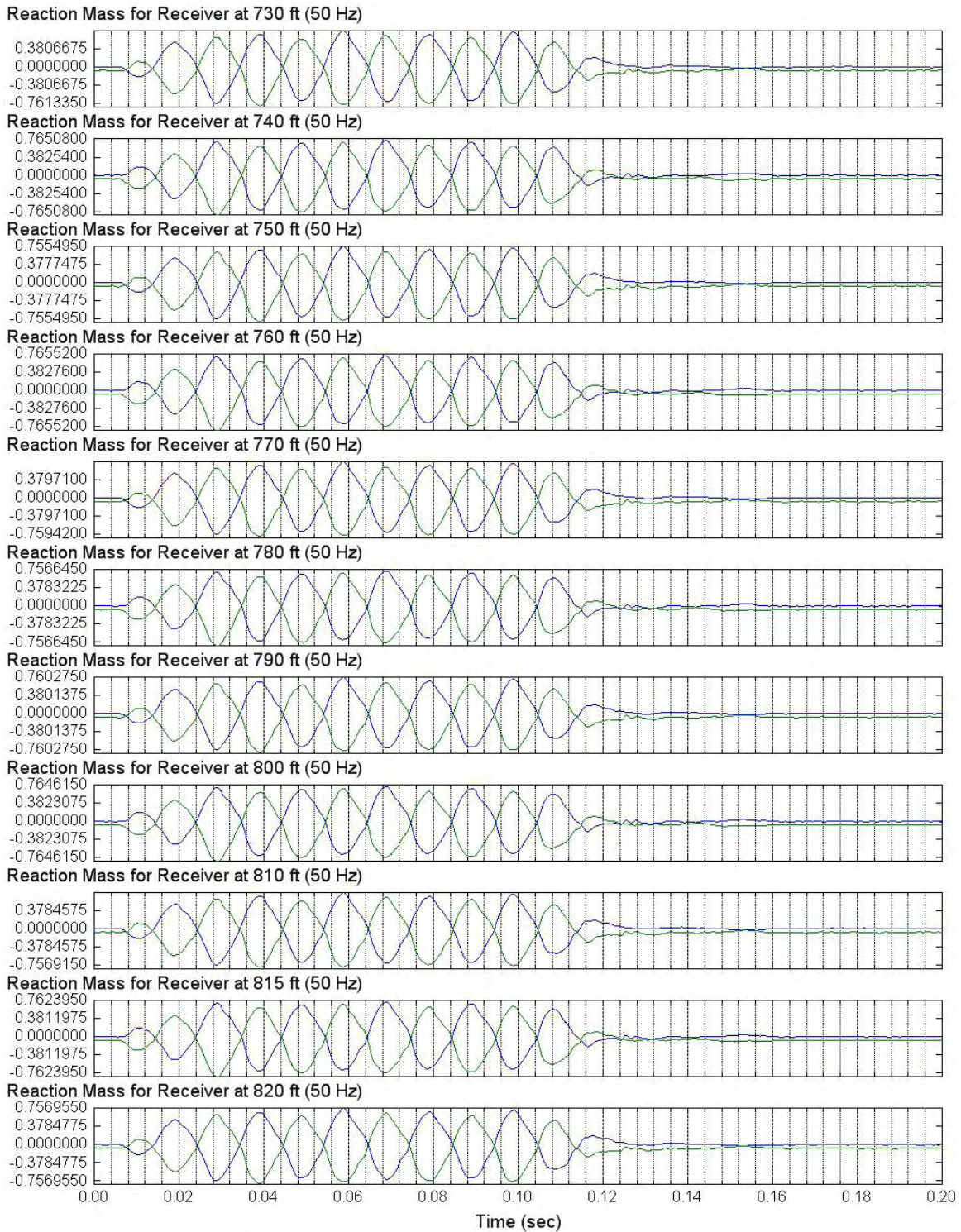


Figure 5.6 Unfiltered S-Wave Signals of Reaction Mass Accelerometer (C4996)
Depths 830 to 960 ft; Input Signal: 5 Cycles of 50-Hz Sine Wave

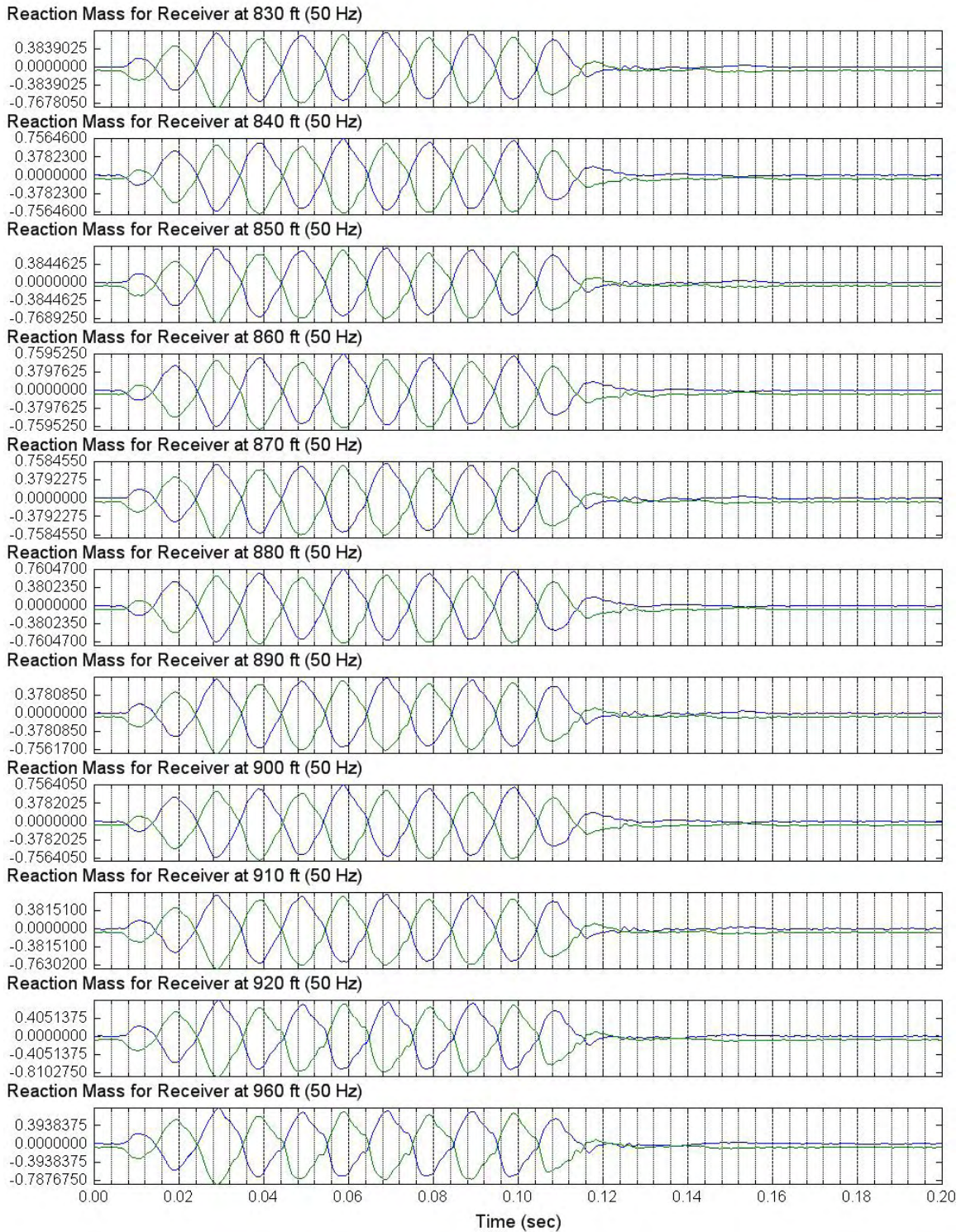


Figure 5.7 Unfiltered S-Wave Signals of Reaction Mass Accelerometer (C4996)
 Depths 910 to 980 ft; Input Signal: 4 Cycles of 20-Hz Sine Wave

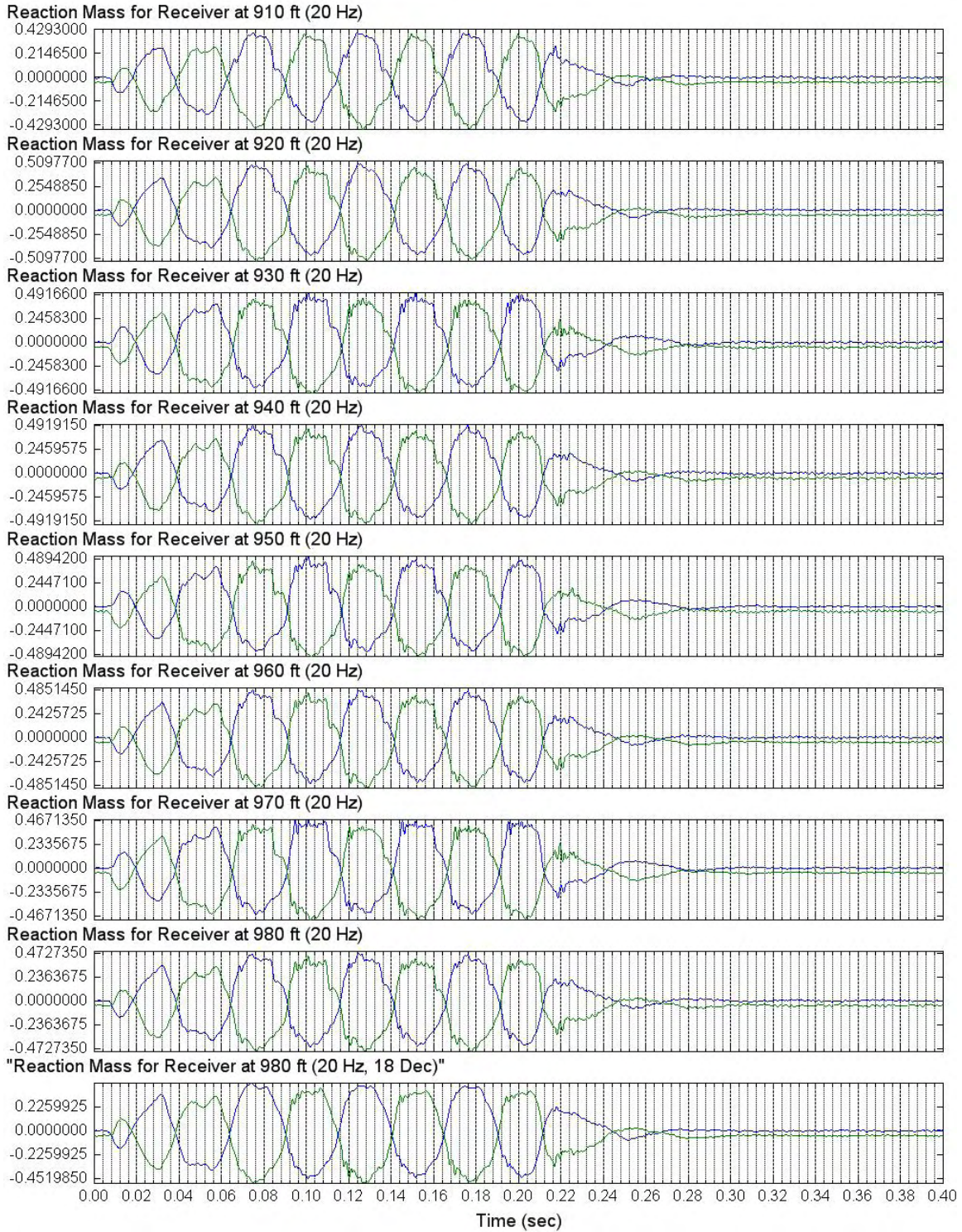


Figure 5.8 Unfiltered S-Wave Signals of Reaction Mass Accelerometer (C4996)
Depths 980 to 1060 ft; Input Signal: 4 Cycles of 30-Hz Sine Wave

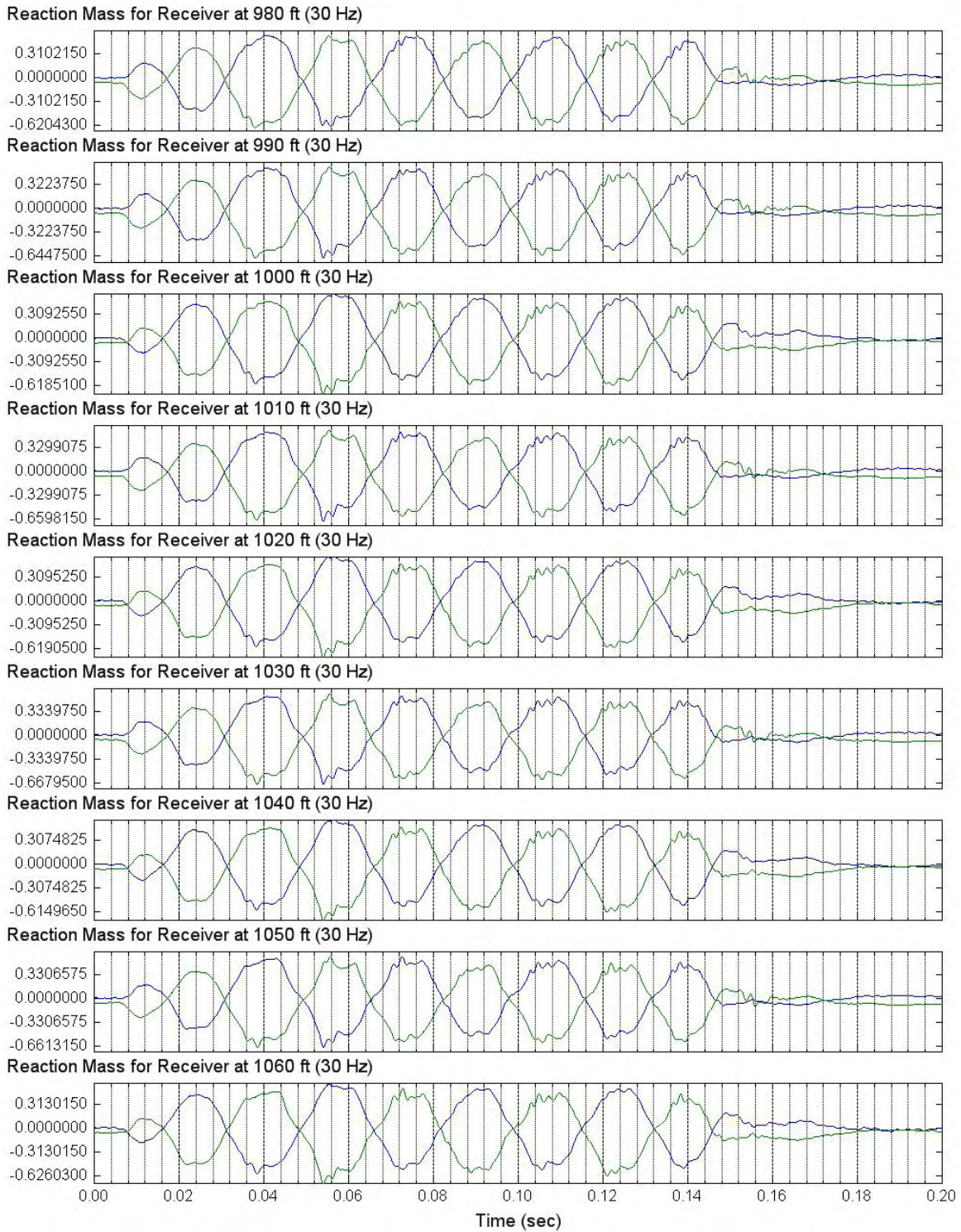
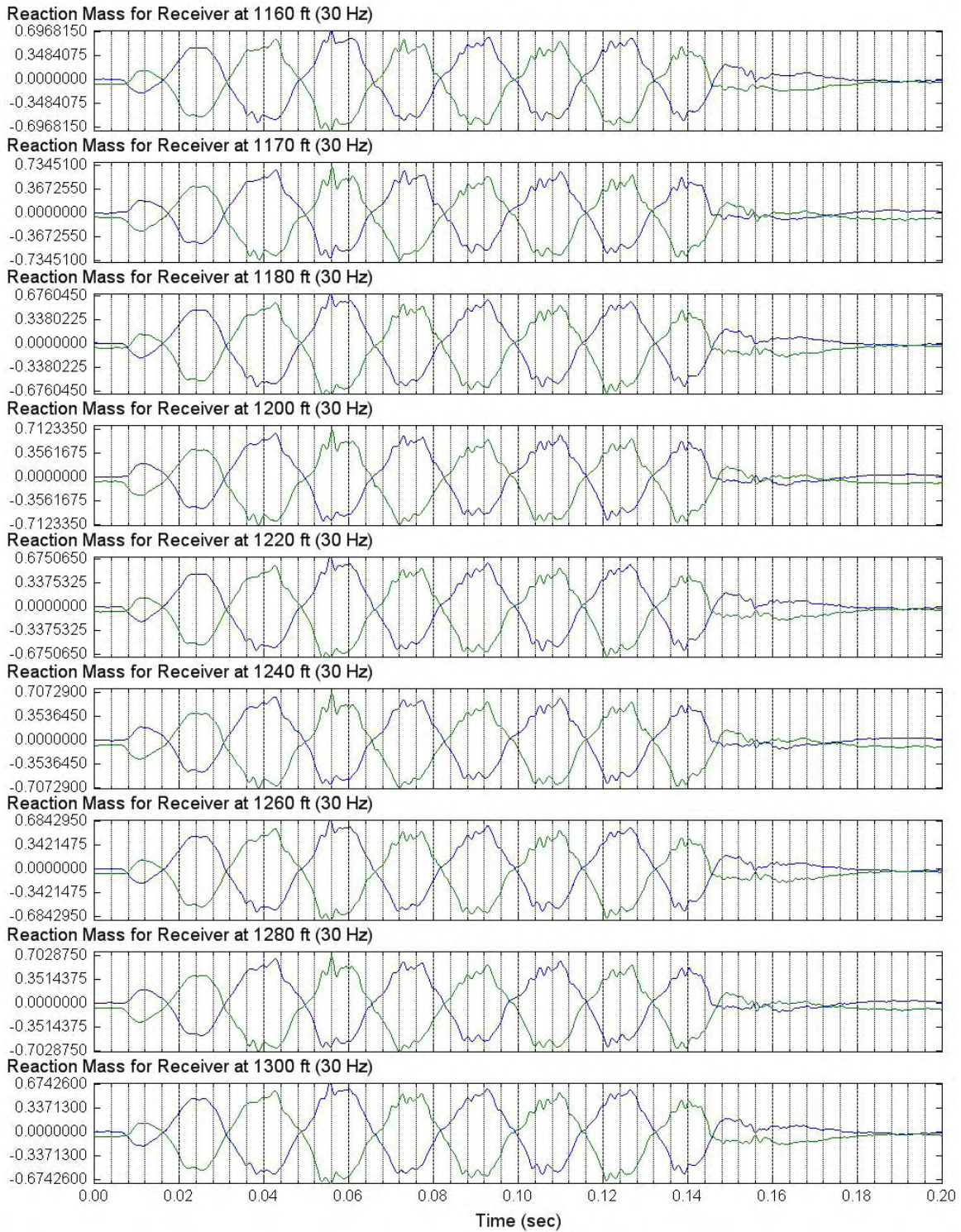


Figure 5.9 Unfiltered S-Wave Signals of Reaction Mass Accelerometer (C4996)
Depths 1070 to 1150 ft; Input Signal: 4 Cycles of 30-Hz Sine Wave



Figure 5.10 Unfiltered S-Wave Signals of Reaction Mass Accelerometer (C4996)
Depths 1160 to 1300 ft; Input Signal: 4 Cycles of 30-Hz Sine Wave



Section 6: Unfiltered S-Wave Records of Reference Receiver

Section 6 includes all unfiltered S-wave signals at the reference receiver.

1. Figures 6.1 to 6.6 present unfiltered reference horizontal receiver (S-wave) signals in Borehole C4996, depths 360 to 960 ft; input signal: 5 cycles of 50-Hz sine wave.
2. Figure 6.7 presents unfiltered reference horizontal receiver (S-wave) signals in Borehole C4996, depths 910 to 980 ft; input signal: 4 cycles of 20-Hz sine wave.
3. Figures 6.8 to 6.10 present unfiltered reference horizontal receiver (S-wave) signals in Borehole C4996, depths 980 to 1300 ft; input signal: 4 cycles of 30-Hz sine wave.

Figure 6.1 Unfiltered S-Wave Signals of Reference Horizontal Receiver (C4996)
Depths 360 to 455 ft; Input Signal: 5 Cycles of 50-Hz Sine Wave

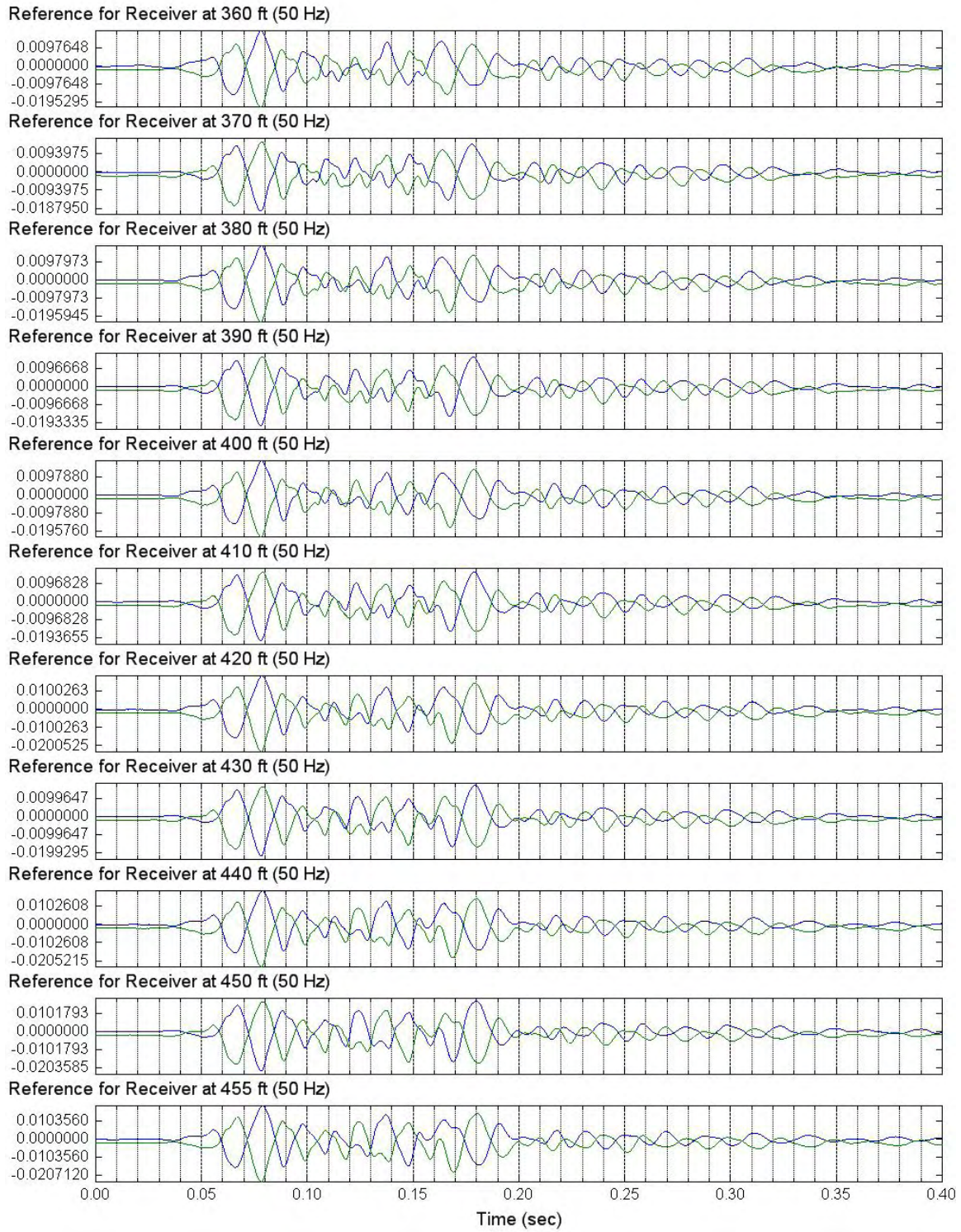


Figure 6.2 Unfiltered S-Wave Signals of Reference Horizontal Receiver (C4996)
Depths 460 to 520 ft; Input Signal: 5 Cycles of 50-Hz Sine Wave

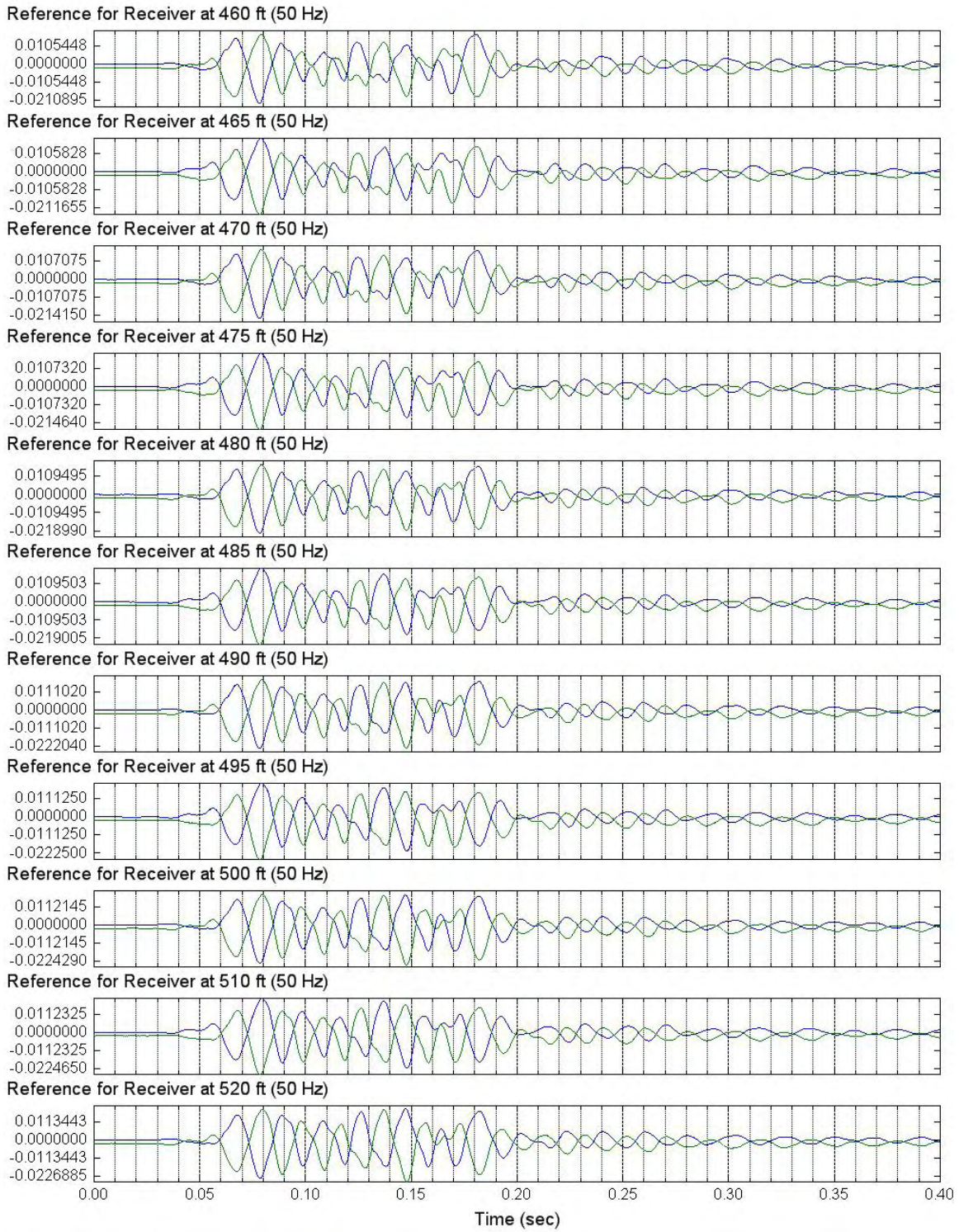


Figure 6.3 Unfiltered S-Wave Signals of Reference Horizontal Receiver (C4996)
Depths 530 to 630 ft; Input Signal: 5 Cycles of 50-Hz Sine Wave

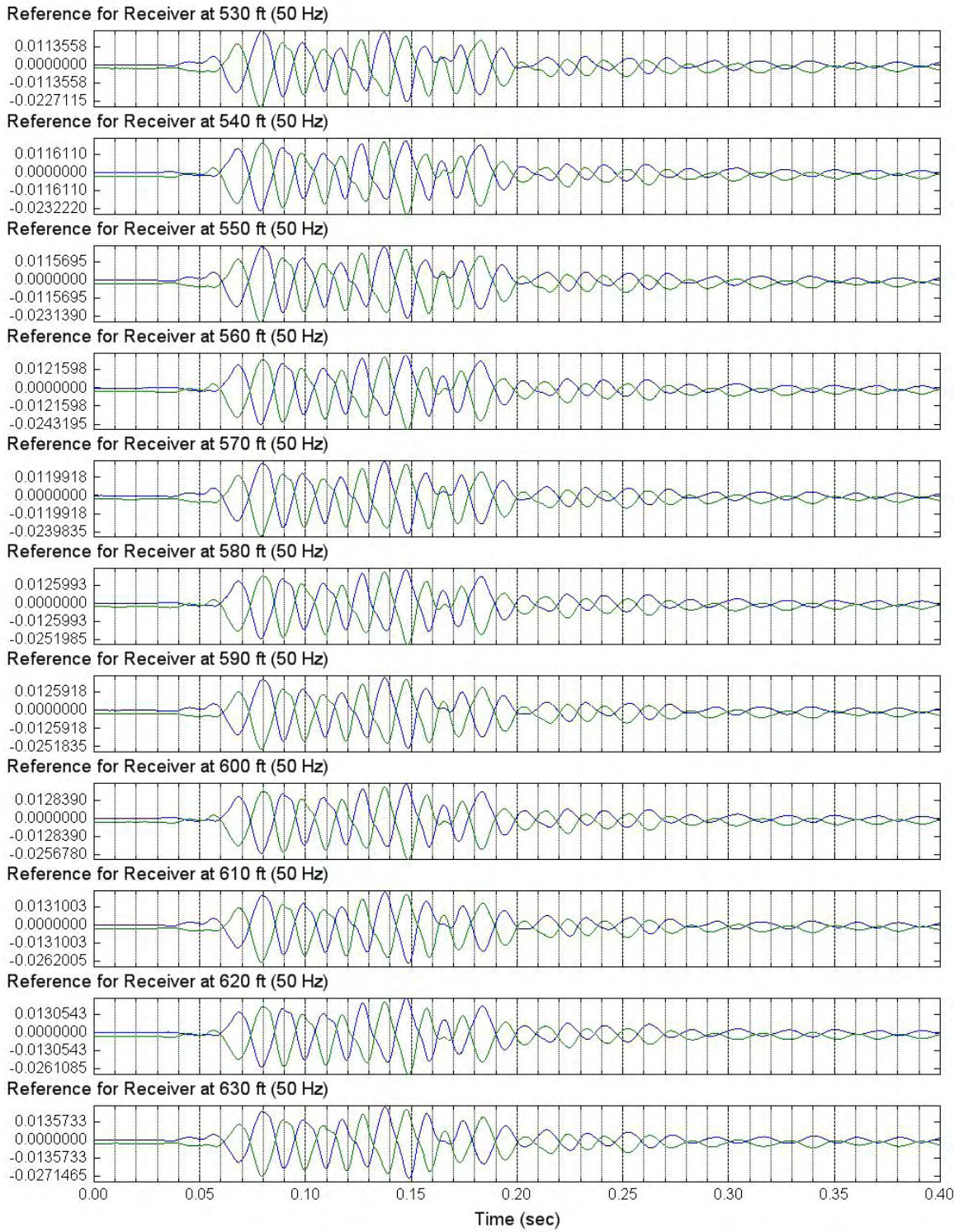


Figure 6.4 Unfiltered S-Wave Signals of Reference Horizontal Receiver (C4996)
Depths 640 to 720 f; Input Signal: 5 Cycles of 50-Hz Sine Wave

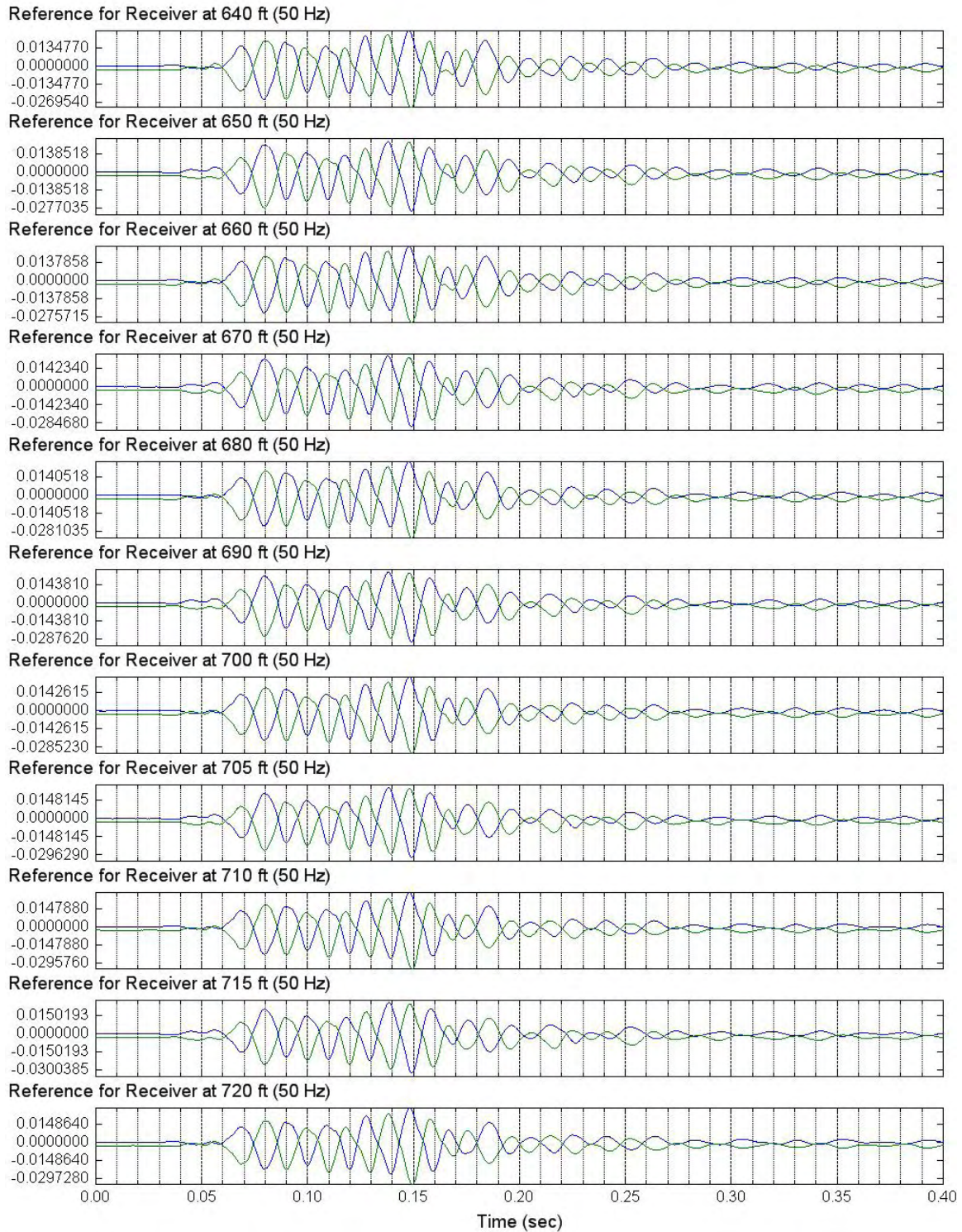


Figure 6.5 Unfiltered S-Wave Signals of Reference Horizontal Receiver (C4996)
Depths 730 to 820 ft; Input Signal: 5 Cycles of 50-Hz Sine Wave

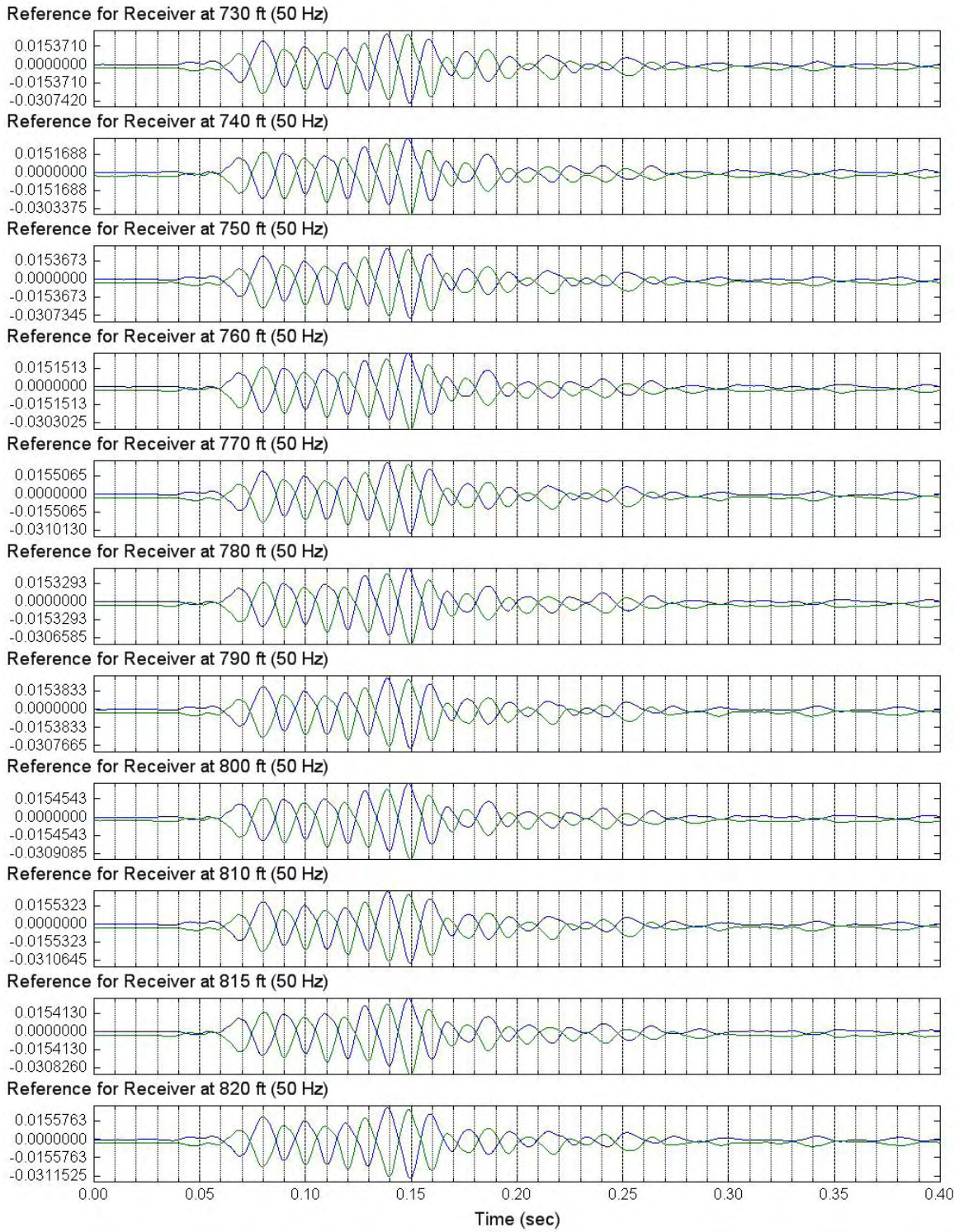


Figure 6.6 Unfiltered S-Wave Signals of Reference Horizontal Receiver (C4996)
Depths 830 to 960 ft; Input Signal: 5 Cycles of 50-Hz Sine Wave

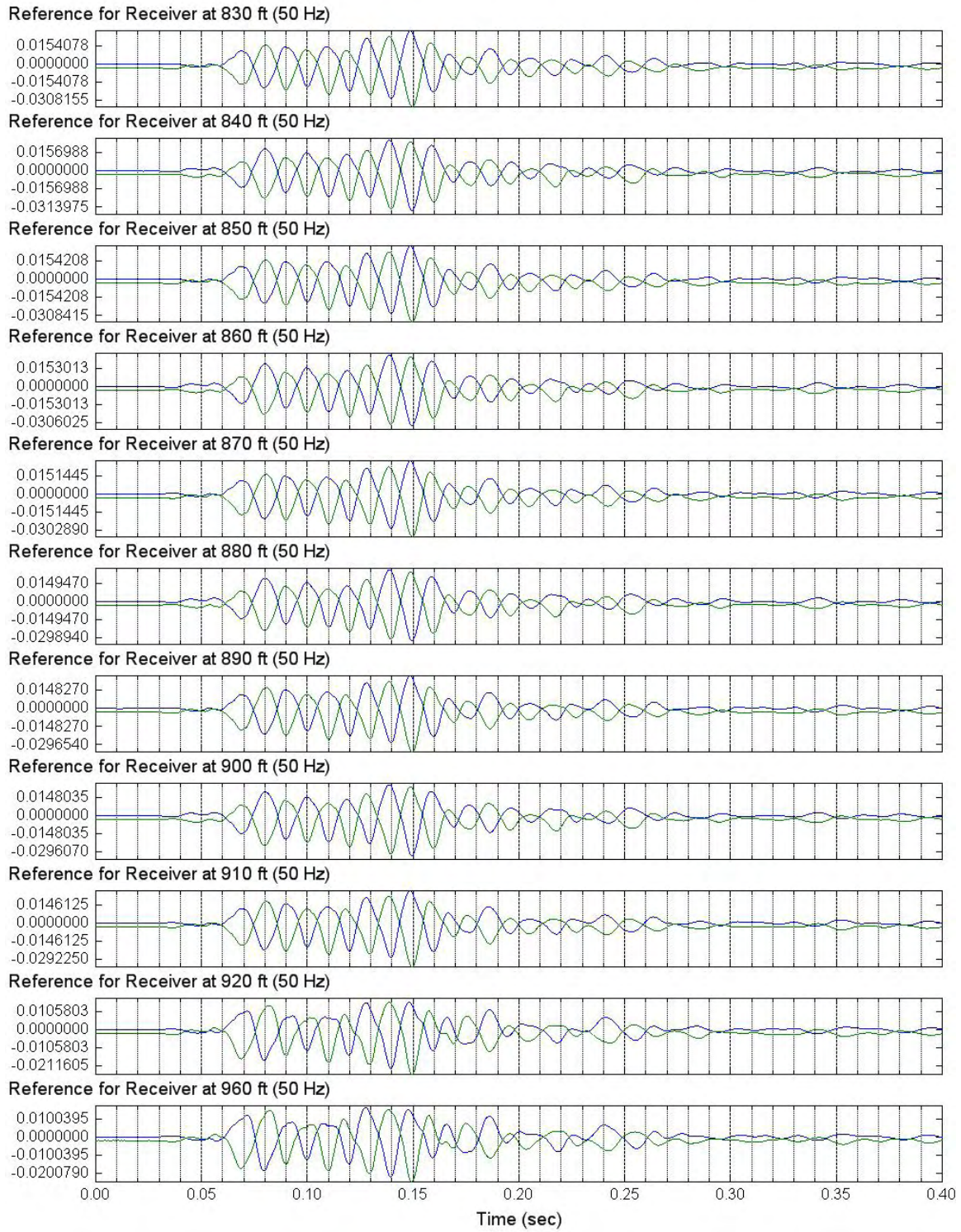


Figure 6.7 Unfiltered S-Wave Signals of Reference Horizontal Receiver (C4996)
Depths 910 to 980 ft; Input Signal: 4 Cycles of 20-Hz Sine Wave

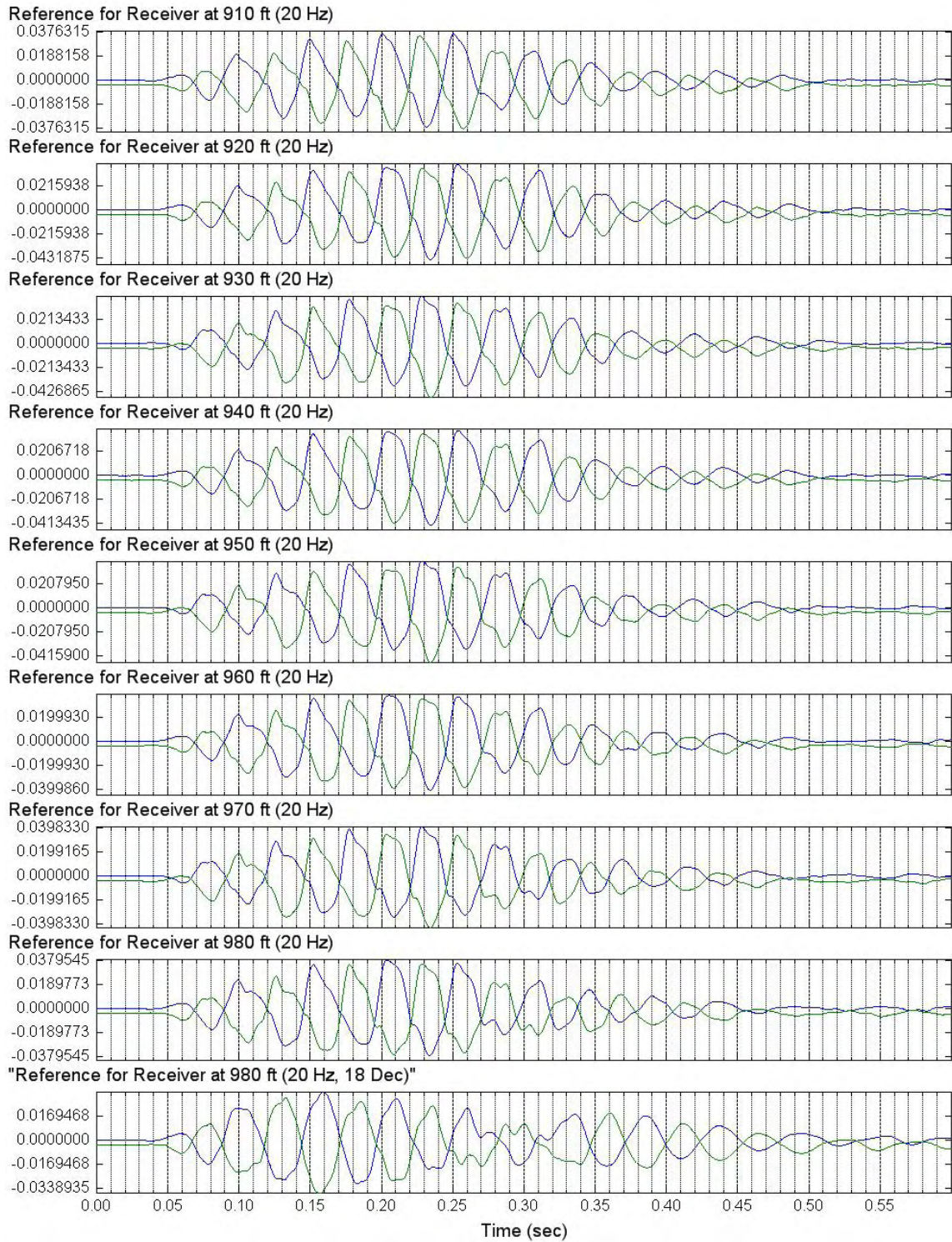


Figure 6.8 Unfiltered S-Wave Signals of Reference Horizontal Receiver (C4996)
Depths 980 to 1060 ft; Input Signal: 4 Cycles of 30-Hz Sine Wave

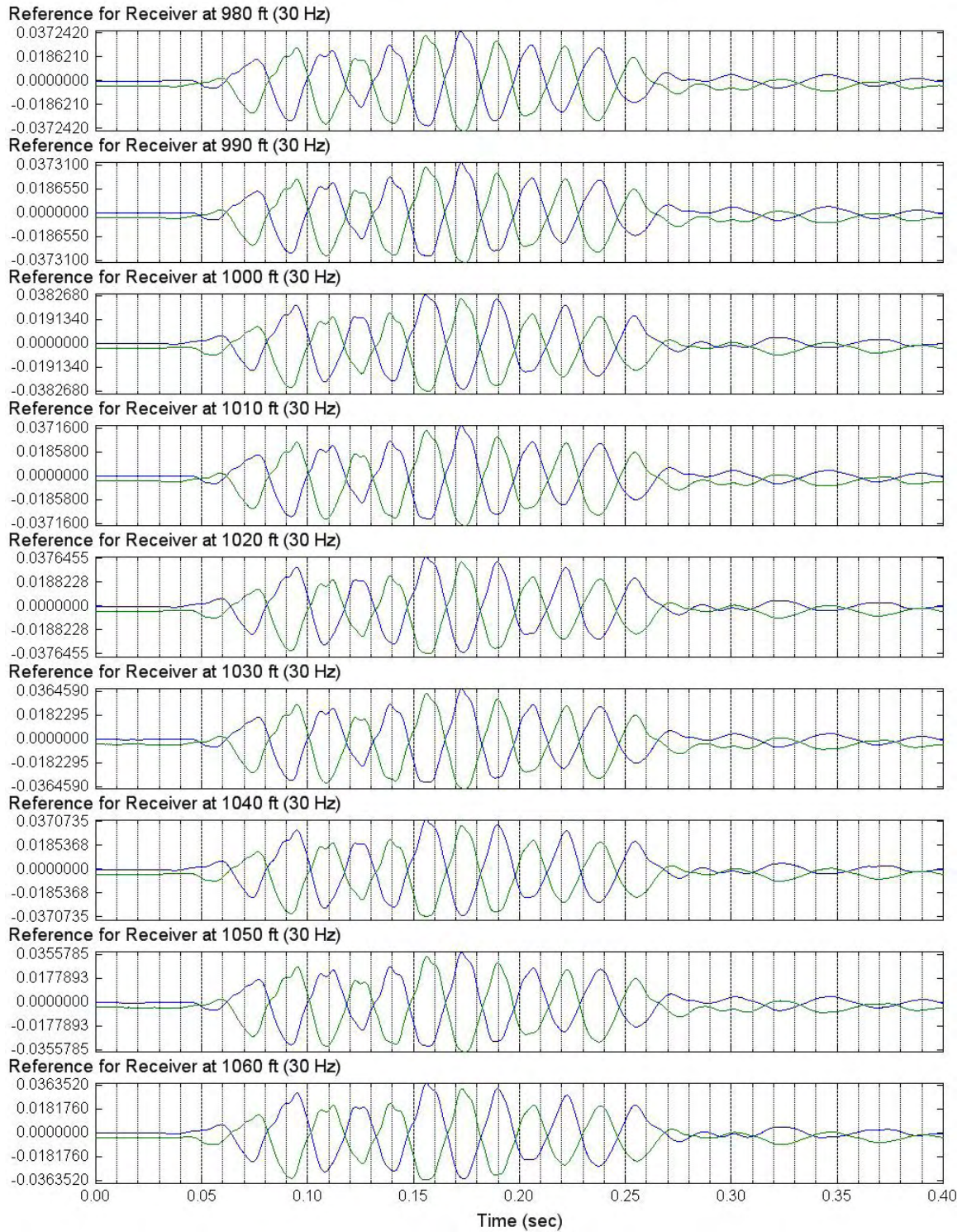


Figure 6.9 Unfiltered S-Wave Signals of Reference Horizontal Receiver (C4996)
Depths 1070 to 1150 ft; Input Signal: 4 Cycles of 30-Hz Sine Wave

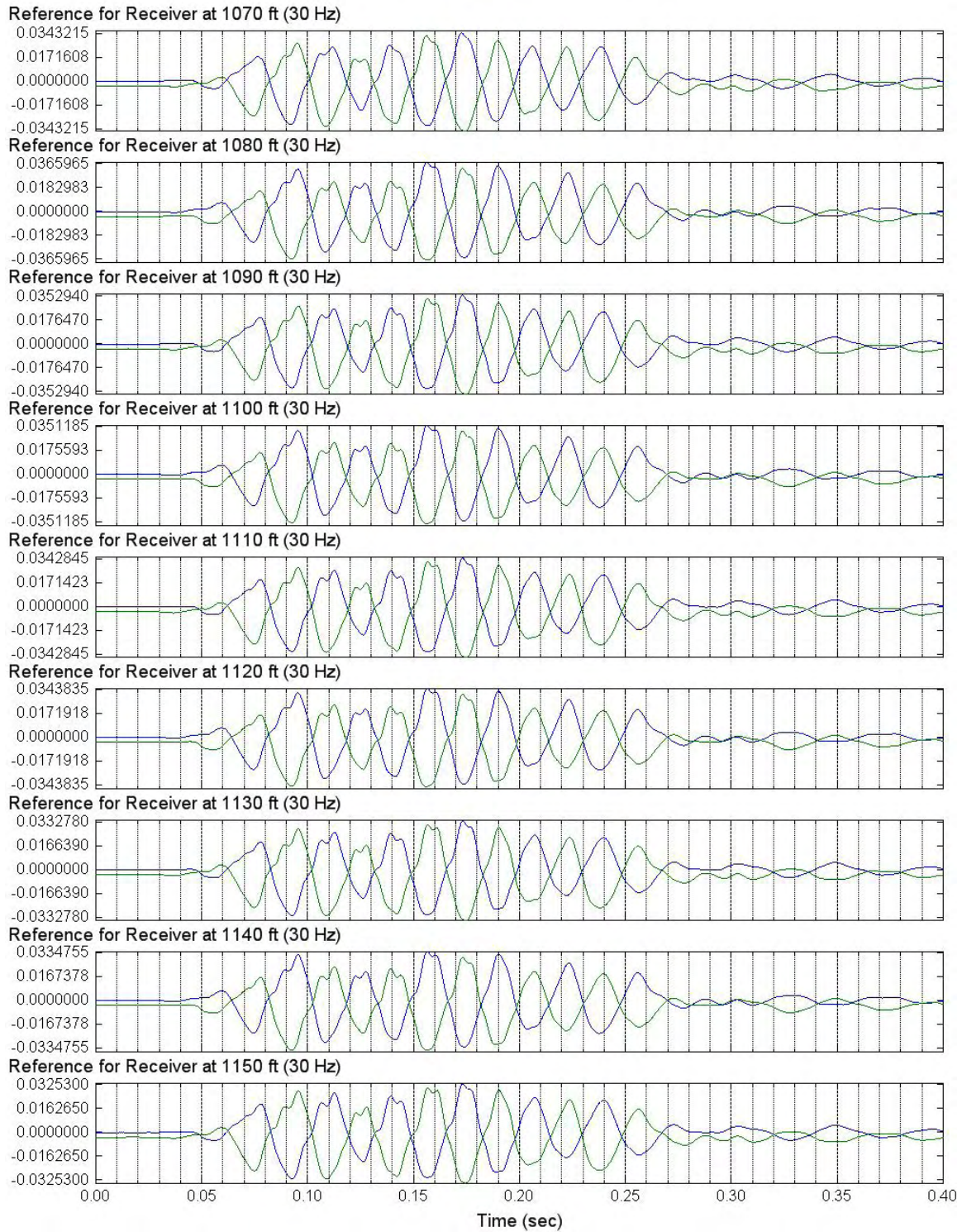
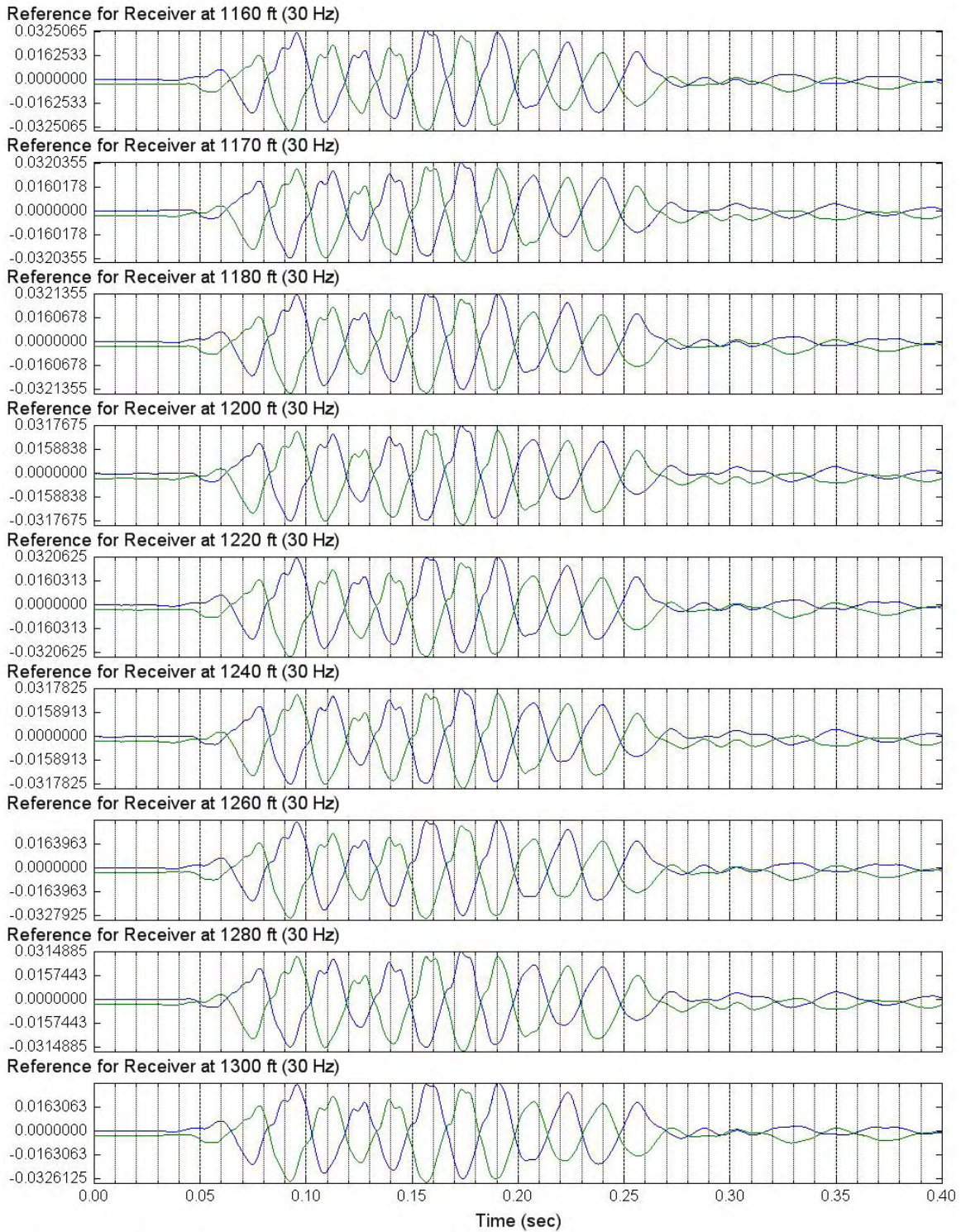


Figure 6.10 Unfiltered S-Wave Signals of Reference Horizontal Receiver (C4996)
Depths 1160 to 1300 ft; Input Signal: 4 Cycles of 30-Hz Sine Wave



Section 7: Filtered S-Wave Signals of Lower Rotated In-Line Receiver

Section 7 includes all filtered S-wave signals at the lower rotated horizontal receiver.

1. Figures 7.1 to 7.6 present filtered lower rotated horizontal receiver (S-wave) signals in Borehole C4996, depths 360 to 960 ft; FFT low pass 60 Hz; input signal: 5 cycles of 50-Hz sine wave.
2. Figure 7.7 presents filtered lower rotated horizontal receiver (S-wave) signals in Borehole C4996, depths 910 to 980 ft; FFT low pass 25 Hz; input signal: 4 cycles of 20-Hz sine wave.
3. Figures 7.8 to 7.10 present filtered lower rotated horizontal receiver (S-wave) signals in Borehole C4996, depths 980 to 1300 ft; FFT low pass 40 Hz; input signal: 4 cycles of 30-Hz sine wave.

Figure 7.1 Filtered S-Wave Signals of Lower Rotated In-Line Receiver (C4996)
Depths 360 to 455 ft; Input Signal: 5 Cycles of 50-Hz Sine Wave; Low Pass 60 Hz

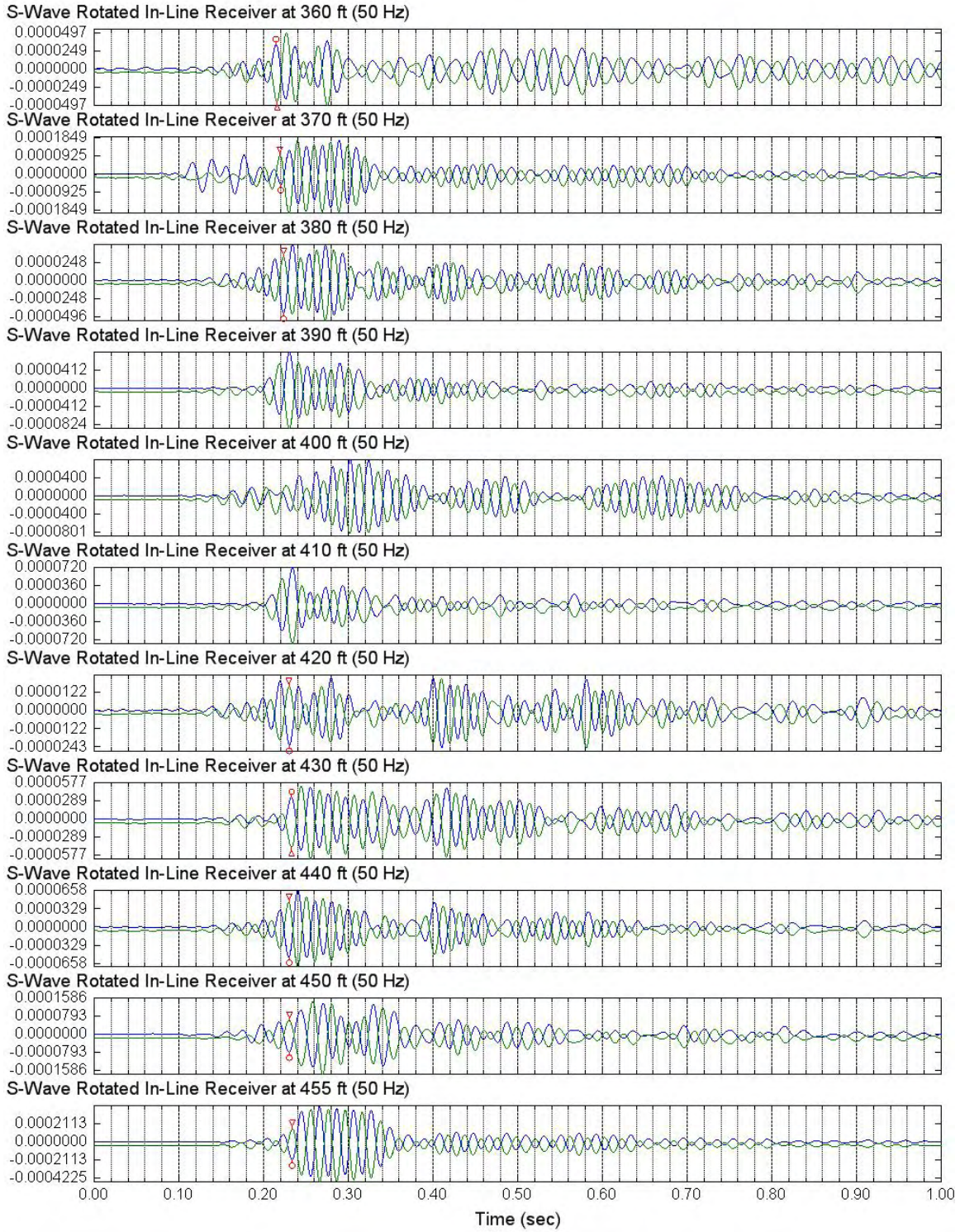


Figure 7.2 Filtered S-Wave Signals of Lower Rotated In-Line Receiver (C4996)
Depths 460 to 520 ft; Input Signal: 5 Cycles of 50-Hz Sine Wave; Low Pass 60 Hz

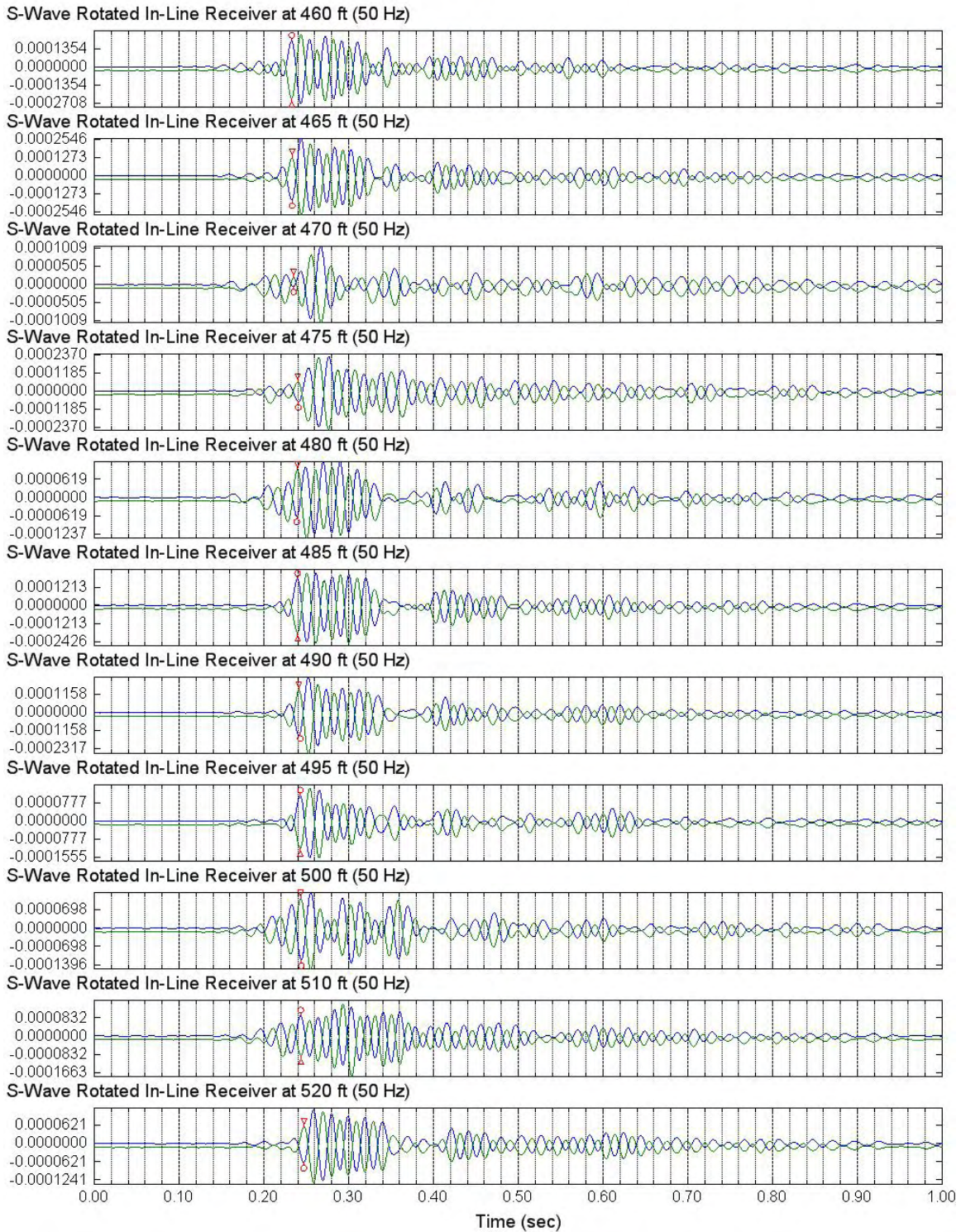


Figure 7.3 Filtered S-Wave Signals of Lower Rotated In-Line Receiver (C4996)
 Depths 530 to 630 ft; Input Signal: 5 Cycles of 50-Hz Sine Wave; Low Pass 60 Hz

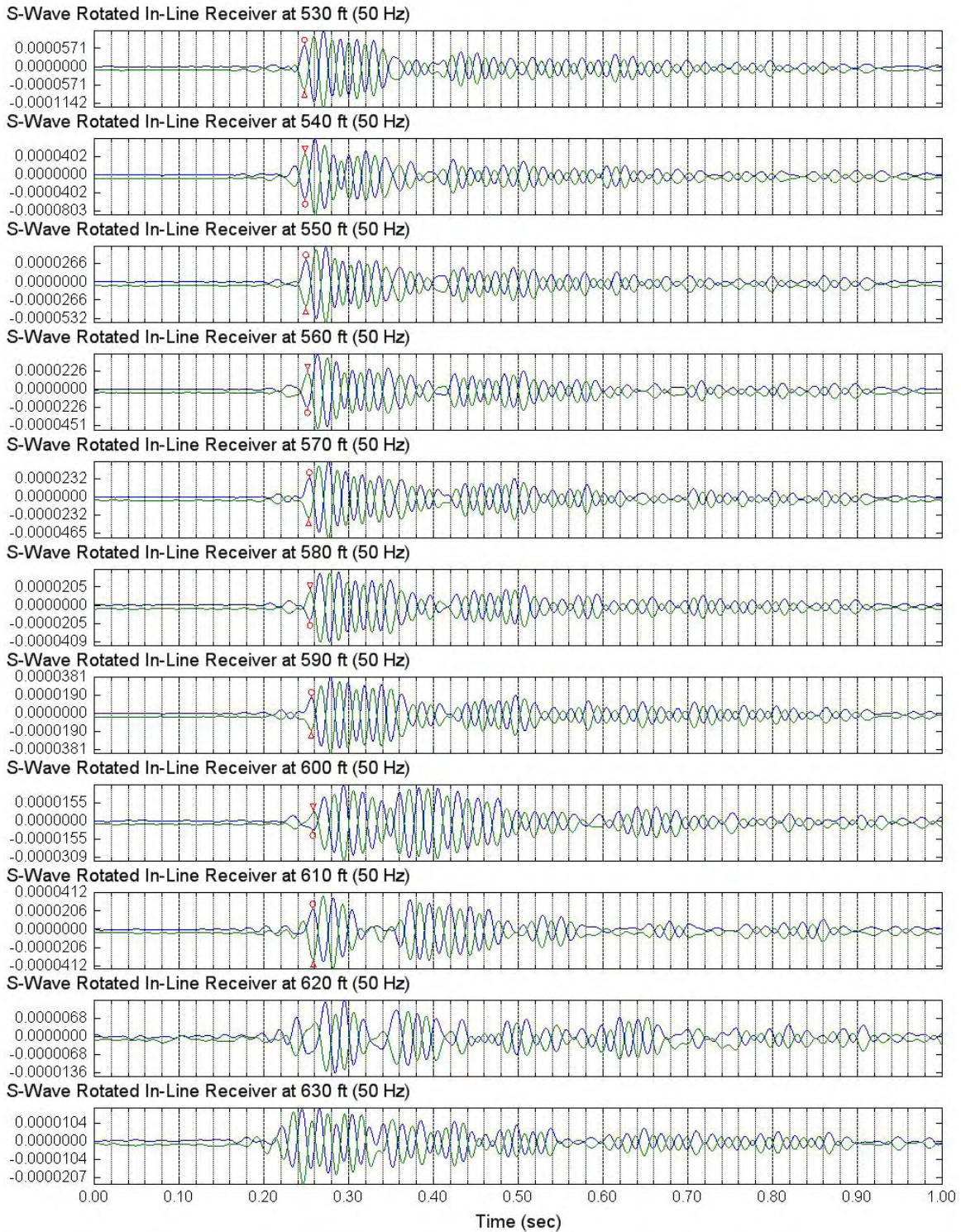


Figure 7.4 Filtered S-Wave Signals of Lower Rotated In-Line Receiver (C4996)
 Depths 640 to 720 ft; Input Signal: 5 Cycles of 50-Hz Sine Wave; Low Pass 60 Hz

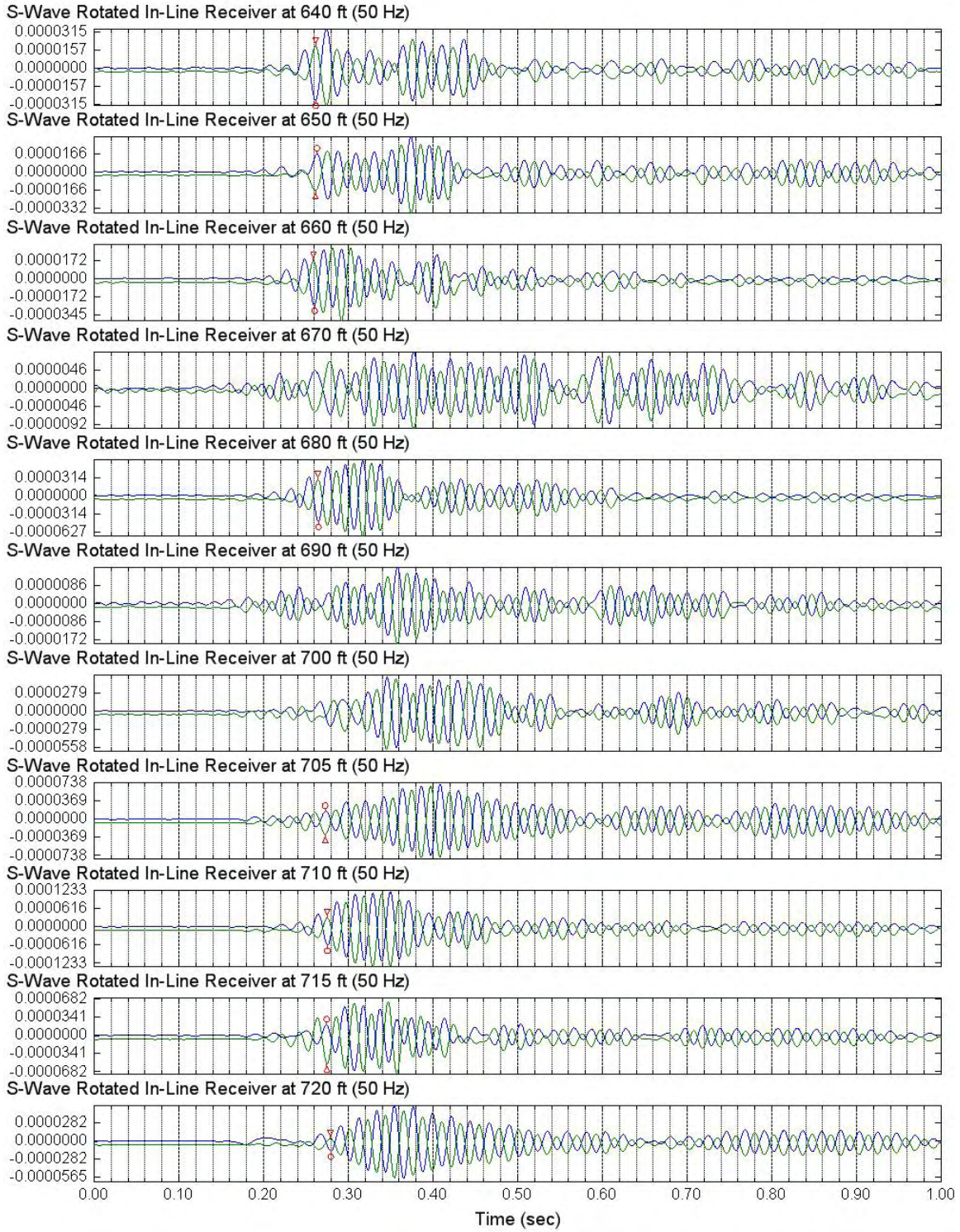


Figure 7.5 Filtered S-Wave Signals of Lower Rotated In-Line Receiver (C4996)
Depths 730 to 820 ft; Input Signal: 5 Cycles of 50-Hz Sine Wave; Low Pass 60 Hz

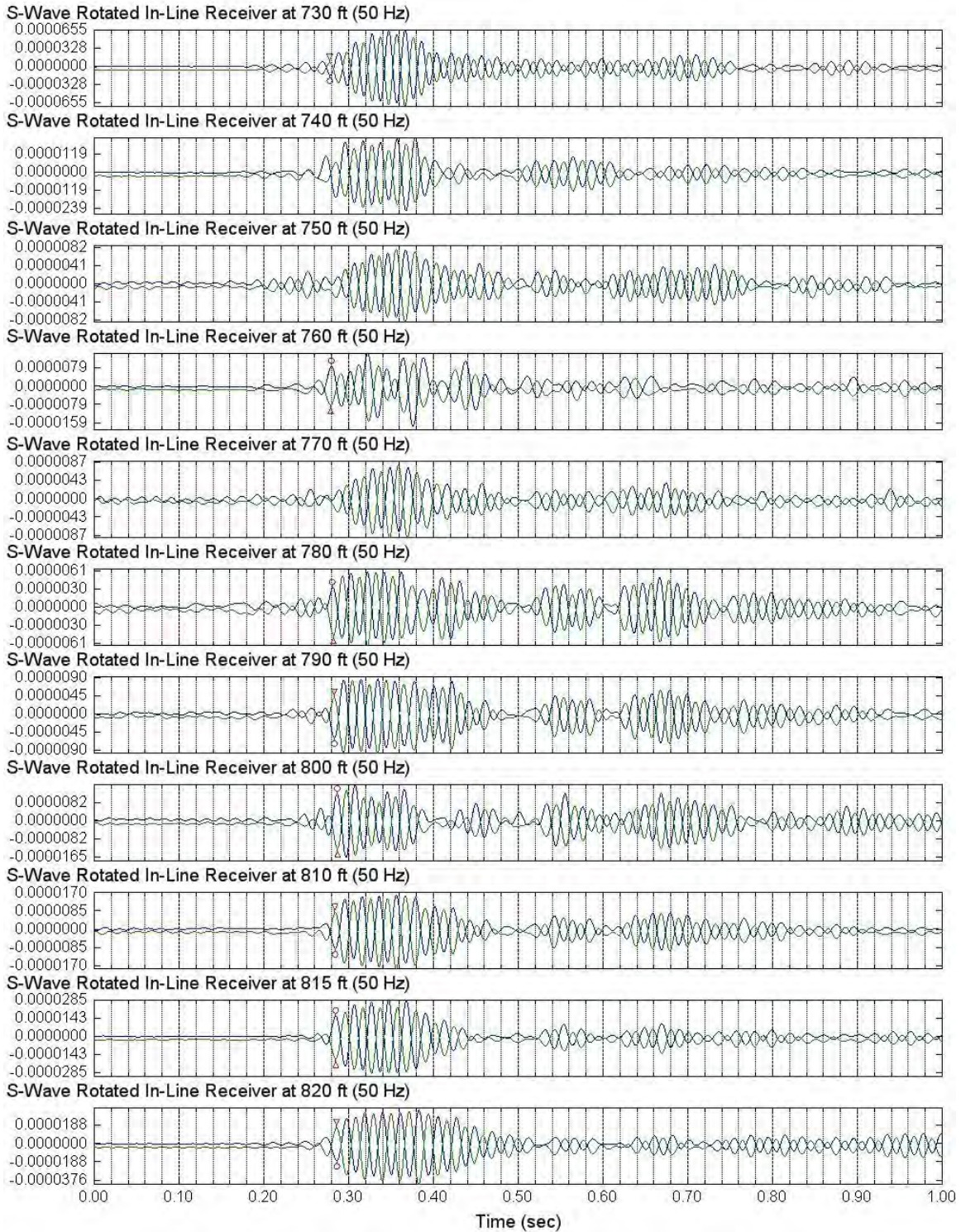


Figure 7.6 Filtered S-Wave Signals of Lower Rotated In-Line Receiver (C4996)
 Depths 830 to 960 ft; Input Signal: 5 Cycles of 50-Hz Sine Wave; Low Pass 60 Hz

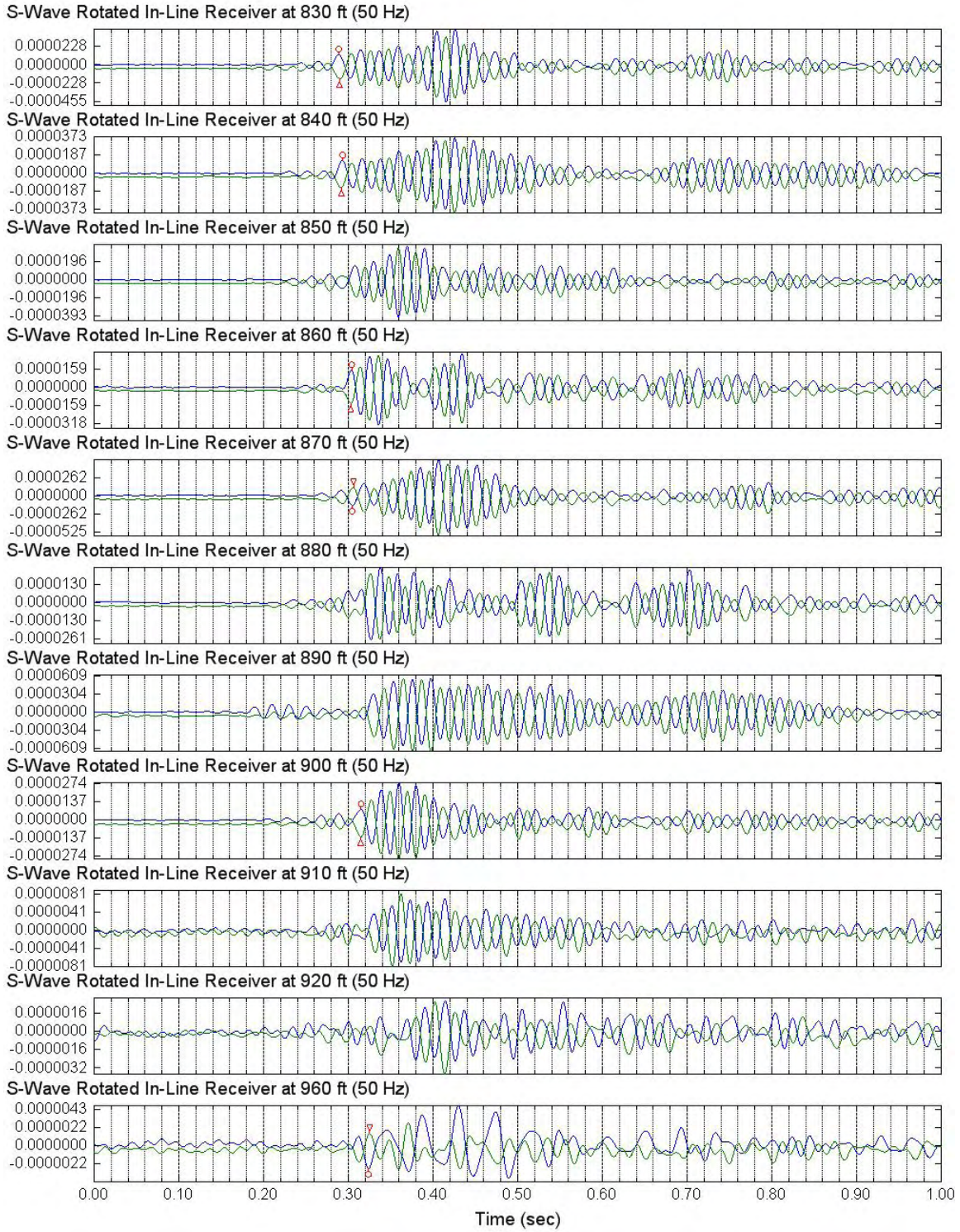


Figure 7.7 Filtered S-Wave Signals of Lower Rotated In-Line Receiver (C4996)
 Depths 910 to 980 ft; Input Signal: 4 Cycles of 20-Hz Sine Wave; Low Pass 25 Hz

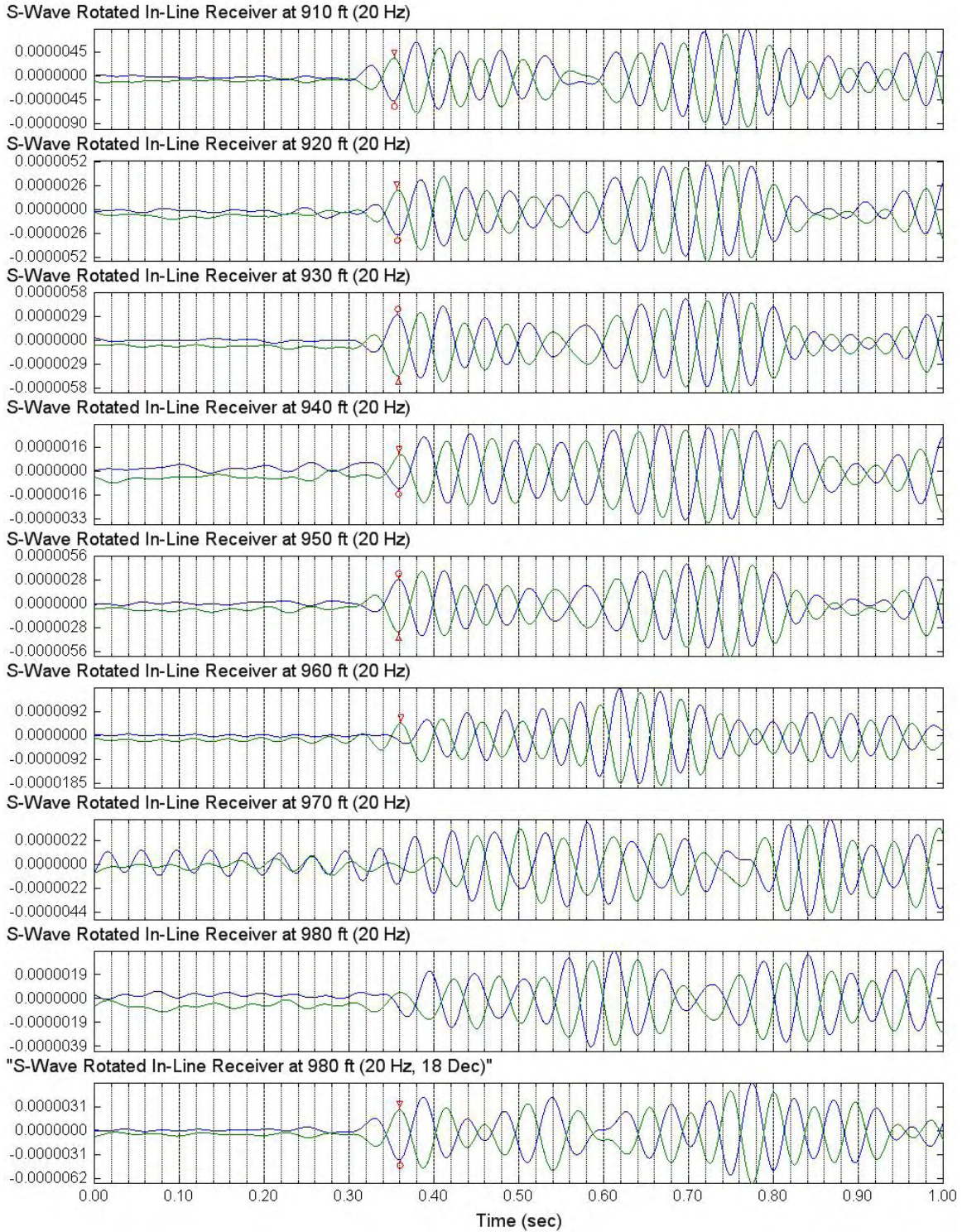


Figure 7.8 Filtered S-Wave Signals of Lower Rotated In-Line Receiver (C4996)
Depths 980 to 1060 ft; Input Signal: 4 Cycles of 30-Hz Sine Wave; Low Pass 40 Hz

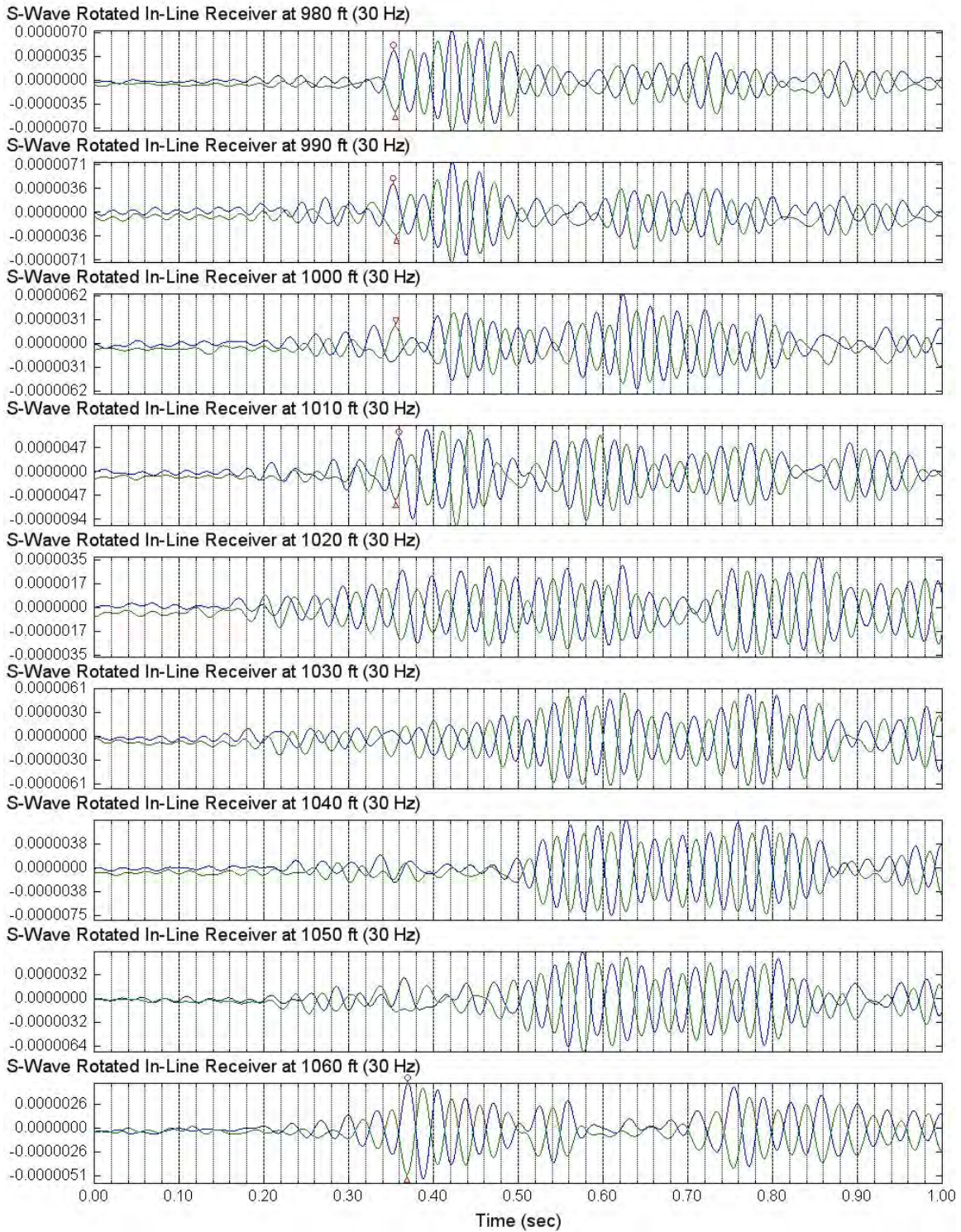


Figure 7.9 Filtered S-Wave Signals of Lower Rotated In-Line Receiver (C4996)
Depths 1070 to 1150 ft; Input Signal: 4 Cycles of 30-Hz Sine Wave; Low Pass 40 Hz

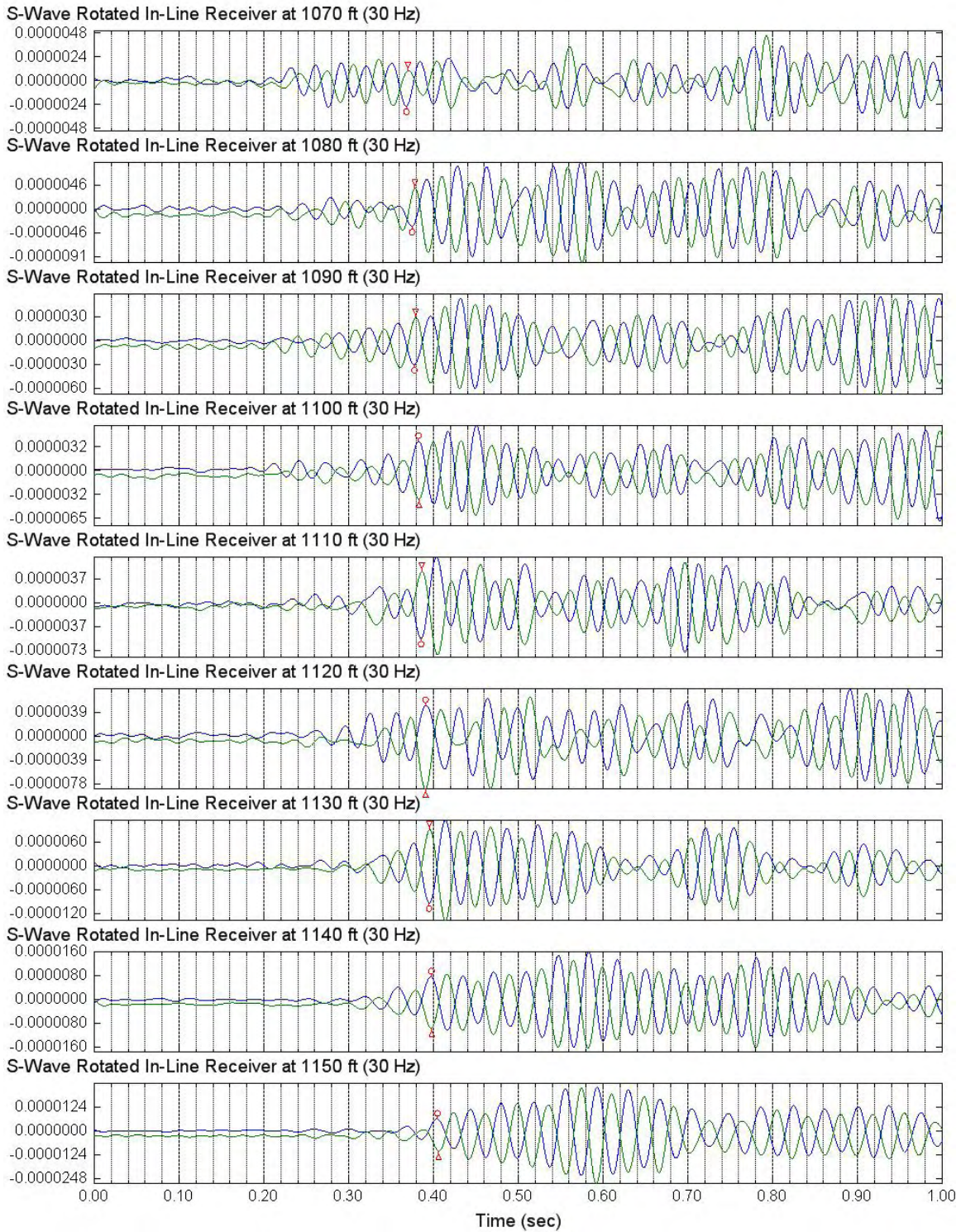
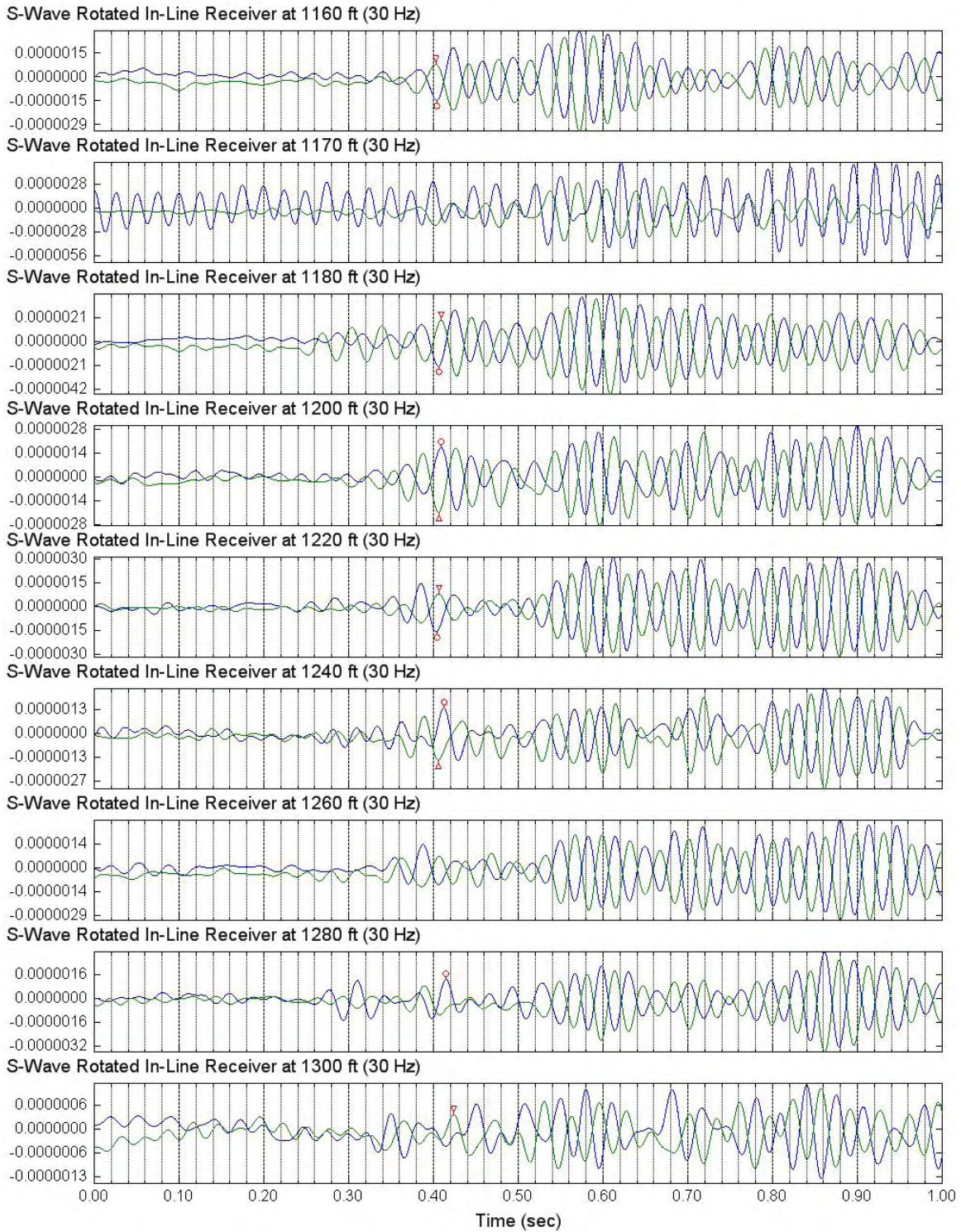


Figure 7.10 Filtered S-Wave Signals of Lower Rotated In-Line Receiver (C4996)
Depths 1160 to 1300 ft; Input Signal: 4 Cycles of 30-Hz Sine Wave; Low Pass 40 Hz



Section 8: Filtered S-Wave Signals of Reaction Mass

Acceleration

1. Figures 8.1 to 8.6 present filtered reaction mass horizontal (S-wave) acceleration at Borehole C4996, depths 360 to 960 ft; FFT low pass 60 Hz; input signal: 5 cycles of 50-Hz sine wave.
2. Figure 8.7 presents filtered reaction mass horizontal (S-wave) acceleration at Borehole C4996, depths 910 to 980 ft; FFT low pass 25 Hz; input signal: 4 cycles of 20-Hz sine wave.
3. Figures 8.8 to 8.10 present filtered reaction mass horizontal (S-wave) acceleration at Borehole C4996, depths 980 to 1300 ft; FFT low pass 40 Hz; input signal: 4 cycles of 30-Hz sine wave.

Figure 8.1 Filtered S-Wave Signals of Reaction Mass Accelerometer (C4996)
 Depths 360 to 455 ft; Input Signal: 5 Cycles of 50-Hz Sine Wave; Low Pass 60 Hz

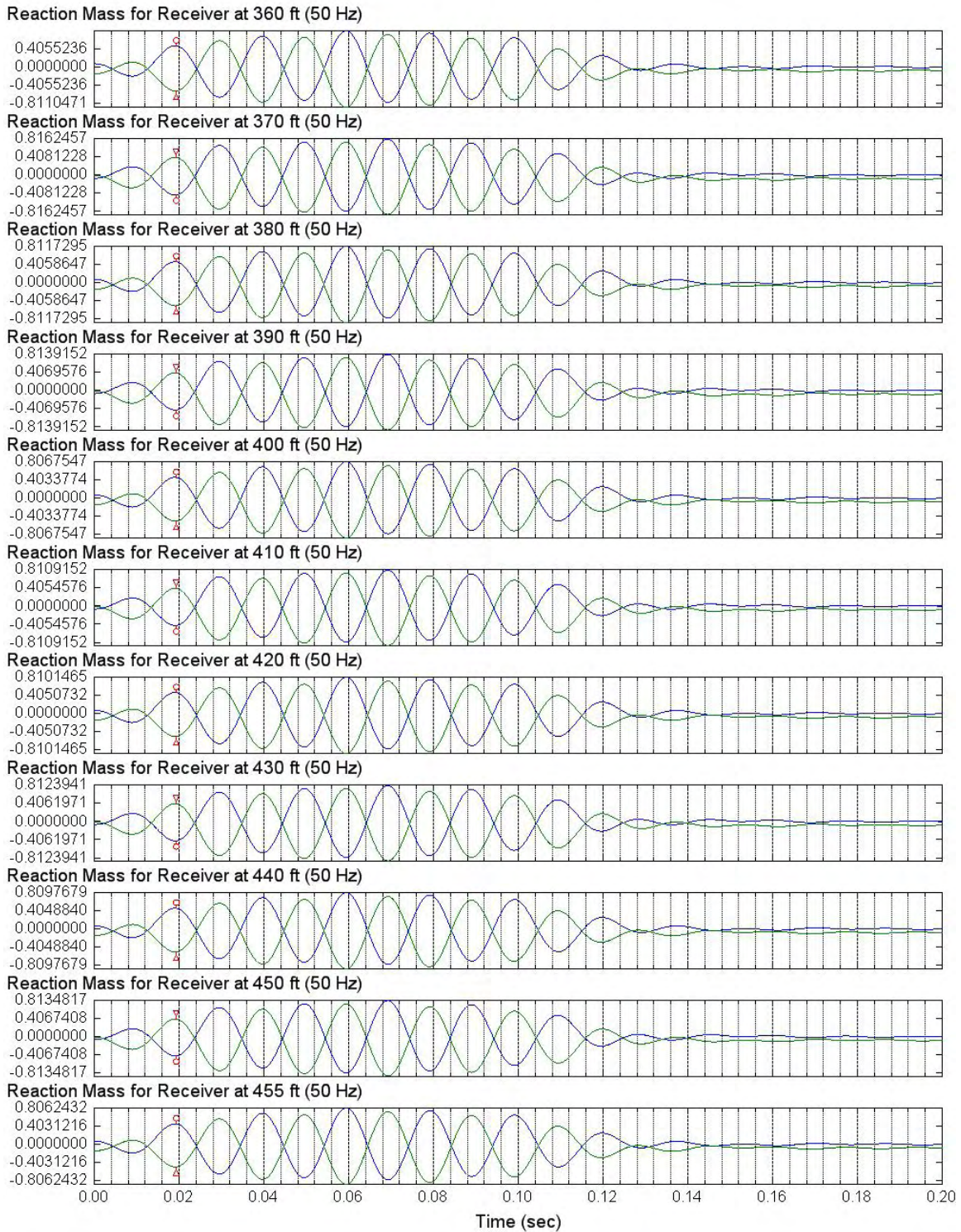


Figure 8.2 Filtered S-Wave Signals of Reaction Mass Accelerometer (C4996)
 Depths 460 to 520 ft; Input Signal: 5 Cycles of 50-Hz Sine Wave; Low Pass 60 Hz

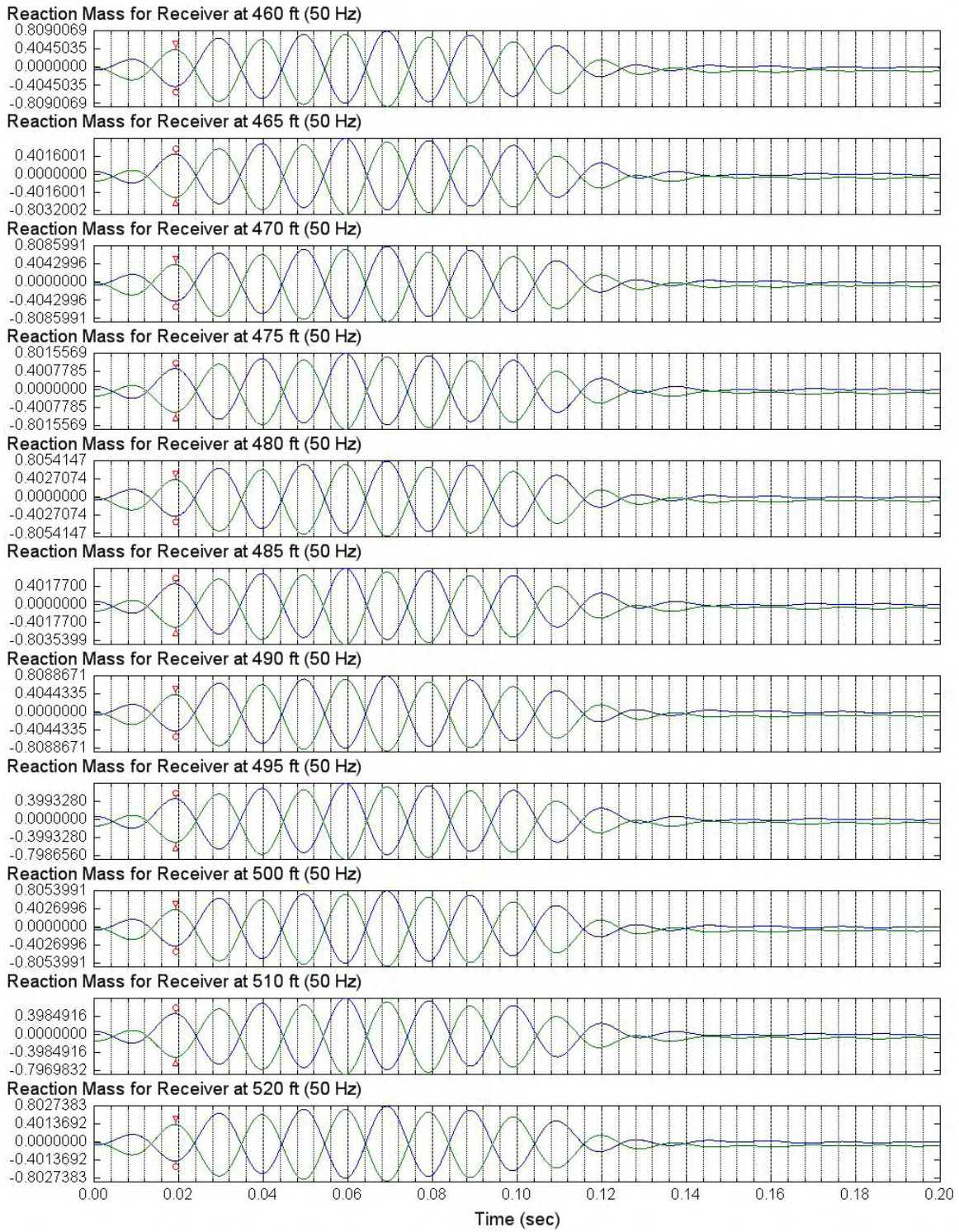


Figure 8.3 Filtered S-Wave Signals of Reaction Mass Accelerometer (C4996)
 Depths 530 to 630 ft; Input Signal: 5 Cycles of 50-Hz Sine Wave; Low Pass 60 Hz

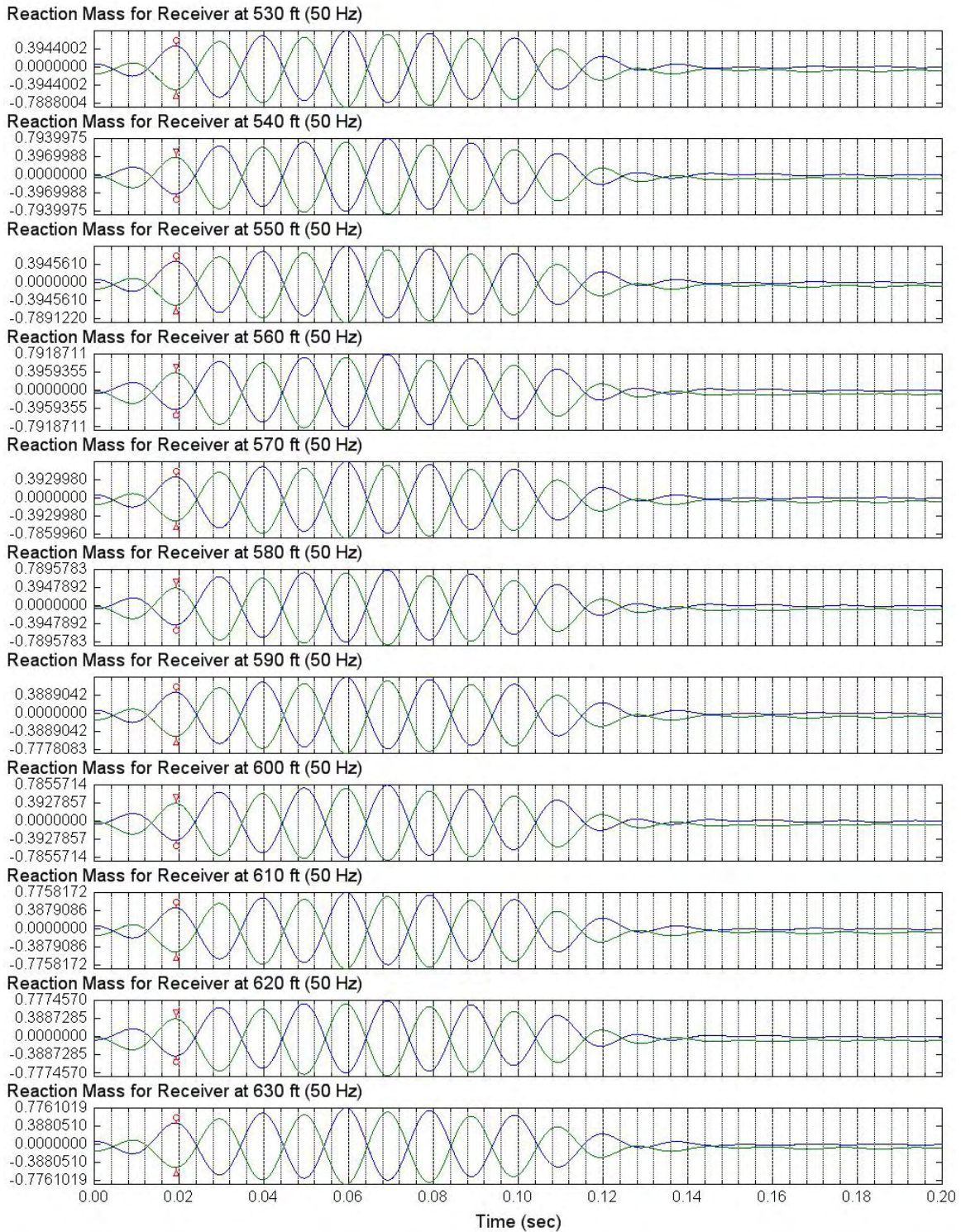


Figure 8.4 Filtered S-Wave Signals of Reaction Mass Accelerometer (C4996)
 Depths 640 to 720 ft; Input Signal: 5 Cycles of 50-Hz Sine Wave; Low Pass 60 Hz

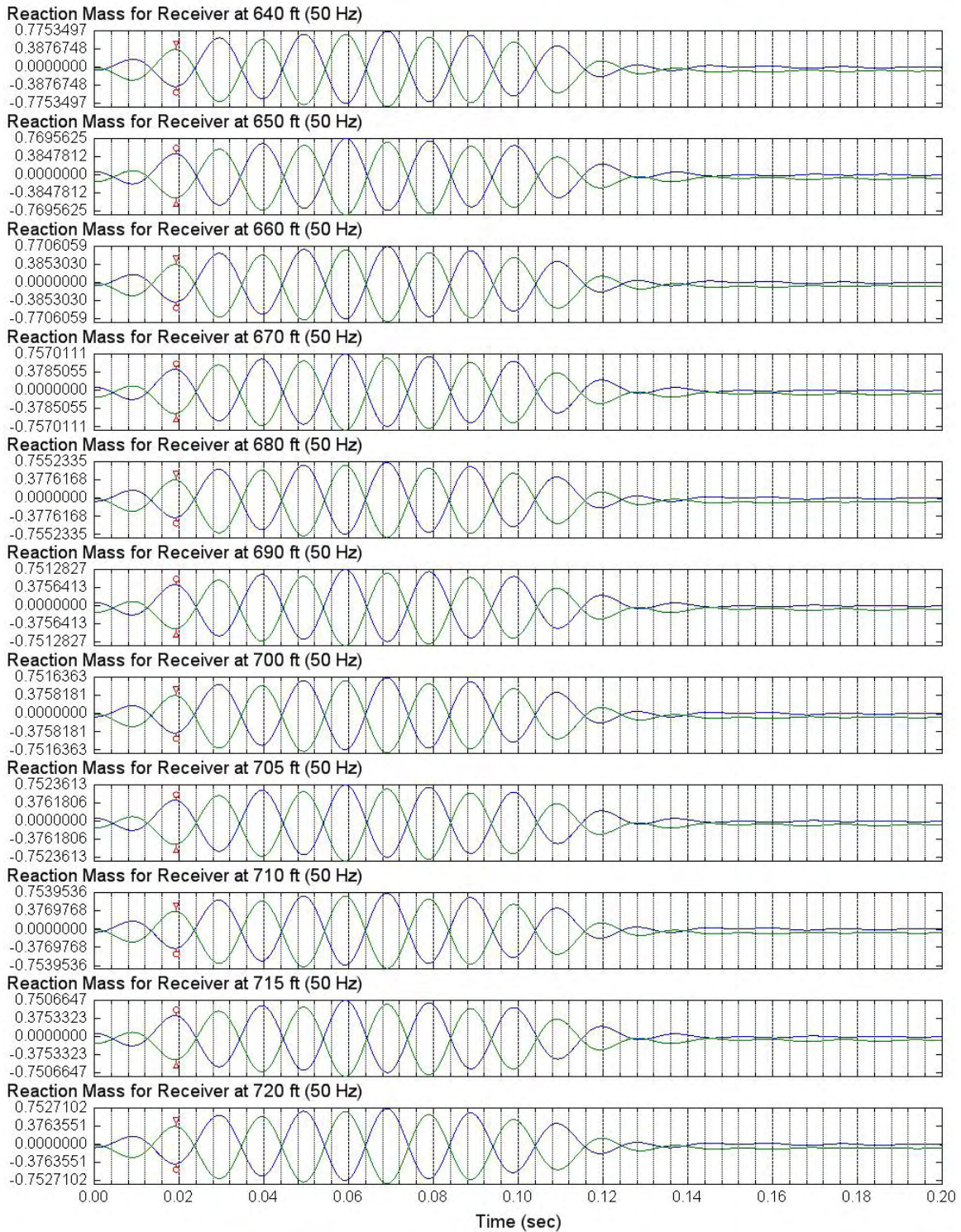


Figure 8.5 Filtered S-Wave Signals of Reaction Mass Accelerometer (C4996)
 Depths 730 to 820 ft; Input Signal: 5 Cycles of 50-Hz Sine Wave; Low Pass 60 Hz

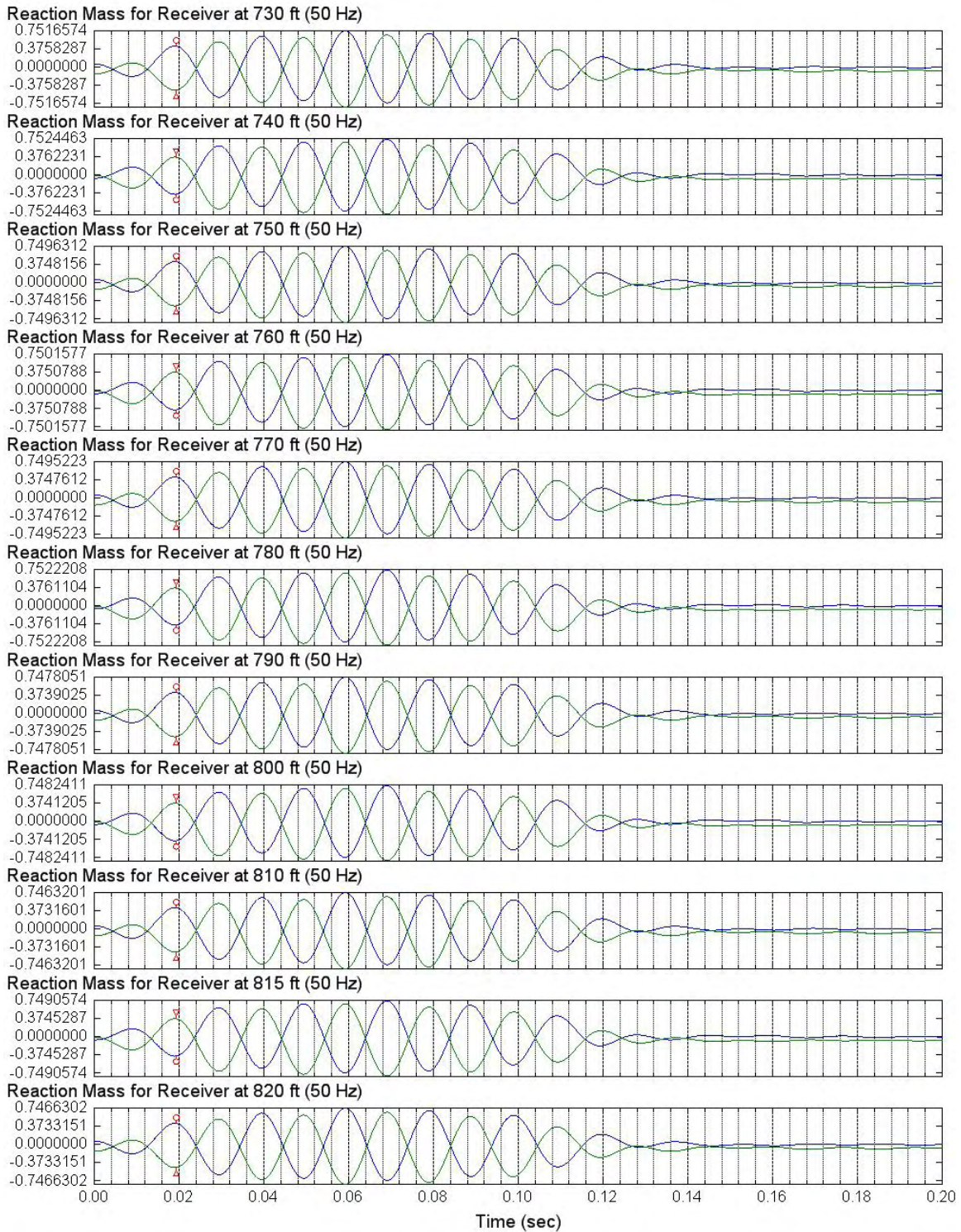


Figure 8.6 Filtered S-Wave Signals of Reaction Mass Accelerometer (C4996)
 Depths 830 to 960 ft; Input Signal: 5 Cycles of 50-Hz Sine Wave; Low Pass 60 Hz

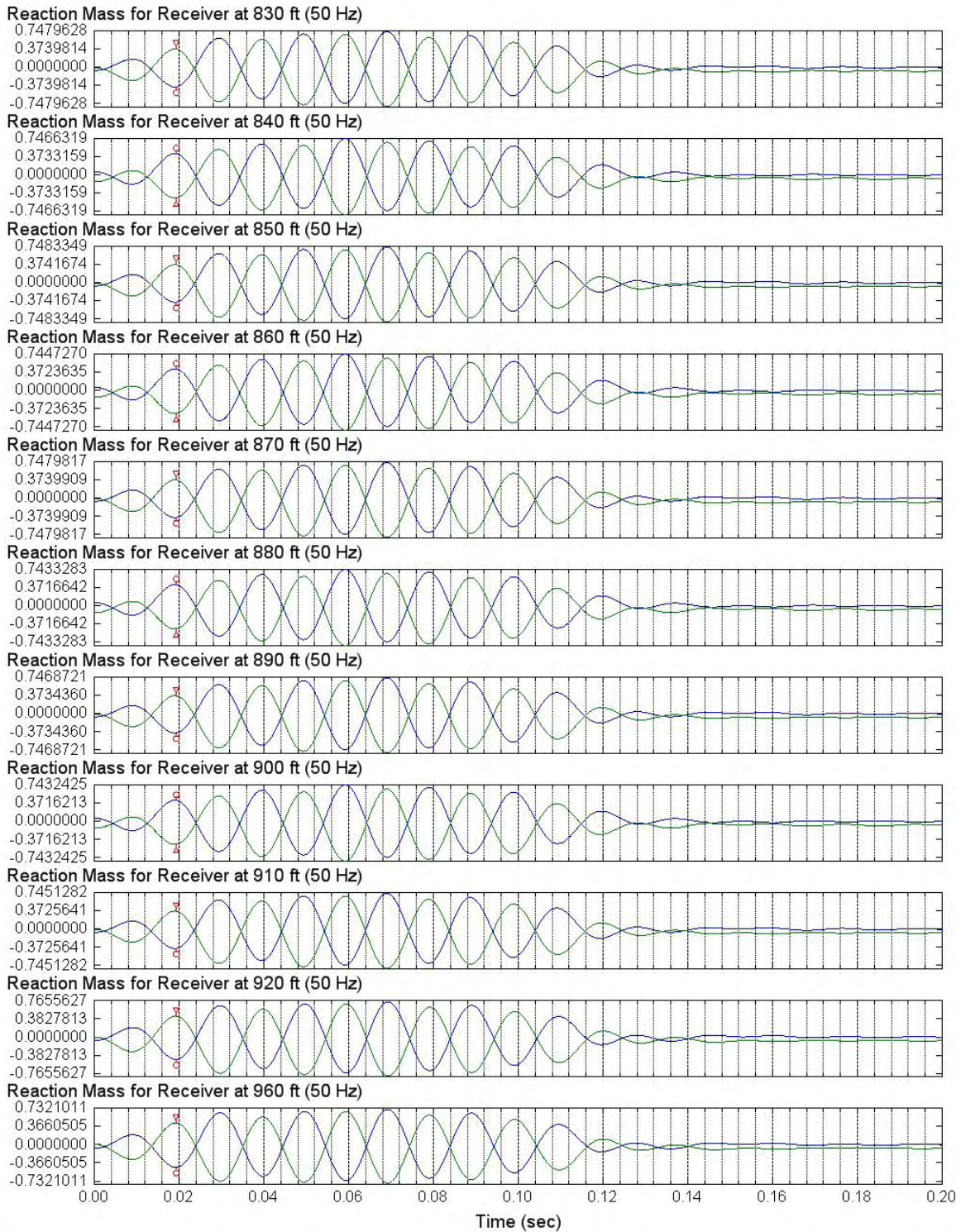


Figure 8.7 Filtered S-Wave Signals of Reaction Mass Accelerometer (C4996)
 Depths 910 to 980 ft; Input Signal: 4 Cycles of 20-Hz Sine Wave; Low Pass 25 Hz

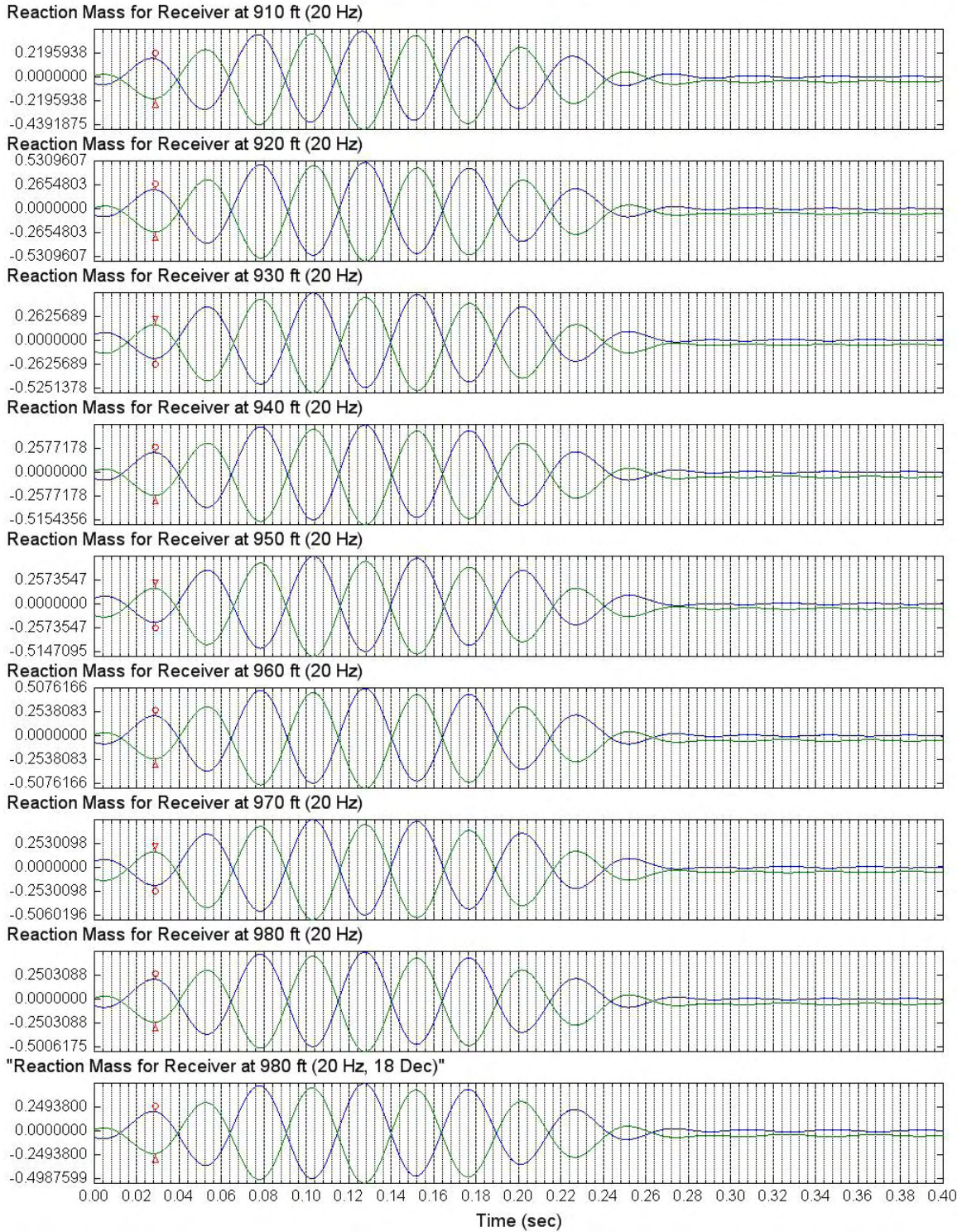


Figure 8.8 Filtered S-Wave Signals of Reaction Mass Accelerometer (C4996)
 Depths 980 to 1060 ft; Input Signal: 4 Cycles of 30-Hz Sine Wave; Low Pass 40 Hz

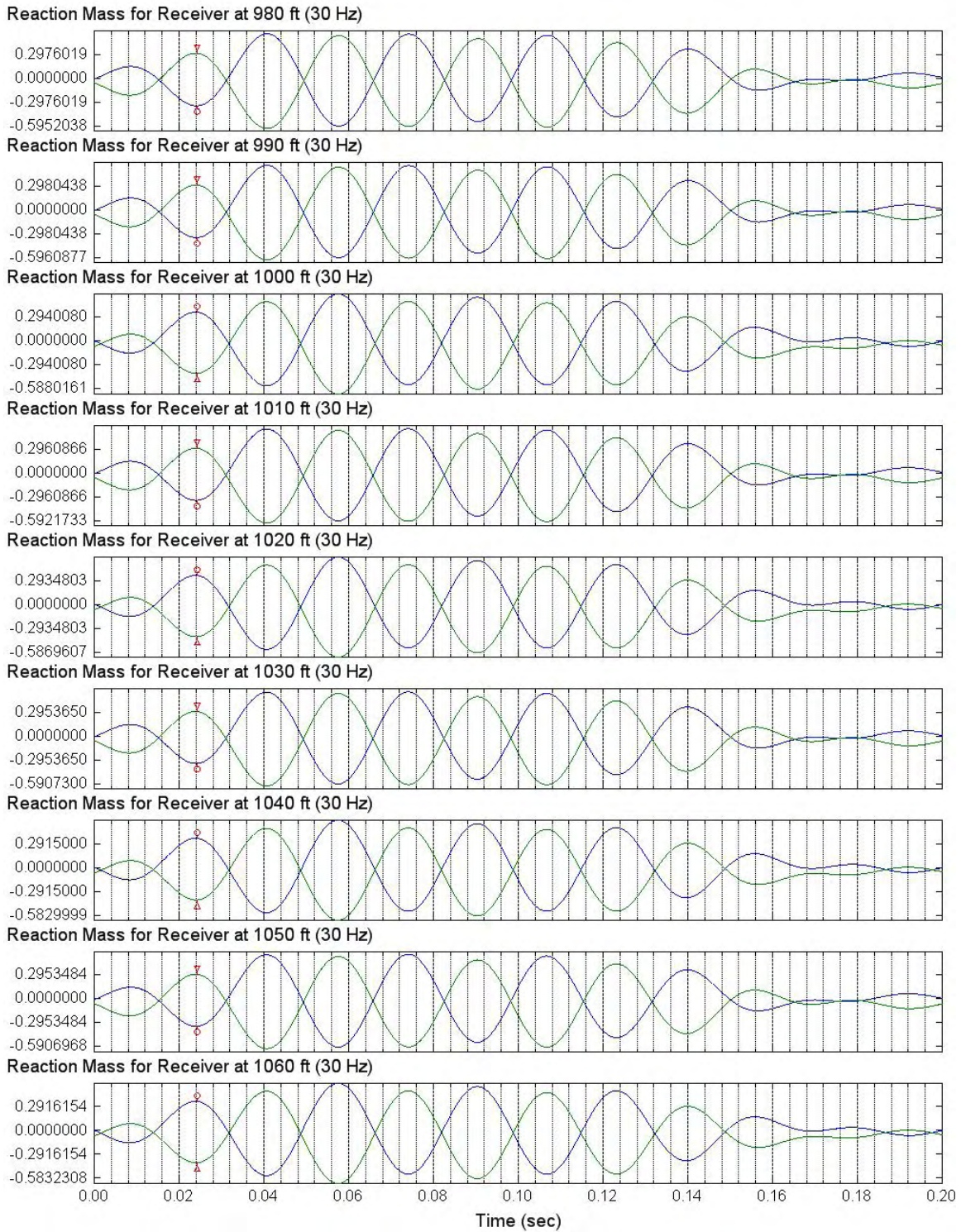


Figure 8.9 Filtered S-Wave Signals of Reaction Mass Accelerometer (C4996)
 Depths 1070 to 1150 ft; Input Signal: 4 Cycles of 30-Hz Sine Wave; Low Pass 40 Hz

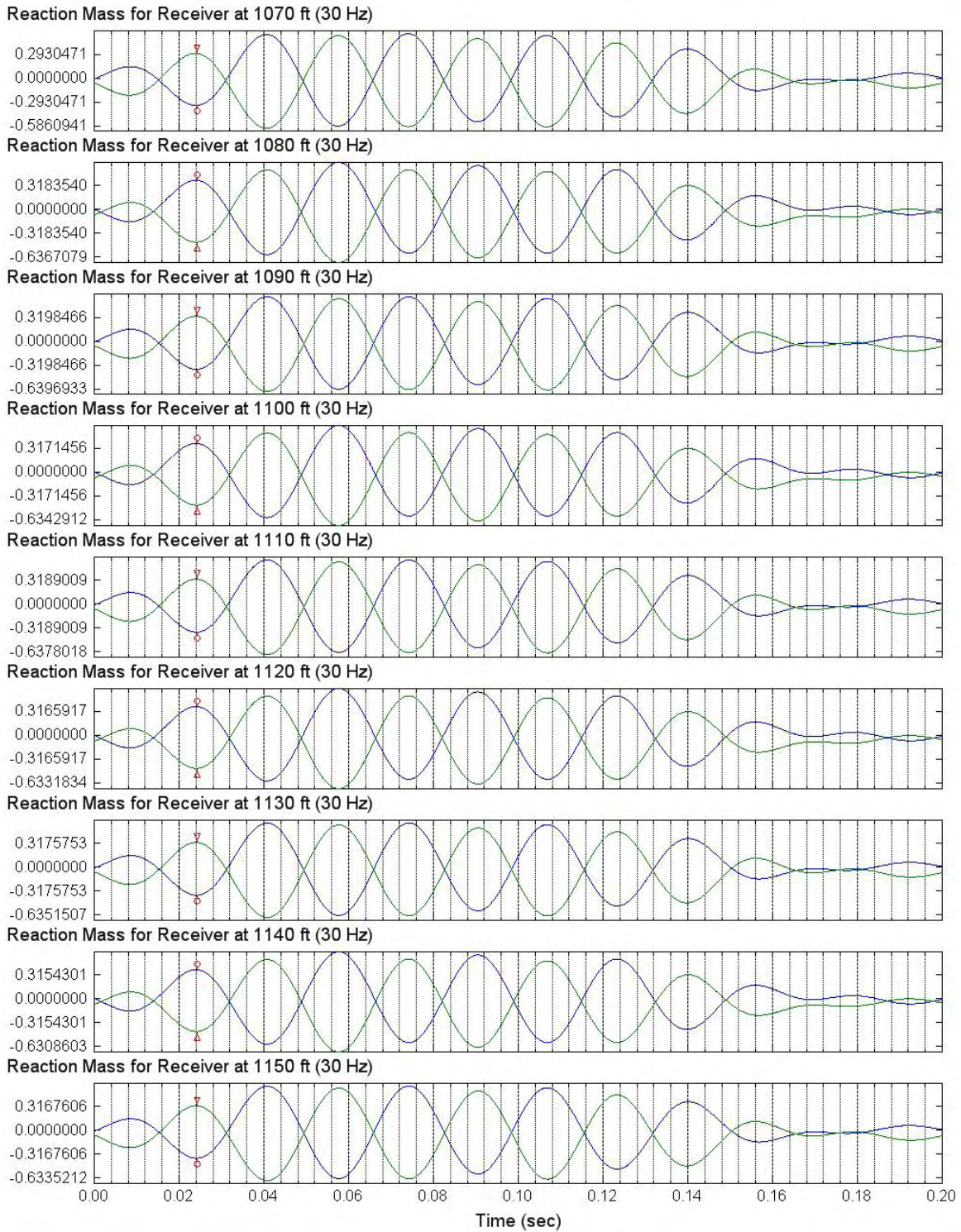
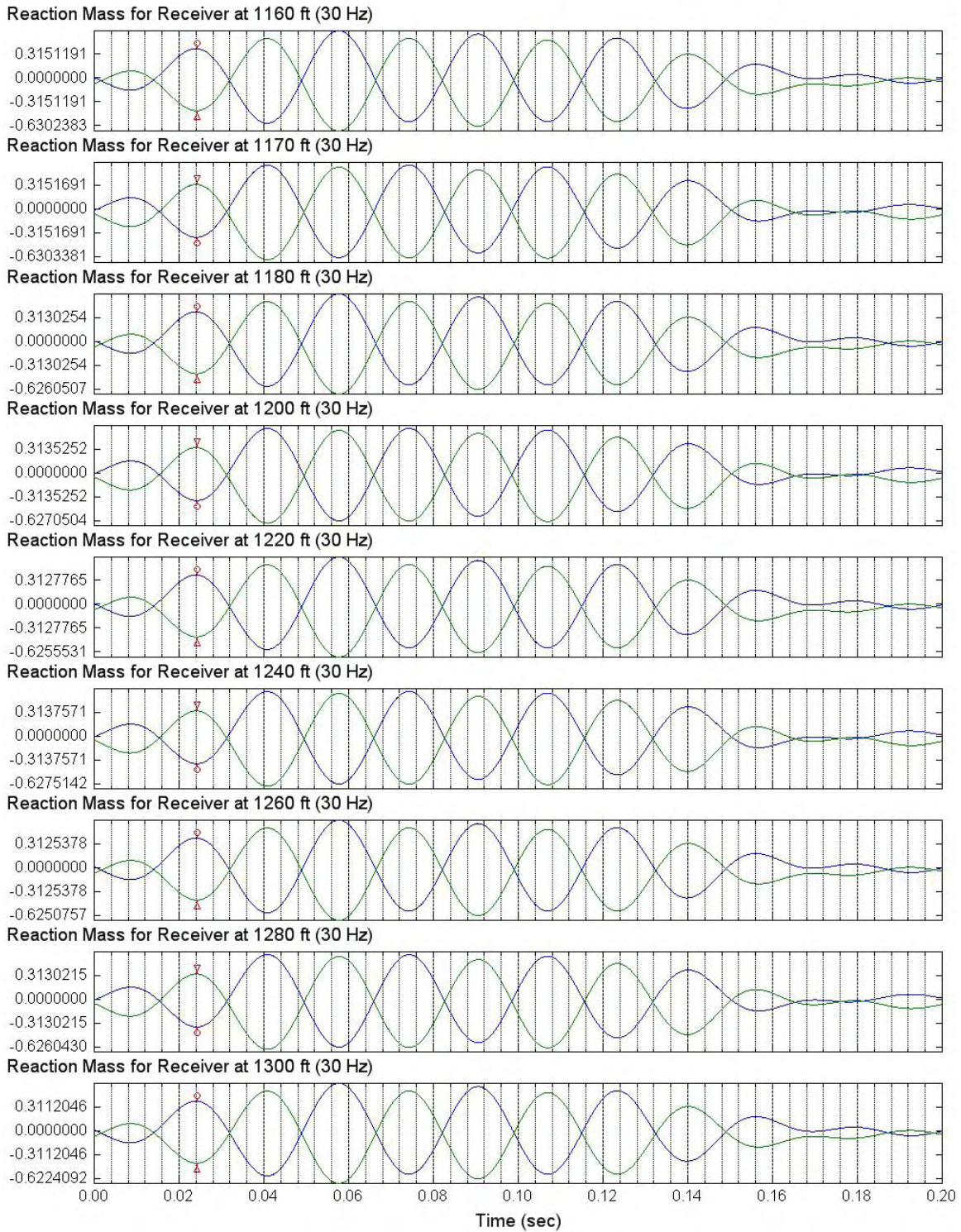


Figure 8.10 Filtered S-Wave Signals of Reaction Mass Accelerometer (C4996)
DDepths 1160 to 1300 ft; Input Signal: 4 Cycles of 30-Hz Sine Wave; Low Pass 40 Hz



Section 9: Filtered S-Wave Signals of Reference Receiver

1. Figures 9.1 to 9.6 present filtered reference horizontal receiver (S-wave) signals in Borehole C4996, depths 360 to 960 ft; FFT low pass 60 Hz; input signal: 5 cycles of 50-Hz sine wave.
2. Figure 9.7 presents filtered reference horizontal receiver (S-wave) signals in Borehole C4996, depths 910 to 980 ft; FFT low pass 25 Hz; input signal: 4 cycles of 20-Hz sine wave.
3. Figures 9.8 to 9.10 present filtered reference horizontal receiver (S-wave) signals in Borehole C4996, depths 980 to 1300 ft; FFT low pass 40 Hz; input signal: 4 cycles of 30-Hz sine wave.

Figure 9.1 Filtered S-Wave Signals of Reference Horizontal Receiver (C4996)
Depths 360 to 455 ft; Input Signal: 5 Cycles of 50-Hz Sine Wave; Low Pass 60 Hz

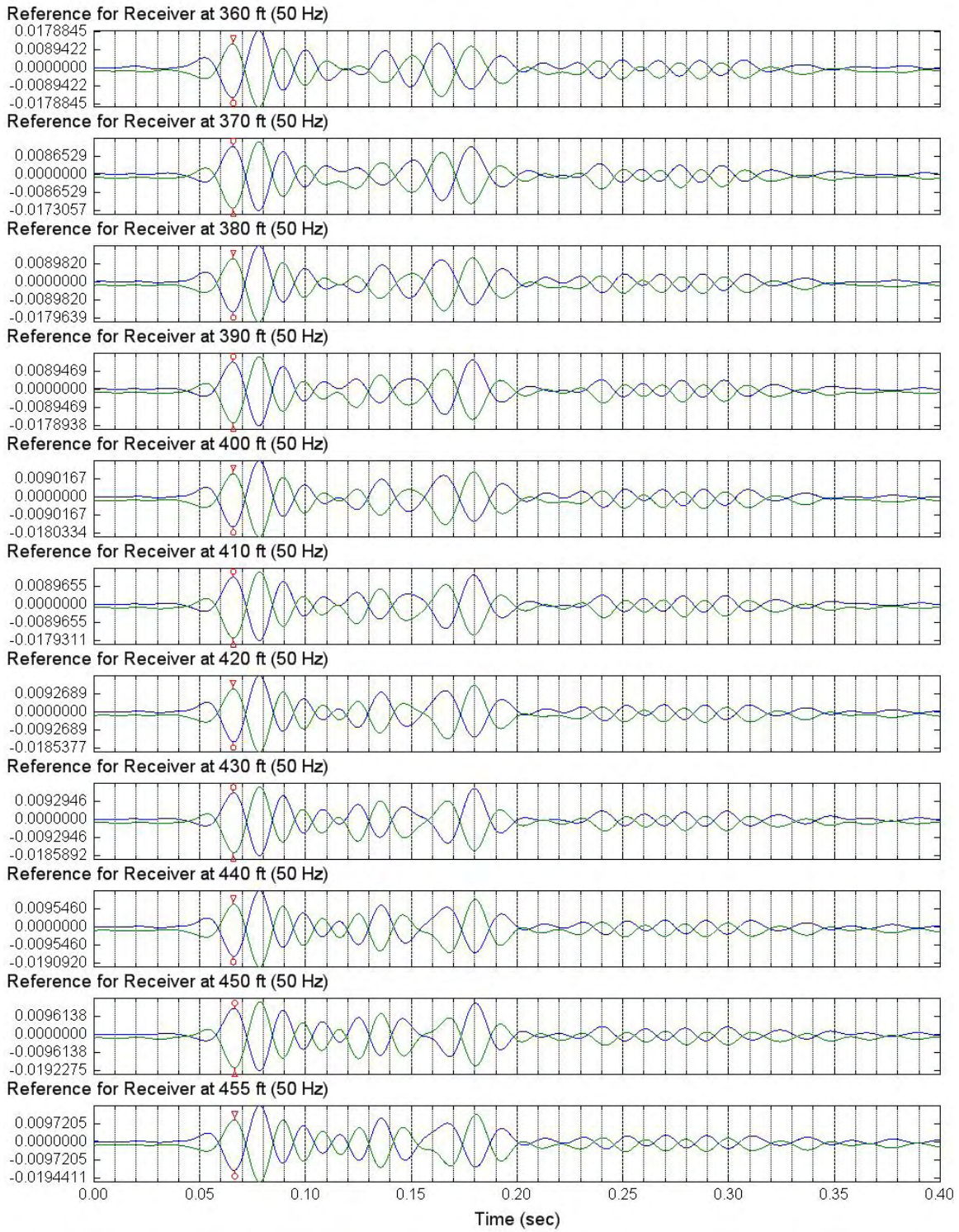


Figure 9.2 Filtered S-Wave Signals of Reference Horizontal Receiver (C4996)
 Depths 460 to 520 ft; Input Signal: 5 Cycles of 50-Hz Sine Wave; Low Pass 60 Hz

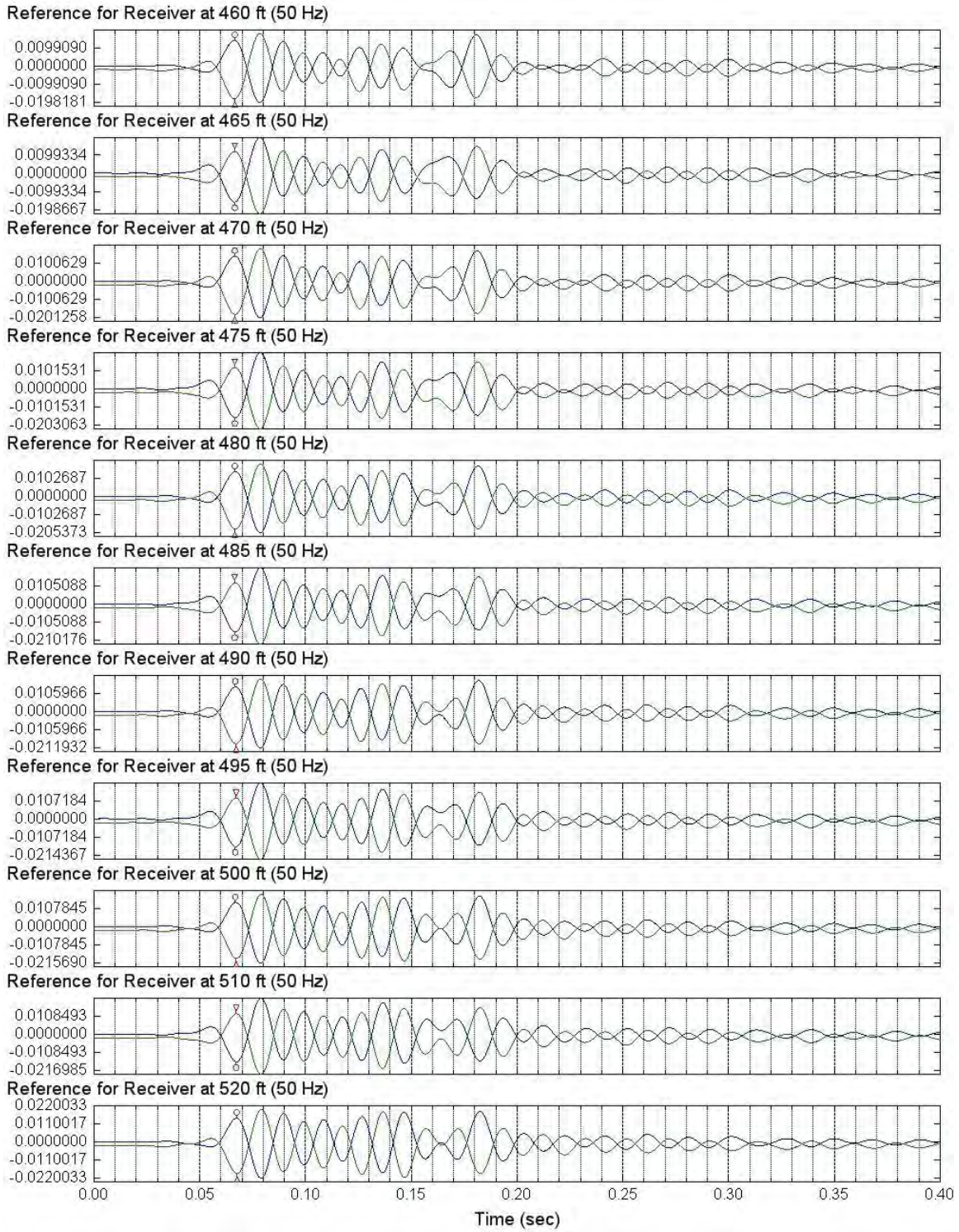


Figure 9.3 Filtered S-Wave Signals of Reference Horizontal Receiver (C4996)
 Depths 530 to 630 ft; Input Signal: 5 Cycles of 50-Hz Sine Wave; Low Pass 60 Hz

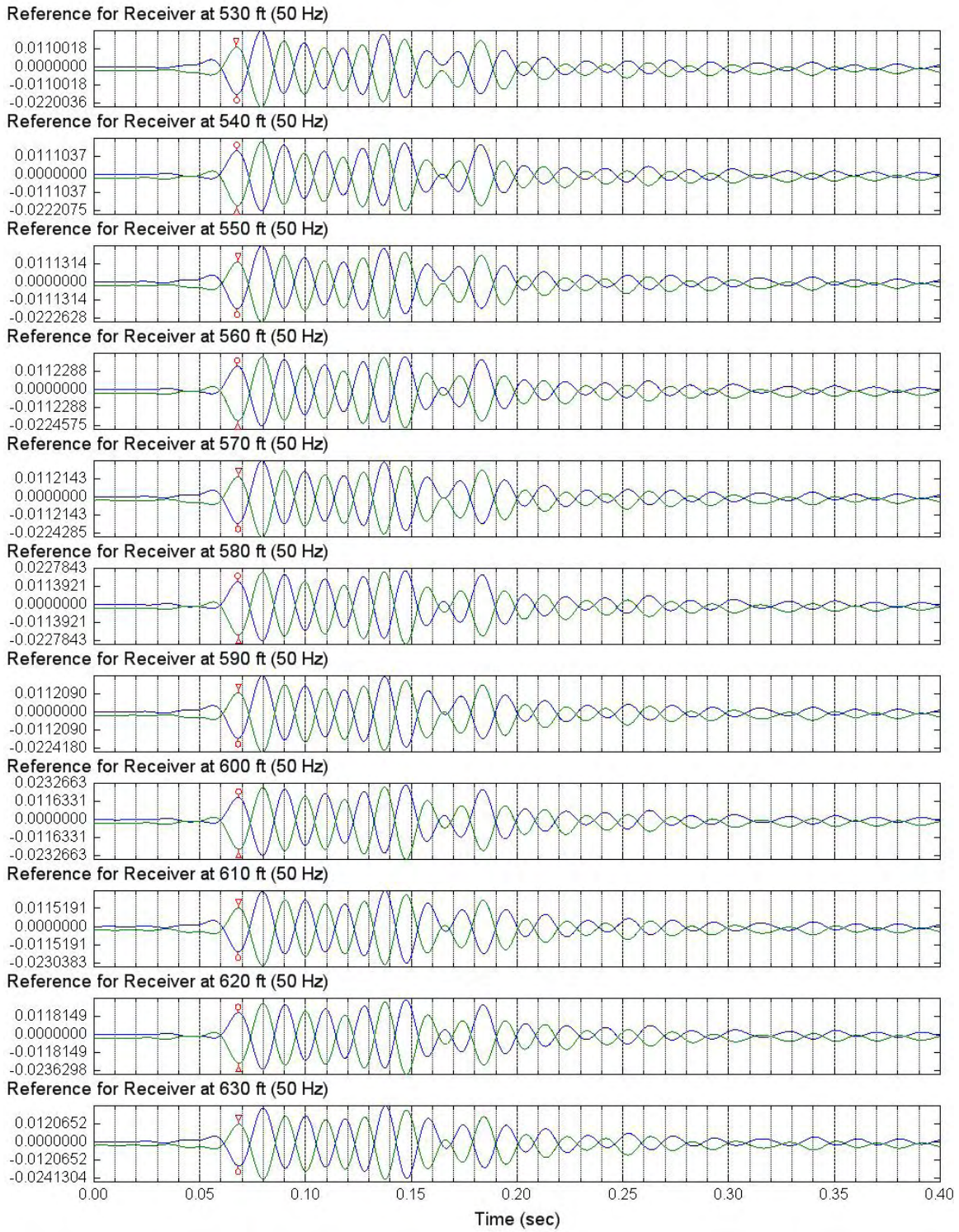


Figure 9.4 Filtered S-Wave Signals of Reference Horizontal Receiver (C4996)
 Depths 640 to 720 ft; Input Signal: 5 Cycles of 50-Hz Sine Wave; Low Pass 60 Hz

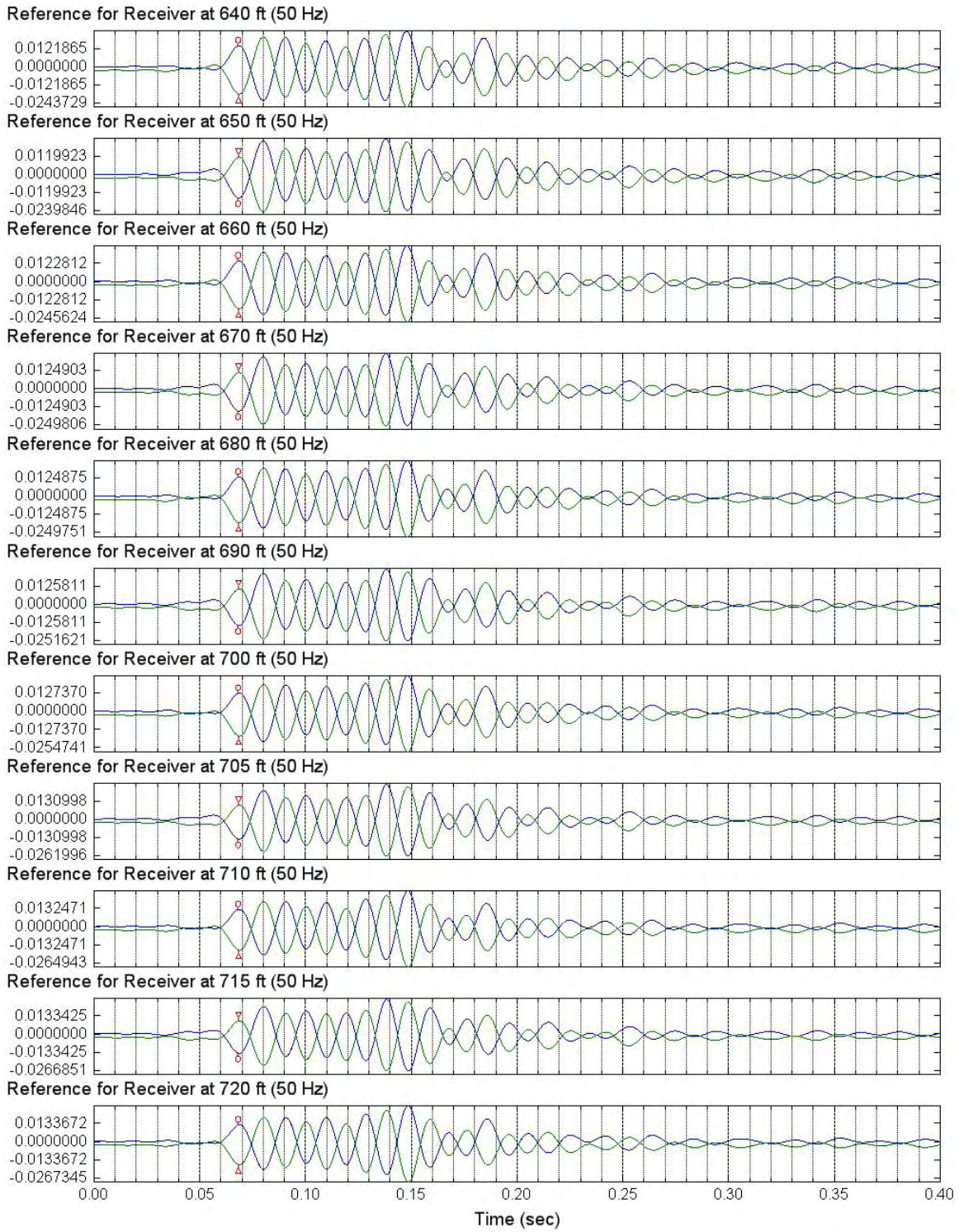


Figure 9.5 Filtered S-Wave Signals of Reference Horizontal Receiver (C4996)
 Depths 730 to 820 ft; Input Signal: 5 Cycles of 50-Hz Sine Wave; Low Pass 60 Hz

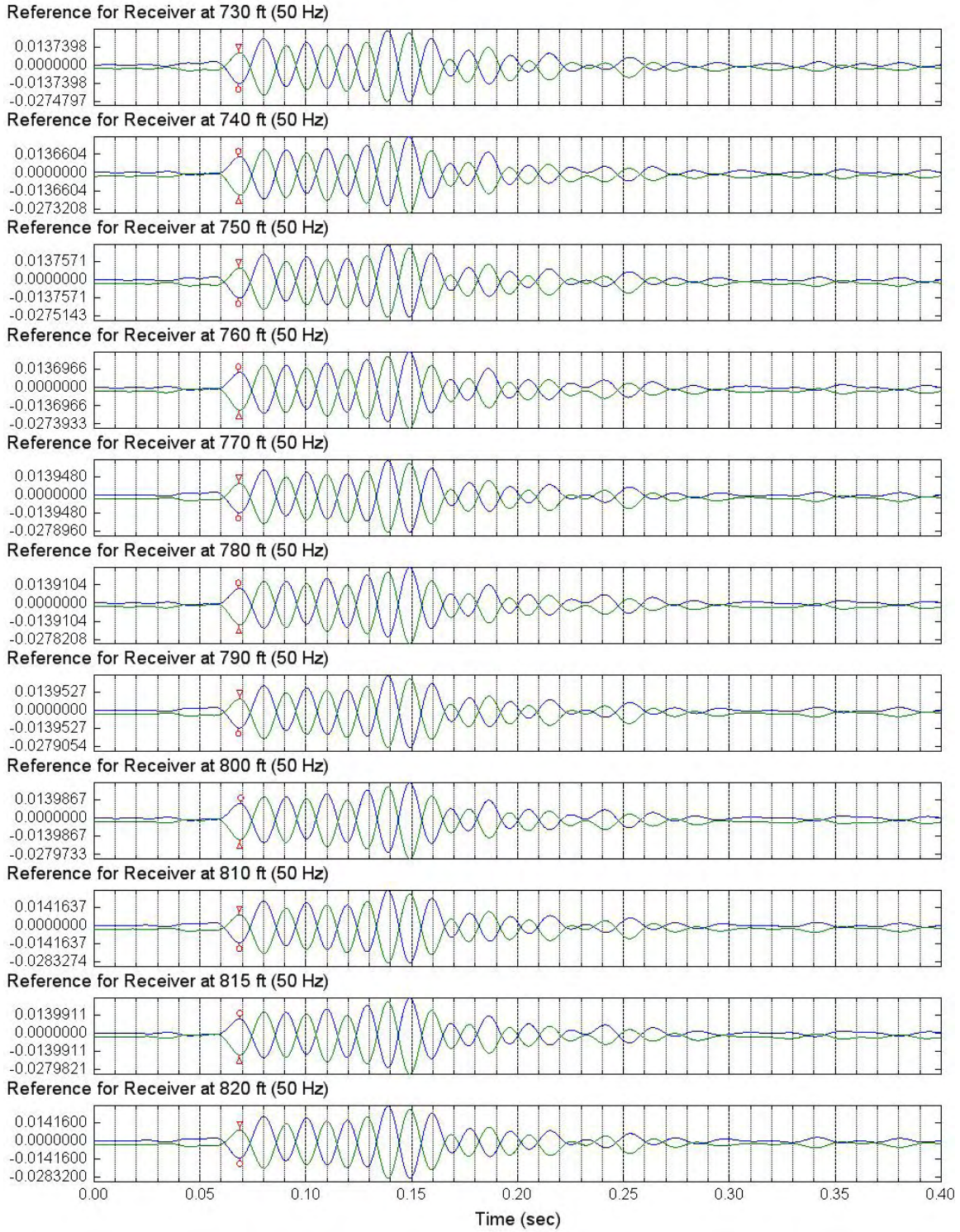


Figure 9.6 Filtered S-Wave Signals of Reference Horizontal Receiver (C4996)
 Depths 830 to 960 ft; Input Signal: 5 Cycles of 50-Hz Sine Wave; Low Pass 60 Hz

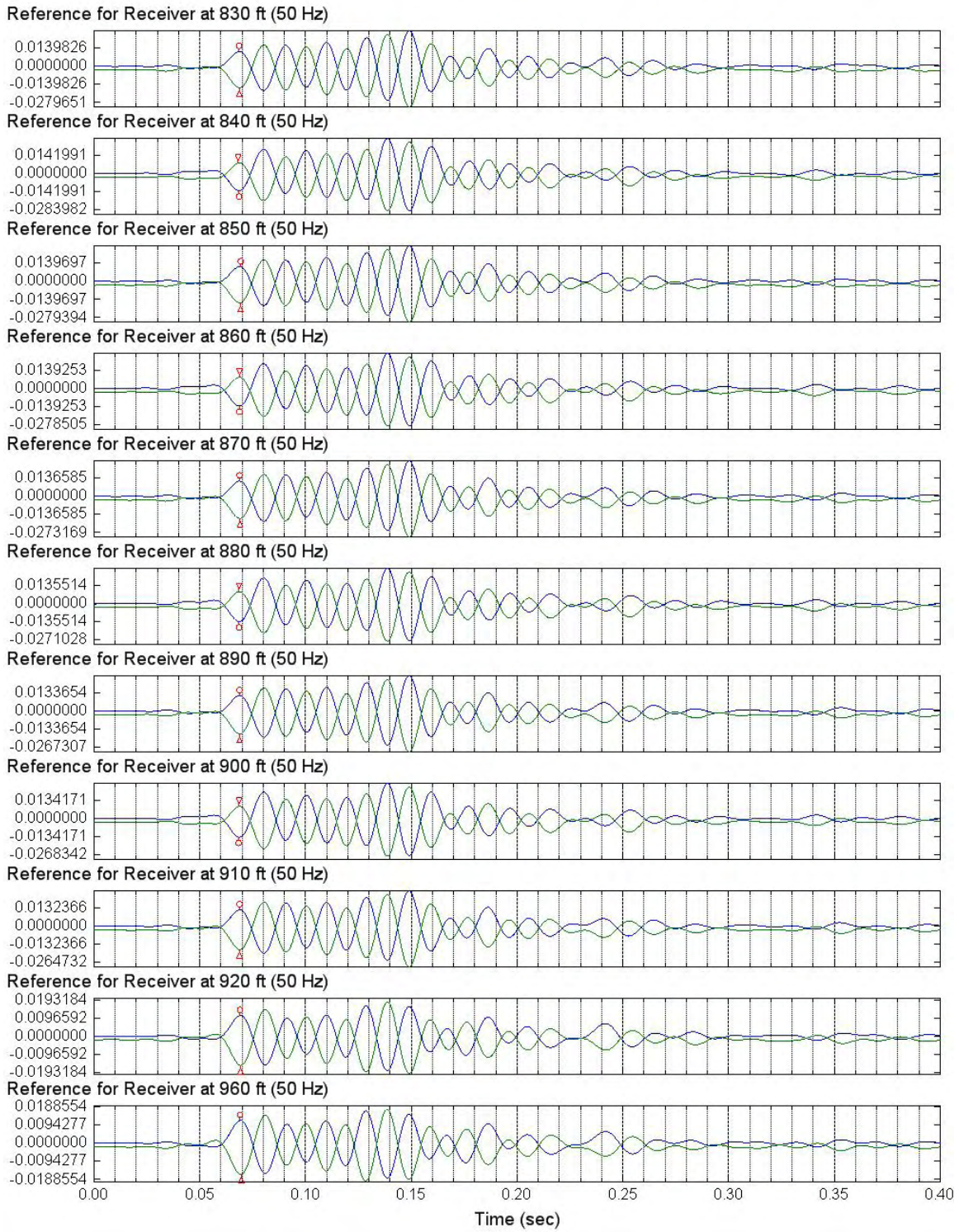


Figure 9.7 Filtered S-Wave Signals of Reference Horizontal Receiver (C4996)
Depths 910 to 980 ft; Input Signal: 4 Cycles of 20-Hz Sine Wave; Low Pass 25 Hz

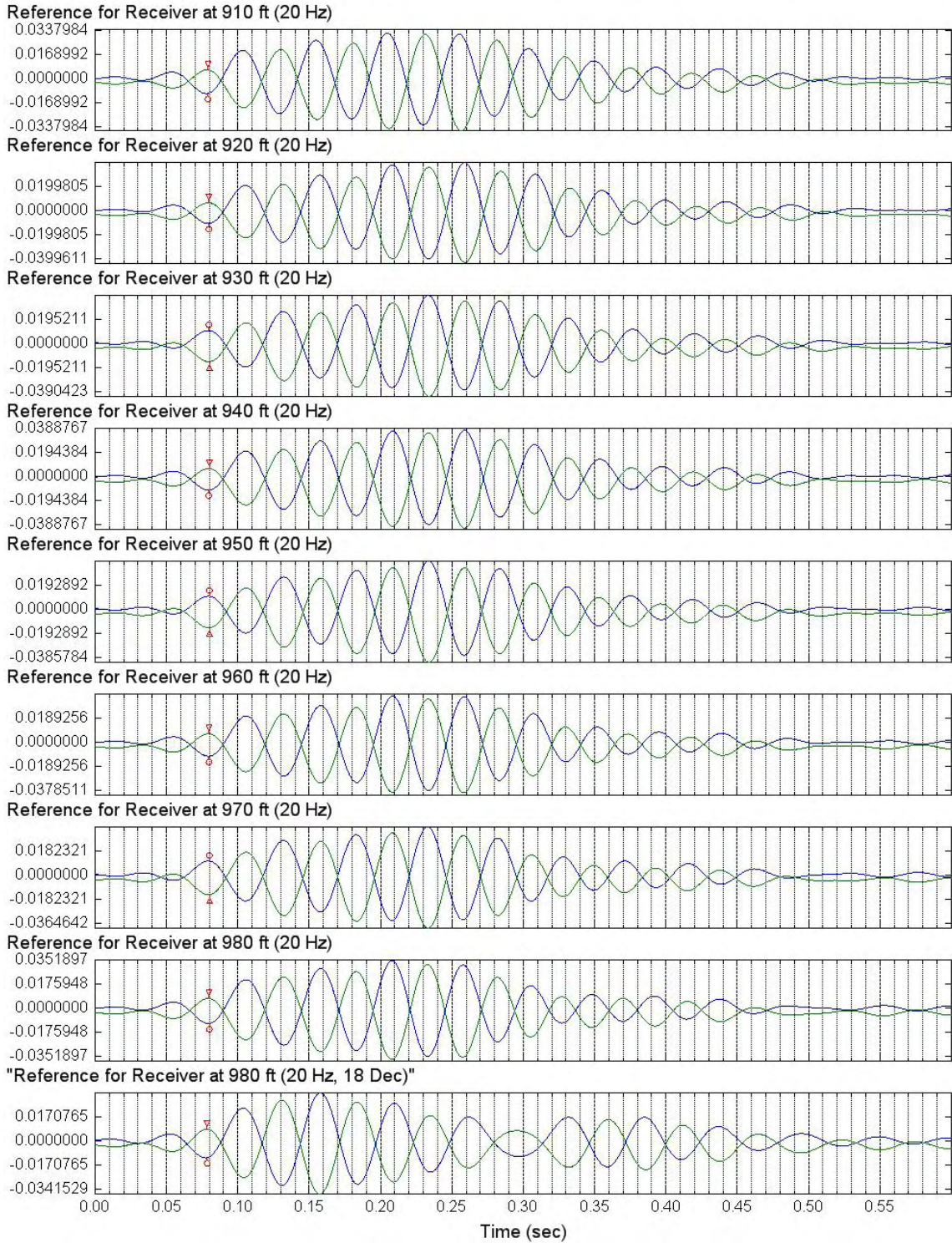


Figure 9.8 Filtered S-Wave Signals of Reference Horizontal Receiver (C4996)
 Depths 980 to 1060 ft; Input Signal: 4 Cycles of 30-Hz Sine Wave; Low Pass 40 Hz

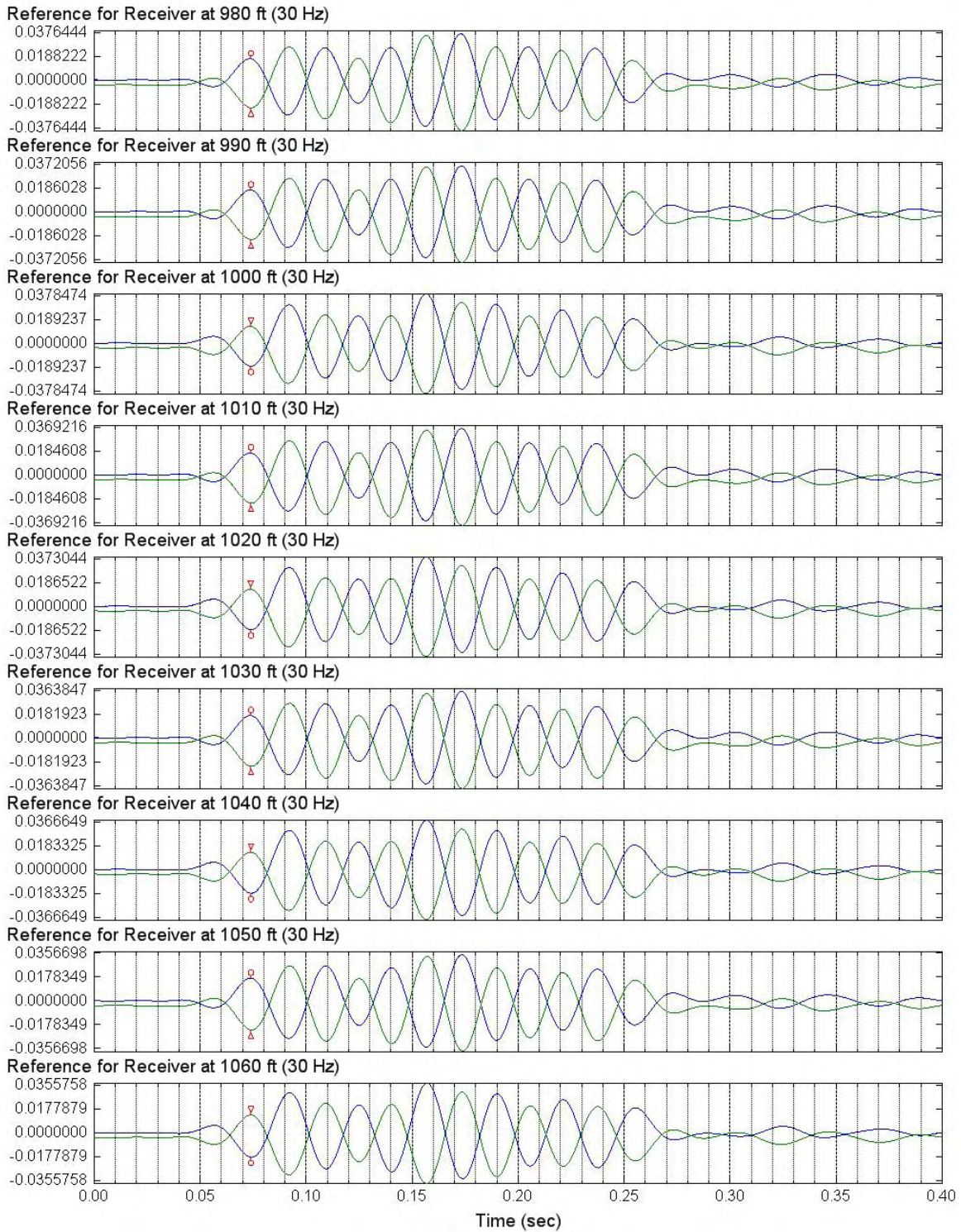


Figure 9.9 Filtered S-Wave Signals of Reference Horizontal Receiver (C4996)
Depths 1070 to 1150 ft; Input Signal: 4 Cycles of 30-Hz Sine Wave; Low Pass 40 Hz

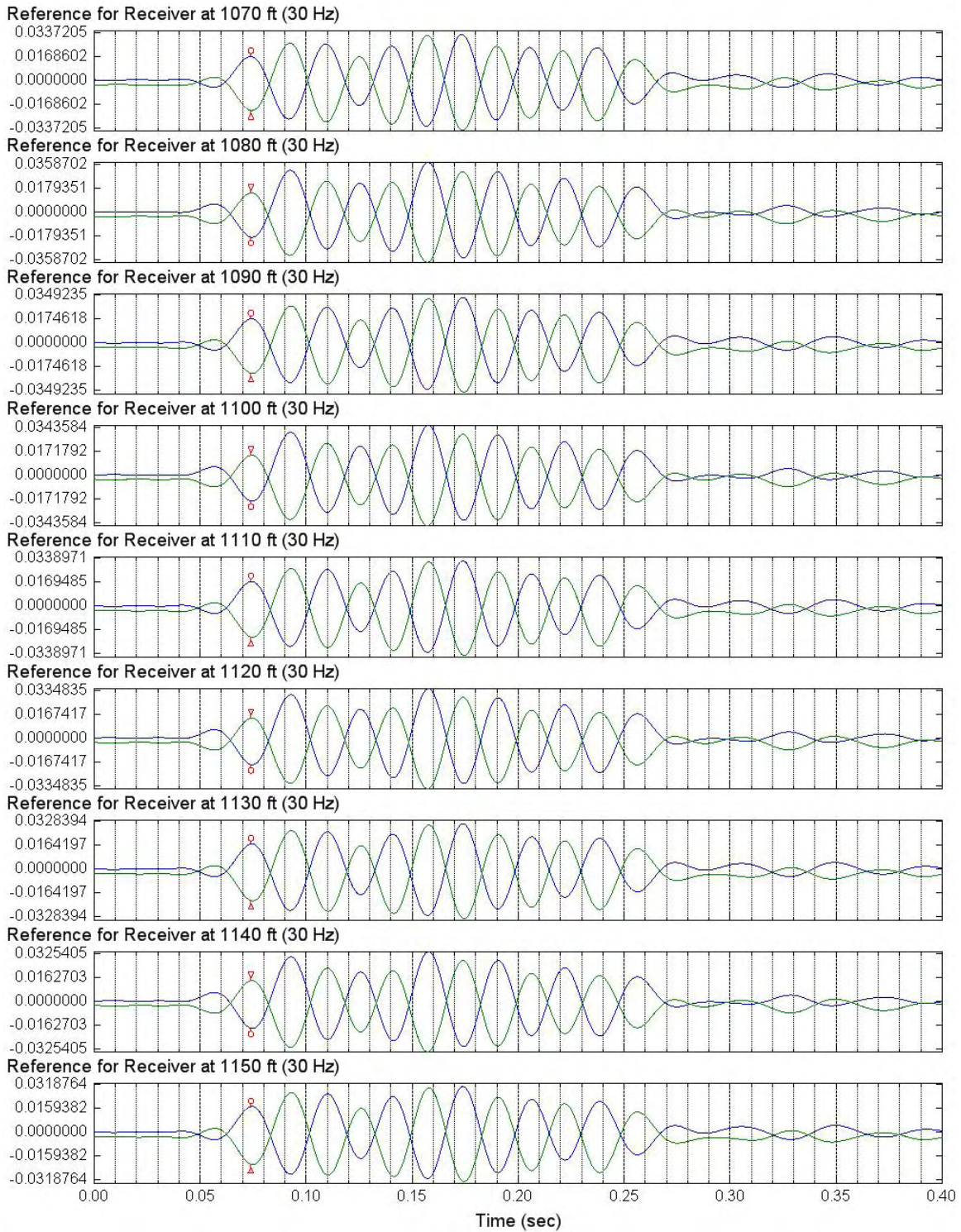
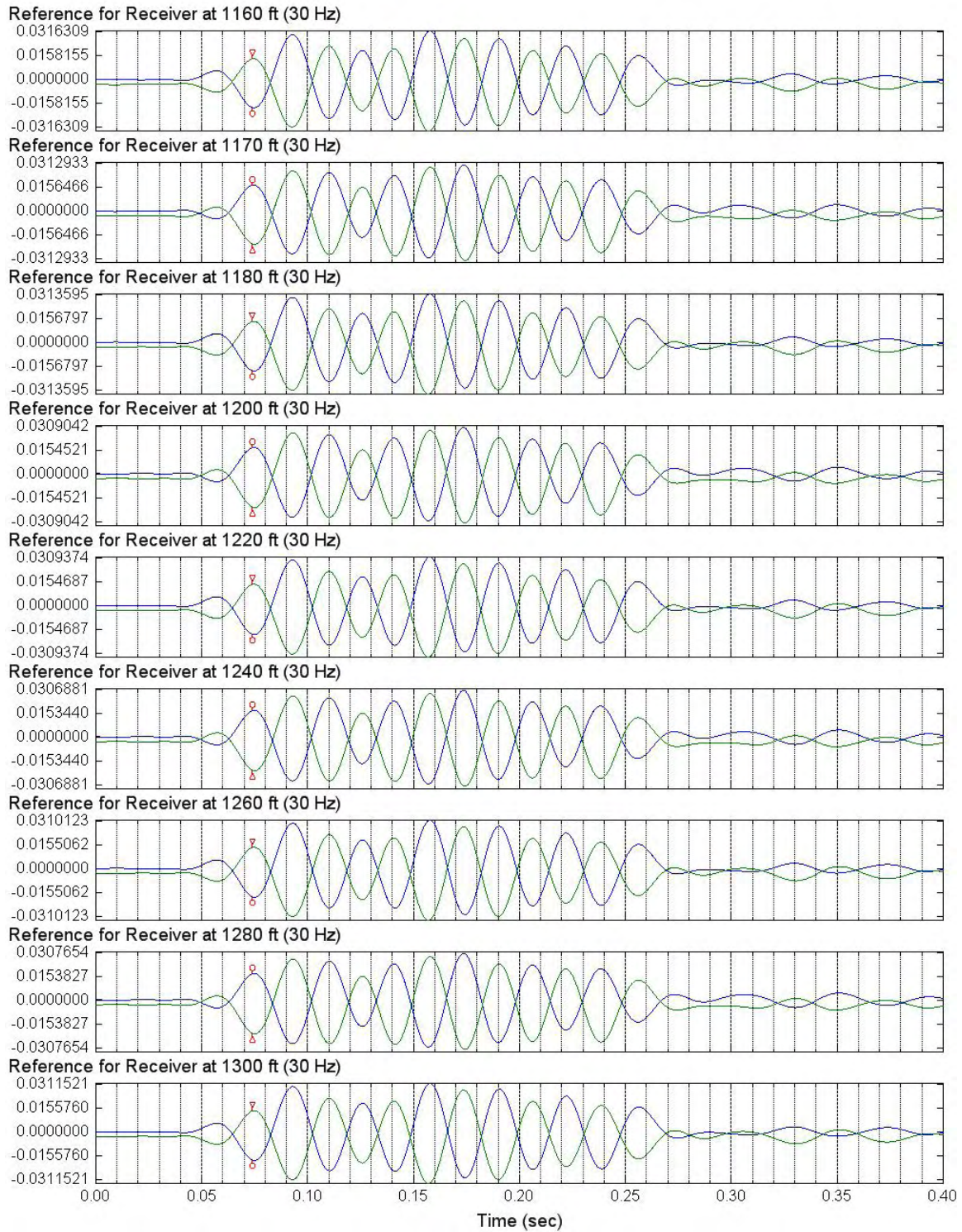


Figure 9.10 Filtered S-Wave Signals of Reference Horizontal Receiver (C4996)
 Depths 1160 to 1300 ft; Input Signal: 4 Cycles of 30-Hz Sine Wave; Low Pass 40 Hz



Section 10: Expanded and Filtered S-Wave Signals of Lower Rotated In-Line Receiver

1. Figures 10.1 to 10.6 present expanded lower rotated in-line receiver (S-wave) signals in Borehole C4996, depths 360 to 960 ft; FFT low pass 60 Hz; input signal: 5 cycles of 50-Hz sine wave.
2. Figure 10.7 presents expanded lower rotated in-line receiver (S-wave) signals in Borehole C4996, depths 910 to 980 ft; FFT low pass 25 Hz; input signal: 4 cycles of 20-Hz sine wave.
3. Figures 10.8 to 10.10 present expanded lower rotated in-line receiver (S-wave) signals in Borehole C4996, depths 980 to 1300 ft; FFT low pass 40 Hz; input signal: 4 cycles of 30-Hz sine wave.

Figure 10.1 Expanded S-Wave Signals of Lower Rotated In-Line Receiver (C4996)
 Depths 360 to 455 ft; Input Signal: 5 Cycles of 50-Hz Sine Wave; Low Pass 60 Hz

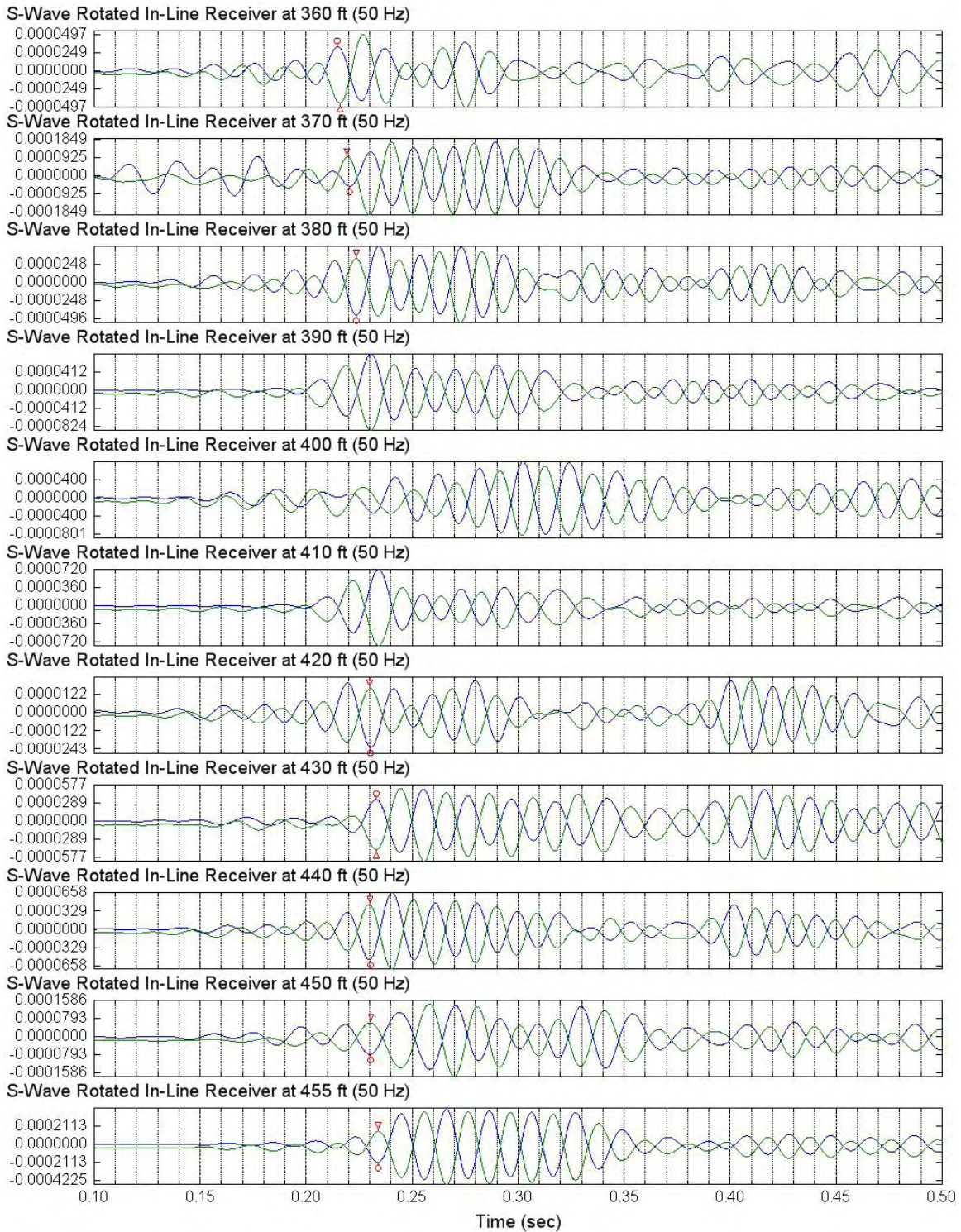


Figure 10.2 Expanded S-Wave Signals of Lower Rotated In-Line Receiver (C4996)
 Depths 460 to 520 ft; Input Signal: 5 Cycles of 50-Hz Sine Wave; Low Pass 60 Hz

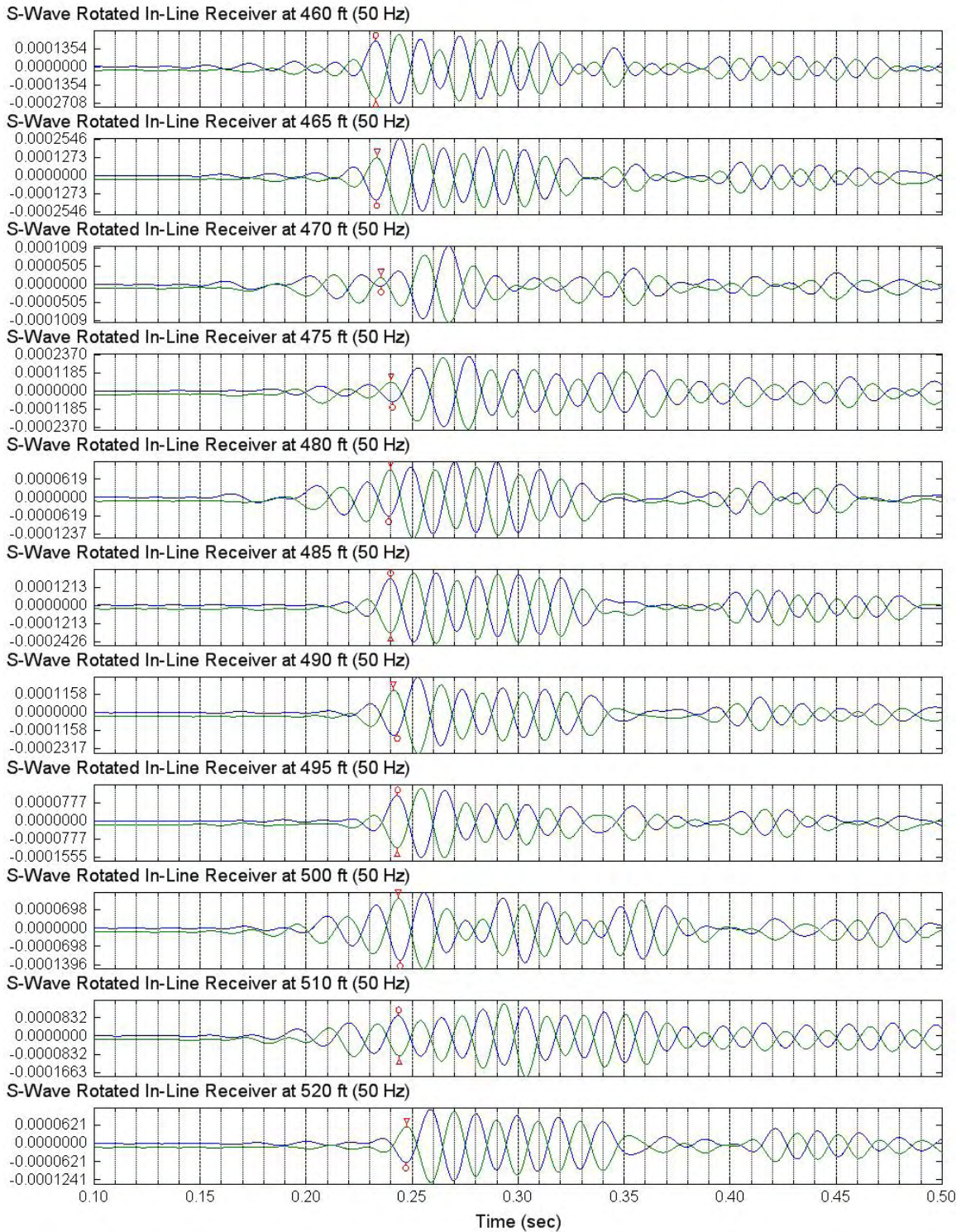


Figure 10.3 Expanded S-Wave Signals of Lower Rotated In-Line Receiver (C4996)
 Depths 530 to 630 ft; Input Signal: 5 Cycles of 50-Hz Sine Wave; Low Pass 60 Hz

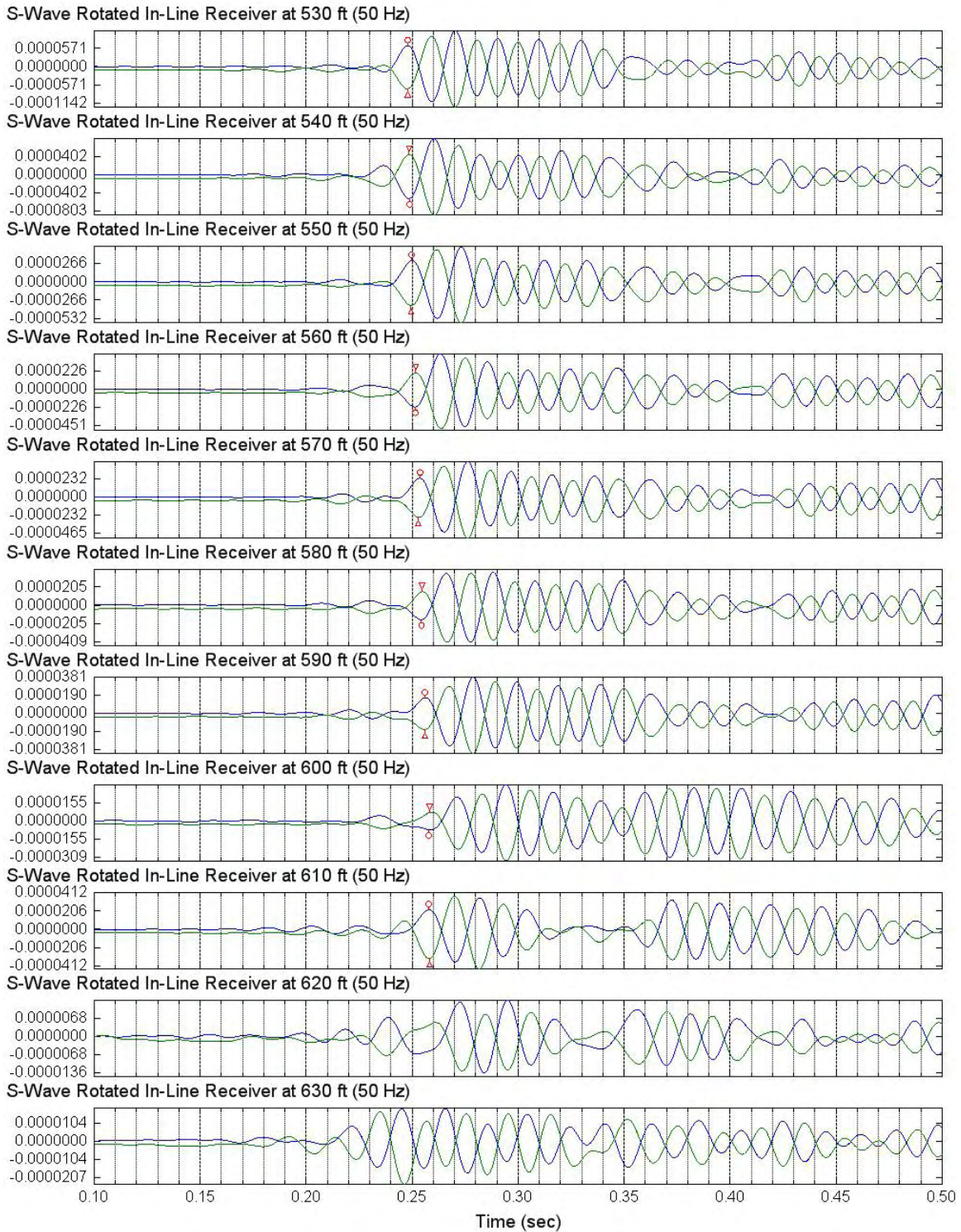


Figure 10.4 Expanded S-Wave Signals of Lower Rotated In-Line Receiver (C4996)
 Depths 640 to 720 ft; Input Signal: 5 Cycles of 50-Hz Sine Wave; Low Pass 60 Hz

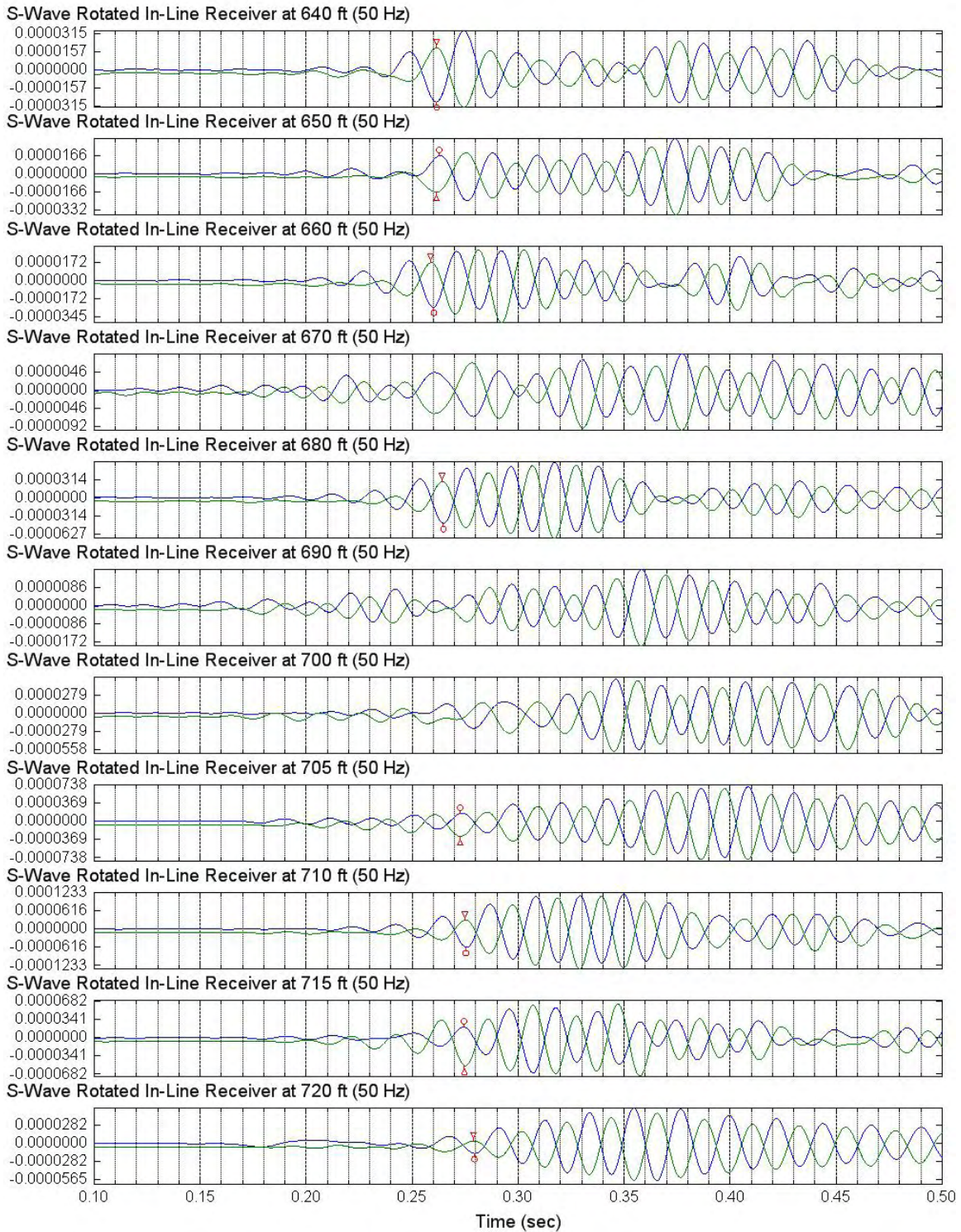


Figure 10.5 Expanded S-Wave Signals of Lower Rotated In-Line Receiver (C4996)
Depths 730 to 820 ft; Input Signal: 5 Cycles of 50-Hz Sine Wave; Low Pass 60 Hz

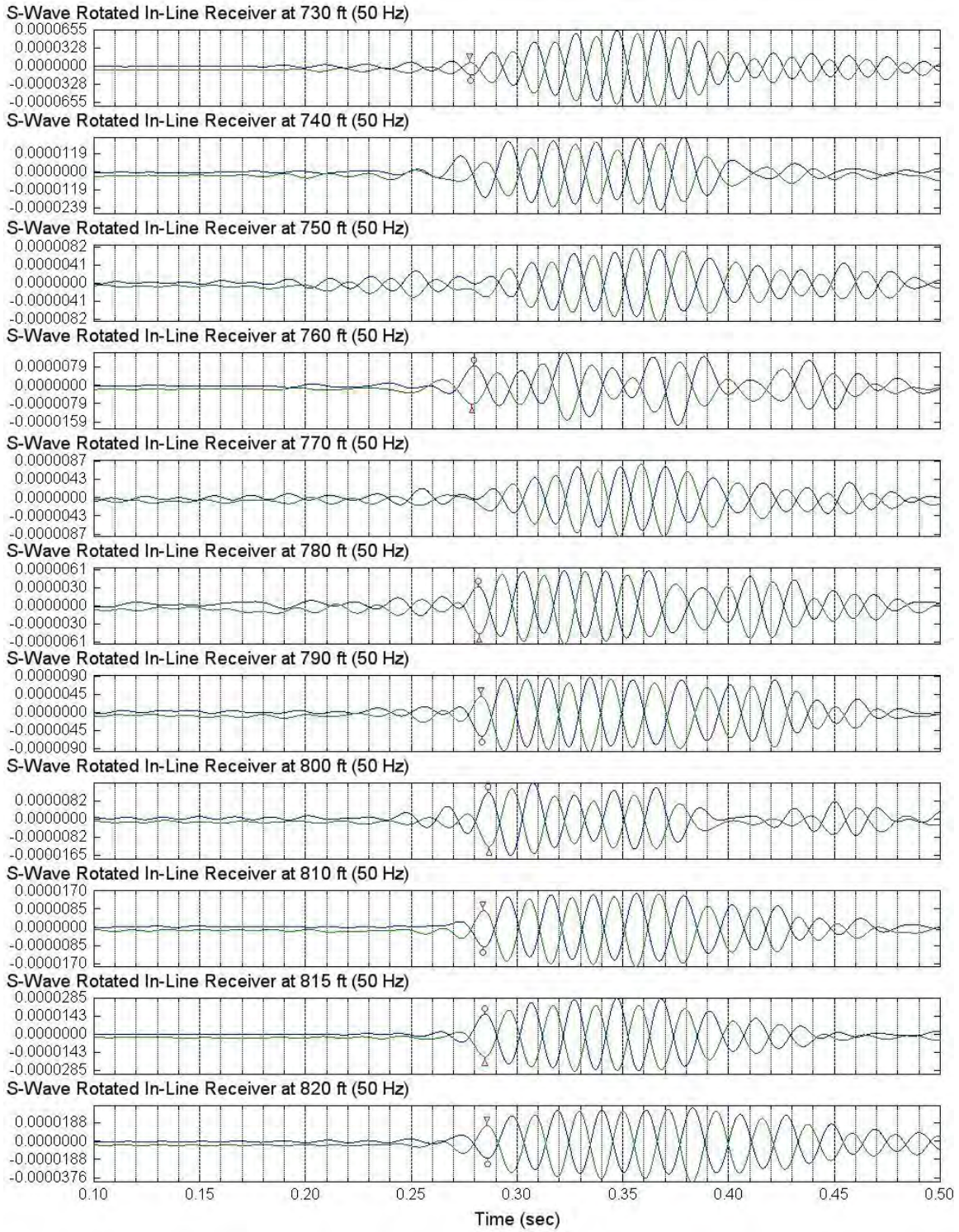


Figure 10.6 Expanded S-Wave Signals of Lower Rotated In-Line Receiver (C4996)
 Depths 830 to 960 ft; Input Signal: 5 Cycles of 50-Hz Sine Wave; Low Pass 60 Hz

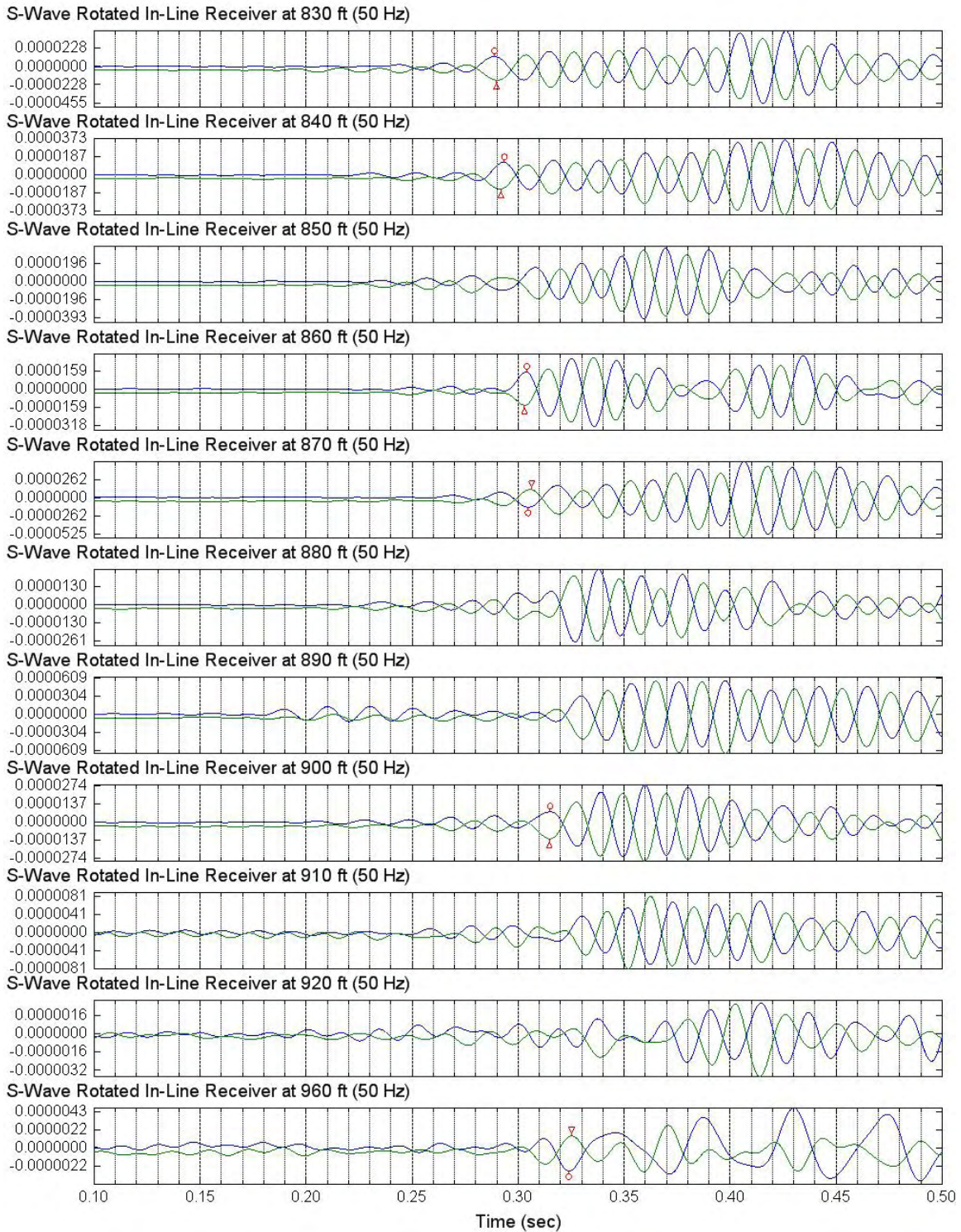


Figure 10.7 Expanded S-Wave Signals of Lower Rotated In-Line Receiver (C4996)
 Depths 910 to 980 ft; Input Signal: 4 Cycles of 20-Hz Sine Wave; Low Pass 25 Hz

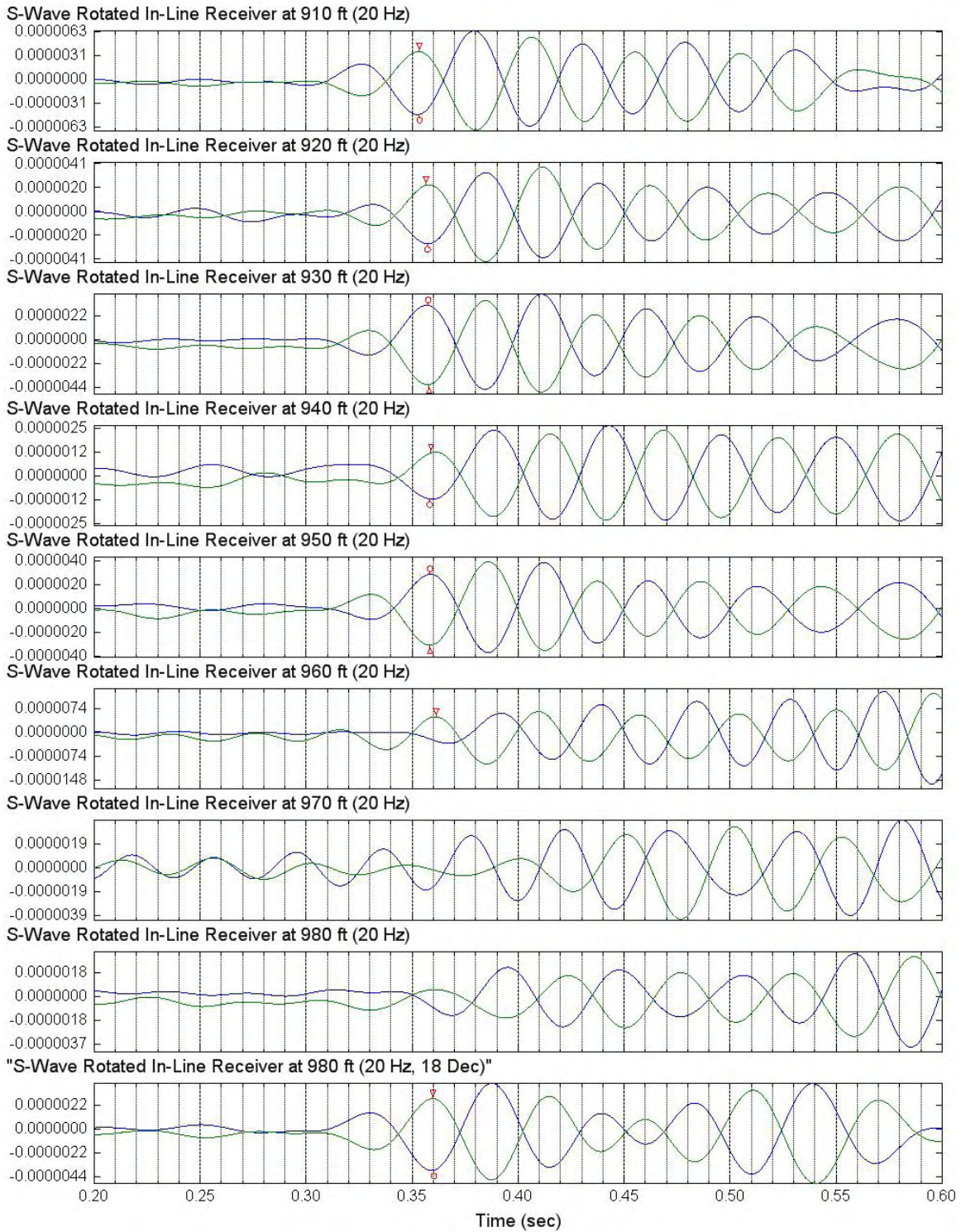


Figure 10.8 Expanded S-Wave Signals of Lower Rotated In-Line Receiver (C4996)
Depths 980 to 1060 ft; Input Signal: 4 Cycles of 30-Hz Sine Wave; Low Pass 40 Hz

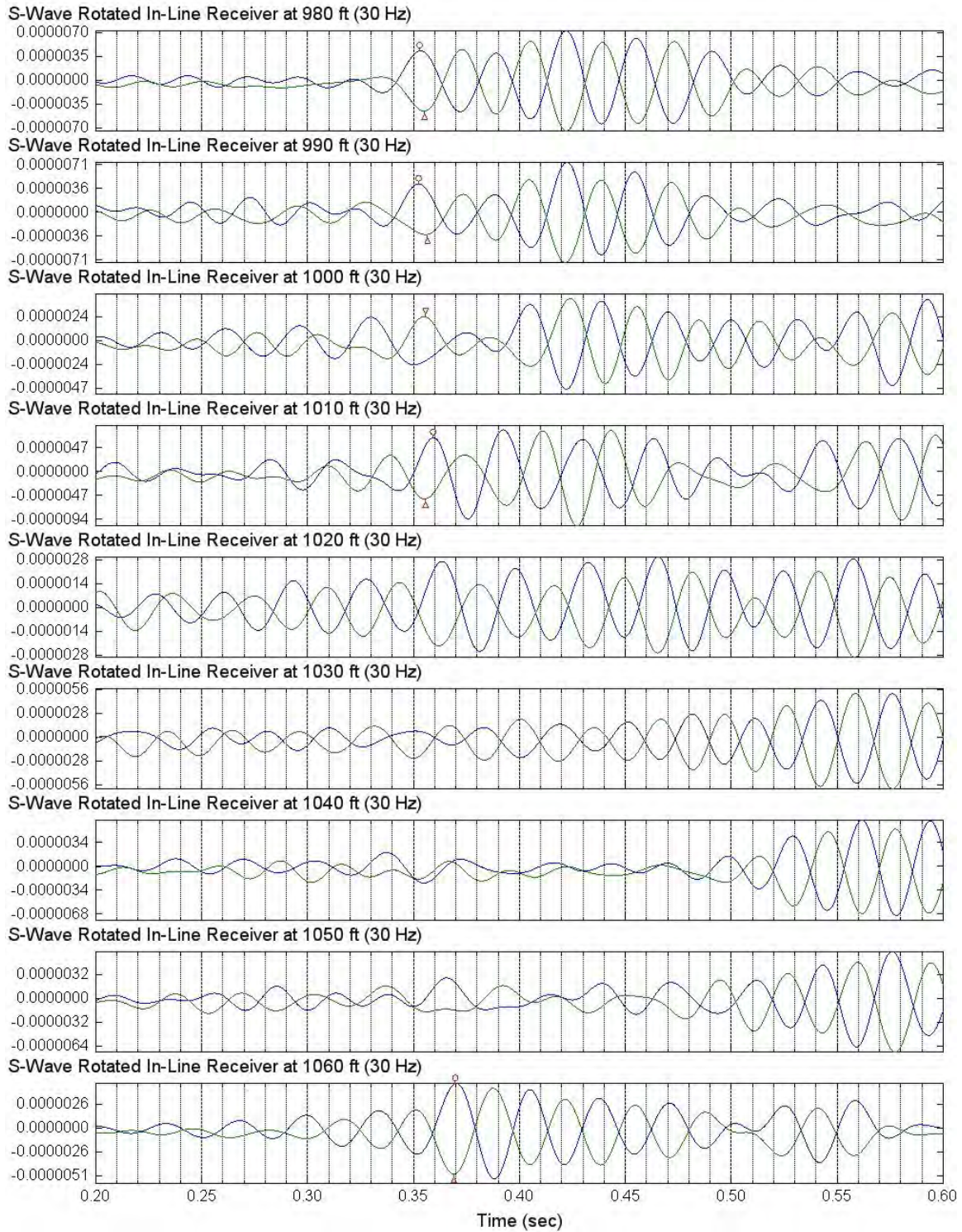


Figure 10.9 Expanded S-Wave Signals of Lower Rotated In-Line Receiver (C4996)
Depths 1070 to 1150 ft; Input Signal: 4 Cycles of 30-Hz Sine Wave; Low Pass 40 Hz

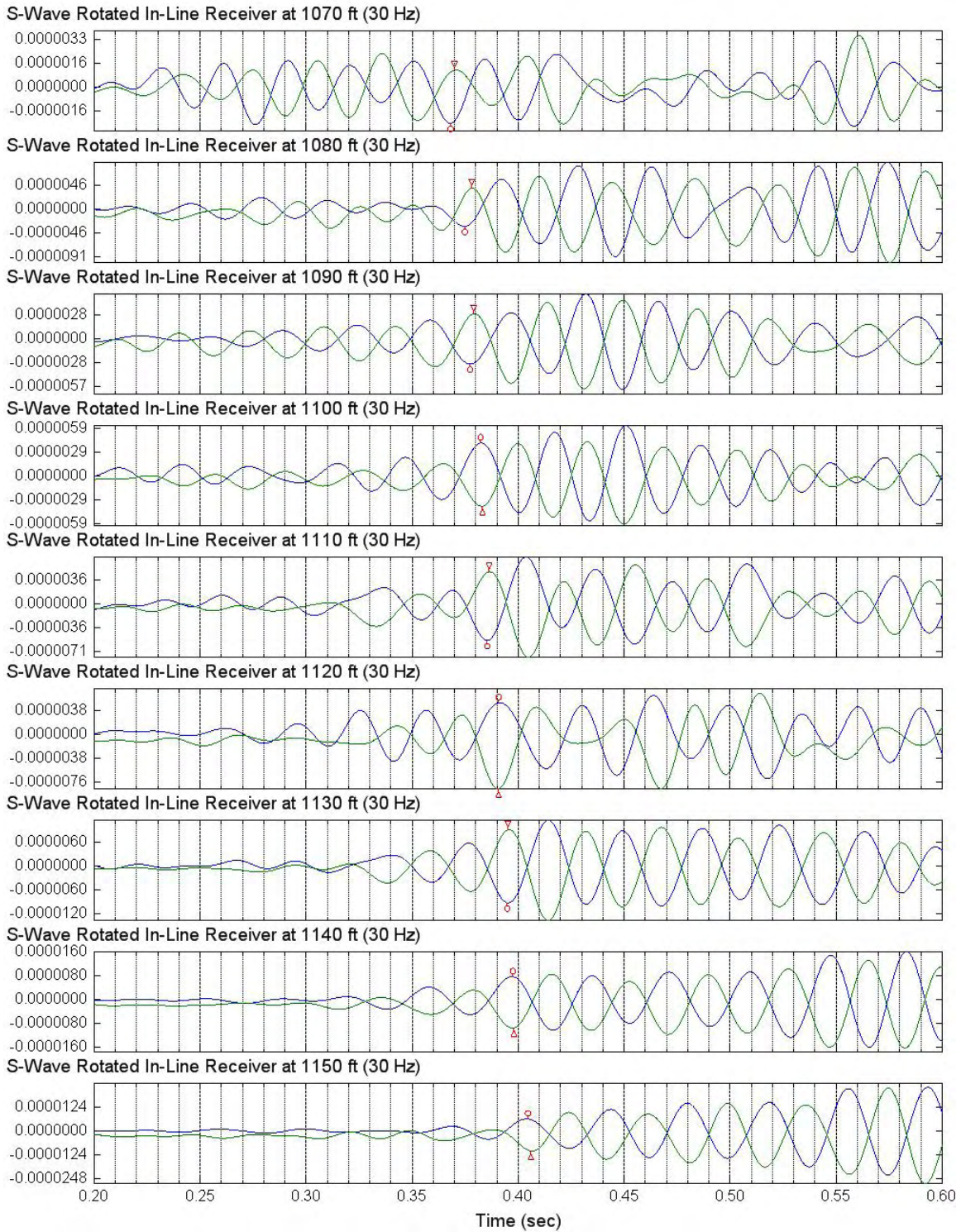
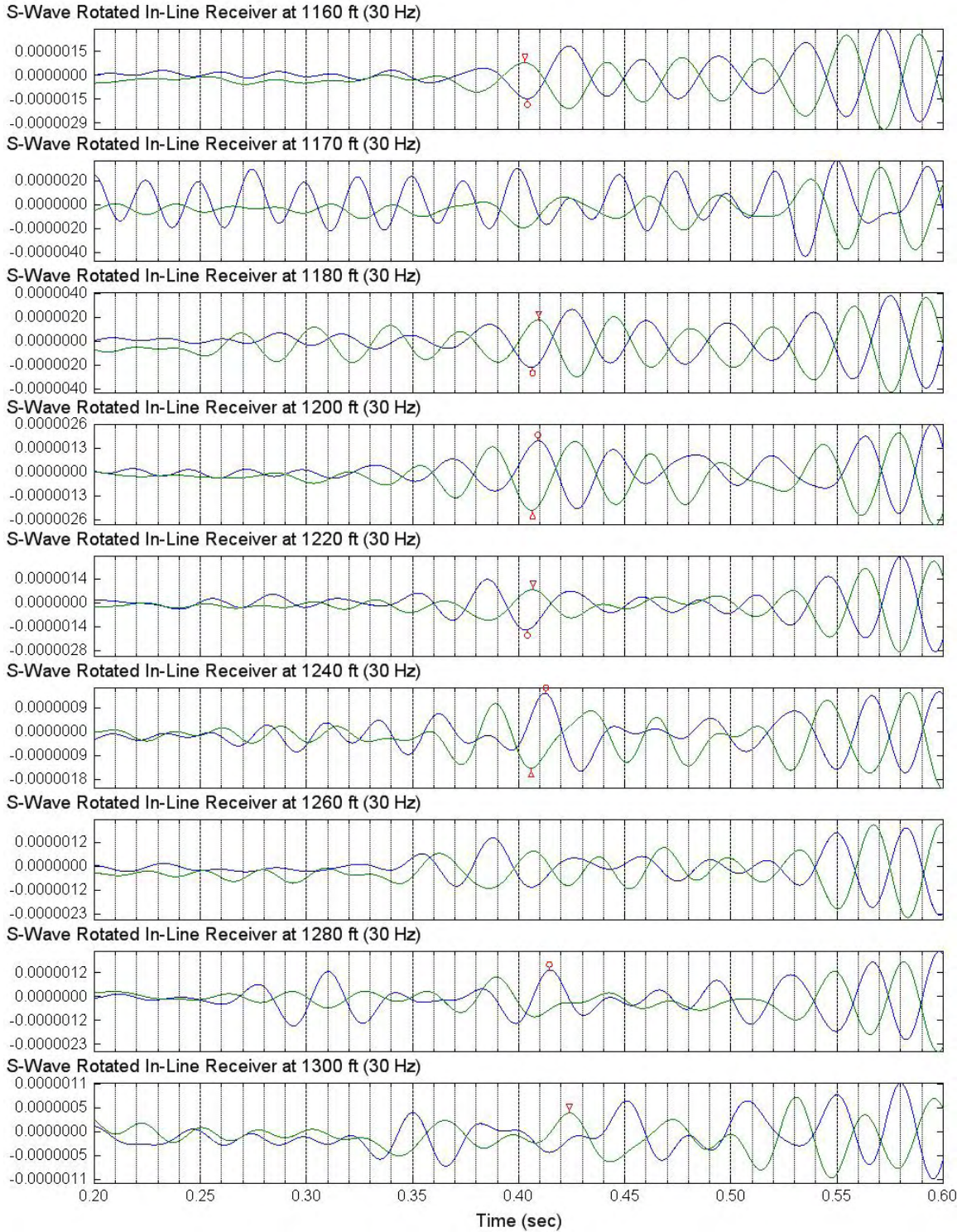


Figure 10.10 Expanded S-Wave Signals of Lower Rotated In-Line Receiver (C4996)
Depths 1160 to 1300 ft; Input Signal: 4 Cycles of 30-Hz Sine Wave; Low Pass 40 Hz



Section 11: Waterfall Plots of Unfiltered S-Wave Signals of Lower Rotated In-Line Receiver

1. Figures 11.1 to 11.3 present waterfall plots of unfiltered lower rotated in-line receiver (S-wave) signals in Borehole C4996, depths 360 to 960 ft; input signal is 5 cycles of 50-Hz sine wave, time shifted by the acceleration of the reaction mass.
2. Figure 11.4 presents waterfall plots of unfiltered lower rotated horizontal receiver (S-wave) signals in Borehole C4996, depths 910 to 980 ft; input signal is 4 cycles of 20-Hz sine wave, time shifted by the acceleration of the reaction mass.
3. Figure 11.5 presents waterfall plots of unfiltered lower rotated horizontal receiver (S-wave) signals in Borehole C4996, depths 980 to 1300 ft; input signal is 4 cycles of 30-Hz sine wave, time shifted by the acceleration of the reaction mass.

Figure 11.1 Waterfall Plot of Unfiltered S-Wave Signals of Lower Rotated In-Line Receiver (C4996)

Depths 360 to 520 ft; Input Signal: 5 Cycles of 50-Hz Sine Wave; Low Pass 60 Hz; Time Shifted by Reaction Mass Acceleration

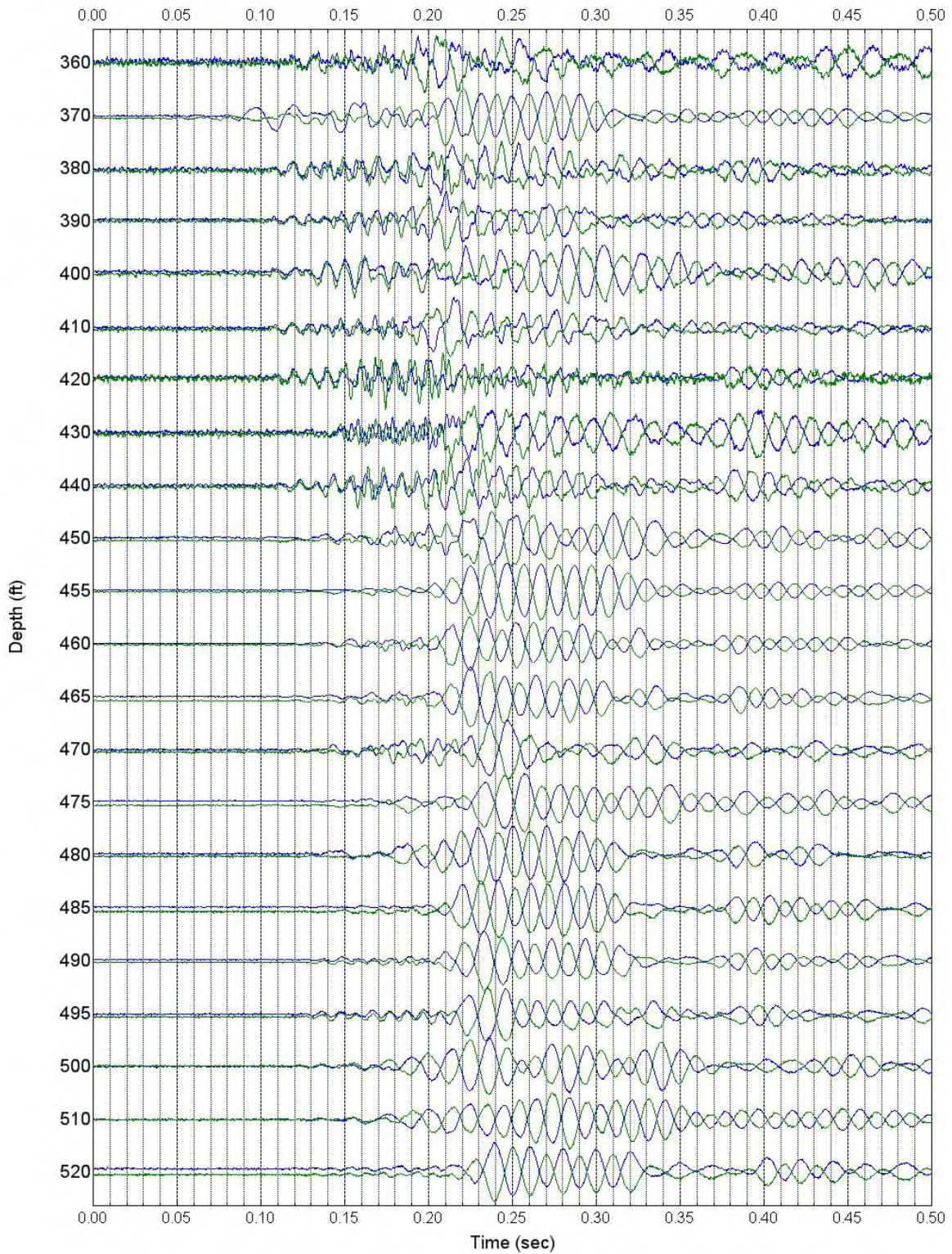


Figure 11.2 Waterfall Plot of Unfiltered S-Wave Signals of Lower Rotated In-Line Receiver (C4996)

Depths 530 to 720 ft; Input Signal: 5 Cycles of 50-Hz Sine Wave; Low Pass 60 Hz; Time Shifted by Reaction Mass Acceleration

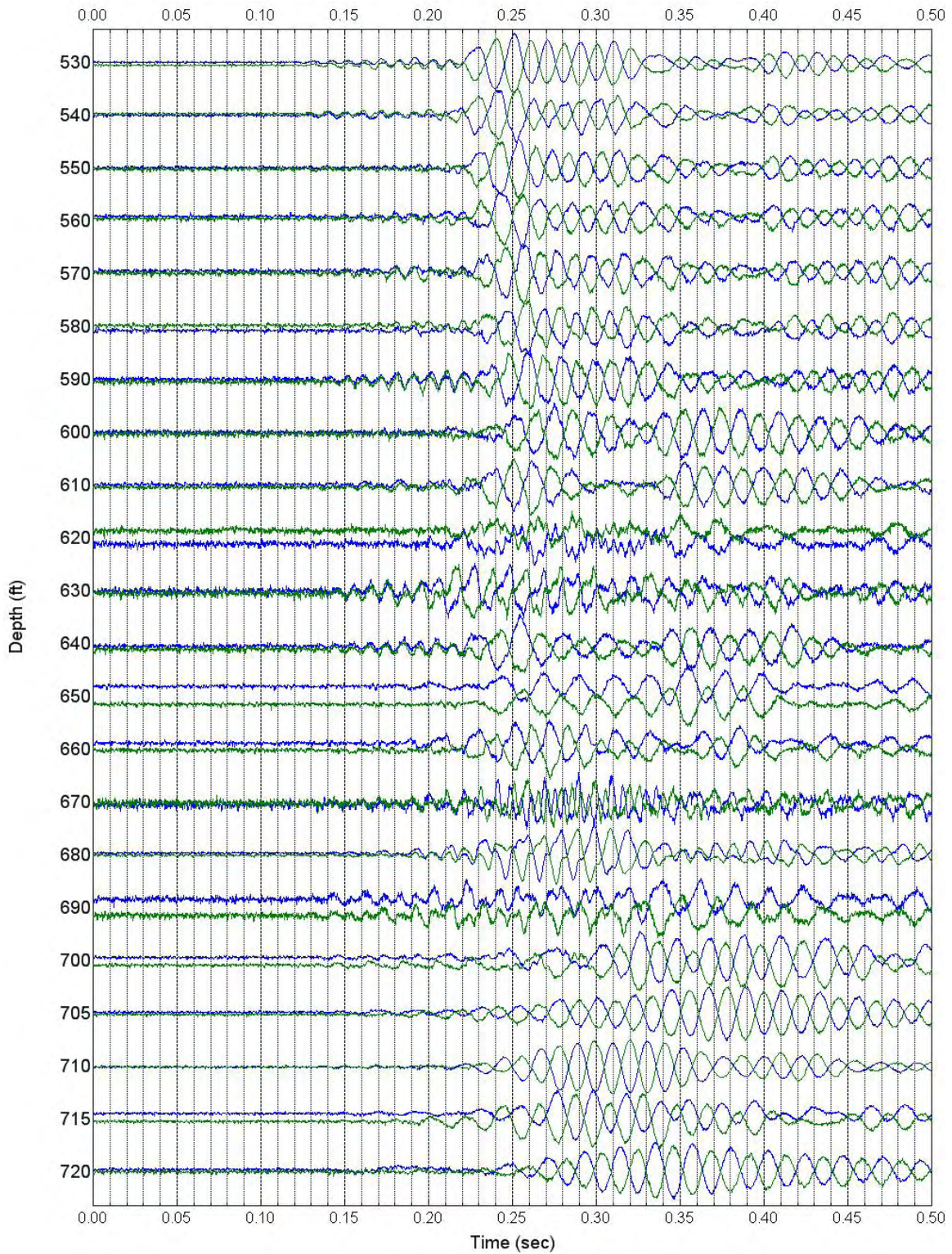


Figure 11.3 Waterfall Plot of Unfiltered S-Wave Signals of Lower Rotated In-Line Receiver (C4996)

Depths 730 to 960 ft; Input Signal: 5 Cycles of 50-Hz Sine Wave; Low Pass 60 Hz; Time Shifted by Reaction Mass Acceleration

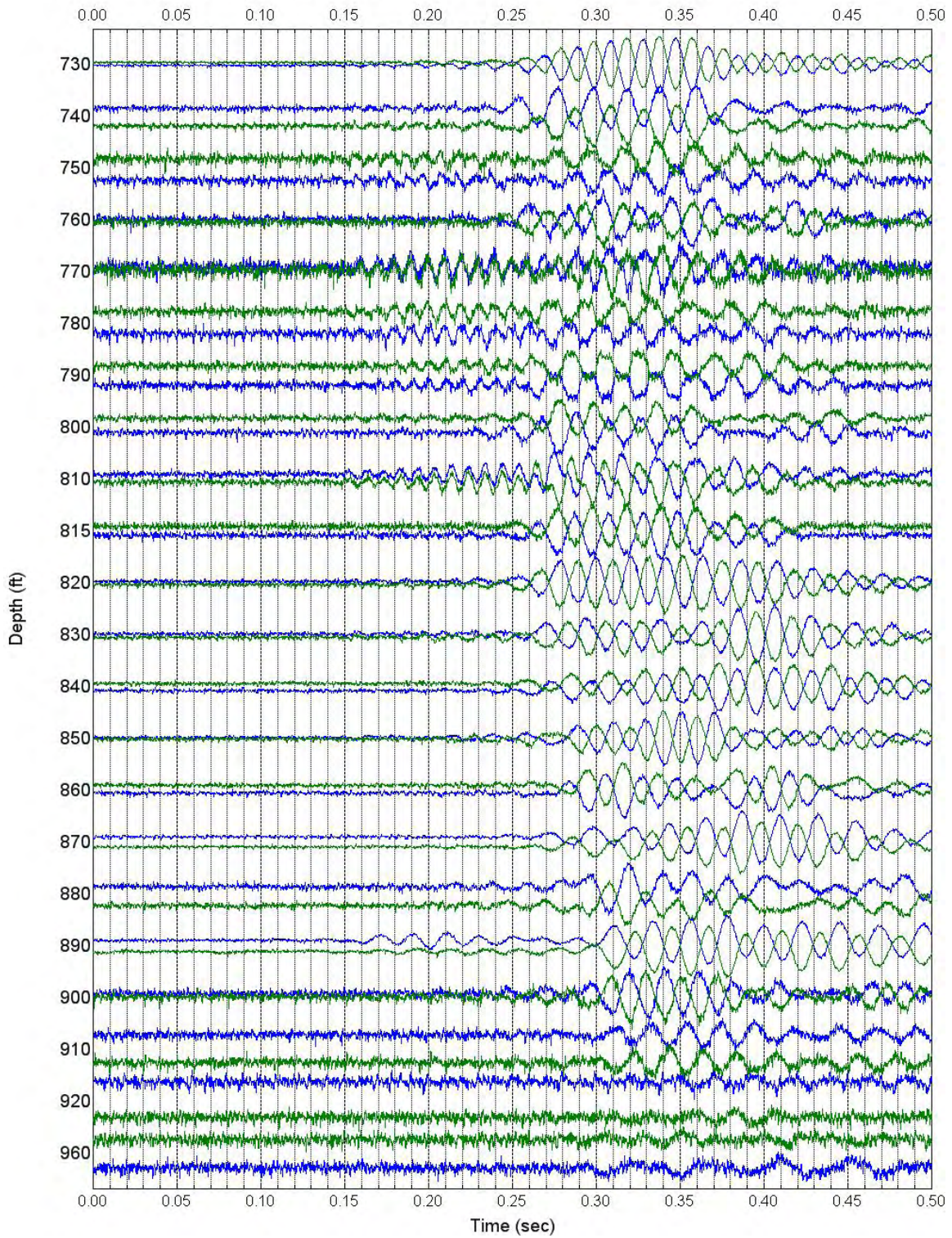


Figure 11.4 Waterfall Plot of Unfiltered S-Wave Signals of Lower Rotated In-Line Receiver (C4996)

Depths 910 to 980 ft; Input Signal: 4 Cycles of 20-Hz Sine Wave; Low Pass 25 Hz; Time Shifted by Reaction Mass Acceleration

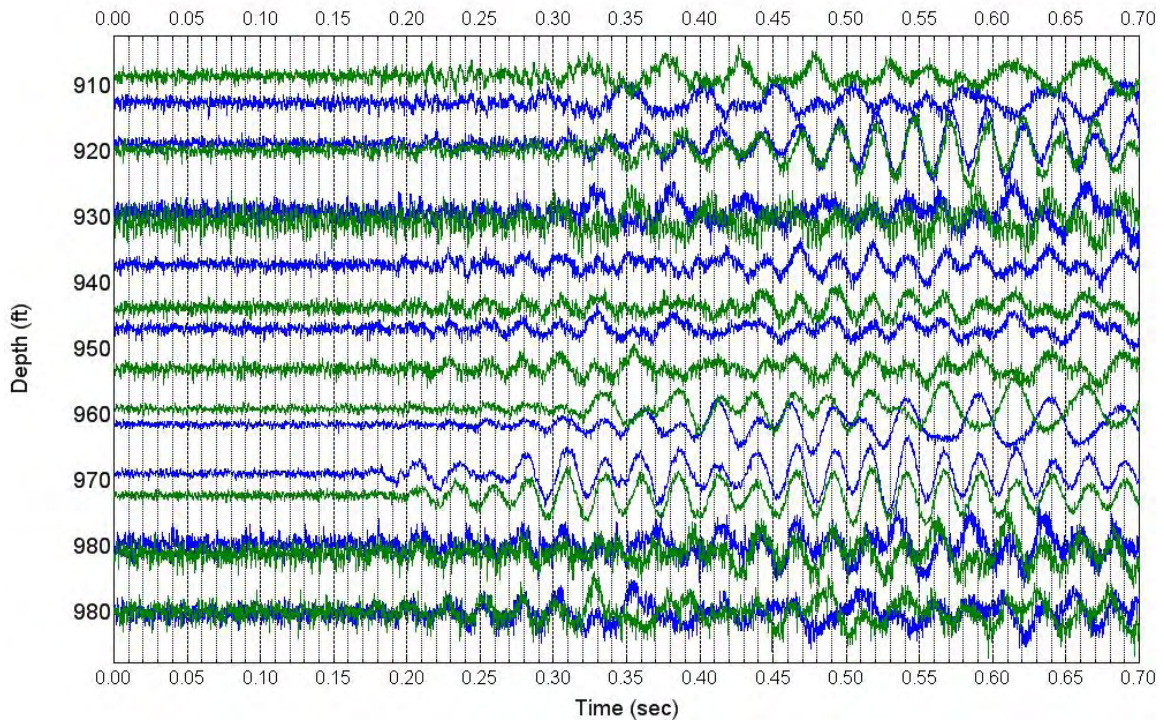
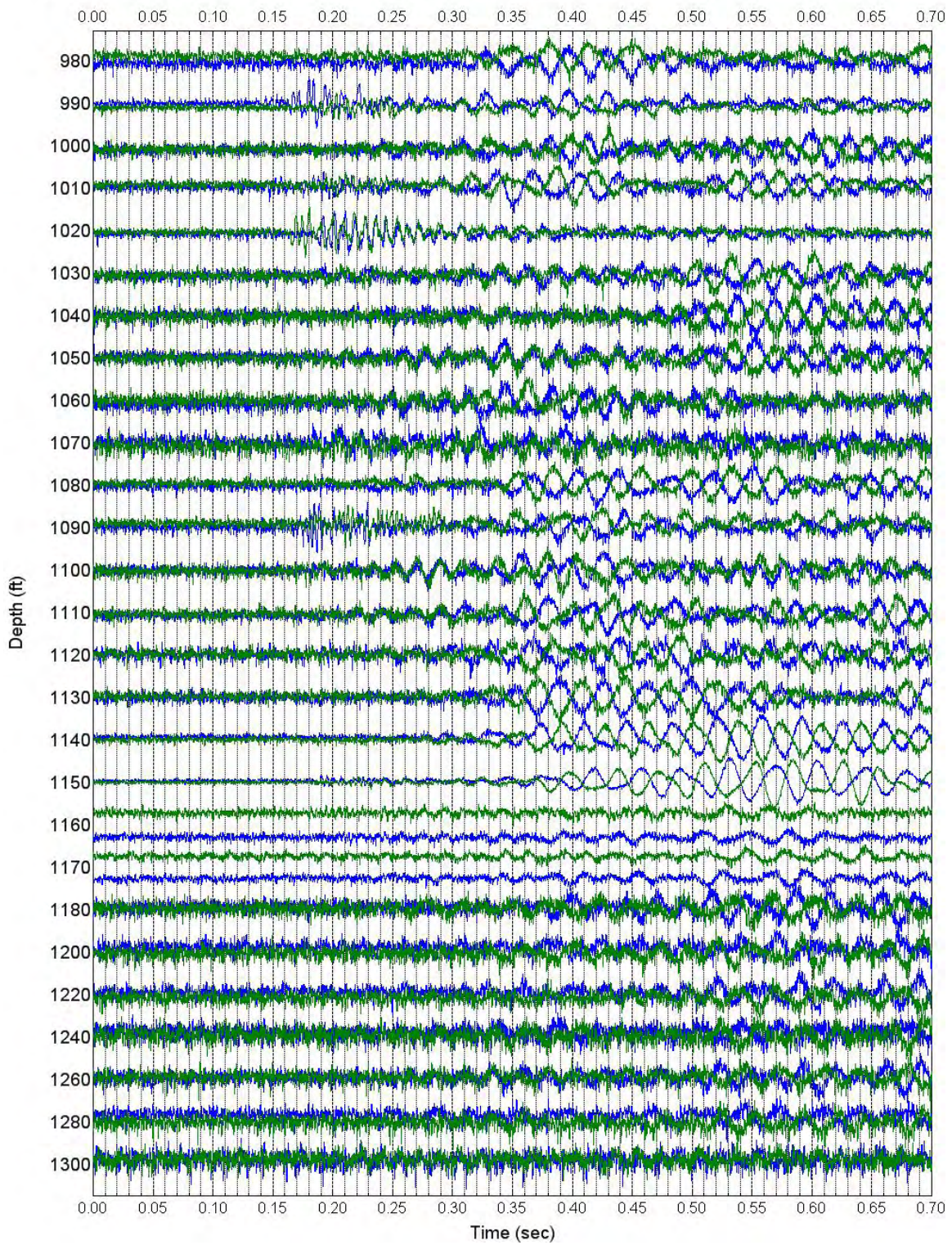


Figure 11.5 Waterfall Plot of Unfiltered S-Wave Signals of Lower Rotated In-Line Receiver (C4996)

Depths 980 to 1300 ft, Input Signal: 4 Cycles of 30-Hz Sine Wave; Low Pass 40 Hz, Time Shifted by Reaction Mass Acceleration



Section 12: Waterfall Plots of Filtered S-Wave Signals of Lower Rotated In-Line Receiver

1. Figures 12.1 to 12.3 present waterfall plots of filtered lower rotated horizontal receiver (S-wave) signals in Borehole C4996, depths 360 to 960 ft; input signal is 5 cycles of 50-Hz sine wave; time shifted by reaction mass acceleration, low pass 60 Hz; depth scaled.
2. Figure 12.4 presents a waterfall plot of filtered lower rotated horizontal receiver (S-wave) signals in Borehole C4996, depths 910 to 980 ft; input signal is 4 cycles of 20-Hz sine wave; time shifted by reaction mass acceleration; low pass 25 Hz; depth scaled.
3. Figure 12.5 presents a waterfall plot of filtered lower rotated horizontal receiver (S-wave) signals in Borehole C4996, depths 980 to 1300 ft; input signal is 4 cycles of 30-Hz sine wave; time shifted by reaction mass acceleration; low pass 40 Hz; depth scaled.

Figure 12.1 Waterfall Plot of Filtered S-Wave Signals of Lower Rotated In-Line Receiver (C4996)

Depths 360 to 520 ft; Input Signal: 50-Hz Sine Wave; Low Pass 60 Hz; Time Shifted by Reaction Mass Acceleration; Depth Scaled

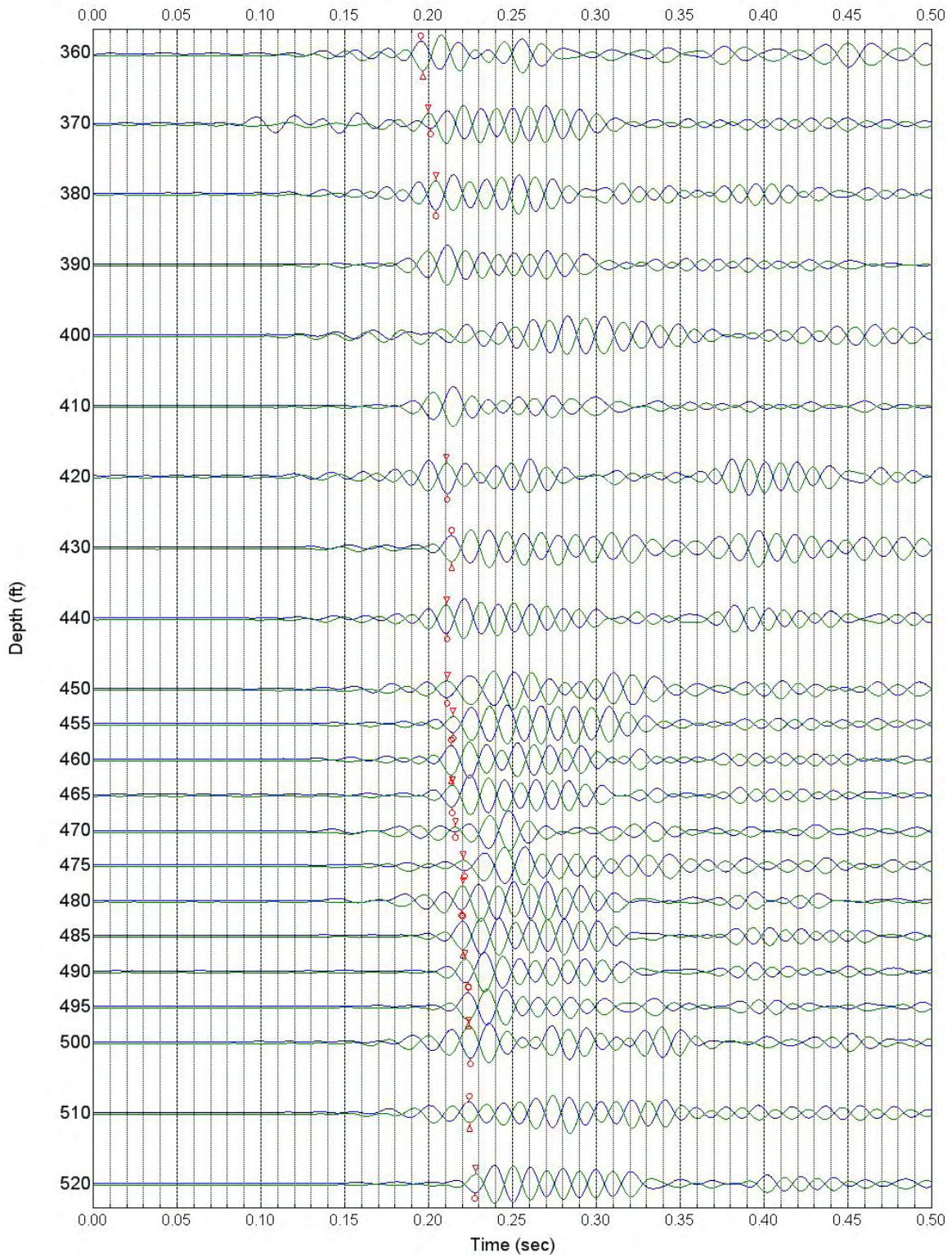


Figure 12.2 Waterfall Plot of Filtered S-Wave Signals of Lower Rotated In-Line Receiver (C4996)

Depths 530 to 720 ft; Input Signal: 50-Hz Sine Wave; Low Pass 60 Hz; Time Shifted by Reaction Mass Acceleration; Depth Scaled

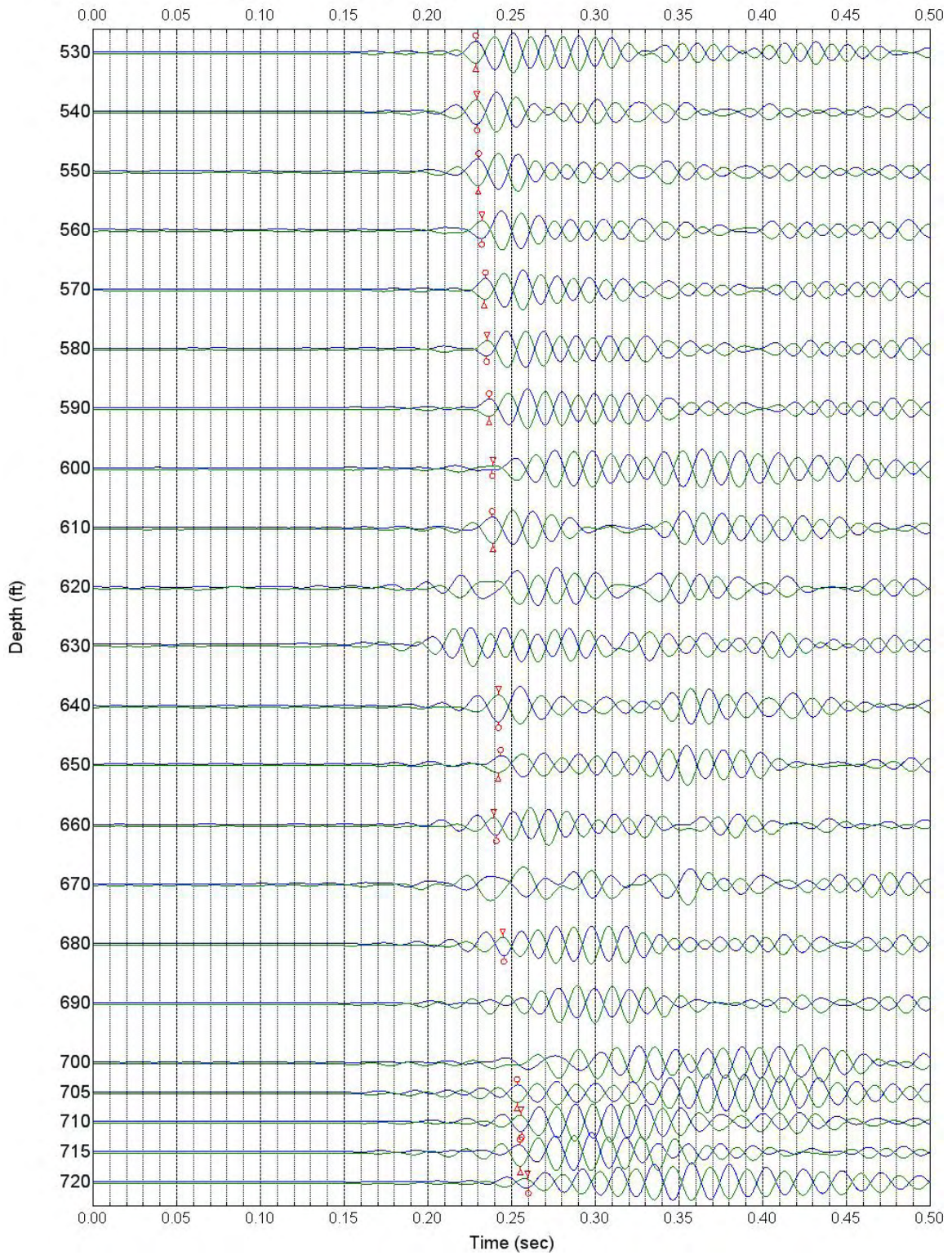


Figure 12.3 Waterfall Plot of Filtered S-Wave Signals of Lower Rotated In-Line Receiver (C4996)

Depths 730 to 960 ft; Input Signal: 50-Hz Sine Wave; Low Pass 60 Hz; Time Shifted by Reaction Mass Acceleration; Depth Scaled

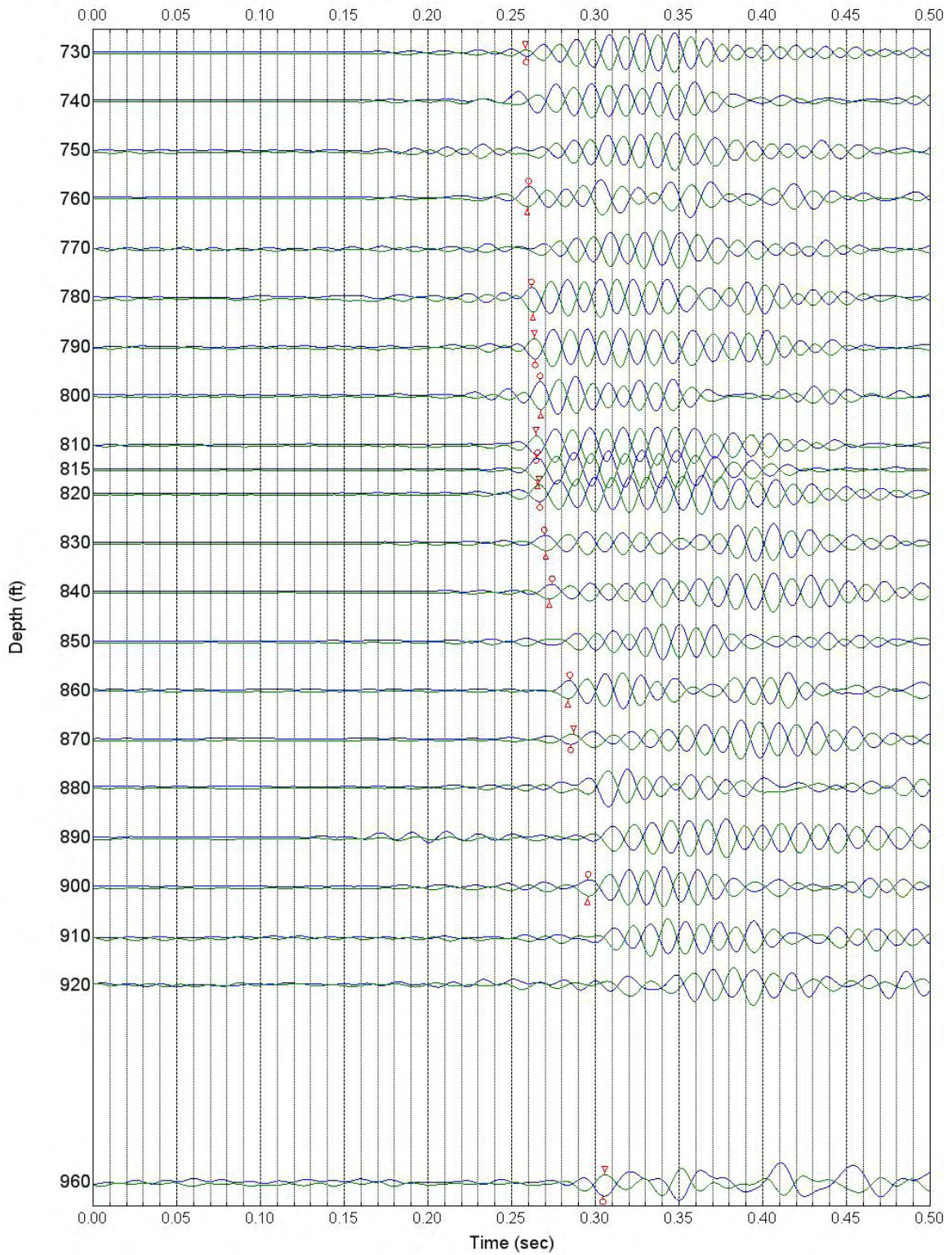


Figure 12.4 Waterfall Plot of Filtered S-Wave Signals of Lower Rotated In-Line Receiver (C4996)

Depths 910 to 980 ft; Input Signal: 20-Hz Sine Wave; Low Pass 25 Hz; Time Shifted by Reaction Mass Acceleration; Depth Scaled

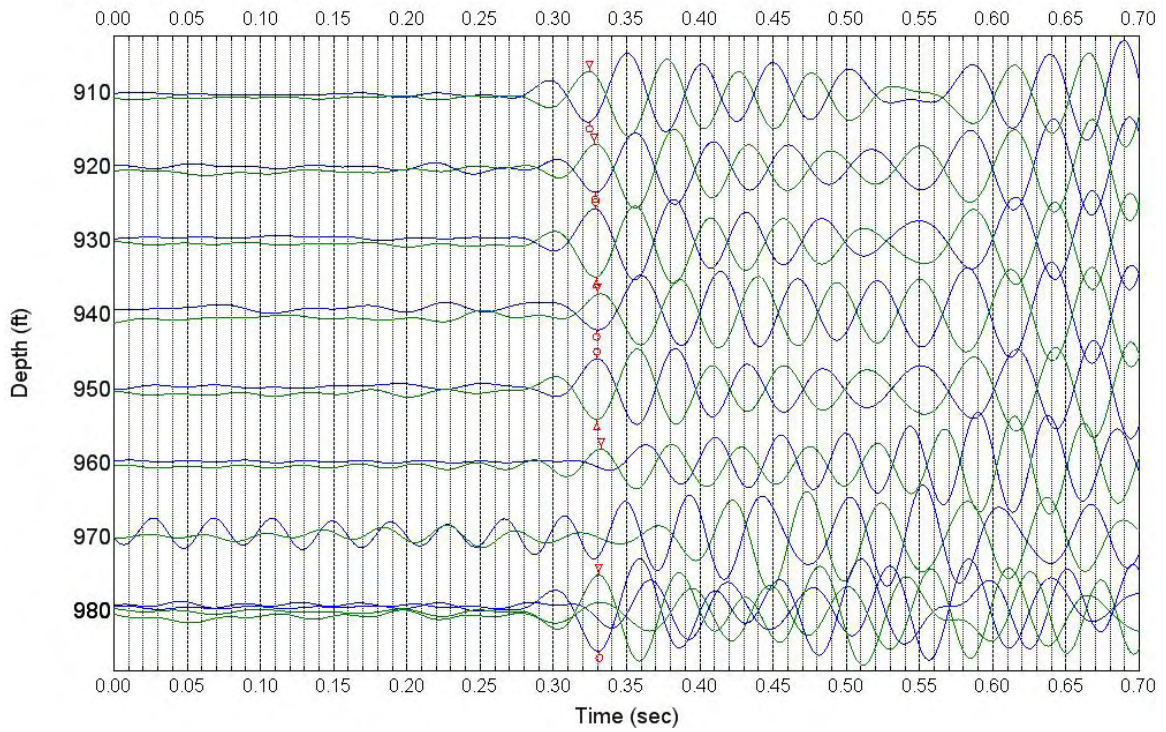
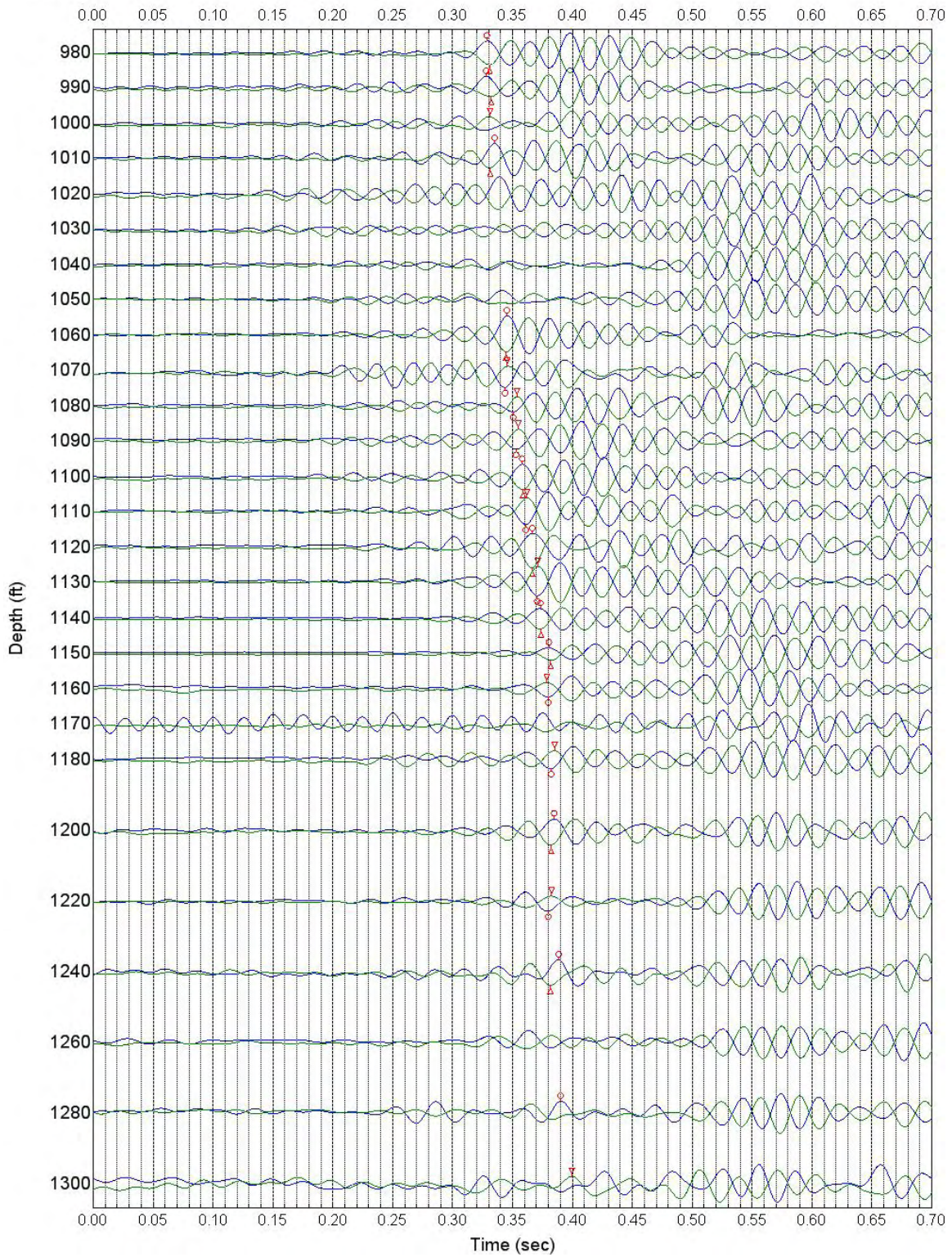


Figure 12.5 Waterfall Plot of Filtered S-Wave Signals of Lower Rotated In-Line Receiver (C4996)

Depths 980 to 1300 ft; Input Signal: 30-Hz Sine Wave; Low Pass 40 Hz; Time Shifted by Reaction Mass Acceleration; Depth Scaled



Section 13 References

1. Barnett, D.B., K.R. Fecht, S.P. Reidel, B.N. Bjornstad, D.C. Lanigan and C.F. Rust. 2007. "*Geology of the Waste Treatment Plant Seismic Boreholes*". PNNL-16407, Rev. 1. Pacific Northwest National Laboratory, Richland, Washington.
2. Gardner, M.G. and R.K. Price. 2007. "*Summary Report of Geophysical Logging for the Seismic Boreholes Project at the Hanford Site Waste Treatment Plant*". DTS-RPT-090 / PNNL-16395. EnergySolutions and Pacific Northwest Geophysics, Richland, Washington.
3. Redpath, B.B. 2007. "*Downhole Measurements of Shear- and Compression-Wave Velocities in Boreholes C4993, C4997, C4997 and C4998 at the Waste Treatment Plant DOE Hanford Site*". PNNL-16559. Redpath Geophysics, Murphys, California.
4. Stokoe, K.H., II, Rathje, E.M., Wilson, C. and Rosenblad, B., 2004. "*Development of Large-Scale Mobile Shakers and Associated Instrumentation for In Situ Evaluation of Nonlinear Characteristics and Liquefaction Resistance of Soils,*" 13th World Conference on Earthquake Engineering, Vancouver, B.C. Canada , August 1-6.
5. Rohay, A.C. and T.M. Brouns. 2007. "*Site-Specific Velocity and Density Model for the Waste Treatment Plant, Hanford, Washington*". PNNL-16652. Pacific Northwest National Laboratory, Richland, Washington.